UNIVERSIDAD COMPLUTENSE DE MADRID

FACULTAD DE CIENCIAS QUÍMICAS

Departamento de Química Orgánica

DESLOCALIZACIÓN ELECTRÓNICA NO CONVENCIONAL: ESTUDIO EXPERIMENTAL Y TEÓRICO DE LA HOMOCONJUGACIÓN AROMÁTICA Y SUS APLICACIONES

MEMORIA PARA OPTAR AL GRADO DE DOCTOR
PRESENTADA POR

Noelia Herrero García

Bajo la dirección del doctor

José Osío Barcina

Madrid, 2013

UNIVERSIDAD COMPLUTENSE DE MADRID

FACULTAD DE CIENCIAS QUÍMICAS

Departamento de Química Orgánica I

DESLOCALIZACIÓN ELECTRÓNICA NO CONVENCIONAL: ESTUDIO EXPERIMENTAL Y TEÓRICO DE LA HOMOCONJUGACIÓN AROMÁTICA Y SUS APLICACIONES

TESIS DOCTORAL

Noelia Herrero García

Madrid, 2012

DESLOCALIZACIÓN ELECTRÓNICA NO CONVENCIONAL: ESTUDIO EXPERIMENTAL Y TEÓRICO DE LA HOMOCONJUGACIÓN AROMÁTICA Y SUS APLICACIONES

Director:

José Osío Barcina

Memoria que para optar al grado de

DOCTOR EN CIENCIAS QUÍMICAS

presenta

Noelia Herrero García

Madrid, 2012

D. José Osío Barcina, Profesor Titular de Química Orgánica de la Facultad de Ciencias Químicas de la Universidad Complutense de Madrid,

CERTIFICA:

Que la presente Memoria, titulada: DESLOCALIZACIÓN ELECTRÓNICA NO CONVENCIONAL: ESTUDIO EXPERIMENTAL Y TEÓRICO DE LA HOMOCONJUGACIÓN AROMÁTICA Y SUS APLICACIONES, se ha realizado bajo su dirección en el Departamento de Química Orgánica I de la Facultad de Ciencias Químicas de la Universidad Complutense de Madrid por la licenciada en Química Dña. Noelia Herrero García, y autoriza su presentación para ser calificada como Tesis Doctoral.

Madrid, -- de 2012

Fdo. D. José Osío Barcina

A mi madrina

Los resultados descritos en la presente Tesis Doctoral se han publicado en los siguientes artículos:

" Electron Delocalization in Homoconjugated 7,7-Diarylnorbornane Systems: A Computational and Experimental Study "

Chem. Eur. J. **2011**, *17*, 7327-7335.

" Efficient Electron Delocalization Mediated by Aromatic Homoconjugation in 7,7-Diphenylnorbornane Derivatives "

J. Org. Chem. **2009**, *74¸7148-7156.*

" A Joint Experimental and Computational Investigation on Homoconjugated Push-Pull Chromophores Derived from 7,7-Diphenylnorbornane "

Eur. J. Org. Chem. **2012**, 2643-2655.

"Efficient Photoinduced Energy Transfer Mediated by Aromatic Homoconjugated Bridges "

Chem. Eur. J. **2010**, *16*, 6033-6040.

"Rational Design of a non-Basic Molecular Receptor for Selective NH_4^+/K^+ Complexation in the Gas-Phase"

Chem. Eur. J. ***2012, 18, DOI:*** *10.1002/chem.201201642*

La presente memoria del trabajo de tesis Doctoral se ha escrito siguiendo el formato de publicaciones. Incluye, además de una introducción general sobre el estado actual del área de investigación en la que se enmarca el trabajo, una discusión integradora de los resultados obtenidos. Los dos capítulos principales se han subdividido según las distintas publicaciones, mientras que en el capítulo de las discusiones generales se han incluido resultados no publicados en el momento de redacción de la Memoria. Los capítulos publicados conservan su formato original en inglés, sin embargo, la introducción, discusión, objetivos y conclusiones se han escrito en castellano de acuerdo a la normativa para este formato de tesis.

La Memoria adjunta un CD en el que se han incluido todas las coordenadas cartesianas y energías totales de todos los puntos estacionarios mencionados obtenidos mediante cálculos computacionales. El CD incluye también un archivo .pdf con la Memoria completa.

Abreviaturas utilizadas en esta Memoria:

anh	Anhidro
Ar	Argón
CT	Transferencia de carga
d	Doblete
dd	Doblete de dobletes
DFT	Teoría del funcional de la densidad
DMF	Dimetilformamida
DPM	Difenilmetano
DPN	Difenilnorbornano
E_{ox}	Potencial de oxidación
eq	Equivalente químico
E_{red}	Potencial de reducción
ESI	Ionización por electroespray
ESI-MS	Espectroscopía de masas por ESI
EtOH	Etanol
Fc	Ferroceno
FTIR	Espectroscopía infrarroja con transformada de Fourier
gap	Salto de energía
HOMO	Orbital molecular ocupado de mayor energía
Hz	Hertzios
L	Ligando
LF	Campo del ligando
K	Kelvin
LUMO	Orbital molecular desocupado de menor energía
m	Multiplete

m/z	Relación masa/carga
MeCN	Acetonitrilo
MeOH	Metanol
MLCT	Transferencia de carga metal-ligando
NLO	Óptica no lineal
nm	Nanómetros
P.f.	Punto de fusión
Ph	Fenilo
ppm	Partes por millón
r_{DA}	Distancia dador-aceptor
RMN	Resonancia Magnética Nuclear
r.t.	Temperatura ambiente
s	Singlete
t	Triplete
TD-DFT	Teoría del funcional de la densidad dependiente del tiempo
THF	Tetrahidrofurano
TMS	Trimetilsililo
UV-vis	Ultravioleta-visible
δ	Desplazimiento
λ	Longitud de onda

ÍNDICE

I. INTRODUCCIÓN GENERAL Y OBJETIVOS 1

I.1 Deslocalización electrónica en moléculas orgánicas 3

I.2 Deslocalización electrónica no convencional 7
I.2.1 Homoconjugación 11
I.2.2 Homoconjugación aromática 13

I.3 El 7,7-difenilnorbornano como subunidad estructural en Química Supramolecular 20

II. CAPÍTULO I 23

1.1 Electron Delocalization in Homoconjugated 7,7-Diarylnorbornane Systems: A Computational and Experimental Study 25
1.1.2 Computational details 29
1.1.3 Results and Discussion 30
1.1.4 Conclusion 44
1.1.5 Experimental Section 46

1.2 Efficient Electron Delocalization Mediated by Aromatic Homoconjugation in 7,7-Diphenylnorbornane Derivatives 51
1.2.1 Introduction 52
1.2.2 Results and Discussion 57
1.2.3 Conclusion 67
1.2.4 Experimental Section 69

1.3 A Joint Experimental and Computational Investigation on Homoconjugated Push-Pull Chromophores Derived from 7,7-Diphenylnorbornane 73
1.3.1 Introduction 74
1.3.2 Computational details 77
1.3.3 Results and Discussion 79
1.3.4 Conclusion 99
1.3.5 Experimental Section 101

III. CAPÍTULO 2 123

2.1 Efficient Photoinduced Energy Transfer Mediated by Aromatic homoconjugated bridges **125**
2.2.1 Introduction 126
2.2.2 Results and Discussion 130
1.1.2.1 Photophysical properties 131
1.1.2.1.1 Absorption and emission spectroscopy 131
1.1.2.1.2 Transient absorption spectroscopy 135
2.2.3 Conclusion 140
2.2.4 Experimental Section 141

2.2 Rational Design of a non-Basic Molecular Receptor for Selective NH_4^+/K^+ Complexation. **149**
2.2.1 Introduction 150
2.2.2 Results and Discussion 151
2.2.3 Conclusion 161
2.2.4 Experimental Section 162

IV. DISCUSIÓN GENERAL **167**

IV.1 Capítulo 1 **169**
IV.1.1 Estudio de la deslocalización electrónica por homoconjugación en compuestos aromáticos y sistemas poliméricos. 169
IV.1.2 Estudio de la deslocalización electrónica por homoconjugación en compuestos con sustituyentes. Sistemas push-pull. 181

IV.2 Capíulo 2 **190**
IV.2.1 Aplicaciones de sistemas homoconjugados en el diseño de cables moleculares y OLEDs 190
IV.2.2 Diseño de receptores moleculares para la complejación selectiva NH_4^+/K^+ 199

V. CONCLUSIONES **207**

I. INTRODUCCIÓN GENERAL Y OBJETIVOS

I.1 Deslocalización electrónica en moléculas orgánicas

Uno de los conceptos más importantes en Química es el de deslocalización electrónica.[1,2,3,4,5] Este concepto es omnipresente en todas las áreas de la Química, pero de manera muy especial en Química Orgánica, en la que aparece fundamentalmente en moléculas π-conjugadas y aromáticas. De acuerdo con la definición establecida por la IUPAC en 1994, "la deslocalización electrónica es un concepto mecano-cuántico empleado principalmente en Química Orgánica para describir los enlaces π en sistemas conjugados. Estos enlaces no están localizados entre dos átomos, sino que en lugar de ello cada unión presenta un carácter parcial de doble enlace o de orden de enlace".[6a] Otra definición, también dada por la IUPAC, define este fenómeno como "la redistribución de la densidad de los electrones de valencia a lo largo de una entidad molecular en comparación con un modelo localizado".[6b] Una idea de la importancia de la deslocalización electrónica la da el hecho de que durante el periodo comprendido entre los años 1990-2004, aparecen 2500 entradas con este término en la Web of Science. Este número aumenta hasta las 8200 entradas durante los años 2005-2011.

El interés por los compuestos orgánicos con deslocalización electrónica derivada de la conjugación no es solo teórico. Desde el descubrimiento por Heeger, MacDiarmid y Shirakawa (galardonados con el premio Nobel el año 2000) de las propiedades conductoras de los polímeros conjugados,[7] la

[1] a) M. J. S. Dewar, en *Modern Models of Bonding and Delocalization*, (Eds.: J. F. Liebman, A. Greenberg) Verlag Chemie, Weinheim, **1988**; b) L. Pauling, en *The Nature of the Chemical Bond*, Cornell University Press, **1960**.
[2] *Curr. Org. Chem.* **2011**, *15(20)*: número especial sobre deslocalización electrónica en Química Orgánica.
[3] *Phys. Chem. Chem. Phys.* **2011**, *13(46)*: número especial sobre deslocalización electronica, aromaticidad y propiedades moleculares relacionadas.
[4] *Chem. Rev.* **2005**, *105(10)*: número especial sobre deslocalización σ y π.
[5] *Chem. Rev.* **2001**, *105(5)*: número especial sobre aromaticidad y deslocalización.
[6] a) P. Muller, *Pure Appl. Chem.* **1994**, *66*, 1077; b) V. I. Minkin, *Glossary of Terms Used in Theoretical Organic Chemistry, Pure Appl. Chem.* **1999**, *71*, 1919-1981.
[7] a) C. K. Chiang, M. A. Druy, S. C. Gau, A. J. Heeger, E. J. Louis, A. G. MacDiarmid, Y. W. Park, H. Shirakawa, *J. Am. Chem. Soc.* **1978**, *100*, 1013; b) C. K. Chiang, C. R., Jr. Fincher, Y. W. Park, A. J. Heeger, H. Shirakawa, E. J. Louis, S. C. Gau, A. G. MacDiarmid, *Phys. Rev. Lett.* **1977**, *39*, 1098; c) H. Shirakawa, E. J. Louis, A. G. MacDiarmid, C. K. Chiang, A. J. Heeger, *J. Chem. Soc., Chem. Commun.* **1977**, 579;

importancia de estos compuestos no ha cesado de crecer y actualmente constituyen la base de áreas tan importantes como la electrónica molecular, los materiales orgánicos y la nanotecnología.[8,9] Las características de los compuestos orgánicos conjugados basadas en sus propiedades eléctricas y ópticas permiten que estos sistemas estén presentes en multitud de aplicaciones tales como semiconductores orgánicos,[10] OLEDs,[11] transistores orgánicos (OFETs),[12] circuitos integrados,[13] células solares,[14] cables moleculares,[15]

---

d) H. Shirakawa, *Angew. Chem. Int. Ed.* **2001**, *40*, 2574-2580; e) A. G. MacDiarmid, *Angew. Chem. Int. Ed.* **2001**, *40*, 2581-2590.

[8] a) *Electronic Materials: The Oligomer Approach*, (Eds: K. Müllen, G. Wegner), Wiley-VCH, New York, **1998**; b) *Introduction to Molecular Electronics*, (Eds: M. C. Petty, M. R. Bryce, D. Bloor), Oxford University Press, New York, **1995**.

[9] a) V. Balzani, A. Credi, M. Venturi, *Molecular Devices. Concepts and Perspectives for the Nanoworld*, Wiley-VCH, Weinheim, **2008**; b) *Dekker Encyclopedia of Nanoscience and Nanotechnology*, Schwarz, J. A., Contescu, C. I., Putyera, K., Eds.; Marcel Dekker, New York, 2004; c) Gómez, R.; Segura, J. L. In *Materials for Organic Solar Cells*, in *Handbook of Organic Electronics and Photonics, Vol. 3*, Nalwa H. S., Ed.; American Scientific Publishers, Valencia, California, 2007; d) *π-Electron Magnetism: From Molecules to Magnetic Materials*, (Ed.: J. Veciana), *Structure & Bonding* **2001**, *100*, 1-207; e) *Tomorrow's Chemistry Today: Concepts in Nanoscience, Organic Materials and Environmental Chemistry*, (Ed.: B. Pignataro), Wiley-VCH, Weinheim, **2009**; f) *Functional Organic Materials: Syntheses, Strategies and Applications*, (Eds.: T. J. J. Müller, U. H. F. Bunz), Wiley-VCH, Weinheim, **2007**.

[10] *Handbook of Conducting Polymers*, (Eds: T. A. Skotheim, J. R. Reynolds), CRC Press, Taylor & Francis Group, London, **2007**; a) James, D. K.; Tour, J. M. *Chem. Mater.* **2004**, *16*, 4423; b) Klauk, H. *Chem. Soc. Rev.* **2010**, *39*, 2643; c) Perepichka, D. F.; Meng, H.; Wuld, F. *Adv. Mater.* **2005**, *17*, 2281; d) Allard, S.; Foster, M.; Souharce, B.; Thiem, H.; Scherf, U. *Angew. Chem. Int. Ed.* **2008**, *47*, 4070; e) Melzer, C.; Von Seggern, H. *Nat. Mater.* **2010**, *9*, 470.

[11] a) Yersin, H. *Highly Efficient OLEDs with Phosphorescent Materials*; Wiley-VCH: Weinheim, Germany, 2008; b) *Organic Light-Emitting Devices. Synthesis, Properties and Applications*, (Eds: K. Müllen, U. Scherf), Wiley-VCH, Weinheim, **2006**; c) Chiu, C.-W.; Chow, T. J.; Chuen, C.-H.; Lin, H.-M.; Tao, Y.-T. *Chem. Mater.* **2003**, *15*, 4527; d) *Organic Electroluminescence*, Kafafi Z. H., Ed.; Taylor Francis, Boca Raton, 2005; e) J. Liu, Q. Pei, *Curr. Org. Chem.* **2010**, *14*, 2133-2144; f) Z. Ma, P. Sonar, Z.-K. Chen, *Curr. Org. Chem.* **2010**, *14*, 2034-2069; g) A. C. Grimsdale, *Curr. Org. Chem.* **2010**, *14*, 2196-2217; h) C. Li, Z. Bo, *Polymer* **2010**, *51*, 4273-4292.

[12] a) Stutzmann, N.; Friend, R. H.; Sirringhaus, H. *Science* **2003**, *299*, 1881; b) J. Zaumseil, H. Sirringhaus, *Chem. Rev.* **2007**, *107*, 1296; c) C. D. Dimitrakopoulos, P. R. L. Malenfant, *Adv. Mater.* **2002**, *14*, 99-117; d) H. Sirringhaus, *Adv. Mater.* **2005**, *17*, 2411-2425; e) A. R. Murphy, J. M. J. Fréchet, *Chem. Rev.* **2007**, *107*, 1066-1096.

[13] a) D. R. Gamota, P. Brazis, K. Kalyanasundaram, J. Zhang, *Printed Organic and Molecular Electronics*; Kluwer Academic Publishers: New York, NY, U.S., 2004; b) M. J. Xu, *Synth. Met.* **2000**, *115*, 1; c) H. Sirringhaus, T. Kawase, R. H. Friend, T.

sensores químicos y biológicos[16] y láseres poliméricos,[17] entre otros.[18] Los materiales orgánicos π-conjugados presentan en muchos casos propiedades similares o mejores que las de los análogos inorgánicos, con las ventajas adicionales de ser con frecuencia más baratos, fáciles de fabricar y más flexibles y ligeros.

Desde un punto de vista cualitativo, cuando los químicos emplean el término "deslocalización electrónica", es relativamente fácil hacerse una idea o crear una imagen mental de lo que significa este concepto. En este sentido, la teoría de la resonancia resulta muy útil ya que permite representar sistemas

---

Shimoda, M. Inbasekaran, W. Wu, E. P. Woo, *Science* **2000**, *290*, 2123; d) Z. Bao, *Adv. Mater.* **2000**, *12*, 227; e) B. Crone, A. Dodabalapur, Y.-Y. Lin, R. W. Filas, Z. Bao, A. LaDuca, R. Sarpeshkar, H. E. Katz, W. Li, *Nature* **2000**, *403*, 521; f) T. B. Singh, N. S. Sariciftci, *Annu. Rev. Mater. Res.* **2006**, *36*, 199.

[14] a) H. Hoppe, N. S. Sariciftci, *Polymer Solar Cells*; Springer: Heidelberg, Berlin, 2008; Vol. 214; b) C. J. Brabec, N. S. Sariciftci, J. C. Hummelen, *Adv. Funct. Mater.* **2001**, *11*, 15-26; c) J. Xue, B. P. Rand, S. Uchida, S. R. Forrest, *Adv. Mater.* **2005**, *17*, 66-71; d) J. Li, F. Dierschke, J. Wu, A. C. Grimsdale, K. Müllen, *J. Mater. Chem.* **2006**, *16*, 96-100; e) S. Günes, H. Neugebauer, N. S. Sariciftci, *Chem. Rev.* **2007**, *107*, 1324-1338; f) P. M. Beaujuge, J. M. J. Fréchet, *J. Am. Chem. Soc.* **2011**, *133*, 20009-20029.

[15] *Molecular Wires. From design to Properties*, (Ed.: L. de Cola); Thematic issue, *Top. Curr. Chem.* **2005**, *257*, 1-170.

[16] a) L. Torsi, M. C. Tanese, N. Cioffi, M. C. Gallazzi, L. Sabbatici, P. G. Zambonin, G. Raos, S. V. Meille, M. M. Giangregorio, *J. Phys. Chem. B* **2003**, *107*, 7589-7564; b) C. Bartic, G. Borghs, *Anal. Bioanal. Chem.* **2006**, *384*, 354-365; c) S. W. Thomas III, G. D. Joly, T. M. Swager, *Chem. Rev.* **2007**, *107*, 1339-1386.

[17] a) F. Hide, M. A. Díaz-García, B. J. Schwartz, A. J. Heeger, *Acc. Chem. Res.* **1997**, *30*, 430-436; b) M. D. McGehee, A. J. Heeger, *Adv. Mater.* **2000**, *12*, 1655-1668; c) G. Kranzelbinder, E. Toussaere, J. Zyss, A. Pogantsch, E. W. J. List, H. Tillmann, H. H. Hörhold, *Appl. Phys. Lett.* **2002**, *80*, 716-718; d) I. W. D. Samuel, G. A. Turnbull, *Chem. Rev.* **2007**, *107*, 1272-1295.

[18] a) R. H. Friend, R. W. Gymer, A. B. Holmes, J. H. Burroughes, R. N. Marks, C. Taliani, D. D. C. Bradley, D. A. Dos Santos, J. L. Bredas, M. Lögdlund, W. R. Salaneck, *Nature* **1999**, *397*, 121; b) B. D. Gates, Q. Xu, M. Stewart, D. Ryan, C. G. Willson, G. M. Whitesides, *Chem. Rev.* **2005**, *105*, 1171; c) H. Sirringhaus, N. Tessler, R. H. Friend, *Science* **1998**, *280*, 1741; d) A. C. Huebler, F. Doetz, H. Kempa, H. E. Katz, M. Bartzsch, N. Brandt, I. Hennig, U. Fuegmann, S. Vaidyanathan, J. Granstrom, S. Liu, A. Sydorenko, T. Zillger, G. Schmidt, K. Preissler, E. Reichmanis, P. Eckerle, F. Richter, T. Fischer, U. Hahn, *Organic Electronics* **2007**, *8*, 480; e) J. A. Rogers, Z. Bao, *J. Polym. Sci. A* **2002**, *40*, 3327; f) S. Lois, J.-C. Flores, J.-P. Lere-Porte, F. Serein-Spirau, J. J. E. Moreau, K. Miqueu, J.-M. Sotiropoulos, P. Baylere, M. Tillard, C. Belin, *Eur. J. Org. Chem.* **2007**, 4019.

deslocalizados mediante varias estructuras de Lewis (estructuras resonantes o formas canónicas) cuya superposición proporciona una descripción de la molécula. Cuantas más estructuras resonantes contribuyan a la descripción, mayor es la deslocalización electrónica del sistema estudiado. La diferencia entre la energía del sistema deslocalizado y la energía de una estructura hipotética con enlaces σ y π localizados, es la energía de deslocalización de la molécula.

Sin embargo, cuando se quiere hacer una descripción cuantitativa de la deslocalización electrónica, la situación es mucho más complicada, ya que la deslocalización no es un observable y por tanto no existe una propiedad que permita medirla directamente. Esta circunstancia ha estimulado el desarrollo de una serie de aproximaciones teóricas que intentan definir y proporcionar una evaluación cuantitativa de la deslocalización (σ y π) en sistemas conjugados, tanto aromáticos como no aromáticos.[2,3,4,5] Cabe destacar a este respecto, como herramientas muy útiles para el estudio teórico de la deslocalización, la ELF (Electron Localization Function), que proporciona una imagen de las regiones donde la localización de los electrones de una molécula es elevada,[19] la QTAIM (Quantum Theory of Atoms in Molecules) que da información sobre la estructura electrónica de sistemas orgánicos,[20] NICS (Nucleus Independent Chemical Shift),[21] y ACID (Anisotropy of Induced Current Density).[22]

A pesar de que la deslocalización electrónica no es un observable y por tanto no puede medirse directamente, además de las aproximaciones teóricas mencionadas anteriormente, es posible estudiar este fenómeno de manera indirecta ya que hay una serie de propiedades moleculares, observables, que están directamente relacionadas con el grado de deslocalización presente en las moléculas.

---

[19] a) P. Fuentealba, J. C. Santos, *Curr. Org. Chem.* **2011**, *15*, 3619-3626; b) B. Silvi, P. Reinhardt, *Curr. Org. Chem.* **2011**, *15*, 3555-3565; c) S. N. Steinmann, Y. Mo, C. Corminboeuf, *Phys. Chem. Chem. Phys.* **2011**, *13*, 20584-20592.

[20] a) C. Silva López, A. R. de Lera, *Curr. Org. Chem.* **2011**, *15*, 3576-3593; b) P. Bultinck, M. Rafat, R. Ponec, B. Van Gheluwe, R. Carbó-Dorca, P. Popelier, *J. Phys. Chem. A* **2006**, *110*, 7642-7648.

[21] a) T. Heine, R. Islas, G. Merino, *J. Comput. Chem.* **2007**, *28*, 302-309; b) Z. Chen, C. S. Wannere, C. Corminboeuf, R. Puchta, P. v. R. Schleyer, *Chem. Rev.* **2005**, *105*, 3842-3888.

[22] D. Geuenich, K. Hess, F. Köhler, R. Herges, *Chem. Rev.* **2005**, *105*, 3758-3772.

Algunas de las evidencias experimentales de la deslocalización electrónica, cuyo estudio permite extrapolar conclusiones acerca de la misma, son la alternancia en las longitudes de enlace en moléculas orgánicas conjugadas, la respuesta de sistemas conjugados a un campo eléctrico externo (polarizabilidad), las espectroscopias UV-vis y fotoelectrónica, la transmisión de los efectos ejercidos por los sustituyentes en compuestos conjugados[23] los tiempos de vida de estados excitados o la reactividad de las moléculas con deslocalización electrónica.[22] De todas estas propiedades, quizás la más accesible y probablemente la que más se ha utilizado, sea el estudio de los espectros UV-vis.[24] Aunque esta técnica espectroscópica presenta ciertas limitaciones,[25] en términos generales existe una relación directa entre el grado de deslocalización electrónica y la longitud de onda de la correspondiente banda en el espectro, cuando se comparan familias de moléculas en las que se van introduciendo variaciones estructurales pequeñas, de tal forma que, cuanto mayor es la deslocalización, mayor es el desplazamiento batocrómico de la banda en el espectro.

I.2 Deslocalización electrónica no convencional

La movilidad de los electrones a lo largo de la estructura de una molécula orgánica no solo puede ser debida a las conjugaciones σ y π mencionadas anteriormente.[26] En los últimos años se han descrito una serie de mecanismos, diferentes de la conjugación, que permiten la deslocalización de los electrones de un sistema molecular. Todos ellos tienen en común que están basados en diferentes topologías moleculares que permiten la comunicación o

[23] *T. M. Krygowski, B. T. Stepien, Chem. Rev.* ***2005****, 105, 3482-3512.*

[24] a) H.-H. Perkampus, *UV-Vis Atlas of Organic Compounds,* VCH, Weinheim, **1992**; b) P. Klán, J. Wirz, *Photochemistry of Organic Compounds. From Concepts to Practice*,Wiley, Chichester, **2009**; c) M. Klessinger, J. Michl, *Excited States and Photochemistry of Organic Molecules*, VCH, Weinheim, **1995**.

[25] C. A. van Walree, J. H. van Lenthe, B. C. van der Wiel, *Chem. Phys. Lett.* **2012**, *528*, 29-33.

[26] Ejemplos de sistemas con deslocalización σ se describen en: a) R. M. Williams, M. Koeberg, J. M. Lawson, Y.-Z. An, Y. Rubin, M. N. Paddon-Row, J. W. Verhoeven, *J. Org. Chem.* **1996**, *61*, 5055-5062; b) H. Oevering, M. N. Paddon-Row, M. Heppener, A. M. Oliver, E. Cotsaris, J. W. Verhoeven, N. S. Hush, *J. Am. Chem. Soc.* **1987**, *109*, 3258-3269.

solapamiento de orbitales y, por tanto, la deslocalización electrónica en mayor o menor grado. Los ejemplos más importantes de deslocalización electrónica no convencional son la spiroconjugación,[27,28,29] la conjugación cruzada,[25,30,31,32,33,34,35] la conjugación toroidal[36,37,38,39,40] y la deslocalización electrónica a lo largo de sistemas con apilamientos π (π-

[27] T. P. I. Saragi, T. Spehr, A. Siebert, T. Fuhrmann-Lieker, J. Salbeck, *Chem. Rev.* **2007**, *107*, 1011-1065.
[28] a) L.-H. Xie, J. Liang, J. Song, C.-R. Yin, W. Huang, *Curr. Org. Chem.* **2010**, *14*, 2169-2195; b) D. Heredia, L. Fernández, L. Otero, M. Ichikawa, C.-Y. Lin, Y.-L. Liao, S.-A. Wang, K.-T. Wong, F. Fungo, *J. Phys. Chem C* **2011**, *115*, 21907-21914; c) D. Vak, J. Jo, J. Ghim, C. Chun, B. Lim, A. J. Heeger, D.-Y. Kim, *Macromolecules* **2006**, *39*, 6433-6439; d) Y. J. Cho, O. Y. Kim, J. Y. Lee, *Org. Electron.* **2012**, *13*, 351-355; e) C. Fan, Y. Chen, P. Gan, C. Yang, C. Zhong, J. Qin, D. Ma, *Org. Lett.* **2010**, *12*, 5648-5651.
[29] a) J. Abe, Y. Shirai, N. Nemoto, Y. Nagase, *J. Phys. Chem. A* **1997**, *101*, 1-4; b) Y. Luo, P. Norman, H. Agren, *Chem. Phys. Lett.* **1999**, *303*, 616-620.
[30] P. A. Limacher, H. P. Lüthi, *Wires Comput. Chem. Sci.* **2011**, *1*, 477-486.
[31] a) D. Q. Andrews, G. C. Solomon, R. P. Van Duyne, M. A. Ratner, *J. Am. Chem. Soc.* **2008**, *130*, 17309-17319; b) G. C. Solomon, D. Q. Andrews, R. H. Goldsmith, T. Hansen, M. R. Wasielewski, R. P. Van Duyne, M. A. Ratner, *J. Am. Chem. Soc.* **2008**, *130*, 17301-17308; c) A. B. Ricks, G. C. Solomon, M. T. Colvin, A. M. Scott, K. Chen, M. A. Ratner, M. R. Wasielewski, *J. Am. Chem. Soc.* **2010**, *132*, 15427-15434.
[32] a) S. Smolarek, A. Vdovin, A. Rijs, C. A. van Walree, M. Z. Zgierski, W. J. Buma, *J. Phys. Chem. A* **2011**, *115*, 9399-9410; b) B. C. van der Wiel, R. M. Williams, C. A. van Walree, *Org. Biomol. Chem.* **2004**, *2*, 3432-3433; c) M. Klokkenburg, M. Lutz, A. L. Spek, J. H. van der Maas, C. A. van Walree, *Chem. Eur. J.* **2003**, *9*, 3544-3554; d) C. A. van Walree, V. E. M. Kaats-Richters, S. J. Veen, B. Wieczorek, J. H. Van der Wiel, B. C. Van der Wiel, B. C. *Eur. J. Org. Chem.* **2004**, 3046-3056.
[33] a) M. Gholami, R. R. Tykwinski, *Chem. Rev.* **2006**, *106*, 4997-5027; b) R. R. Tykwinski, Y. Zhao, *Synlett* **2002**, 1939-1953.
[34] R. Ponce Ortíz, R. Malavé Osuna, V. Hernández, J. T. López Navarrete, B. Vercelli, G. Zotti, V. V. Sumerin, E. S. Balenkova, V. G. Nenajdenko, *J. Phys. Chem. A* **2007**, *111*, 841-851.
[35] C. Lepetit, M. B. Nielsen, F. Diederich, R. Chauvin, *Chem. Eur. J.* **2003**, *9*, 5056-5066.
[36] C. Lambert, *Angew. Chem. Int Ed.* **2005**, *44*, 7337-7339.
[37] Y. Tanaka, T. Koike, M. Akita, *Chem. Commun.* **2010**, *46*, 4529-4531.
[38] a) S. V. Rosokha, I. S. Neretin, D. Sun, J. K. Kochi, *J. Am. Chem. Soc.* **2006**, *128*, 9394-9407; b) D. Sun, S. V. Rosokha, J. K. Kochi, *Angew. Chem. Int. Ed.* **2005**, *44*, 5133-5136.
[39] a) V. J. Chebny, R. Shukla, R. Rathore, *J. Phys. Chem. A* **2006**, *110*, 13003-13006; b) R. Shukla, S. V. Lindeman, R. Rathore, *Org. Lett.* **2007**, *9*, 1291-1294.
[40] A. Wakamiya, T. Ide, S. Yamaguchi, *J. Am. Chem. Soc.* **2005**, *127*, 14859-14866.

stacking).[41,42,43,44,45,46,47,48,49,50,51,52,53,54] Ejemplos representativos de moléculas que presentan estos tipos de deslocalización electrónica no convencional pueden verse en la Figura1. También cabe mencionar, aunque tienen menos

[41] S. P. Jagtap, S. Mukhopadhyay, V. Coropceanu, G. L. Brizius, J.-L. Brédas, D. M. Collard, *J. Am. Chem. Soc.* **2012**, *134*, DOI: 10.1021/ja3019065.
[42] S. T. Schneebeli, M. Kamenetska, Z. Cheng, R. Skouta, R. A. Friesner, L. Venkataraman, R. Breslow, *J. Am. Chem. Soc.* **2011**, *133*, 2136-2139.
[43] G. C. Solomon, C. Herrmann, J. Vura-Weis, M. R. Wasielewski, M. A. Ratner, *J. Am. Chem. Soc.* **2010**, *132*, 7887-7889.
[44] M. Supur, Y. Yamada, M. E. El-Khouly, T. Honda, S. Fukuzumi, *J. Phys. Chem. C* **2011**, *115*, 15040-15047.
[45] Y. Che, A. Datar, X. Yang, T. Naddo, J. Zhao, L. Zang, *J. Am. Chem. Soc.* **2007**, *129***,** 6354-6355.
[46] a) Y. Morisaki, T. Murakami, Y. Chujo, *Macromolecules* **2008**, *41*, 5960-5963; b) Y. Morisaki, T. Murakami, T. Sawamura, Y. Chujo, *Macromolecules* **2009**, *42*, 3656-3660.
[47] a) J. Zyss, I. Ledoux, S. Volkov, V. Chernyak, S. Mukamel, G. P. Bartholomew, G. C. Bazan, *J. Am. Chem. Soc.* **2000**, *122*, 11956-11962; b) G. P. Bartholomew, G. C. Bazan, *Acc. Chem. Res.* **2001**, *34*, 30-39; c) D. S. Seferos, S. A. Trammell, G. C. Bazan, J. G. Kushmerick, *Proc. Natl. Acad. Sci. U.S.A.* **2005**, *102*, 8821-8825; d) J. W. Hong, H. Y. Woo, B. Liu, G. C. Bazan, *J. Am. Chem. Soc.* **2005**, *127*, 7435-7443.
[48] a) W. Wang, J. Xu, Y.-H. Lai, F. Wang, *Macromolecules* **2004**, *37*, 3546-3553; b) W. Wang, J. Xu, Z. Sun, X. Zhang, Y. Lu, Y.-H. Lai, *Macromolecules* **2006**, *39*, 7277-7285.
[49] a) R. Rathore, S. H. Abdelwahed, I. A. Guzei, *J. Am. Chem. Soc.* **2003**, *125*, 8712-8713; b) R. Rathore, S. H. Abdelwahed, M. K. Kiesewetter, R. C. Reiter, C. D. Stevenson, *J. Phys Chem. B* **2006**, *110*, 1536-1540.
[50] a) Y. K. Kang, I. V. Rubtsov, P. M. Iovine, J. Chen, M. J. Therien, *J. Am. Chem. Soc.* **2002**, *124*, 8275-8279; b) J. Zheng, Y. K. Kang, M. J. Therien, D. N. Beratan, *J. Am. Chem. Soc.* **2005**, *127*, 11303-11310.
[51] a) T. Nakano, T. Yade, *J. Am. Chem. Soc.* **2003,** *125*, 15474-15484; b) V. Coropceanu, T. Nakano, N. E. Gruhn, O. Kwon, T. Yade, K. Katsukawa, J.-L. Brédas, *J. Phys. Chem. B* **2006**, *110*, 9482-9487.
[52] a) T. A. Zeidan, Q. Wang, T. Fiebig, F. D. Lewis *J. Am. Chem. Soc.* **2007**, *129*, 9848-9849; b) M. Smeu, R. A. Wolkow, H. Guo *J. Am. Chem. Soc.* **2009**, *131*, 11019-11029; c) S. Mataka, T. Thiemann, M. Taniguchi, T. Sawada, *Synlett* **2000**, 1211-1227; d) M. Shibahara, M. Watanabe, T. Iwanaga, T. Matsumoto, K. Ideta, T. Shinmyozu, *J. Org. Chem.* **2008**, *73*, 4433-4442.
[53] a) *Modern Cyclophane Chemistry* (Eds.: R. Gleiter, H. Hopf), Wiley-VCH, Weinheim, **2004**; b) F. Diederich, *Cyclophanes*, Royal Society of Chemistry, Cambridge, **1991**; c) *Cyclophanes* (Ed.: F. Vögtle), Springer, Heidelberg, **1983**.
[54] a) F. D. Lewis, J. Liu, W. Weigel, W. Rettig, I. V. Kurnikov, D. N. Beratan, *Proc. Natl. Acad. Sci. U.S.A.* **2002**, *99*, 12536-12541; b) C. R. Treadway, M. G. Hill, J. K. Barton, *Chem. Phys.* **2002**, *281*, 409-428 y referencias incluidas en la publicación.

relación con el presente trabajo, la conjugación curva,[55] presente por ejemplo en fullerenos, nanotubos y cintas moleculares, así como también la conjugación meta.[56]

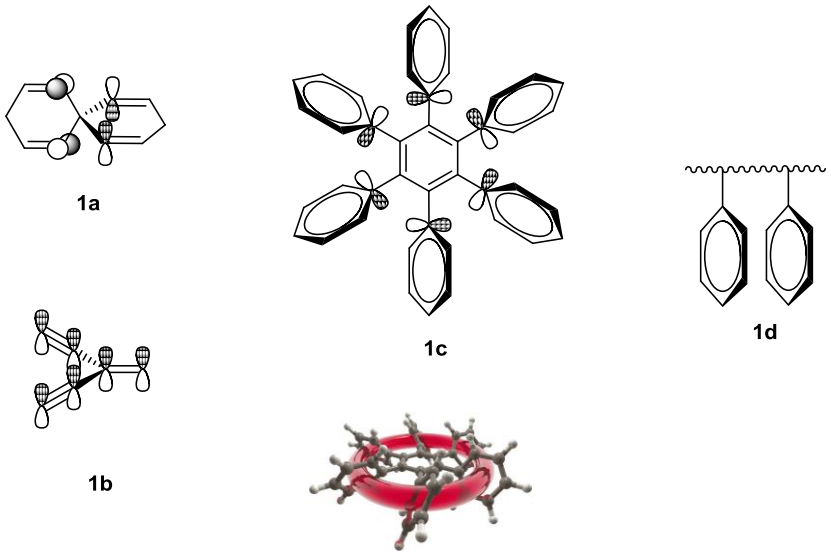

Figura 1. Ejemplos de sistemas con spiro-conjugación (**1a**), conjugación cruzada (**1b**), conjugación toroidal (**1c**) y apilamiento-π (π-stacking) (**1d**).

En los ejemplos expuestos en la Figura 1, la disposición de los orbitales p_z de los dobles enlaces y de los anillos aromáticos, es tal que posibilita su solapamiento y la deslocalización electrónica. Esta comunicación es muy eficaz en el caso de los derivados del hexafenilbenceno (**1c**) y análogos con

[55] a) J. Xia, R. Jasti, *Angew. Chem. Int. Ed.* **2012**, *51*, 2474-2476; b) M. Iyoda, J. Yamakawa, M. J. Rahman, *Angew. Chem. Int. Ed.* **2011**, *50*, 10522-10553; c) H. Omachi, S. Matsuura, Y. Segawa, K. Itami, *Angew. Chem. Int. Ed.* **2010**, *49*, 10202-10205; d) D. Eisenberg, R. Shenhar, M. Rabinovitz, *Chem. Soc. Rev.* **2010**, *39*, 2879-2890; X. Lu, Z. Chen, *Chem. Rev.* **2005**, *105*, 3643-3696; e) K. Tahara, Y. Tobe, *Chem. Rev.* **2006**, *106*, 5274-5290; f) Z. Chen, R. B. King, *Chem. Rev.* **2005**, *105*, 3613-3642; g) S. Taubert, D. Sundholm, F. Pichierri, *J. Org. Chem.* **2010**, *75*, 5867-5874; h) P. W. Fowler, A. Soncini, *Phys. Chem. Chem. Phys.* **2011**, *13*, 20637-20643.

[56] a) A. L. Thompson, T.-S. Ahn, K. R. J. Thomas, S. Thayumanaban, T. J. Martinez, C. J. Bardeen, *J. Am. Chem. Soc.* **2005,** *127*, 16348-16349; b) Y.-S. Yang, K.-L- Liau, C.-Y. Li, M.-Y. Chen, *J. Am. Chem. Soc.* **2007,** *129*, 13183-13192; c) C. Song, T. M. Swager, *Macromolecules* **2005**, *38*, 4569-4576; d) M. Moreno Oliva, J. Casado, G. Hennrich, J. T. López Navarrete, *J. Phys. Chem. B* **2006**, *110*, 19198-19206.

anillos heterocíclicos,[37] en los que solapan los orbitales de los anillos situados en conformación perpendicular respecto al fenilo central, dando lugar a sistemas con una deslocalización en forma de toroide. En el caso de los spirocompuestos del tipo **1a**, es posible la comunicación entre los dos fragmentos unidos mediante el carbono sp^3 central, por el solapamiento de los orbitales π que, aunque están situados ortogonalmente uno del otro, se sitúan suficientemente próximos en el espacio. Este tipo de deslocalización es muy importante en el caso de los spirofluorenos, de los que se han descrito en los últimos años un gran número de ejemplos con aplicaciones en diferentes dispositivos orgánicos.[27,28]

En los compuestos con conjugación cruzada también es posible el solapamiento entre todos los orbitales π (**1b**). Aunque el grado de deslocalización electrónica parece ser menor que en derivados con spiroconjugación y conjugación toroidal, muy recientemente se ha demostrado que este tipo de moléculas pueden emplearse como materiales orgánicos.[30,31]

Por lo que respecta a derivados que presentan deslocalización por apilamiento de sistemas aromáticos (π-stacking) (**1d**), la comunicación entre los anillos aromáticos es similar a la descrita para la deslocalización toroidal (**1c**). El número de ejemplos de este tipo de sistemas es muy elevado, sobre todo teniendo en cuenta el caso de los ciclofanos.[53]

En publicaciones recientes se ha demostrado que en los sistemas con apilamiento-π pueden darse tanto la transferencia electrónica fotoinducida como la conductividad eléctrica a través de los anillos aromáticos cofaciales.[41-45] Este fenómeno tiene especial relevancia en los procesos de transferencia electrónica en las moléculas de DNA.[50,54]

I.2.1 Homoconjugación

Además de la spiroconjugación, la conjugación cruzada, la conjugación toroidal y la deslocalización en sistemas con apilamiento-π, existe otro posible mecanismo no convencional por el cual los electrones pueden deslocalizarse a lo largo de la estructura de una molécula: la homoconjugación. De acuerdo con la IUPAC, se entiende por homoconjugación el solapamiento de orbitales π

separados por un grupo no conjugativo, como un CH_2.[57,58,59,60,61,62,63] En la Figura 2 se muestran algunos ejemplos de moléculas con dobles y triples enlaces homoconjugados. Hasta ahora la deslocalización por homoconjugación se ha estudiado sobre todo en sistemas cíclicos con dobles y triples enlaces. La deslocalización en estos compuestos ha sido objeto de controversia, ya que el grado de deslocalización en estos sistemas depende en gran medida de las características estructurales de cada molécula. Así, por ejemplo, se ha podido comprobar que la deslocalización electrónica por homoconjugación es muy eficaz en sistemas homoaromáticos cíclicos cargados positivamente, como el catión homotropilio (**2a**).[57] En estos derivados la carga positiva hace posible una fuerte deslocalización.

[57] Una revisión sobre homoaromaticidad puede verse en: R. V. Williams, *Chem. Rev.* **2001**, *101*, 1185-1204.

[58] Estudios recientes sobre el homobenceno: a) Z. Chen, H. Jiao, J. I. Wu, R. Herges, S. B. Zhang, P. von R. Schleyer, *J. Phys. Chem. A* **2008**, *112*, 10586-10594; b) F. Stahl, P. von R. Schleyer, H. Jiao, H. F. Schaefer III, K.-H. Chen, N. Allinger, *J. Org. Chem.* **2002**, *67*, 6599-6611.

[59] a) P. W. Fowler, M. Lillington, L. P. Olson, *Pure Appl. Chem.* **2007**, *79*, 969-979. Ver también, b) P. K. Freeman, *J. Org. Chem.* **2005**, *70*, 1998-2001; c) T. Bajorek, N. H. Werstiuk, *Can. J. Chem.* **2005**, *83*, 1352-1359.

[60] Moléculas inorgánicas con homoconjugación/homoaromaticidad se describen en: Q. Zhang, S. Yue, X. Lu, Z. Chen, R. Huang, L. Zheng, P. von R. Schleyer, *J. Am. Chem. Soc.* **2009**, *131*, 9789-9799.

[61] a) V. Maraval, R. Chauvin, *Chem. Rev.* **2006**, *106*, 5317-5343; b) C. Lepetit, B. Silvi, R. Chauvin, *J. Phys. Chem. A* **2003**, *107*, 464-473; c) A. de Meijere, S. I. Kozhushkov, R. Boese, T. Haumann, D. S. Yufit, J. A. K. Howard, L. S. Khaikin, M. Trætteberg, *Eur. J. Org. Chem.* **2002**, 485-492; d) A. de Meijere, S. I. Kozhushkov, *Top. Curr. Chem.* **1999**, *201*, 1-42; e) B. Leibrock, O. Vostrowsky, A. Hirsch, *Eur. J. Org. Chem.* **2001**, 4401-4409; f) H. Jiao, N. J. R. van Eikema Hommes, P. v. R. Schleyer, A. de Meijere, *J. Org. Chem.* **1996**, *61*, 2826-2828.

[62] Estudios recientes sobre homoconjugación en metano[10]anulenos se describen en: a) G. F. Caramori, K. T. De Oliveira, S. E. Galembeck, P. Bultinck, M. G. Constantino, *J. Org. Chem.* **2007**, *72*, 76-85; b) Y. Zhang, E. Hisano, R. Ohta, R. Miyatake, Y. Horino, M. Oda, S. Kuroda, *Tetrahedron Lett.* **2008**, *49*, 888-892. Un estudio teórico sobre moléculas deslocalizadas con interacciones homoconjugativas se describe en: c) D. J. Tantillo, R. Hoffmann, K. N. Houk, P. M. Warner, E. C. Brown, D. K. Henze, *J. Am. Chem. Soc.* **2004**, *126*, 4256-4263.

[63] Interacciones homoconjugativas estabilizantes entre dobles y triples enlaces se describen en: R. Gleiter, R. Merger, H. Irngartinger, *J. Am. Chem. Soc.* **1992**, *114*, 8927-8932.

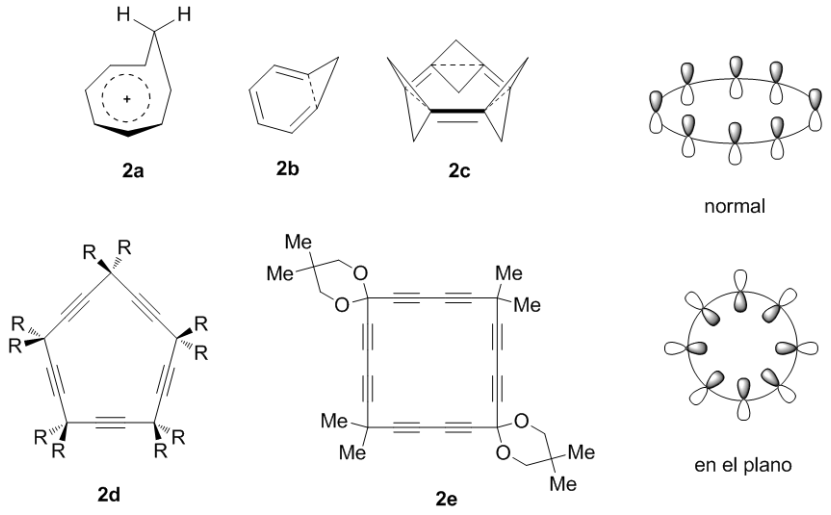

Figura 2. Ejemplos de moléculas homoconjugadas.

Sin embargo, la situación descrita para sistemas cíclicos neutros, y más aún en sus análogos de cadena abierta, es más compleja y continúa siendo objeto de debate. Así, se ha descrito la existencia de interacciones homoconjugativas, aunque débiles, en los casos del cicloheptatrieno (**2b**) y de varios sistemas trishomoaromáticos, como el trishomobenceno (**2c**).[58-60] Sin embargo, en el caso de sistemas cíclicos con triples enlaces como los periciclenos **2d** y **2e**, en los que tiene lugar un solapamiento "en el plano", no se detecta deslocalización electrónica por interacciones homoconjugativas entre los orbitales π de los alquinos.[61-63] Tan sólo en el caso de alquinos cíclicos muy tensos parece haber deslocalización por homoconjugación.[61b,64]

I.2.2 Homoconjugación aromática

Si bien los sistemas homoconjugados formados por dobles y triples enlaces se han estudiado en profundidad durante los últimos años, no ha ocurrido lo

[64] I. Fernández, G. Frenking, *Faraday Discuss*. **2007**, *135*, 403-422.

mismo con la deslocalización electrónica debida a homoconjugación aromática, de la que apenas hay precedentes en la bibliografía.[65,66,67] El caso más investigado es el del tripticeno y compuestos análogos (ipticenos) (Figura 3).

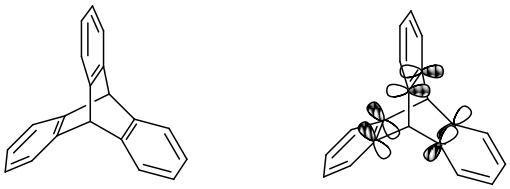

Figura 3. Estructura del tripticeno.

La molécula de tripticeno es un ejemplo de homoconjugación aromática lateral, ya que los anillos aromáticos se encuentran separados por carbonos con hibridación sp^3 y la deslocalización electrónica en este caso tendría lugar a través del solapamiento de los orbitales de un lado de cada uno de los anillos aromáticos. Hasta la fecha, se han llevado a cabo numerosos estudios basados en este tipo de derivados y de sus aplicaciones.[65-66] Sin embargo, mientras que

[65] Revisiones recientes sobre el tripticeno y derivados análogos se describen en: a) L. Zhao, Z. Li, T. Wirth, *Chem. Lett.* **2010**, *39*, 658-667; b) J. H. Chong, M. J. MacLachlan, *Chem. Soc. Rev.* **2009**, *38*, 3301-3315; c) T. M. Swager, *Acc. Chem. Res.* **2008**, *41*, 1181-1189; d) J.-S. Yang, J.-L. Yan, *Chem. Commun.* **2008**, 1501-1512. Ver también: e) V. R. Skvarchenko, V. K. Shalaev, E. I. Klabunovskii, *Russ. Chem. Rev.* **1974**, *43*, 951-966.

[66] a) G. Jansen, B. Kahlert, F.-G. Klämer, R. Boese, D. Bläser, *J. Am. Chem. Soc.* **2010**, *132*, 8581-8592; b) T. Kobayashi, S. Kobayashi, *Eur. J. Org. Chem.* **2002**, 2066-2073; c) M. Kamieth, F.-G. Klärner, F. Diederich, *Angew. Chem. Int. Ed.* **1998**, *37*, 3303-3306; d) T. Doerner, R. Gleiter, F. A. Neugebauer, *Eur. J. Org. Chem.* **1998**, 1615-1623; e) T. Nakazawa, I. Murata, *J. Am. Chem. Soc.* **1977**, *99*, 1996-1997; f) K. Yamamura, T. Nakazawa, I. Murata, *Angew. Chem. Int. Ed.* **1980**, *19*, 543-546; g) K. Yamamura, K. Nakasuji, H. Yamochi, *Chem. Let.* **1983**, 627-630.

[67] Las interacciones homoconjugativas laterales en ipticenos no están establecidas de manera concluyente y son objeto de controversia: a) X. Gu, Y.-H. Lai, *Org. Lett.* **2010**, *12*, 5200-5203. b) V. J. Chebny, T. S. Navale, R. Shukla, S. V. Lindeman, R. Rathore, *Org. Lett.* **2009**, *11*, 2253-2256; c) L. Zhao, Z. Li, T. Wirth, *Chem. Lett.* **2010,** 658-667; d) H.-D. Martin, B. Mayer, *Angew. Chem. Int. Ed.* **1983**, *22*, 283-314. e) V. R. Skvarchenko, V. K. Shalaev, E. I. Klabunovskii, *Russian Chem. Rev.* **1974**, *43*, 951-966; f) W. Theilacker, K. Albrecht, H. Uffmann, *Chem. Ber.* **1965**, *98*, 428-432. La estructura cristalina del tripticeno se describe en: g) R. G. Hazell, G. S. Pawley, C. E. Lund Petersen, *J. Cryst. Mol. Struct.* **1971**, *1*, 319-324.

algunas investigaciones consideran que existe deslocalización electrónica por interacción entre los orbitales de los anillos aromáticos, trabajos más recientes ponen en duda que tal deslocalización se produzca, al menos de forma importante, por lo que este aspecto es actualmente objeto de controversia.[67] La razón puede ser la geometría del sistema biciclo[2.2.2]octano, que obliga a que el ángulo entre los planos de dos anillos aromáticos sea bastante elevado (120^{o}), y como consecuencia, la orientación de los orbitales de los mismos no sea la más adecuada para que tenga lugar un solapamiento efectivo entre dichos orbitales, a pesar de que la distancia mínima entre dos fenilos (2.41 Å) es bastante corta.[67g] Esto podría explicar que en el tripticeno se diera una homoconjugación muy limitada, variando el grado de deslocalización electrónica de unos derivados a otros.

En principio, el candidato más sencillo para estudiar la deslocalización electrónica en sistemas con homoconjugación aromática, es el difenilmetano (Figura 4). Sin embargo, esta molécula presenta algunas características que hacen que no sea un buen modelo para el estudio de la deslocalización mediante homoconjugación. Aunque de acuerdo con la estructura de rayos-x, tanto el ángulo C_{ipso}-CH_2-$C_{ipso'}$ (112.4^{o}) como la distancia C_{ipso}-$C_{ipso'}$ (2.52 Å, algo mayor que en el tripticeno)[68] son adecuados para que exista homoconjugación entre los fenilos, hay otra razón, más importante, que impide el solapamiento de los orbitales aromáticos y la deslocalización electrónica entre los anillos aromáticos del difenilmetano: su libertad conformacional (Figura 4).

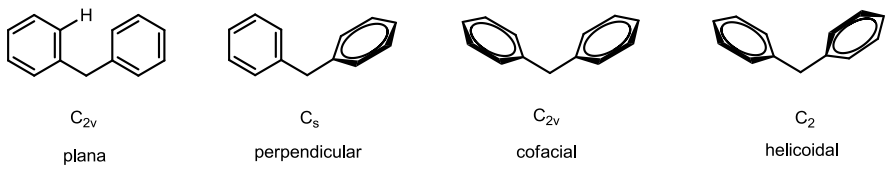

Figura 4. Conformaciones más representativas del difenilmetano.

En la Figura 4 se representan las conformaciones más representativas del difenilmetano. La menos estable, debido al impedimento estérico de los átomos

[68] J. C. Barnes, J. D. Paton, J. R. Damewood, K. Mislow, *J. Org. Chem.* **1981**, *46*, 4975-4979.

de hidrógeno en posición orto, es la conformación plana, y la más estable la disposición helicoidal. Sin embargo, la diferencia de energías entre las tres conformaciones más estables es pequeña, lo que hace que el difenilmetano se comporte como un rotor, en el que la conformación en la cual la homoconjugación estaría favorecida (la cofacial), no es la más estable.[69] De hecho, en estado sólido el difenilmetano cristaliza en la conformación helicoidal, con valores de los ángulos torsionales C_{orto}-C_{ipso}-CH_2-$C_{ipso'}$ y C_{ipso}-CH_2-$C_{ipso'}$-$C_{orto'}$ de 71.8º y 63.5º, respectivamente.[68]

Un factor muy importante que influye en la estabilidad de la conformación cofacial, son las interacciones aromáticas entre los fenilos. En el difenilmetano y derivados pueden darse, en principio, tres tipos de interacciones importantes diferentes: a) las interacciones homoconjugativas, que serían estabilizantes debido al aumento de deslocalización electrónica; b) la transferencia de carga entre los anillos cuando en ellos haya sustituyentes dadores y aceptores, también estabilizante; y c) repulsión electrostática entre las nubes electrónicas de los anillos aromáticos, interacción esta desestabilizante. En trabajos anteriores hemos estudiado la importancia relativa de estas interacciones, concluyendo que la predominante es la repulsión electrostática entre los anillos aromáticos, lo cual explicaría la menor estabilidad de la conformación cofacial frente a la helicoidal en el difenilmetano y, por tanto, la dificultad para que se produzcan interacciones hommoconjugativas.[69,70,71] De hecho, en compuestos en los que se encuentra el difenilmetano como subunidad estructural, éste se comporta como un interruptor, impidiendo la deslocalización electrónica entre las dos regiones unidas a los anillos aromáticos.[72]

---

[69] A. García Martínez, J. Osío Barcina, *The Diphenylmethane Moiety* in *Encyclopedia of Supramolecular Chemistry*, (Eds.: J. L. Atwood, J. W. Steed), Marcel Dekker, New York, **2004**, 452-456.

[70] A. García Martínez, J. Osío Barcina, A. de Fresno Cerezo, R. Gutiérrez Rivas, *J. Am. Chem. Soc.* **1998**, *120*, 673-679.

[71] Para estudios relacionados, ver: a) F. Cozzi, F. Ponzini, R. Annunziata, M. Cinquini, J. S. Siegel, *Angew. Chem., Int. Ed. Engl.* **1995**, *34*, 1019-1020; b) C. A. Hunter, K. Lawson, J. Perkins and C. Urch, *J. Chem. Soc. Perkin Trans. 2* **2001**, 651-669.

[72] a) D. K. James, J. M. Tour, *Top. Curr. Chem.* **2005**, *257*, 33-62. Ejemplos de copolímeros en los que el difenilmetano actúa como interruptor de la conjugación se describen en: b) K.-Y. Peng, S.-A. Chen, W.-S. Fann, *J. Am. Chem. Soc.* **2001**, *123*, 11388-11397; c) P. G. Del Rosso, M. F. Almassio, S. S. Antollini, R. O. Garay, *Opt. Mater.* **2007**, *30*, 478-485; d) M. Beinhoff, L. D. Bozano, J. C. Scott, K. R. Carter,

La situación descrita anteriormente para el difenilmetano, según la cual no existen interacciones homoconjugativas ni por tanto deslocalización electrónica entre los anillos aromáticos, puede alterarse si se obliga de alguna manera a que los fenilos se dispongan cofacialmente, lo que favorecería el solapamiento entre los orbitales π . Para ello es necesario idear un sistema que compense la repulsión electrostática haciendo posible la deslocalización electrónica mediante homoconjugación aromática. Nosotros hemos comprobado que estas condiciones se dan en el 7,7-difenilnorbornano (DPN) (**3**) y sus derivados (Figura 5).

3

Figura 5. Estructura del 7,7-difenilnorbornano.

En el DPN el giro de los anillos aromáticos se encuentra dificultado por el impedimento estérico entre los átomos de hidrógeno situados en posición *exo* del norbornano, y los situados en posición *orto* en los fenilos. La barrera de giro de los anillos es de 12.5 kcal.mol^{-1}, muy superior a la descrita para el difenilmetano.[69,73] Este hecho, junto con la simetría que presenta el sistema bicíclico del norbornano, hacen que en el DPN los fenilos se dispongan en conformación cofacial, con lo que la interacción homoconjugativa de los orbitales π es máxima en este hidrocarburo y en sus derivados, constituyendo ejemplos de homoconjugación aromática apical.

La estructura de rayos-X del DPN confirma esta situación, siendo el ángulo C_{ipso}-C_7-$C_{ipso'}$ 107.0^o y la distancia C_{ipso}-$C_{ipso'}$ 2.46 Å,[73] muy por debajo de la suma de los radios de van der Waals de dos fenilos (3.4 Å).[74] Por otra parte, estos valores son inferiores a los descritos para el difenilmetano (112.4^o y 2.52 Å, respectivamente). Estas características estructurales, hacen que el DPN

Macromolecules **2005**, *38*, 4147-4156; e) P. G. Del Rosso, M. F. Almassio, P. Aramendia, S. S. Antollini, R. O. Garay, *Eur. Polym. J.* **2007**, *43*, 2584-2593.

[73] A. García Martínez, J. Osío Barcina, A. Albert, F. H. Cano, *Tetrahedron Lett.* **1993**, *34*, 6736–6753.

[74] L. Yu, H.-J. Schneider, *Eur. J. Org. Chem.* **1999**, 1619–1625.

presente analogías importantes, y también diferencias, con los compuestos conjugados y los sistemas con apilamiento π. De hecho, puede considerarse que esta molécula, por su topología, se encuentra en una posición intermedia entre los sistemas conjugados (como el bifenilo) y los compuestos con "π-stacking" (como el [2,2]paraciclofano) (Figura 6).

Figura 6. Estructuras del bifenilo (**4**), DPN (**3**) y [2,2]paraciclofano (**5**).

En el bifenilo (**4**), los dos anillos aromáticos se encuentran alineados y, aunque no son coplanares debido al impedimento estérico de los átomos de hidrógenos en posición *orto*, la deslocalización electrónica (conjugación) se produce por el solapamiento de los orbitales π a ambos lados del plano medio horizontal de la molécula. En cambio, en el DPN la disposición relativa en ángulo de los orbitales π aromáticos hace que estos se aproximen por la parte superior cóncava de la molécula, mientras que se separan por la parte inferior. Esto se traduce en una fuerte interacción entre los orbitales, pero a diferencia de lo que ocurre en los compuestos conjugados, solamente por un lado de los anillos aromáticos.

Por lo que respecta a las similitudes y diferencias entre el DPN y el [2,2]paraciclofano (**5**), en ambos casos se trata de moléculas con anillos aromáticos cofaciales, pero mientras que en **5** los fenilos se disponen paralelamente, con lo que el área de contacto y la interacción entre los orbitales π es máxima, en el DPN los anillos forman un ángulo de 107^{o}. Esto se traduce en que en el DPN los fenilos están mucho más próximos (2.43 Å) que en **5** (2.99 Å) en la región cercana al norbornano, mientras que se alejan considerablemente hacia el exterior de la molécula.

Teniendo en cuenta todos estos factores, el DPN es un modelo idóneo para el estudio de las interacciones homoconjugativas en sistemas aromáticos, y para evaluar si en este tipo de derivados la deslocalización electrónica es importante o si, como ocurre con los dobles y triples enlaces homoconjugados

en moléculas neutras, e incluso en los ipticenos, esta deslocalización es pequeña o incluso inapreciable.

En nuestro grupo de investigación se han llevado a cabo estudios previos sobre la homoconjugación aromática en DPN's. Estos estudios muestran que existe una fuerte interacción entre los orbitales de los anillos aromáticos cofaciales, lo que se traduce en la aparición de una banda nueva en el espectro UV-vis del DPN a 228 nm (banda de homoconjugación), que no se observa en el difenilmetano.[69,70,75] Esta banda es consecuencia de la deslocalización electrónica homoconjugativa, como prueba el hecho de que experimente un desplazamiento batocrómico en oligómeros del DPN (Figura 7), de manera análoga a lo observado en sistemas conjugados.[75]

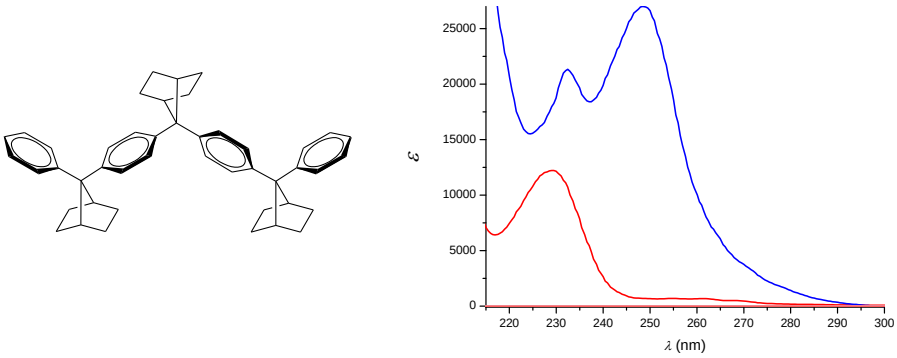

Figura 7. Estructura del trímero del DPN y espectros UV-vis del DPN (rojo, λ_{max} = 228 nm) y del trímero (azul, λ_{max} = 248 nm).

La deslocalización electrónica en DPN's también se ha puesto de manifiesto en estudios de polímeros deslocalizados que alternan homoconjugación y conjugación[76] y de las propiedades ópticas no lineales en derivados del DPN[77] llevadas a cabo en nuestro laboratorio.

El principal objetivo del presente trabajo, es profundizar en el estudio de la deslocalización electrónica debida a homoconjugación aromática. Para ello, se

[75]N. Caraballo-Martínez, M. R. Colorado Heras, M. M. Blázquez, J. Osío Barcina, A. García Martínez, M. R. Torres Salvador, *Org. Lett.* **2007**, *9*, 2943-2946.
[76] A. García Martínez, J. Osío Barcina, A. de Fresno Cerezo, A.-D. Schlüter, J. Frahn, *Adv. Mater.* **1999**, *11*, 27-31.
[77] A. García Martínez, J. Osío Barcina, A. de Fresno Cerezo, G. Rojo, F. Agulló-López, *J. Phys Chem. B* **2000**, *104*, 43-47.

sintetizarán una serie de derivados del DPN así como de sistemas análogos no homoconjugados que servirán como referencias. El estudio de las propiedades químicas y espectroscópicas de estos compuestos, se completará con información obtenida mediante cálculos computacionales DFT. El conjunto de estas investigaciones aportará datos acerca del grado de deslocalización electrónica en estos sistemas y sobre las características de este fenómeno. También se estudia la aplicación de derivados homoconjugados en la construcción de materiales orgánicos. En concreto, los objetivos de esta parte de la Tesis Doctoral pueden resumirse en los siguientes puntos:

- Estudio teórico-experimental de la homoconjugación aromática en hidrocarburos derivados del DPN.
- Estudio teórico-experimental de la homoconjugación aromática en derivados sustituidos del DPN, con especial énfasis en sistemas push-pull.
- Síntesis y propiedades de polímeros homoconjugados.
- Diseño y propiedades de cables moleculares homoconjugados.
- Aplicaciones de sistemas homoconjugados en la preparación de OLED's.

I.3 El 7,7-difenilnorbornano como subunidad estructural en Química Supramolecular

Una de las subunidades más utilizadas en el diseño de estructuras supramoleculares es el difenilmetano.[69,78,79,80,81] La principal razón por la que

[78] *Comprehensive Supramolecular Chemistry*, (Eds.: J. L. Atwood, J. E. D. Davies, D. D. MacNicol, F. Vögtle), Vol. 1, *Molecular Recognition: Receptors for Cationic Guests*, Pergamon, **1996**.
[79] *Encyclopedia of Supramolecular Chemistry* (Eds.: J. L. Atwood, J. W. Steed), Marcel Dekker, New York, **2004**.
[80] J. W. Steed, J. L. Atwood, *Supramolecular Chemistry*, John Wiley & Sons, Chichester, **2009**.

aparece con gran frecuencia como parte de la estructura de receptores moleculares de muy diversa índole, es que el difenilmetano proporciona una región de geometría cóncava y rica en electrones que favorece la formación de complejos con huéspedes catiónicos o neutros mediante interacciones no-covalentes de tipo catión···π, π···π, X-H···π, etc. Sin embargo, esta subunidad presenta una limitación importante a la hora de formar complejos estables receptor-huésped: su falta de preorganización. Tal y como se comentó anteriormente, el difenilmetano no presenta una conformación preferente, comportándose como un rotor. Es más, la conformación cofacial, que es la que presenta una geometría más adecuada para el establecimiento de interacciones complementarias con diferentes huéspedes, no es la más estable, por lo que el receptor debe experimentar una modificación estructural adoptando una conformación que, aunque no sea la más estable, favorece la complejación receptor-huésped. Esto supone un gasto energético considerable, que se ve reflejado en la estabilidad del correspondiente complejo, de acuerdo con el principio de que cuanto más preorganizado sea el receptor y mayor grado de complemetaridad presenten el receptor y el huésped, mayor es la estabilidad del complejo supramolecular. En sistemas supramoleculares en los que están involucradas interacciones no covalentes débiles, los factores entrópicos pueden resultar determinantes en la formación y estabilidad de los correspondientes complejos, por lo que el grado de preorganización del receptor resulta ser fundamental.[69,82]

Aunque en principio este factor puede parecer de poca importancia, no resulta ser así en absoluto. En efecto, en nuestro grupo de investigación hemos demostrado que la utilización de subunidades más preorganizadas que el difenilmetano, como el 7,7-difenilnorbornano, presenta ventajas muy importantes a la hora de diseñar sistemas que permitan estudiar interacciones supramoleculares y formar complejos estables receptor-huésped. La elevada estabilidad de la conformación cofacial del DPN ha permitido emplear esta

[81] T. Schrader, M. Maue, in *Functional Synthetic Receptors*, (Eds.: T. Schrader, A. D. Hamilton), WILEY-VCH, Weinheim, **2005**.
[82] a) M. S. Searle, D. H. Williams, *J. Am. Chem. Soc.* **1992**, *114*, 10690-10697; b) C. T. Calderone, D. H. Williams, *J. Am. Chem. Soc.* **2001**, *123*, 6262-6267; c) H.-J. Scheneider, *Angew. Chem. Int Ed.* **2009**, *48*, 3924-3977.

subunidad en el estudio de interacciones aromáticas cara-cara[70] y lado-cara (Figura 8a),[83] así como también interacciones C-H···π y O-H···π.[84]

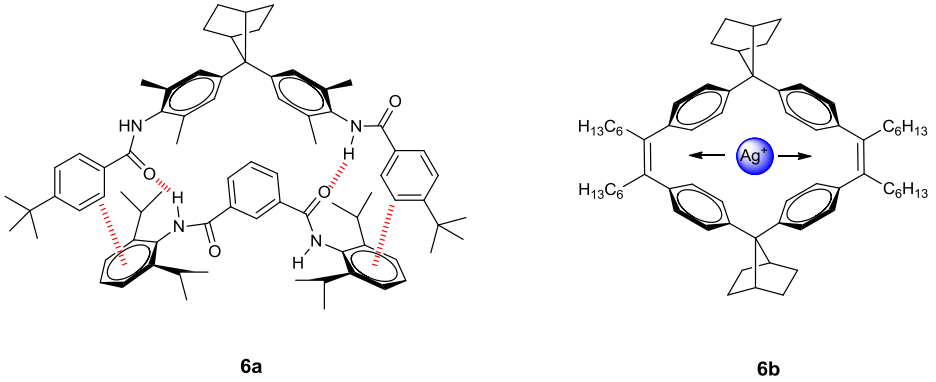

6a **6b**

Figura 8. Estructuras de complejos supramoleculares formados por subunidades de DPN.

El ejemplo más significativo de la importancia de la utilización del DPN en complejos supramoleculares lo constituye el sistema ciclofano·Ag^+ representado en la Figura 8. Este complejo entre el catión Ag^+ y un receptor aromático es el más estable descrito hasta la fecha. Su estabilidad es muy superior a la del sistema análogo con un receptor con subunidades de difenilmetano.[85]

Otro de los objetivos de la presente Tesis Doctoral es la utilización del DPN como subunidad estructural en el diseño de estructuras supramoleculares que formen complejos estables con huéspedes catiónicos, en concreto con el ión amonio.

[83] A. García Martínez, J. Osío Barcina, A. de Fresno Cerezo, *Chem. Eur. J.* **2001**, *7*, 1171-1175.
[84] J. Osío Barcina, I. Fernández, M. R. Colorado Heras, *Eur. J. Org. Chem.* **2012**, 940-947.
[85] A. García Martínez, J. Osío Barcina, M. R. Colorado Heras, A. de Fresno Cerezo, M. R. Torres Salvador, *Chem. Eur. J.* **2003**, *9*, 1157-1165.*7*

II. CAPÍTULO 1

1.1 Electron Delocalization in Homoconjugated 7,7-Diarylnorbornane Systems: A Computational and Experimental Study

A joint computational-experimental study has been carried out to analyze the homoconjugative interactions in 7,7-diarylnorbornane (DPN) derivatives. The experimentally observed new bands in their UV/Vis have been accurately assigned by means of TD-DFT calculations. Both experimental data and computations show that aromatic homoconjugation in acyclic systems is an effective mechanism for electron delocalization that resembles the situation described for polyphenylenes and polyenes. The effective homoconjugation length in homoconjugated oligomers is in the range of 6-7 aryl rings. The effect of substituents directly attached to the para carbon atom of the DPN moiety have been also studied. We found that HOMO-LUMO can indeed be modified by the nature of the aromatic substituents in order to provoke dramatic changes in the electronic properties (i.e. in the absorption spectra) of the studied species.

(*Chem. Eur. J.* **2011,** *17*, 7327 – 7335)

1.1.1 Introduction

Electron delocalization in molecules is one of the most important phenomena in chemistry.[1] Many properties and applications of conjugated compounds are controlled by the way that electrons delocalize between the atoms along the structure of the molecules.[2] Besides classical π- and σ-delocalization,[3] in recent years alternative modes of electronic interaction have led to a large variety of systems with interesting electronic properties: cross-conjugation,[4] spiro-conjugation,[5] toroidal conjugation,[6] and π-stacking.[7] A different alternative for electron delocalization is found in homoconjugated systems.

---

[1] a) M. J. S. Dewar, in *Modern Models of Bonding and Delocalization*, (Eds.: J. F. Liebman, A. Greenberg), Verlag Chemie, Weinheim, **1988**; b) D. Geuenich, K. Hess, F. Köhler, R. Herges, *Chem. Rev*. **2005**, *105*, 3758-3772.

[2] a) *Handbook of Conducting Polymers*, (Eds: T. A. Skotheim, J. R. Reynolds), CRC Press, Taylor & Francis Group, London, **2007**; b) *Organic Light-Emitting Devices. Synthesis, Properties and Applications*, (Eds: K. Müllen, U. Scherf), Wiley-VCH, Weinheim, **2006**; c) *Electronic Materials: The Oligomer Approach*, (Eds: K. Müllen, G. Wegner), Wiley-VCH, New York, **1998**; d) *Introduction to Molecular Electronics*, (Eds: M. C. Petty, M. R. Bryce, D. Bloor), Oxford University Press, New York, **1995**.

[3] *Chem. Rev.* **2005**, *105*, number 10: special issue on delocalization-pi and sigma.

[4] a) M. Gholami, R. R. Tykwinski, *Chem. Rev.* **2006**, *106*, 4997-5027; b) R. R. Tykwinski, Y. Zhao, *Synlett* **2002**, 1939-1953; c) M. Klokkenburg, M. Lutz, A. L. Spek, J. H. van der Maas, C. A. van Walree, *Chem. Eur. J.* **2003**, *9*, 3544-3554; d) C. A. van Walree, V. E. M. Kaats-Richters, S. J. Veen, B. Wieczorek, J. H. Van der Wiel, B. C. Van der Wiel, B. C. *Eur. J. Org. Chem.* **2004**, 3046-3056; e) R. Ponce Ortíz, R. Malavé Osuna, V. Hernández, J. T. López Navarrete, B. Vercelli, G. Zotti, V. V. Sumerin, E. S. Balenkova, V. G. Nenajdenko, *J. Phys. Chem. A* **2007**, *111*, 841-851.

[5] a) T. P. I. Saragi, T. Spehr, A. Siebert, T. Fuhrmann-Lieker, J. Salbeck, *Chem. Rev.* **2007**, *107*, 1011-1065; b) J. Abe, Y. Shirai, N. Nemoto, Y. Nagase, *J. Phys. Chem. A* **1997**, *101*, 1-4; c) Y. Luo, P. Norman, H. Agren, *Chem. Phys. Lett.* **1999**, *303*, 616-620.

[6] a) C. Lambert, *Angew. Chem. Int. Ed.* **2005**, *44*, 7337-7339; b) V. J. Chebny, R. Shukla, R. Rathore, *J. Phys. Chem. A* **2006**, *110*, 13003-13006; c) R. Shukla, S. V. Lindeman, R. Rathore, *Org. Lett.* **2007**, *9*, 1291-1294; d) D. Sun, S. V. Rosokha, J. K. Kochi, *Angew. Chem. Int. Ed.* **2005**, *44*, 5133-5136; e) S. V. Rosokha, I. S. Neretin, D. Sun, J. K. Kochi, *J. Am. Chem. Soc.* **2006**, *128*, 9394-9407; f) A. Wakamiya, T. Ide, S. Yamaguchi, *J. Am. Chem. Soc.* **2005**, *127*, 14859-14866.

[7] a) T. A. Zeidan, Q. Wang, T. Fiebig, F. D. Lewis *J. Am. Chem. Soc.* **2007**, *129*, 9848-9849; b) M. Smeu, R. A. Wolkow, H. Guo *J. Am. Chem. Soc.* **2009**, *131*, 11019-11029; c) Y. Morisaki, Y. Chujo, *Angew. Chem. Int. Ed.* **2006**, *45*, 6430-6437; d) S. Mataka, T. Thiemann, M. Taniguchi, T. Sawada, *Synlett* **2000**, 1211-1227; e) J. W. Hong, H. Y. Woo, B. Liu, G. C. Bazan, *J. Am. Chem. Soc.* **2005**, *127*, 7435-7443.

Homoconjugation can be defined as the orbital overlap of two π-systems separated by a non-conjugated group, such as CH_2 (IUPAC). However, the degree of electron delocalization in homoconjugated systems strongly depends on the structure of the corresponding compounds. Thus, in cyclic charged homoaromatic[8] compounds (e.g. homotropylium cation **1**, Figure 1) in which the positive charge is the driving force, electron delocalization is well established.

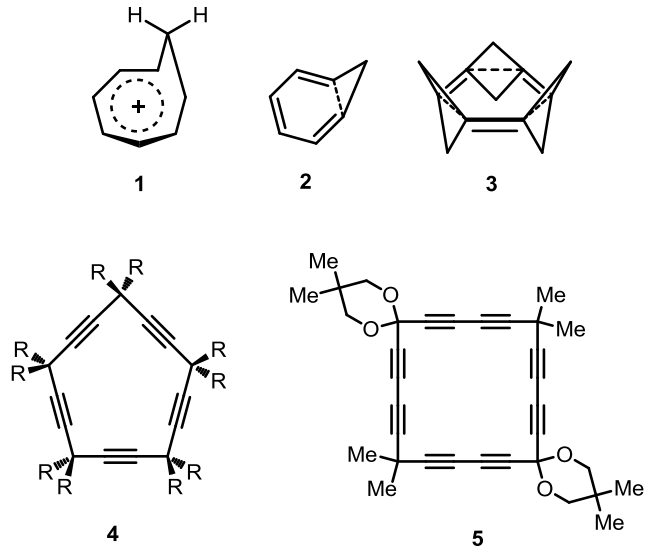

Figure 1. Examples of homoconjugated alkenes and alkynes.

However, the situation in neutral analogous is still controversial and remains the subject of an interesting debate. In the case of cycloheptatriene (**2**, Figure 1) and several model tris-homoaromatics such as "in plane" trishomobenzene **3** (Figure 1), weak stabilization by through-space homoconjugative interactions has been described.[9]

[8] R. V. Williams, *Chem. Rev.* **2001**, *101*, 1185-1204.

[9] a) Z. Chen, H. Jiao, J. I. Wu, R. Herges, S. B. Zhang, P. v. R. Schleyer, *J. Phys. Chem. A* **2008**, *112*, 10586-10594; b) F. Stahl, P. v. R. Schleyer, H. Jiao, H. F. Schaefrer III, K.-H. Chen, N. L. Allinger, *J. Org. Chem.* **2002**, *67*, 6599-6611; c) P. W. Fowler, M. Lillington, L. P. Olson, *Pure Appl. Chem.* **2007**, *79*, 969-979. See also, d) Q. Zhang, S. Yue, X. Lu, Z. Chen, R. Huang, L. Zheng, P. v. R. Schleyer, *J. Am. Chem. Soc.* **2009**, *131*, 9789-9799; e) P. K. Freeman, *J. Org. Chem.* **2005**, *70*, 1998-2001; f) T. Bajorek, N. H. Werstiuk, *Can. J. Chem.* **2005**, *83*, 1352-1359. For recent studies on homoconjugation in methano[10]annulenes, see: g) G. F. Caramori, K. T.

This situation differs from that found in macrocyclic oligoacetylenes and oligodiacetylenes (e.g. pericyclene **4** and **5**, Figure 1),[10] compounds which are not homoaromatic and no electron delocalization by homoconjugative interactions between the triple bonds is detected. Only in highly strained cyclic alkynes homoconjugative interactions seem to be appreciable.[10b] In this respect, it should be pointed out that a CH_2 group in planar cyclic systems such as cyclopropene and cyclobutene has two π electrons. This means that, as instance, cyclopropene is formally a homoantiaromatic molecule because it has four π electrons while cyclobutene is a six π electrons homoaromatic compound.[11]

Despite the large amount of research carried out on homoconjugated alkenes and alkynes, aromatic homoconjugated systems have received less attention. In this chapter, a systematic theoretical and experimental study of homoconjugative interactions between aromatic rings is reported. As a measure of electron delocalization in our systems we have chosen the corresponding absorption spectra since it is well established that increased electron delocalization reduces the HOMO-LUMO energy gap causing a bathochromic shift in the UV absorption if a set of related molecules is considered.[12]

De Oliveira, S. E. Galembeck, P. Bultinck, M. G. Constantino, *J. Org. Chem.* **2007**, *72*, 76-85; h) Y. Zhang, E. Hisano, R. Ohta, R. Miyatake, Y. Horino, M. Oda, S. Kuroda, *Tetrahedron Lett.* **2008**, *49*, 888-892. An interesting (theoretical) class of delocalized molecules with homoconjugative interactions between polyenyl chains is described in: i) D. J. Tantillo, R. Hoffmann, K. N. Houk, P. M. Warner, E. C. Brown, D. K. Henze, *J. Am. Chem. Soc.* **2004**, *126*, 4256-4263.

[10] a) V. Maraval, R. Chauvin, *Chem. Rev.* **2006**, *106*, 5317-5343; b) C. Lepetit, B. Silvi, R. Chauvin, *J. Phys. Chem. A* **2003**, *107*, 464-473; c) A. de Meijere, S. I. Kozhushkov, R. Boese, T. Haumann, D. S. Yufit, J. A. K. Howard, L. S. Khaikin, M. Trætteberg, *Eur. J. Org. Chem.* **2002**, 485-492; d) A. de Meijere, S. I. Kozhushkov, *Top. Curr. Chem.* **1999**, *201*, 1-42; e) B. Leibrock, O. Vostrowsky, A. Hirsch, *Eur. J. Org. Chem.* **2001**, 4401-4409; f) H. Jiao, N. J. R. van Eikema Hommes, P. v. R. Schleyer, A. de Meijere, *J. Org. Chem.* **1996**, *61*, 2826-2828. See also: g) R. Gleiter, R. Merger, H. Irngartinger, *J. Am. Chem. Soc.* **1992**, *114*, 8927-8932.

[11] I. Fernández, G. Frenking, *Faraday Discuss*. **2007**,*135*, 403-422.

[12] a) P. Klán, J. Wirz, *Photochemistry of Organic Compounds. From Concepts to Practice*,Wiley, Chichester, **2009**; b) M. Klessinger, J. Michl, *Excited States and Photochemistry of Organic Molecules*, VCH, Weinheim, **1995**.

1.1.2 Computational details

Geometry optimizations without symmetry constraints were carried out using the Gaussian03 optimizer[13] together with TurboMole5[14] energies and gradients at the BP86[15]/def-SVP[16] level of theory using the resolution-of-identity (RI)[17] method. This level is denoted as RI-BP86/def2-SVP. Stationary points were characterized as minima by calculating the Hessian matrix analytically at this level. Calculations of absorption spectra were accomplished by using the time-dependent density functional theory (TD-DFT)[18] method at the same level. The assignment of the excitation energies to the experimental bands was performed on the basis of the energy values and oscillator strengths. The B3LYP[19] Hamiltonian was chosen because it was proven to provide reasonable UV/Vis spectra for a variety of chromophores[20] including

[13] Gaussian 03, Revision D.01, M. J. Frisch, G. W. Trucks, H. B. Schlegel, G. E. Scuseria, M. A. Rob, J. R. Cheeseman, J. A. Montgomery, Jr., T. Vreven, K. N. Kudin, J. C. Burant, J. M. Millam, S. S. Iyengar, J. Tomasi, V. Barone, B. Mennucci, M. Cossi, G. Scalmani, N. Rega, G. A. Petersson, H. Nakatsuji, M. Hada, M. Ehara, K. Toyota, R. Fukuda, J. Hasegawa, M. Ishida, T. Nakajima, Y. Honda, O. Kitao, H. Nakai, M. Klene, X. Li, J. E. Knox, H. P. Hratchian, J. B. Cross, V. Bakken, C. Adamo, J. Jaramillo, R. Gomperts, R. E. Stratmann, O. Yazyev, A. J. Austin, R. Cammi, C. Pomelli, J. W. Ochterski, P. Y. Ayala, K. Morokuma, G. A. Voth, P. Salvador, J. J. Dannenberg, V. G. Zakrzewski, S. Dapprich, A. D. Daniels, M. C. Strain, O. Farkas, D. K. Malick, A. D. Rabuck, K. Raghavachari, J. B. Foresman, J. V. Ortiz, Q. Cui, A. G. Baboul, S. Clifford, J. Cioslowski, B. B. Stefanov, G. Liu, A. Liashenko, P. Piskorz, I. Komaromi, R. L. Martin, D. J. Fox, T. Keith, M. A. Al-Laham, C. Y. Peng, A. Nanayakkara, M. Challacombe, P. M. W. Gill, B. Johnson, W. Chen, M. W. Wong, C. Gonzalez, J. A. Pople, Gaussian, Inc., Wallingford, CT, **2003**.

[14] Turbomole v. 5.10. R. Ahlrichs, M. Baer, M. Haeser, H. Horn, C. Koelmel, *Chem. Phys. Lett*. **1989**, *162*, 165-169.

[15] a) A. D. Becke, *Phys. Rev. A* **1988**, *38*, 3098-3100; b) J. P. Perdew, *Phys. Rev. B* **1986**, *33*, 8822-8824.

[16] F. Weigend, R. Ahlrichs, *Phys. Chem. Chem. Phys*. **2005**, *7*, 3297-3305.

[17] K. Eichkorn, O. Treutler, H. Öhm, M. Häser, R. Ahlrichs, *Chem. Phys. Lett*. **1995**, *242*, 652-660.

[18] a) M. E. Casida, *Recent Developments and Applications of Modern Density Functional Theory*, Vol. 4, Elsevier, Amsterdam, **1996**; b) M. E. Casida, D. P. Chong, *Recent Advances in Density Functional Methods*, Vol. 1, World Scientific, Singapore, **1995**, p. 155.

[19] a) A. D. Becke, *J. Chem. Phys*. **1993**, *98*, 5648-5652; b) C. Lee, W. Yang, R. G. Parr, *Phys. Rev. B* **1988**, *37*, 785-789.

[20] For a review, see: A. Dreuw, M. Head-Gordon, *Chem. Rev*. **2005**, *105*, 4009-4037.

organometallic species.[21] Donor–acceptor interactions were computed by using the natural bond orbital (NBO) method.[22] The energies associated with these two-electron interactions were computed according to the following equation:

$$\Delta E^{(2)}_{\phi\phi^*} = -n_\phi \frac{\left\langle \phi^* \left| \hat{F} \right| \phi \right\rangle^2}{\varepsilon_{\phi^*} - \varepsilon_\phi}$$

Equation 1

1.1.3 Results and Discussion

The simplest example of apical[23] aromatic homoconjugated compound should be diphenylmethane (DPM, **16**, Figure 2).[24] However, aryl-aryl interactions in diarylmethanes are governed by repulsive electrostatic forces[25] and, therefore, the most stable conformation of **16** is the helical disposition, in which the homoconjugative interaction between the phenyl rings is not possible.

---

[21] Some recent examples: a) V. N. Nemykin, E. A. Makarova, J. O. Grosland, R. G. Hadt, A. Y. Koposov, *Inorg. Chem*. **2007**, *46*, 9591-9601; b) M. L. Lage, I. Fernández, M. J. Mancheño, M. A. Sierra, *Inorg. Chem*. **2008**, *47*, 5253-5258; c) M. L. Lage, I. Fernández, M. J. Mancheño, M. A. Sierra, *Chem. Eur. J*. **2010**, *16*, 6616-6624.

[22] a) J. P. Foster, F. Weinhold, *J. Am. Chem. Soc*. **1980**, *102*, 7211-7218; b) A. E. Reed, F. J. Weinhold, *J. Chem. Phys*. **1985**, *83*, 1736-1740; c) A. E. Reed, R. B. Weinstock, F. Weinhold, *J. Chem. Phys*. **1985**, *83*, 735-746; d) A. E. Reed, L. A. Curtiss, F. Weinhold, *Chem. Rev*. **1988**, *88*, 899-926.

[23] Lateral homoconjugative interactions in iptycenes such as trypticene are not clear and remains controversial: a) X. Gu, Y.-H. Lai, *Org. Lett.* **2010**, *12*, 5200-5203. b) V. J. Chebny, T. S. Navale, R. Shukla, S. V. Lindeman, R. Rathore, *Org. Lett.* **2009**, *11*, 2253-2256; c) L. Zhao, Z. Li, T. Wirth, *Chem. Lett.* **2010,** 658-667; d) H.-D. Martin, B. Mayer, *Angew. Chem. Int. Ed.* **1983**, *22*, 283-314. e) V. R. Skvarchenko, V. K. Shalaev, E. I. Klabunovskii, *Russian Chem. Rev.* **1974**, *43*, 951-966; f) W. Theilacker, K. Albrecht, H. Uffmann, *Chem. Ber*. **1965**, *98*, 428-432.

[24] "The Diphenylmethane Moiety": A. García Martínez, J. Osío Barcina in *Encyclopedia of Supramolecular Chemistry* (Eds.: J. L. Atwood, J. W. Steed), Marcel Dekker, New York, **2004**, pp. 452-456.

[25] A. García Martínez, J. Osío Barcina, A. De Fresno Cerezo, R. Gutiérrez Rivas, *J. Am. Chem. Soc.* **1998**, *120*, 673-679.

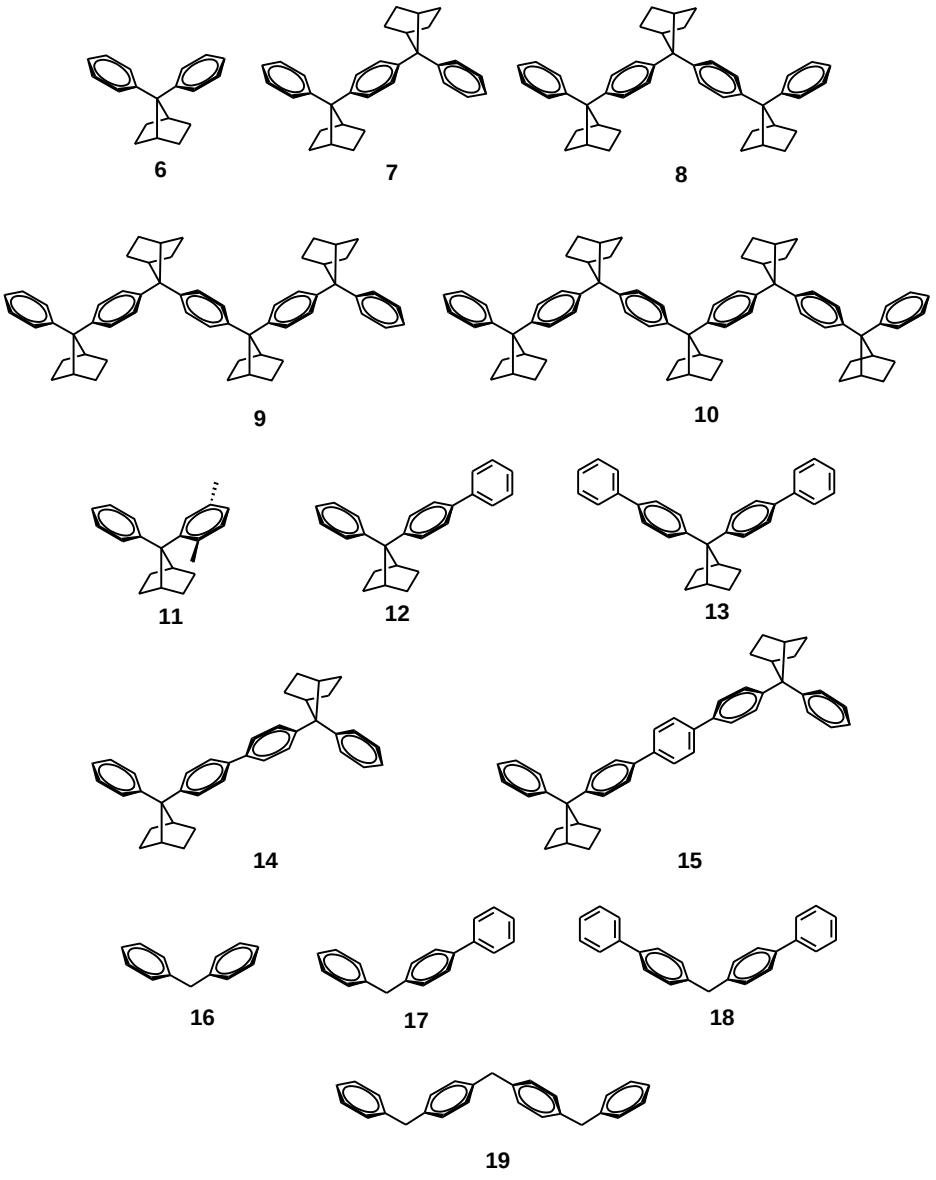

Figure 2. Structures of homoconjugated systems **6**-**15** and non-homoconjugated reference compounds **16**-**19**.

This situation can be modified substantially if the aromatic rings are forced to adopt a cofacial conformation as it happens in 7,7-diphenylnorbornane (DPN, **6**, Figure 2) due to the steric hindrance of the H-*exo* of the bicycle. This is clearly shown in the fully optimized (RI-BP86/def2-SVP level) geometries of both compounds (Figure 3a). As a consequence, homoconjugative interaction between the aromatic rings is now possible and a new homoconjugation band at 228 nm is observed in the UV spectrum of DPN.[24,25] The second-order perturbation theory of the NBO-method agrees with this description. In fact, stabilizing two-electrons delocalizations from the π molecular orbital of a phenyl ring to the π*-molecular orbital of the adjacent phenyl group were found (associated second-order energies of $\Delta E^{(2)}$ = -0.91 kcal.mol^{-1}). Moreover, the HOMO-3 and the LUMO of **6** clearly show the electronic communication between both phenyl groups (Figure 3b).

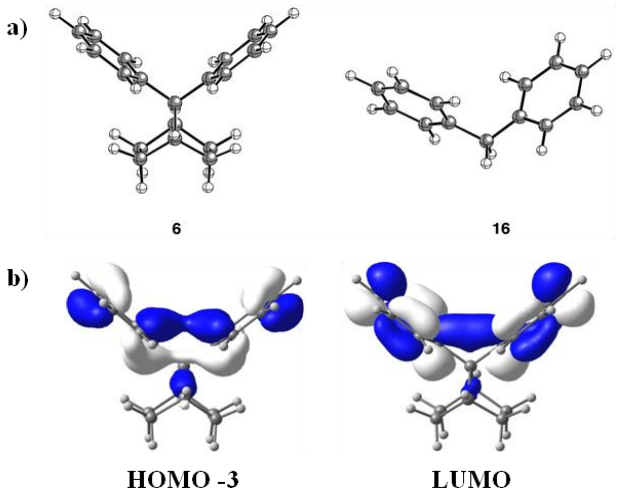

Figure 3. a) Fully optimized geometries (RI-BP86/def2-SVP level) of compounds **6** and **16**. **b)** HOMO-3 and LUMO of compound **6** (isosurface value of 0.035 a.u.).

It should be noted that the NBO-method was not able to find a similar π -π* interaction in the DPM analogue and no similar molecular orbitals connecting both aryl moieties were found either.

We also used the Truhlar's meta hybrid exchange-correlation functional M06-2X developed to account for dispersive corrections for the parent homoconjugated compound **6** and found that there are no significant

differences between the optimized geometries with M06-2X and RI-BP86 methods. In fact, the relevant C_{ipso}-C_{ipso} (phenyl groups) bond length is practically the same (2.459 and 2.466 Å, respectively).

Table 1. Comparison of main UV/Vis excitation energies λ_{max} and the corresponding oscillator strengths (in parentheses) for compound **6**-**19**.

Compound	λ_{exp}/nm [a]	λ_{calc}/nm[b]	Transition[c]	δ_r (BLA)[d]
6	228	237 (0.18)	HOMO-LUMO (5.75)	0.0039
7	242[e]	255 (0.42)	HOMO-LUMO (5.38)	0.0077
	222	220 (0.02)	HOMO-5-LUMO	0.0068
8	248[e]	265 (0.63)	HOMO-LUMO (5.21)	0.0076
	232	232 (0.01)	(combination band)	0.0077
9	250[e]	272 (0.84)	HOMO-LUMO (5.12)	
	231	240	HOMO-1-LUMO+1	
10	---	273 (1.07)	HOMO-LUMO (5.06)	
11	218	234 (0.08)	HOMO-1-LUMO (46%)[f]	
			HOMO-LUMO (29%)	
12	259	274 (0.67)	HOMO-LUMO (4.94)	
13	268	292 (0.70)	HOMO-LUMO (4.70)	
14	272	288 (0.98)	HOMO-LUMO (4.74)	
15	295	316 (1.51)	HOMO-LUMO (4.34)	
17	251	265 (0.65)	HOMO-LUMO (5.06)	
18	257	276 (0.67)	HOMO-LUMO (4.94)	
19	---	246 (0.13)	(combination band)	

[a] Experimental data, recorded at room temperature in MeOH. [b] Computed TD-B3LYP/def2-SVP gas-phase vertical excitation energies. [c] HOMO-LUMO gap energies (in eV) are given in parentheses. [d] Computed bond length alternation (BLA). [e] In hexane. [f] Transition contribution.

Therefore, we think that the dispersion effects are not important in our molecules. We can therefore conclude that this electronic communication between the cofacial aryl groups, which is enforced by the imposed geometry

of the DPN moiety, is responsible for the electronic delocalization (and therefore, for the special electronic properties) of the studied homoconjugated species.

In the present work we have also studied computationally systems with extended homoconjugation (DPN olygomers **7**-**10**), several homoconjugated 7,7-diarylnorbornanes (aryl = phenyl and biphenyl) (**11**-**13**), and compounds with alternating homoconjugation-conjugation-homoconjugation (**14** and **15**) (Figure 2). The results of these calculations have been compared with experimental data obtained from the corresponding absorption spectra. For comparison, a series of non-homoconjugated DPM derivatives (**17**-**19**) were also synthesized and studied. The synthesis of compounds **6**-**9**,[25,26] **12**-**13**,[27] and **14**-**15**[28] was carried out according to the general procedure described in Scheme 1. For the preparation of the reference compounds **17**-**19** we used a synthetic route described in the literature for DPM derivatives,[29] also depicted in Scheme 1.

Table 1 gathers the wavelengths of the absorption maxima together with the corresponding computed gas-phase TD-DFT vertical transitions and associated oscillator strengths.

[26] N. Caraballo-Martínez, M. R. Colorado Heras, M. M. Blázquez, J. Osío Barcina, A. García Martínez, M. R. Torres Salvador, *Org. Lett.* **2007**, *9*, 2943-2946.
[27] A. García Martínez, J. Osío Barcina, A. de Fresno Cerezo, A.-D. Schlüter, J. Frahn, *Adv. Mater.* **1999**, *11*, 27-31.
[28] J. Osío Barcina, M. R. Colorado Heras, M. Mba, R. Gómez Aspe, N. Herrero García, *J. Org. Chem.* **2009**, *74*, 7148-7156.
[29] a) J. M. Tour, A. M. Rawlett, M. Kozaki, Y. Yao, R. C. Jagessar, S. M. Dirk, D. W. Price, M. A. Reed, C.-W. Zhou, J. Chen, W. Wang, I. Campbell, *Chem. Eur. J.* **2001**, *7*, 5118-5134; b) J. M. Tour, M. Kozaki, J. M. Seminario, *J. Am. Chem. Soc.* **1998**, *120*, 8486-8493.

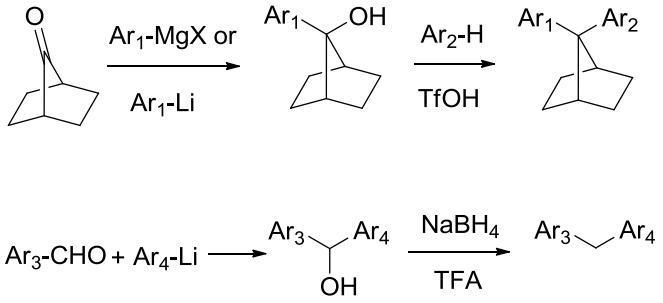

Scheme 1. General synthetic methods for the preparation of homoconjugated systems **6**-**15** and diphenylmethane derivates **17**-**19**.

1.1.3.1 DPN oligomers

In the case of systems with extended homoconjugation (DPN oligomers) **7**-**10**, two intriguing questions are of interest. On the one hand, it is important to study the relative enegies of the different cofacial conformations that can be adopted by these compounds. Secondly, it is important to know how electrons delocalize along the structure of the oligomers and the effect of the chain length on this delocalization (effective homoconjugation length).[26]

With regard to the first question, in the case of the DPN dimer **7**, two stable cofacial conformations (*U* and *Z* or *zig-zag*) are possible (Scheme 2).[30] Obviously, as the chain of the oligomers becomes longer, the number of these conformers increases. As an example, the conformations of trimer **8** are depicted schematically in Scheme 2.

The crystal structure of dimer **7** has been elucidated and, in the solid state, the zig-zag conformation is observed (Figure 4).[26] Whether this is an effect of crystal packing forces or the result of energy differences between the conformers is one of the aspects than we have studied in this chapter.

[30] For a review on molecular zig-zag rods, see: P. F. H. Schwab, J. R. Smith, J. Michl, *Chem. Rev.* **2005**, *105*, 1197-1279.

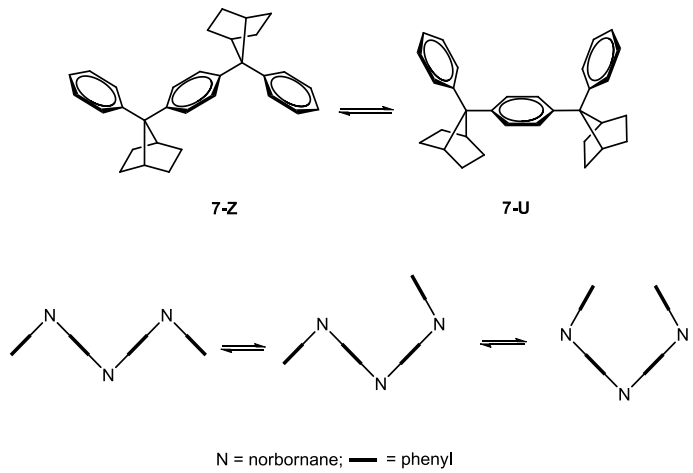

Scheme 2. Stable cofacial conformations of dimer **7** and trimer **8**.

Our calculations indicate that the **7-*Z*** conformer is only 0.7 kcal.mol^{-1} more stable than the **7-*U*** isomer. This practically negligible total energy difference between both conformers points to the crystal packing forces as the main factor responsible for the structure adopted by compound **7** in the solid state. In fact, the crystal packing of **7-*Z*** is stabilized by CH-π interactions between the *para* hydrogen atom of one molecule and the central aryl ring of the neighbouring dimer.[26]

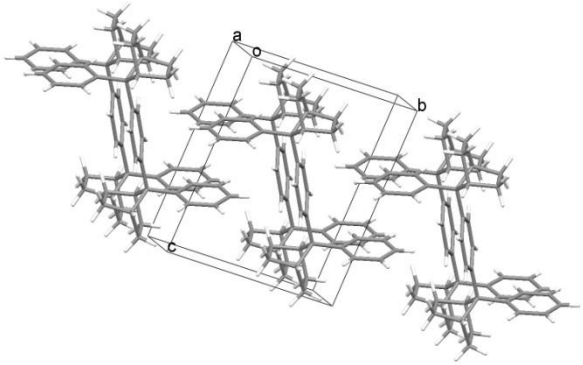

Figure 4. Crystal packing of dimer **7** showing the preferred zig-zag conformation in the solid state.

The UV/Vis spectra of oligomers **7-9** show two important features. Firstly, the homoconjugation band of DPN (228 nm) is bathochromically shifted on going from the dimer (242 nm) to the trimer (248 nm) and the tetramer (250 nm) as a consequence of extended homoconjugation. The electron delocalization shows a limit (effective homoconjugation length)[31] around the pentamer or hexamer.[26] Interestingly, both the experimental wavelengths of the absorption maxima and the corresponding calculated wavelengths of the vertical transition show a clear exponential behaviour (correlation coefficient R^2 of 0.9998 and 0.998, respectively) with an asymptotical maximum reached at five or six DPN units (Figure 5).

We want to point out that this behaviour is also found in π conjugated polyenes and polyphenylenes, although the effect in the homoconjugated systems described is obviously less pronounced. In conjugated systems properties such as absorption or the total π conjugation increases with the number of conjugated C=C units or aryl rings exhibiting a maximum around 12 to 16 carbon atoms in the case of polyenes.[2,11b,31] The value obtained by us for homoconjugated aryl rings is almost the same than the described recently for *ortho*-phenylenes in which the effective conjugation length is approximately eight repeated units.[31a] This clear analogy shows that homoconjugation is an effective mechanism for the delocalization of electrons within the molecule.

On the other hand, the absorption spectra of the DPM trimer (reference compound **19**), resembles that of DPM. In this case, only forbidden transitions with low ε values in the region 260-275 nm are observed (244-269 nm, ε = 265-490 for DPM). No trace of homoconjugation band at 248 nm was detected.

[31] For studies on effective conjugation length, see: a) J. He, L. C. Jason, S. H. Wadumethrige, K. Thakur, L. Dai, S. Zou, R. Rathore, S. Hartley, *J. Am. Chem. Soc.* **2010**, *132*, 13848-13857; b) M. Banerjee, R. Shukla, R. Rathore, *J. Am. Chem. Soc.* **2009**, *131*, 1780-1786; c) J. Rissler, *Chem. Phys. Lett.* **2004**, *395*, 92-96; d) H. Meier, U. Stalmach, H. Kolshorn, *Acta Polym.* **1997**, *48*, 379-384; e) R. E. Martin, U. Gubler, J. Cornil, M. Balakina, C. Boudon, C. Bosshard, J.-P. Gisselbrecht, F. Diederich, P. Günter, M. Gross, J.-L. Brédas, *Chem. Eur. J.* **2000**, *6*, 3622-3635; f) R. E. Martin, T. Mäder, F. Diederich, *Angew. Chem. Int. Ed.* **1999**, *38*, 817-821; g) J. Grimme, M. Kreyenschmidt, F. Uckert, K. Müllen, U. Scherf, *Adv. Mater.* **1995**, *7*, 292-295.

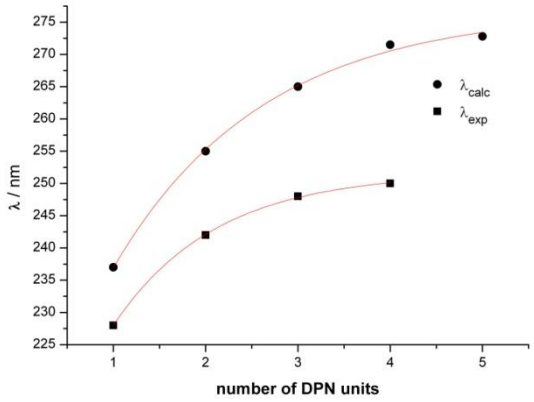

Figure 5. Plot of the experimental and computed λ_{max} versus the number of DPN units.

To further support this finding, we also computed the bond alternation parameter δ_r of the aryl group in the considered oligomers:

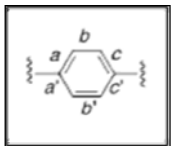

$$\delta_r = \frac{[(a + c - 2b) + (a' + c' - 2b')]}{4}$$

Equation 2

The δ_r parameter has been traditionally used as indicator of the strength of π conjugation in typical push-pull systems (i.e. the amount of charge-transfer from the donor to the acceptor moiety).[32] In benzene, the δ_r value equals 0, whereas values between 0.08 and 0.10 are found in fully quinoid rings. The computed δ_r values using the fully optimized geometries of compounds **6-10** are low (in the range of 0.003 to 0.008) in comparison to π conjugated systems. This is of course not surprising if we take into account the homoconjugated nature of these oligomers. However, the calculated numbers clearly indicate

[32] a) C. Dehu, F. Meyers, J.-L. Brédas, *J. Am. Chem. Soc*. **1993**, *115*, 6198-6206; b) A. Hilger, J.-P. Gisselbrecht, R. R. Tykwinski, C. Boudon, M. Schreiber, R. E. Martin, H. P. Lüthi, M. Gross, F. Diederich, *J. Am. Chem. Soc*. **1997**, *119*, 2069-2078; c) I. Fernández, G. Frenking, *Chem. Comm*. **2006**, 5030-5032.

that the δ_r (that is, the electronic delocalization) increases with the number of DPN units in the oligomer[33] reaching again a maximum around the pentamer or hexamer (see Table 1). TD-DFT calculations assign the experimentally observed absorptions to the HOMO-LUMO vertical transition. From the data in Table 1, the oscillator strength of the vertical transition steadily increases with the length of the oligomer, thus indicating stronger transitions for the higher members of the series.

As readily seen in Figure 6, both the HOMO and LUMO can be viewed as delocalized molecular orbitals which involve the π systems of the aryl groups. Interestingly, in the LUMO there exists a clear electronic communication between the π* molecular orbitals of each aryl groups. This π* extended molecular orbitals also resemble the π* molecular orbitals of conjugated polyenes. Similarly, the HOMO-LUMO gap of the considered homoconjugated oligomers steadily decreases with the number of DPN units.

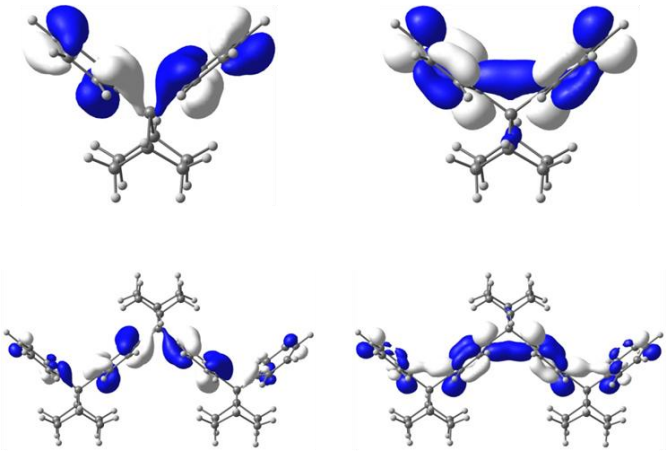

Figure 6. Frontier orbitals of compounds **6** (top) and **8** (bottom).

Besides this, new absorptions at shorter wavelengths are observed in the spectra of the oligomers: **10** (222 nm), **11** (232 nm) and **12** (228 and 231 nm). TD-DFT calculations also reproduce these high-energy absorptions well. As seen in Table 1, the nature of these vertical transitions depends on the

[33] Compound **7** possesses a surprisingly high δ_r value. The reasons for this anomalous behaviour are not fully understood so far.

considered system. Moreover, their corresponding oscillator strength is quite low, indicating weak electronic transitions.

1.1.3.2 7,7-Diarylnorbornanes 11-13

As mentioned previously, the absorption spectrum of DPN shows a new homoconjugation band centered at 228 nm (ε = 103400) that is not observed in DPM. This absorption is due to the cofacial conformation of DPN. Small deviations from cofaciallity should affect the orbital overlap between the aryl rings and diminish the homoconjugation. Thus, the homoconjugation band in DPN derivative **11** is hypso- and hypochromically shifted (λ_{max} = 218 nm, ε = 10900). In this case, the steric hindrance between the methyl group at the *orto* position and the bridgehead hydrogen atom forces the rotation of the aryl ring resulting in a computed torsional angle C_{orto}-C_{ipso}-C_7-C_{ipso} of 77.4^0 (88.3^0 in DPN).

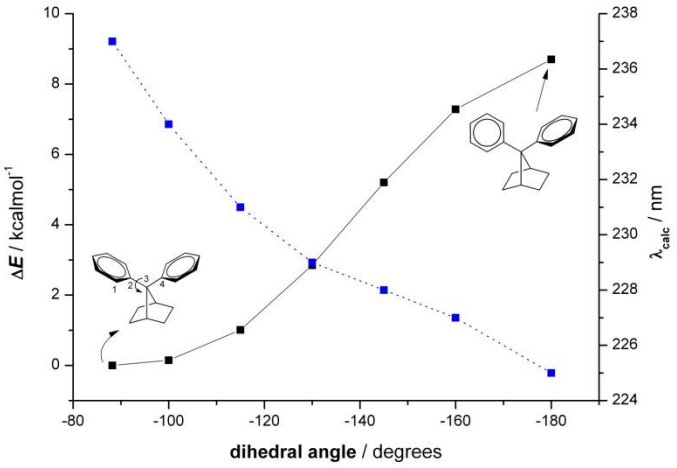

Figure 7. Variation of energy (Δ*E*) (black line) and λ_{calc} (dotted line) with the torsional angle in **6**.

In order to gain information about the influence of the torsional angle on the homoconjugation between the aryl rings of DPN's, we have computed the variation of the energy and λ_{calc} of the different conformations of the parent

homoconjugated compound **6** from the cofacial disposition to the orthogonal conformation (Figure 7).

As readily seen, the homoconjugation band is blue shifted as the torsional angle increases from -80^0 to 180^0 as a consequence of the decrease in the orbital overlap. According to these calculations, the energy difference between the cofacial and orthogonal conformations, which is a transition state, is 9.1 kcal.mol^{-1}. From this value, the ΔG at 25 ^{0}C (ΔG_{298}), that is the rotational barrier in DPN, was estimated to be 11.2 kcal.mol^{-1}. This result seems to be quite reliable since a value of 16.7 kcal.mol^{-1} is obtained for 7-(2-fluorophenyl)-7-phenylnorbornane following the same methodology. The librational barrier obtained by D-NMR in this case is 17.0 kcal.mol^{-1}.[25]

On the other hand, the spectra of **12** and **13** show broad absorption bands in the region 228-300 nm with λ_{max} at 259 nm and 268 nm respectively, bathochromically shifted by 12 nm and 21 nm in comparison to the absorption of biphenyl (247 nm) due to homoconjugative interaction.[25,27]

On the contrary, the spectra of reference compounds **17** and **18** show λ_{max} at 251 nm and 257 nm respectively. The observed red-shifts can be ascribed to the higher electronic delocalization in **12** and **13** due to homoconjugation compared to the parent compounds **17** and **18**, respectively, as reflected in the high computed second-order perturbation energies for the π-π^* donations. As instance, a value of $\Delta E^{(2)}$ = -1.63 kcal.mol^{-1} is found for compound **13** whereas no similar donation was found for compound **18**. Moreover, the absorption maxima of **12** and **13** are also red-shifted respect to the parent homoconjugated compound **6**. As expected, the donation from the biphenyl group to the adjacent phenyl group in **12** is $\Delta\Delta E^{(2)}$ = -0.66 kcal.mol^{-1} higher than the donation from the phenyl group in the parent homoconjugated **6** species in good agreement with the higher π-donation ability of the biphenyl substitutent. Similarly, the π-acceptor ability of the biphenyl group is also higher ($\Delta\Delta E^{(2)}$ = -0.67 kcal.mol^{-1}).

Analogously to the above discussed oligomers, TD-DFT calculations also assign the observed UV/Vis absorptions to the HOMO-LUMO vertical transitions whose oscillator strengths are comparable to compounds **7**-**10**. Again, the HOMO can be considered as a π-molecular orbital involving the

aromatic rings while the LUMO is the π*-extended molecular orbital similar to those depicted in Figure 6.

1.1.3.3 Systems with alternating homoconjugation conjugation

The UV/Vis spectra of compounds **14** and **15** show absortion maxima at 272 nm and 295 nm respectively.[28] Comparison of these data with the λ_{max} of biphenyl (247 nm), *p*-terphenyl (274 nm) and *p*-quaterphenyl clearly demonstrates the effect of electron delocalization by homoconjugation. Thus, the λ_{max} of biphenyl is red shifted by 25 nm when two homoconjugated subunits are attached at the *para* positions (compound **14**). A similar effect is observed for *p*-terphenyl and compound **15** (a red shift of 21 nm). According to these data, the effect of two homoconjugated phenyl rings on the HOMO-LUMO energy gap is similar to that caused by one conjugated phenyl ring since the λ_{max} of **14** and *p*-terphenyl (272 *vs.* 274 nm) and **15** and *p*-quaterphenyl (295 nm *vs.* 292 nm) are very similar.[28]

In this occasion, TD-DFT calculations assign the observed UV/Vis absorptions to the HOMO-LUMO vertical transitions as well, that is a π-π* transition. The shape of the molecular orbitals is similar to those of the previously discussed systems with the remarkable difference that the HOMO is practically localized in the biphenyl or *p*-terphenyl fragment with negligible coefficients in the adjacent phenyl groups (Figure 8).

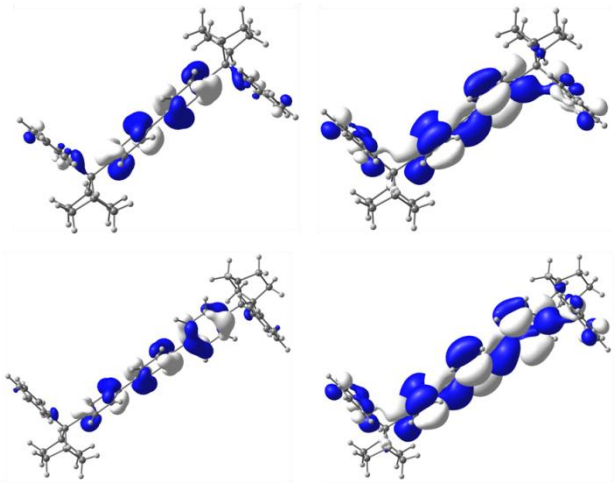

Figure 8. Frontier orbitals of compounds **14** (top) and **15** (bottom).

From the above findings, it can be concluded that the DPN moiety permits the electronic communication/delocalization between the homoconjugated aryl groups directly attached to the C7 carbon atom of norbornane. Therefore, adequate modifications of the electronic structure of these aromatic substituents should effectively alter the electronic properties of the systems.

To check this hypothesis and to provide further support to our study on electron delocalization in homoconjugated systems, we decided to computationally study push-pull systems based on the parent homoconjugated compound **6**. Thus, a nitro group was introduced as π-acceptor group in *para* position of one of the phenyl rings, while different π-donor and π-acceptors groups were added in the *para* position of the adjacent phenyl ring.

The calculated TD-DFT wavelengths (again ascribed to the HOMO-LUMO vertical transitions) nicely correlate with the corresponding Taft-σ_R substituent constants[34] as clearly seen from the excellent linear relationship found when plotting both parameters (correlation coefficient of 0.999 and standard deviation of 0.009, see Figure 9). This latter result confirms the ability of the homoconjugation to provoke the delocation of electrons between both arylic substituents. Furthermore, the calculations also predict that the different chemical modifications in the substituents attached to the DPN fragment can indeed induce dramatic changes in their absorption spectra by modifying the electronic structure of the system.

[34] C. Hansch, A. Leo, R. W. Taft, *Chem. Rev*. **1991**, *91*, 165-195.

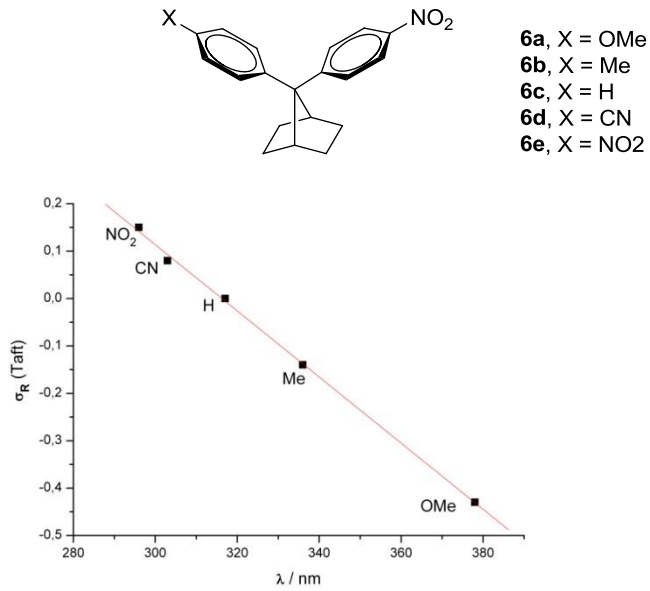

Figure 9. Plot of the computed λ_{max} versus the σ_R-Taft constants for compounds **6a**-**e**.

1.1.4 Conclusion

Neutral homoconjugation is quite an elusive phenomenon that has been described only in cyclic systems such as cycloheptatriene and some tris-homoaromatics (homobenzenes). On the contrary, in macrocyclic oligoacetylenes no electron delocalization mediated by homoconjugative interactions is observed. The situation in open chain aromatic homoconjugated molecules described in this work seems to be completely different. Thus, from the joint computational-experimental study reported in this paper, the following conclusions can be drawn:

i. The DPN moiety effectively allows the electronic communication/delocalization between the homoconjugated aryl groups directly attached to the C7 carbon atom. This is mainly due to the enforced cofacial conformation imposed by the norbornane fragment.

ii. The observed new bands in the corresponding UV/Vis spectra can be ascribed to the HOMO-LUMO transition. Both orbitals possess a remarkable π-character and thus, the transition can be considered as π-π*.

iii. Aromatic homoconjugated compounds, mainly in the case of systems with extended homoconjugation, behave similarly to analogous polyphenylenes and polyenes. The effective homoconjugatuion length has been estimated in the range of 6-7 aromatic rings. Consequently, DPN derivatives can be successfully used in the synthesis of chromophores with NLO properties[35] or as efficient bridges in D-B-A systems for Dexter type photoinduced energy transfer.[36]

iv. The homoconjugative interaction between the aromatic rings can be clearly demonstrated in substituted systems. Adequate chemical modifications in the aromatic substituents attached to the DPN fragment can indeed induce dramatic changes in their absorption spectra by modifying the electronic structure of the system.

[35] A. García Martínez, J. Osío Barcina, A. de Fresno Cerezo, G. Rojo, F. Agulló-López, *J. Phys Chem. B* **2000**, *104*, 43-47.

[36] J. Osío Barcina, N. Herrero-García, F. Cucinotta, L. De Cola, P. Contreras-Carballada, R. M. Williams, A. Guerrero-Martínez, *Chem. Eur. J.* **2010**, *16*, 6033-6040.

1.1.5 Experimental Section

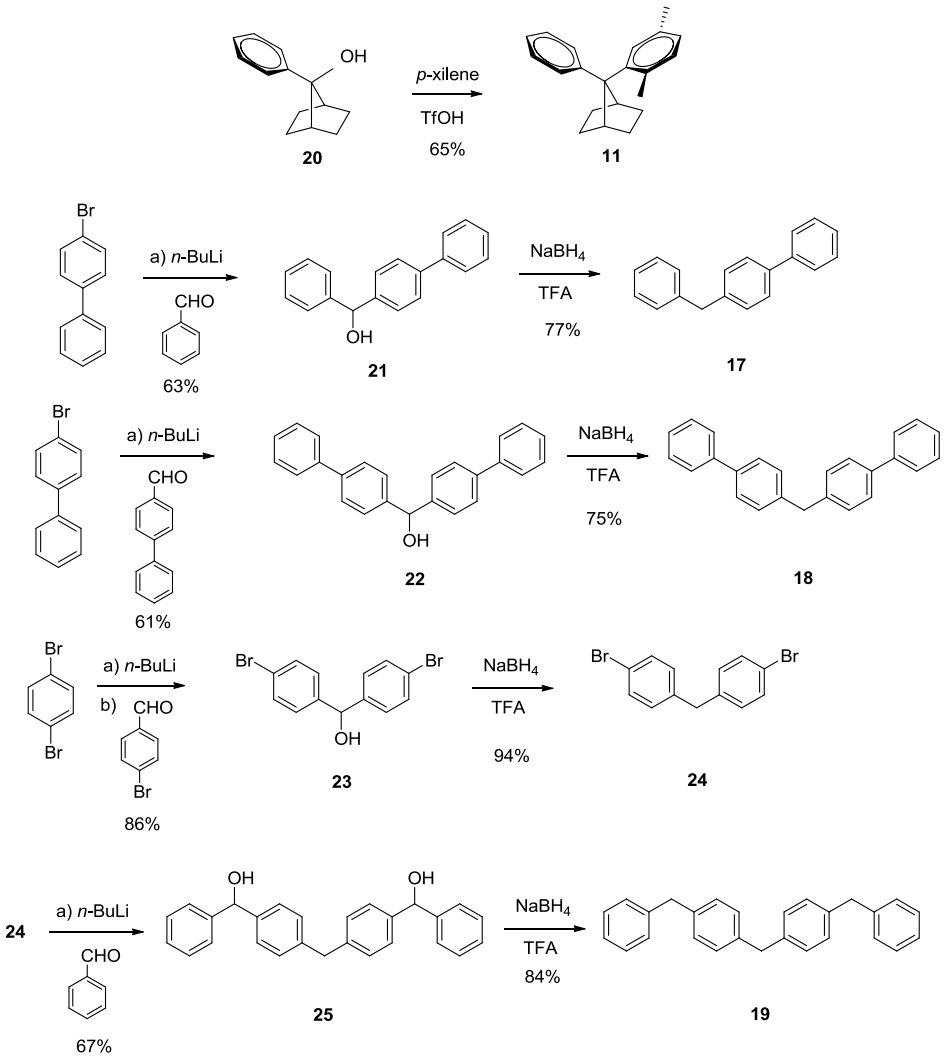

Scheme 3. Synthetic route for the preparation of **11**, **17**, **18** and **19**.

General Information:

^{1}H and ^{13}C NMR spectra were recorded on a 300 MHz spectrometer. Chemical shifts are given in ppm relative to TMS (^{1}H, 0.0 ppm) and $CDCl_3$ (^{13}C, 77.0 ppm). Coupling constants are given in Hertz. All experiments involving organometallic reagents were carried out under argon atmosphere using standard Schlenk techniques. Anhydrous

solvents were distilled under argon following standard procedures. Flash chromatography was performed over silica gel 60 (230-400 mesh). All commercially available compounds were purchased from commercial suppliers and used without further purification. The preparation of **20**,[26] **23** and **24**[29] have been described previously.

Experimental procedures:

Compound 11: 1.20 mL (13.65 mmol) of TfOH were slowly added to a solution of 2.57 g (13.56 mmol) of **20** in 25 mL of *p*-xilene, vigorously stirred at 0º C. After 1 h, the reaction mixture was poured on 25 mL of water and washed with saturated $NaHCO_3$ solution (2 x 25mL) and water (1 x 25mL). After drying the organic solution over $MgSO_4$ the solvent was evaporated and the residue purified by flash chromatography (silica gel/hexane) to give 2.45 g (65%) of **11**. ^{1}H NMR (300 MHz, $CDCl_3$): δ = 7.50-7.41 (m, 3H), 7.23 (t, *J* = 7.8 Hz, 2H), 7.09 (t, *J* = 7.2 Hz, 1H), 6.88-6.85 (m, 2H), 3.18-3.10 (m, 1H), 2.96-2.90 (m, 1H), 2.29 (s, 3H), 2.22 (s, 3H), 2.15-1.86 (m, 2H), 1.50-1.00 ppm (m, 6H); ^{13}C NMR ($CDCl_3$, 75 MHz): δ = 143.7, 142.9, 134.7, 133.2, 131.9, 129.4, 128.2, 127.6, 126.5, 125.0, 65.7, 45.3, 39.6, 29.0, 28.7, 27.9, 27.5, 21.7, 21.2 ppm; IR (neat): ϋ= 3010 (m), 2980 (s), 2880 (m), 1600 (w), 1500 (m), 1475 (m), 1455 (m), 810 (m), 710 cm^{-1} (m); MS (EI, 70 eV) *m/z* (%): 276 (87) [M$^+$], 262 (17), 261 (74), 247 (25), 233 (15), 221 (16), 219 (32), 207 (22), 205 (22), 203 (17), 202 (15), 195 (56), 193 (57), 192 (17), 191 (24), 180 (19), 179 (29), 178 (41), 171 (66), 170 (22), 165 (41), 157 (24), 143 (46), 142 (22), 141 (30), 129 (59), 128 (47), 119 (25), 118 (17), 117 (29), 116 (18), 115 (76), 105 (75), 103 (18), 91 (100), 79 (25), 77 (39), 67 (22), 55 (27), 53 (18), 51 (19); Elemental analysis (%) calc for $C_{21}H_{24}$ (276.42): C 91.25, H 8.75; found: C 91.28, H 8.71.

General procedure for the synthesis of alcohols 21, 22 and 25: In a dry Schlenk flask placed under argon *n*-BuLi (1.4 mL, 2.2 mmol, 1.6M in hexane) was added dropwise to a solution of the corresponding bromide (2.2 mmol) in 5 mL of THF at -78 ºC. After stirring 15 min, a solution of 2.2 mmol of the aldehyde in 5 mL of THF was added to the slurry. The reaction mixture was allowed to warm to room temperature, stirred for 2 h, poured into water (50 mL) and extracted with dichloromethane (3 x 15 mL). The organic solution was washed with water (40 mL) and dried over $MgSO_4$. After removal of the solvent under reduced pressure, the resulting crude product was purified by flash chromatography (silica gel, hexane/Et_2O 9:1).

Alcohol 21:[37] Yield: 63%; ^{1}H NMR (300 MHz, $CDCl_3$): δ = 7.67-7.55 (m, 4H), 7.53-7.29 (m, 14H), 5.88 (s, 1H), 2.52 ppm (bs, 1H, OH); ^{13}C NMR ($CDCl_3$, 75 MHz): δ = 143.8, 142.9, 140.8, 140.5, 128.9, 128.6, 127.7, 127.4, 127.3, 127.2, 127.1, 126.7, 76.1 ppm.

[37] A. F. Trindade, P. M. P. Gois, L. F. Veiros, V. André, M. T. Duarte, C. A. M. Afonso, S. Caddick, F. G. N. Cloke, *J. Org. Chem*. **2008**, *73*, 4076-4086.

Alcohol 22:[38] Yield: 61%; ^{1}H NMR (300 MHz, $CDCl_3$): δ = 7.61 (m, 8H), 7.59-7.42 (m, 8H), 7.37 (t, *J* = 7.2 Hz, 2H), 5.94 (s, 1H), 2.32 ppm (bs, 1H, OH); ^{13}C NMR ($CDCl_3$, 75 MHz): δ = 142.9, 140.9, 140.7, 128.9, 127.4, 127.2, 127.1, 75.9 ppm.

Alcohol 25:[39] Yield: 67%; ^{1}H NMR (300 MHz, $CDCl_3$): δ = 7.42-7.22 (m, 10H), 7.18-7.07 (m, 4H), 5.81 (s, 2H), 3.93 (s, 2H), 2.18 ppm (bs, 2H); ^{13}C NMR ($CDCl_3$, 75 MHz): δ = 143.9, 141.8, 140.5, 129.2, 128.6, 127.7, 126.9, 126.6, 76.2, 41.4 ppm.

General procedure for the synthesis of aromatic hydrocarbons 17, 18 and 19: The alcohol (0.8 mmol) was dissolved in 10 mL of TFA and 302 mg (0.8 mmol) of sodium borohydride were added in small portions during 5 min. The reaction mixture was stirred for 40 min and poured into 50 ml of water. The suspension was made alkaline by addition of sodium hydroxide solution (10%) and extracted with Et_2O (3 x 20 mL). The organic solution was washed with water (2 x 20 mL) and brine (20 mL) and dried over $MgSO_4$. After removal of the solvent under reduced pressure the crude product was purified by flash chromatography (silica gel, hexane).

Compound 17:[40] Yield: 77%; ^{1}H NMR (300 MHz, $CDCl_3$): δ = 7.66 (d, *J* = 7.9 Hz, 2H), 7.61 (d, 8.1 Hz, 2H), 7.50 (t, *J* = 7.2 Hz), 7.45-7.32 (m, 8H), 4.10 ppm (s, 2H); ^{13}C NMR ($CDCl_3$, 75 MHz): δ = 141.1, 141.1, 140.4, 139.1, 129.4, 129.1, 128.8, 128.6, 127.3, 127.2, 127.1, 126.3, 41.7 ppm.

Compound 18:[41] Yield: 75%; ^{1}H NMR (300 MHz, $CDCl_3$): δ = 7.69-7.61 (m, 8H), 7.50 (t, *J* = 7.2 Hz, 4H), 7.43-7.33 (m, 6H), 4.12 ppm (s, 2H); ^{13}C NMR ($CDCl_3$, 75 MHz): δ = 141.1, 140.3, 139.2, 129.5, 128.9, 127.4, 127.2, 127.1, 41.3 ppm.

Compound 19:[42] Yield: 84%; ^{1}H NMR (300 MHz, $CDCl_3$): δ = 7.41-7.33 (m, 4H), 7.32-7.24 (m, 6H), 7.19 (s, 8H), 4.03 (s, 4H), 4.00 ppm (s, 2H); ^{13}C NMR ($CDCl_3$, 75 MHz): δ = 141.3, 139.0, 138.9, 129.1, 129.0, 128.5, 126.1, 41.6, 41.2 ppm.

[38] E. Weber, W. Seichter, I. Goldberg, *Chem. Ber.* **1990**, *123*, 811-820.
[39] a) D. Braun, H. Maid, *Angew. Makromol. Chem.* **1993**, *212*, 93-102; b) F. C. De Schryver, T. Van Thien, G. Smets, *J. Polymer Sci.,Polymer Chem Ed.* **1975**, *13*, 227-252.
[40] J. R. Schmink, N. E. Leadbeater, *Org. Lett.* **2009**, *11*, 2575-2578.
[41] S. E. Asher, S. E. Browne, E. H. Cornwall, J. K. Frisoli, E. A. Salot, E. A. Sauter, M. A. Trecoske, P. S. Veale, Jr., *J. Am. Chem. Soc.* **1984**, *106*, 1432-1440.
[42] A. R. Katritzky, M. Balasubramanian, M. Siskin, E*nergy & Fuels* **1990**, *4*, 499-505.

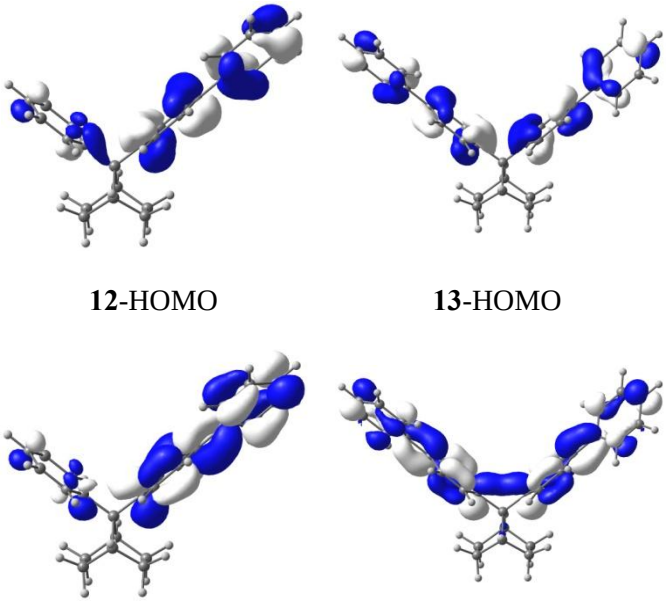

	12-HOMO	**13**-HOMO
	12-LUMO	**13-**LUMO
HOMO-LUMO gap /eV	4.94	4.70

Figure 10. Frontier orbitals of compounds **12** and **13**.

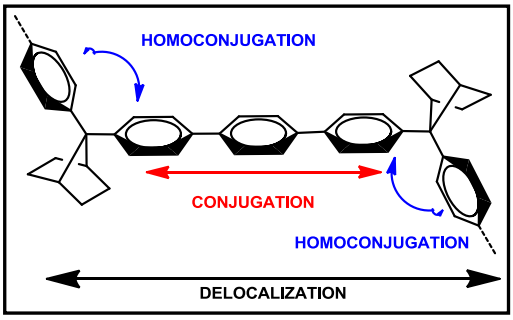

1.2 Efficient Electron Delocalization Mediated by Aromatic Homoconjugation in 7,7-Diphenylnorbornane Derivatives

Efficient electron delocalization by aromatic homoconjugated 7,7-diphenylnorbornane (DPN) in alternated homoconjugated-conjugated block copolymers and reference compounds is revealed by photophysical and electrochemical measurements. The synthesis of the polymers was achieved by Suzuki polycondensation reaction. Effective electron delocalization by DPN is demonstrated by the significant red shifts observed in the absorption and emission spectra and the variation of the energy band gap of the polymers and monomeric model compounds in comparison to a series of oligophenylenes used as references (p-quaterphenyl, p-terphenyl and biphenyl). The electron delocalization is also clearly demonstrated by the lower oxidation potential measured for homoconjugated model compound in comparison to p-terphenyl. The results show that the electron delocalization caused by two homoconjugated aryl rings is comparable to the effect produced by one conjugated aryl ring.

(*J. Org. Chem.* **2009,** *47*, 7148-7156)

1.2.1 Introduction

Electron delocalization in covalently linked molecules is one of the most important and widely studied phenomena in organic chemistry.[1] During the last decades, conjugated polymers[2] and oligomers[3] have attracted great interest in material science due to their fascinating semiconducting and NLO properties, among others. Orbital overlap in these systems is the basis of their potential applications in the emerging areas of molecular electronics and nanotechnology,[4] as organic semiconductors,[5] light-emitting diodes (OLEDs),[6] organic field effect transistors (OFEDs),[7] polymer lasers,[8] organic photovoltaic and solar cells[9] and biological and chemical sensors.[10] It is well-known that the

[1] *Chem. Rev.* **2005**, *105*, number 10: special issue on delocalization-pi and sigma.
[2] *Handbook of Conducting Polymers*, Skotheim, T. A., Reynolds, J. R., Eds.; CRC Press, Taylor & Francis Group, London, 2007.
[3] *Electronic Materials: The Oligomer Approach*, Müllen K., Wegner, G., Eds.; Wiley-VCH, New York, 1998.
[4] a) *Introduction to Molecular Electronics*, Petty, M. C., Bryce, M. R., Bloor, D., Eds.; Oxford University Press, New York, 1995. b) Tour, J. M. *Acc. Chem. Res.* **2000**, *33*, 791-804. c) Wassel, R. A.; Gorman, C. B. *Angew. Chem. Int. Ed.* **2004**, *43*, 5120-5123. d) *Dekker Encyclopedia of Nanoscience and Nanotechnology*, Schwarz, J. A., Contescu, C. I., Putyera, K., Eds.; Marcel Dekker, New York, 2004. e) *Organic Light-Emitting Devices. Synthesis, Properties and Applications*, Müllen, K., Scherf U., Eds.; Wiley-VCH, Weinheim, 2006. f) Gómez, R.; Segura, J. L. In *Materials for Organic Solar Cells*, in *Handbook of Organic Electronics and Photonics, Vol. 3*, Nalwa H. S., Ed.; American Scientific Publishers, Valencia, California, 2007.
[5] a) Shirakawa, H. *Angew. Chem. Int. Ed.* **2001**, *40*, 2574-2580. b) MacDiarmid, A. G. *Angew. Chem. Int. Ed.* **2001**, *40*, 2581-2590.
[6] a) Kraft, A.; Grimsdale, A. C.; Holmes, A. B. *Angew. Chem. Int. Ed.* **1998**, *37*, 402-428. b) Mitschke, U.; Baüerle, P. *J. Mater. Chem.* **2000**, *10*, 1471-1507. c) Heeger, A.; *Angew. Chem. Int. Ed.* **2001**, *40*, 2591-2611. d) Veinot, J. G. C.; Marks, T. J. *Acc. Chem. Res.* **2005**, *38*, 632-643. e) *Organic Electroluminescence*, Kafafi Z. H., Ed.; Taylor Francis, Boca Raton, 2005.
[7] a) Dimitrakopoulos, C. D.; Malenfant, P. R. L. *Adv. Mater.* **2002**, *14*, 99-117. b) Sirringhaus, H. *Adv. Mater.* **2005**, *17*, 2411-2425. c) Murphy, A. R.; Fréchet, J. M. J. *Chem. Rev.* **2007**, *107*, 1066-1096.
[8] a) Hide, F.; Díaz-García, M. A.; Schwartz, B. J.; Heeger, A. J. *Acc. Chem. Res.* **1997**, *30*, 430-436. b) McGehee, M. D.; Heeger, A. J. *Adv. Mater.* **2000**, *12*, 1655-1668. c) Kranzelbinder, G.; Toussaere, E.; Zyss, J.; Pogantsch, A.; List, E. W. J.; Tillmann, H.; Hörhold, H. H. *Appl. Phys. Lett.* **2002**, *80*, 716-718. d) Samuel, I. W. D.; Turnbull, G. A. *Chem. Rev.* **2007**, *107*, 1272-1295.
[9] a) Brabec, C. J.; Sariciftci, N. S.; Hummelen, J. C. *Adv. Funct. Mater.* **2001**, *11*, 15-26. b) Xue, J.; Rand, B. P.; Uchida, S.; Forrest, S. R. *Adv. Mater.* **2005**, *17*, 66-71. c) Li, J.; Dierschke, F.; Wu, J.; Grimsdale, A. C.; Müllen, K. *J. Mater. Chem.* **2006**, *16*,

nature of the interactions between the π systems in these oligomers and polymers govern their properties and that small variations in their structures can modify the characteristics and, as a result, the applications of these materials. Therefore, the study of structure/properties relationships to develop new applications is of great importance.[2-4,11]

A very interesting way to achieve structure/properties studies is incorporating non-conventional ways of electronic communication in electron delocalized molecules. In that respect, the search of alternative modes of interaction between organic π systems has recently led to a variety of new structures with promising electronic features: aromatic derivatives with toroidal delocalization,[12,13,14,15] spiro-compounds,[16,17,18] cross-conjugated molecules[19,20,21] and π-stacked systems.[22,23,24,25,26,27,28,29] In particular, π-stacked

96-100. d) Günes, S.; Neugebauer, H.; Sariciftci, N. S. *Chem. Rev.* **2007**, *107*, 1324-1338.

[10] a) Torsi, L.; Tanese, M. C.; Cioffi, N.; Gallazzi, M. C.; Sabbatici, L.; Zambonin, P. G.; Raos, G.; Meille, S. V.; Giangregorio, M. M. *J. Phys. Chem. B* **2003**, *107*, 7589-7564. b) Bartic, C.; Borghs, G. *Anal. Bioanal. Chem.* **2006**, *384*, 354-365.

[11] a) Roncali, J. *Chem. Rev.* **1997**, *97*, 173-205. b) Horowitz, G. *J. Mater. Chem.* **1999**, *9*, 2021-2026.

[12] Lambert, C. *Angew. Chem. Int. Ed.* **2005**, *44*, 7337-7339.

[13] a) Chebny, V. J.; Shukla, R.; Rathore, R. *J. Phys. Chem. A* **2006**, *110*, 13003-13006. b) Shukla, R.; Lindeman, S. V.; Rathore, R. *Org. Lett.* **2007**, *9*, 1291-1294.

[14] a) Sun, D.; Rosokha, S. V.; Kochi, J. K. *Angew. Chem. Int. Ed.* **2005**, *44*, 5133-5136. b) Rosokha, S. V.; Neretin, I. S.; Sun, D.; Kochi, J. K. *J. Am. Chem. Soc.* **2006**, *128*, 9394-9407.

[15] Wakamiya, A.; Ide, T.; Yamaguchi, S. *J. Am. Chem. Soc.* **2005**, *127*, 14859-14866.

[16] Saragi, T. P. I.; Spehr, T.; Siebert, A.; Fuhrmann-Lieker, T.; Salbeck, J. *Chem. Rev.* **2007**, *107*, 1011-1065.

[17] Abe, J.; Shirai, Y.; Nemoto, N.; Nagase, Y. *J. Phys. Chem. A* **1997**, *101*, 1-4.

[18] Luo, Y.; Norman, P.; Agren, H. *Chem. Phys. Lett.* **1999**, *303*, 616-620.

[19] a) Tykwinski, R. R.; Zhao, Y. *Synlett* **2002**, 1939-1953. b) Gholami, M.; Tykwinski, R. R. *Chem. Rev.* **2006**, *106*, 4997-5027.

[20] a) Klokkenburg, M.; Lutz, M.; Spek, A. L.; van der Maas, J. H.; van Walree, C. A. *Chem. Eur. J.* **2003**, *9*, 3544-3554. b) van Walree, C. A.; Kaats-Richters, V. E. M.; Veen, S. J.; Wieczorek, B.; Van der Wiel, J. H.; Van der Wiel, B. C. *Eur. J. Org. Chem.* **2004**, 3046-3056.

[21] Ponce Ortíz, R.; Malavé Osuna, R.; Hernández, V.; López Navarrete, J. T.; Vercelli, B.; Zotti, G.; Sumerin, V. V.; Balenkova, E. S.; Nenajdenko, V. G. *J. Phys. Chem. A* **2007**, *111*, 841-851.

[22] a) Morisaki, Y.; Chujo, Y. *Angew. Chem. Int. Ed.* **2006**, *45*, 6430-6437. b) Morisaki, Y.; Murakami, T.; Chujo, Y. *Macromolecules* **2008**, *41*, 5960-5963. c) Morisaki, Y.; Murakami, T.; Sawamura, T.; Chujo, Y. *Macromolecules* **2009**, *42*, 3656-3660.

systems are very interesting as model compounds in the study of electron transfer processes mediated by DNA oligonucleotides.[27,30,31]

In recent years we have focused our attention on aromatic homoconjugated systems derived from 7,7-diphenylnorbornane (**1**, DPN, Figure 1).[32] DPN is an easily accessible homoconjugated and preorganized system that can be considered as an example of open-chain cyclophane (protophane, according to the definition by Vögtle)[33,34] since the H-*exo* atoms of the norbornane skeleton hinders the rotation of the aryl rings, resulting in a cofacial aromatic π-system

[23] Mataka, S.; Thiemann, T.; Taniguchi, M.; Sawada, T. *Synlett* **2000**, 1211-1227.
[24] a) Zyss, J.; Ledoux, I.; Volkov, S.; Chernyak, V.; Mukamel, S.; Bartholomew, G. P.; Bazan, G. C. *J. Am. Chem. Soc.* **2000**, *122*, 11956-11962. b) Bartholomew, G. P.; Bazan, G. C. *Acc. Chem. Res.* **2001**, *34*, 30-39. c) Seferos, D. S.; Trammell, S. A.; Bazan, G. C.; Kushmerick, J. G. *Proc. Natl. Acad. Sci. U.S.A.* **2005**, *102*, 8821-8825. d) Hong, J. W.; Woo, H. Y.; Liu, B.; Bazan, G. C. *J. Am. Chem. Soc.* **2005**, *127*, 7435-7443.
[25] a) Wang, W.; Xu, J.; Lai, Y.-H.; Wang, F. *Macromolecules* **2004**, *37*, 3546-3553. b) Wang, W.-L.; Xu, J.; Sun, Z.; Zhang, X.; Lu, Y.; Lai, Y.-H. *Macromolecules* **2006**, *39*, 7277-7285.
[26] a) Rathore, R.; Abdelwahed, S. H.; Guzei, I. A. *J. Am. Chem. Soc.* **2003**, *125*, 8712-8713. b) Rathore, R.; Abdelwahed, S. H.; Kiesewetter, M. K.; Reiter, R. C.; Stevenson, C. D. *J. Phys Chem. B* **2006**, *110*, 1536-1540.
[27] a) Kang, Y. K.; Rubtsov, I. V.; Iovine, P. M.; Chen, J.; Therien, M. J. *J. Am. Chem. Soc.* **2002**, *124*, 8275-8279. b) Zheng, J.; Kang, Y. K.; Therien, M. J.; Beratan, D. N. *J. Am. Chem. Soc.* **2005**, *127*, 11303-11310.
[28] Shibahara, M.; Watanabe, M.; Iwanaga, T.; Matsumoto, T.; Ideta, K.; Shinmyozu, T. *J. Org. Chem.* **2008**, *73*, 4433-4442.
[29] a) Nakano, T.; Yade, T. *J. Am. Chem. Soc.* **2003,** *125*, 15474-15484. b) Coropceanu, V.; Nakano, T.; Gruhn, N. E.; Kwon, O.; Yade, T.; Katsukawa, K.; Brédas, J.-L. *J. Phys. Chem. B* **2006**, *110*, 9482-9487.
[30] Lewis, F. D.; Liu, J.; Weigel, W.; Rettig, W.; Kurnikov, I. V.; Beratan, D. N. *Proc. Natl. Acad. Sci. U.S.A.* **2002**, *99*, 12536-12541.
[31] Treadway, C. R.; Hill, M. G.; Barton, J. K. *Chem. Phys.* **2002**, *281*, 409-428 and references therein.
[32] a) García Martínez, A.; Osío Barcina, J. *The Diphenylmethane Moiety* In *Encyclopedia of Supramolecular Chemistry*, Atwood, J. L., Steed J. W., Eds.; Marcel Dekker, New York, 2004. b) García Martínez, A.; Osío Barcina, J.; Albert, A.; Cano, F. H.; Subramanian, L. R. *Tetrahedron Lett.* **1993**, *34*, 6753-6756.
[33] Vögtle, F. In *Cyclophane Chemistry*, Wiley, New York, 1993. Chap. 9, p. 405.
[34] For recent examples of π-stacked protophanes, see: a) Kurth, T. L.; Lewis, F. D. *J. Am. Chem. Soc.* **2003**, *125*, 13760-13767. b) Lewis, F. D.; Daublain, P.; Delos Santos, G. B.; Liu, W.; Asatryan, A. M.; Markarian, S. A.; Fiebig, T.; Raytchev, M.; Wang, Q. *J. Am. Chem. Soc.* **2006**, *128*, 4792-4801. c) Zeidan, T. A.; Wang, Q.; Fiebig, T.; Lewis, F. D. *J. Am. Chem. Soc.* **2007**, *129*, 9848-9849.

bridged by a sp^3-hybridized spacer (homoconjugated), with barriers to rotation of the aryl rings in DPN´s in the range of 12.5-17.5 kcal.mol^{-1}.[32,35] On the basis of these characteristics, DPN has shown to be a good model system for the study of aromatic face-to-face[35] and edge to face[36] interactions, the design of homoconjugated NLO-active chromophores[37] and the synthesis of preorganized macrocycles able to act as molecular clocks.[38]

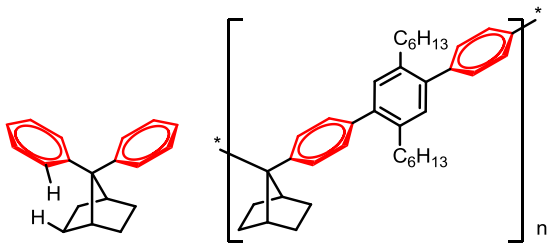

1 (DPN) **2**

Figure 1. Structures of 7,7-diphenylnorbornane (**1**) (DPN) and polymer **2**.

On the other hand, organic oligomers and polymers in which electron delocalization takes place through aromatic homoconjugation remain almost unexplored, despite their potential interest due to the similar properties that these non-conventional delocalized systems could exhibit in comparison to conjugated oligomers and polymers. In previous works we have described the first examples of a soluble polymer with alternating conjugation-homoconjugation[39] as well as homoconjugated oligomers[40] based on DPN. In

[35] García Martínez, A.; Osío Barcina, J.; de Fresno Cerezo, A.; Gutiérrez Rivas, R. *J. Am. Chem. Soc.* **1998**, *120*, 673-679.
[36] García Martínez, A.; Osío Barcina, J.; de Fresno Cerezo, A. *Chem. Eur. J.* **2001**, *7*, 1171-1175.
[37] García Martínez, A.; Osío Barcina, J.; de Fresno Cerezo, A.; Rojo, G.; Agulló-López, F. *J. Phys Chem. B* **2000**, *104*, 43-47.
[38] García Martínez, A.; Osío Barcina, J.; Colorado Heras, M. R.; de Fresno Cerezo, A.; Torres Salvador, M. R. *Chem. Eur. J.* **2003**, *9*, 1157-1165. For a description of stereorigid *ansa*-titanocenes derived from 7,7-bisindenylnorbornane, see: Lobón-Poo, M.; Osío Barcina, J.; García Martínez, A.; Expósito, M. T.; Vega, J. F.; Martínez-Salazar, J. Reyes, M. L. *Macromolecules* **2006**, *39*, 7479-7482.
[39] García Martínez, A.; Osío Barcina, J.; de Fresno Cerezo, A.; Schlüter, A.-D.; Frahn, J. *Adv. Mater.* **1999**, *11*, 27-31.

both cases, the cofacial DPN subunits contribute effectively to the electronic delocalization along the structures of the molecules. In the case of homoconjugated oligomers derived from DPN we have shown that the effective length of homoconjugation is in the range 5-6 phenyl rings.[40]

Some examples of systems that include diphenylmethane (DPM) subunits in their structure have been described, but in these cases, non-cofacial DPM acts mainly as conjugation interrupter or barrier.[4b,41,42,43,44] In conjugated polymeric systems, block copolymers are obtained by the introduction of non-conjugative interrupters in the main chain. The strategy of including conjugated sequences separated by non-conjugated spacers or fragments is an important tool in order to tailor the morphology, processability, stability as well as optical and electrical properties of the corresponding materials since such polymers are expected to retain the electronic and optical properties of the conjugated oligomeric chromophores.[2,4,45]

In the present work we gain further insight into the synthesis and properties of a new class of fluorescent polymers with alternated homoconjugated-conjugated backbone structure. Unlike similar block copolymers, cofacial DPN´s contribute efficiently to electron delocalization along the polymer chain.

[40] Caraballo-Martínez, N.; Colorado Heras, M. R.; Mba Blázquez, M.; Osío Barcina, J.; García Martínez, A.; Torres Salvador, M. R. *Org. Lett.* **2007**, *9*, 2943-2946.
[41] Tour, J. M.; Rawlett, A. M.; Kozaki, M.; Yao, Y.; Jagessar, R. C.; Dirk, S. M.; Price, D. W.; Reed, M. A.; Zhou, C.-W.; Chen, J.; Wang, W.; Campbell, I. *Chem. Eur. J.* **2001**, *7*, 5118-5134.
[42] Peng, K.-Y.; Chen, S.-A.; Fann, W.-S. *J. Am. Chem. Soc.* **2001**, *123*, 11388-11397.
[43] For examples of systems with alternating conjugation-π-stacking, see references 22, 24 and 25.
[44] Cofacial π-stacked fluorenes with methylene bridges are described in reference 26.
[45] *Handbook of Polymer Synthesis*, Kricheldorf, H. R., Nuyken, O., Swift G., Eds.; Marcel Dekker, New York, 2005.

1.2.2 Results and Discussion

1.2.2.1 Synthesis of polymers and reference compounds

In a previous paper[39] we have described the synthesis of the alternating homoconjugated-conjugated polymer **2** (Figure 1) by Suzuki polycondensation reaction.[46] Hexyl alkyl chains were introduced in the *p*-terphenyl segment in order to increase the solubility of the polymer. However, the steric hindrance caused by these chains increases the torsional angle between the aryl rings and, as a consequence, the conjugation in the *p*-terphenyl subunit and the electronic delocalization in the polymer decreased.

Now we report the syntheses of two new block-copolymers with alternating homoconjugation-conjugation, **8** and **11** (Scheme 1) and compare their electronic properties with those found in polymer **2**. Alkyl chains (*n*-C_8H_{17}), necessary to ensure the solubility of the polymers, are now introduced as substituents in the norbornane skeleton with the idea of increasing the conjugation in the *p*-terphenyl and biphenyl subunits. As can be seen, the main difference between **8** and **11** is the relative contribution of homoconjugation *vs.* conjugation to the backbone structure of the polymers, since **8** can be described as a series of DPN subunits bridged by *p*-phenylene rings, while in the case of **11**, the DPN´s are linked together, yielding a polymer with a higher degree of homoconjugation than **8**.

[46] For reviews on synthesis of conjugated polymers by organometallic polycondensation reactions, see: a) Yamamoto, T. *Macromol. Rapid Commun.* **2002**, *23*, 583-606. b) Babudri, F.; Farinda, G. M.; Naso, F. *J. Mater. Chem.* **2004**, *14*, 11-34. For some recent examples of Suzuki polycondensation reactions, see: c) Kandre, R.; Feldman, K.; Meijer, H. E. H.; Schlüter, A. D. *Angew. Chem. Int. Ed.* **2007**, *46*, 4956-4959. d) Yokoyama, A.; Suzuki, H.; Kubota, Y.; Ohuchi, K.; Higashimura, H.; Yokozawa, T. *J. Am. Chem. Soc.* **2007**, *129*, 7236-7237. e) Brookins, R. N.; Schanze, K. S.; Reynolds, J. R. *Macromolecules* **2007**, *40*, 3524-3526. f) Kowitz, C.; Wegner, G. *Tetrahedron* **1996**, *53*, 15553-15574. g) Goodson, F. E.; Novak, B. M. *Macromolecules* **1997**, *30*, 6047-6055.

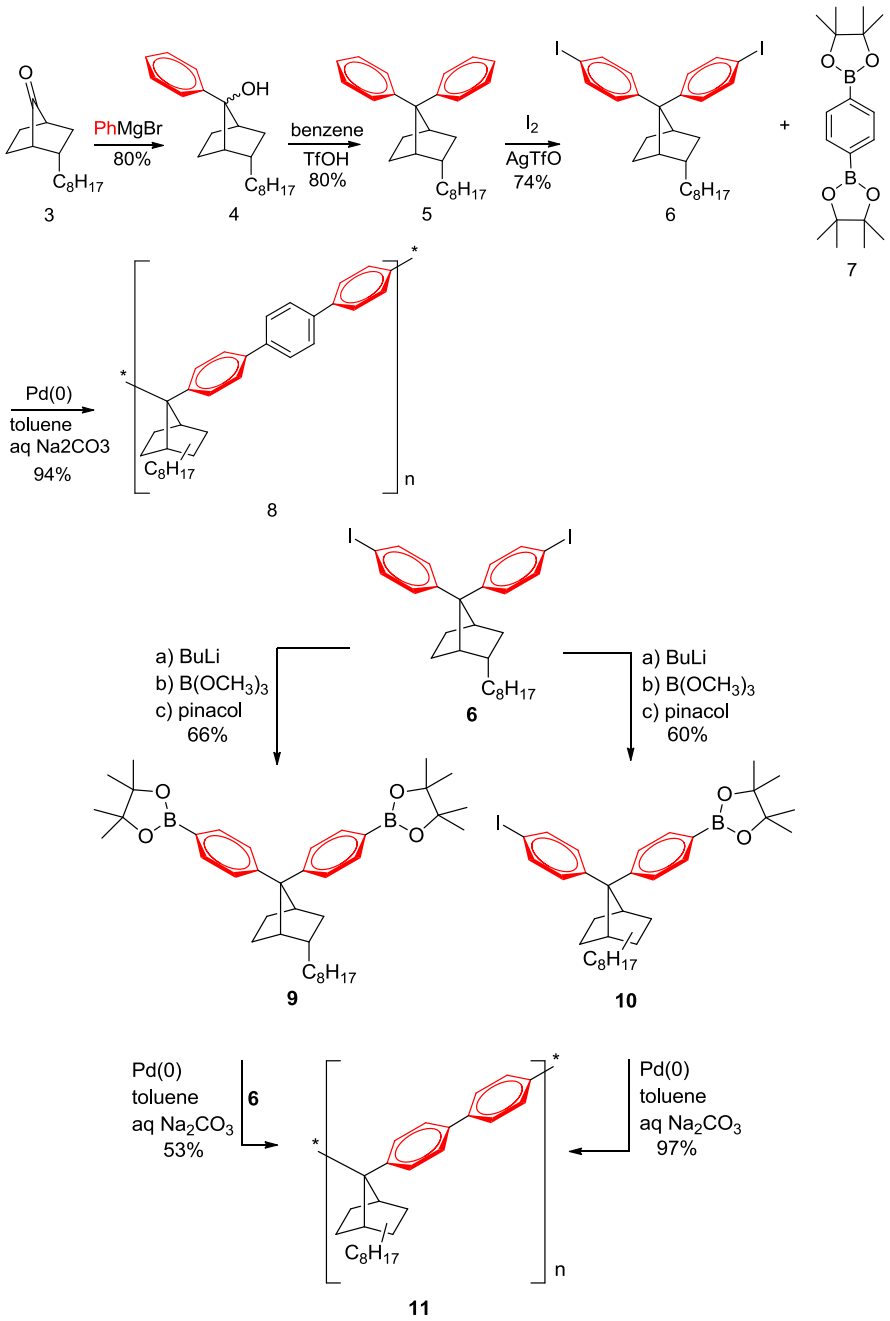

Scheme 1. Synthetic route for the preparation of polymers **8** and **11**.

Polymers **8** and **11** were prepared starting from 2-*endo*-octyl-7-norbornanone (**3**)[40] according to the synthetic procedure described in Scheme 1 employing the Suzuki polycondensation methodology followed previously by us in the case of **2**.[39] In order to facilitate the elucidation of the structures of polymers **8** and **11** as well as the study of their properties, we have also synthesized the corresponding monomeric reference compounds **13** and **15** by Suzuki coupling reactions of iodide **12** and boronates **7** or **14** (Scheme 2).

Although boronic acids have been often directly used as reagents in poly-Suzuki couplings, boronic esters like **9**, **10**, or **14** have proven to be more advantageous in this kind of reactions, since the presence of the 1,1,2,2-tetramethylethylene glycol units has a protective effect on the labile boronic acid precursor. Simultaneously to the polymerization, a hydroxylation deprotection process takes place, in which the removal of such protecting groups as ethylene glycol does not affect the couplings.[46f,g] Polymer **8** is obtained in almost quantitative yield by Pd(0) catalyzed reaction of diiodide **6** with diboronate **7** (Scheme 1). If benzene-1,4-diboronic acid is used instead of **7**, the yield of polymer **8** diminishes considerably.

As it can be seen in Scheme 1, two different protocols were followed for the synthesis of polymer **11**: (i) condensation of two different monomers **9** and **6** (AA-type monomer + BB-type monomer) and (ii) condensation of bifunctional monomer **10** (AB-type monomer). The best results (97%) were obtained by polycondensation reaction of iodoboronate **10** catalyzed by [$Pd(PPh_3)_4$]. Both polymers were obtained as white solids, soluble in common organic solvents (toluene, THF, $CHCl_3$) and show the expected spectroscopic (^{1}H- and ^{13}C-NMR) signals. We have shown that one of the main advantages of Suzuki polycondensation reactions is the high regioselectivity of the catalytic process that allows the synthesis of structurally well defined polymers.[39,46] The structures of **8** and **11** were confirmed by comparison of their NMR spectra with those of reference compounds **13** and **15**.

Gel permeation chromatography (GPC) revealed the following degrees of polymerization and polydispersities (PDI): **8**: M_w = 3470, M_n = 2600, *PDI* = 1.3; **11**: M_w = 6440, M_w = 4650, *PDI* = 1.4 (Table 1). The degrees of polymerization of **8** and **11** are lower than the obtained previously for the analogous polymer **2** under the same reaction conditions. The reason is

probably their lower solubility due to the fact that only one alkyl chain has been introduced in the structure of norbornane.

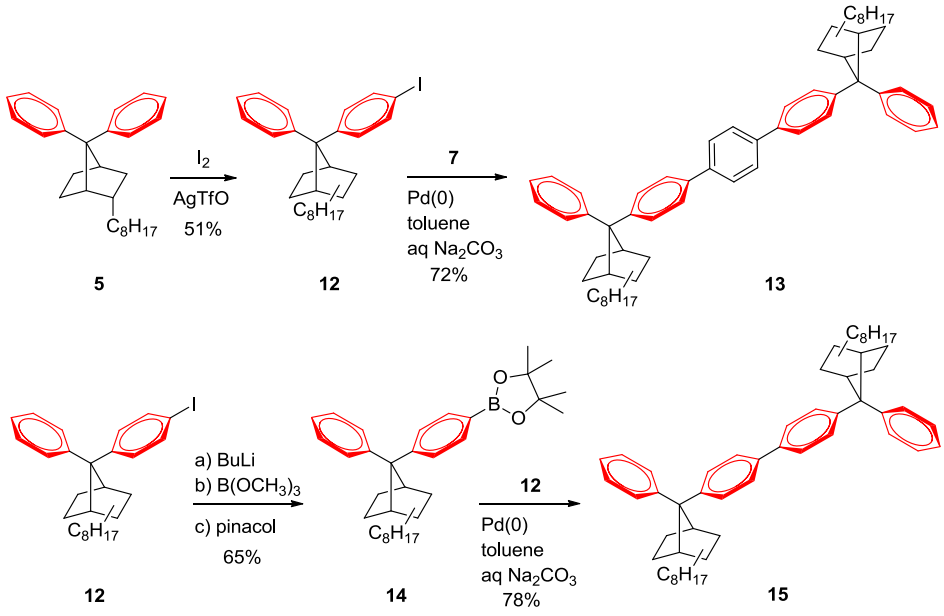

Scheme 2. Synthetic route for the preparation of reference compounds **13** and **15**.

1.2.2.2 Optical and Electrochemical Properties

The most relevant information from polymers **8** and **11** in relation to the extension of electron delocalization is obtained from their absorption spectra (Table 1) and the electrochemical behaviour of reference compound **13** (Table 2). It is well established that a convenient way to study electron delocalization in polymers is by means of absorption spectroscopy, comparing the spectra of the polymers and monomeric model compounds.[47] Extension of π-conjugation causes bathochromic shifts of the π-π* bands of the polymers relative to the

[47] a) Morisaki, Y.; Chujo, Y. *Macromolecules* **2002**, *35*, 587-589. b) Morisaki, Y.; Ishida, T.; Chujo, Y. *Macromolecules* **2002**, *35*, 782-7877. c) Morisaki, Y.; Chujo, Y. *Macromolecules* **2003**, *36*, 9319-9324. d) Morisaki, Y.; Chujo, Y. *Bull. Chem. Soc. Jpn.* **2005**, *78*, 288-293.

absorption of the reference compounds. The λ_{max} values of **8** and **11** as well as of polymer **2** are shown in Table 1.

Table 1. Properties of Polymers **8**, **11** and **2**.

Comp.	Yield (%)	M_w[a]	M_n[a]	PDI[a]	λ_{abs} /nm	λ_{em} /nm	Stokes shift[b]	λ_{onset} /nm	E_g^{opt} /eV
8	94	3470	2600	1.3	298	366	68	342	3.62
11	97	6440	4650	1.4	283	337	54	319	3.89
2	94	21600	8820	2.4	268	348	80	308	4.02

[a] Determined by GPC in THF by using a calibration curve of polystyrene standards. [b] In nm.

The λ_{max} values of reference compounds **13** and **15** as well as those of *p*-quaterphenyl, *p*-terphenyl and biphenyl are also included in Table 2 for comparison. The corresponding absorption spectra are displayed in Figure 2.

Table 2. Properties of reference compounds **13** and **15**, and p-quaterphenyl, p-terphenyl and biphenyl.

Compound	λ_{abs} [a,b]	λ_{em} [a,b]	Stokes shift[b]	λ_{onset} [b]	E_g^{opt} /eV	$E_{oxd}^{1/2}$ /V	E^{HOMO} /eV	E^{LUMO} /eV
13	295	361	66	335	3.70	1.11[c] 1.18,1.43[d]	-5.37	-1.67
15	272	325	53	310	4.00	-	-	-
p-quaterphenyl	292	364	72	334	3.71	1.09[c]	-5.41	-1.70
p-terphenyl	274	338	64	312	3.97	1.44[d] (1.5[e])	-5.56	-1.59
biphenyl	247	315	68	278	4.46	-	-	-

[a] In CH_2Cl_2. [b] In nm. [c] In CH_2Cl_2 containing 0.1M nBu$_4$NClO$_4$ as supporting electrolyte; potentials were recorded using Ag/AgCl as reference electrode and values are given *vs.* Fc/Fc$^+$. [d] In CH_3CN containing 0.1M nBu$_4$NClO$_4$ as supporting electrolyte; potentials were recorded *vs.* Ag/AgCl and calibrated with Fc/Fc$^+$. [e] See ref. [50b].

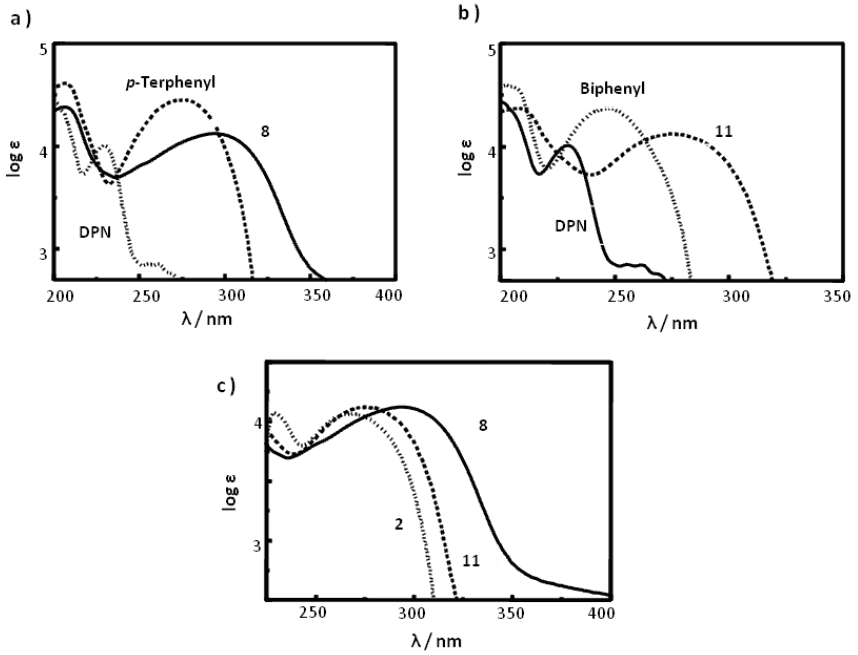

Figure 2. a) Absorption spectra of polymer **8**, 7,7-diphenylnorbornane (DPN) and p-terphenyl; b) Absorption spectra of polymer **11**, DPN and biphenyl; c) Absorption spectra of polymers **8**, **11**, and **2**.

In previous works we shown that, as a result of aromatic homoconjugation, the absorption spectrum of cofacial DPN shows an additional band centred at 228 nm (Figure 2).[32,35,40] In DPN oligomers, this band shows a red shift on going from the monomer to the tetramer (250 nm), pointing to effective electron delocalization in aromatic homoconjugated systems. When DPN subunits are attached at the end of *p*-terphenyl (reference compound **13**) or biphenyl (reference compound **15**), the characteristics absorption bands of these hydrocarbons[48] are bathochromically shifted from 274 nm to 295 nm in the case of *p*-terphenyl ($\Delta\lambda$ = 21 nm) and from 247 nm to 272 nm in the case of biphenyl ($\Delta\lambda$ = 25 nm) (Table 2), showing the effect that the addition of

[48] For a study on absorption spectra and effective conjugation length of oligo-*p*-phenylenes, see: Grimme, J.; Kreyenschmidt, M.; Uckert, F.; Müllen, K. *Adv. Mater.* **1995**, *7*, 292-295.

homoconjugated subunits exerts on the electronic properties of the corresponding systems.

On the other hand, the corresponding spectra of polymers **8** and **11** are red shifted in comparison to reference compounds **13** and **15**, which further evidences the effect of homoconjugation on the electronic properties of these materials. Figure 2a shows the spectra of DPN, **8** and *p*-terphenyl and, as can be seen, the spectrum of **8** shows a broad absorption between 235-350 nm, centred at 298 nm and red shifted in comparison to *p*-terphenyl (24 nm). Polymer **11** (Figure 2b) shows also a broad band, centred at 283 nm and bathochromically shifted in comparison to biphenyl (36 nm) and **15** (11 nm). Finally, Figure 2c shows the spectra of polymers **8**, **11** and **2**.

The higher value of λ_{max} is observed for the polymer containing the longest conjugated subunit (polymer **8**, *p*-terphenyl). As expected, introduction of alkyl chains, needed to ensure the solubility of the materials, in the structure of norbornane instead of in the *p*-terphenyl subunit (polymers **8** and **2**) increases the conjugation and, as a consequence, a bathochromic shift (30 nm) of the corresponding absorption band is observed (Table 1). It should be noted that the λ_{max} of polymer **11**, with biphenyl instead of *p*-terphenyl subunits, is red shifted in comparison to polymer **2**, also because of the distorting influence of the alkyl chains in the case of **2**.

The optical band gap (E_g^{opt}) of polymers **8**, **11**, and **2** (Table 1) and reference compounds **13** and **15** (Table 2) can be obtained from the edge of the absorption spectra (λ_{onset}) using the equation $E_g^{opt} = 1240 / \lambda_{onset}$. The smaller band gap is obtained for polymer **8** (3.62 eV), which shows higher electron delocalization than polymers **11** (3.89 eV) and **2** (4.02 eV). Comparison of the band gaps of compounds **13** (3.70) and **15** (4.00 eV) with those of *p*-terphenyl (3.97 eV) and biphenyl (4.46 eV) respectively indicates again an extension of the electron delocalization via homoconjugation with the DPN subunits. Therefore, the band gap of **13** (3.70 eV) is almost the same than the obtained for *p*-quaterphenyl (3.71 eV) and the corresponding band gap obtained for **15** (4.00 eV) very similar to the value measured for *p*-terphenyl (3.97 eV). These results, as well as the data obtained from the emission spectra (*vide supra*), suggest that the homoconjugative effect of two DPN´s is comparable to the delocalization caused by an additional conjugated phenyl ring.

In summary, the results obtained from the absorption spectra of all the compounds described in this work clearly show that the homoconjugated subunits of DPN contribute significantly to electron delocalization and, hence, to the electronic properties of the polymers. This situation differs from the described for other poly(biphenylmethylene)s in which the methylene group interrupts the conjugation between the aromatic groups.[49]

We have also used cyclic voltammetry to prove the electronic delocalization caused by the homoconjugated DPN subunits. The compounds described in this work are relatively difficult to oxidize and reduce and, for this reason, we have limited the study to model compound **13** as well as *p*-terphenyl and *p*-quaterphenyl.[50] We have determined the oxidation potentials both in CH_2Cl_2 and acetonitrile due to the different solubility of *p*-terphenyl and *p*-quaterphenyl. The results are summarized in Table 2. In CH_2Cl_2, **13** exhibited one reversible oxidation potential at 1.11 V (Figure 3) (two irreversible oxidation processes at 1.18 and 1.43 V were recorded in acetonitrile). As can be seen, the oxidation potential of **13** (1.11 V, CH_2Cl_2) is almost the same than the oxidation potential of *p*-quaterphenyl (1.09 V, CH_2Cl_2), but considerably lower than the oxidation potential of *p*-terphenyl (1.18 *vs.* 1.44 V, both measured in acetonitrile), which further supports the previously mentioned similar effect of two DPN's and one phenyl ring on electron delocalization. On the other hand, the difference between the first and the second oxidation potentials in **13** (0.25 V, acetonitrile) points to efficient radical cation delocalization along the homoconjugated backbone.

The corresponding HOMO energy values (Table 2) have been calculated from the onset of the oxidation potentials (**13**: 1.03 eV; *p*-quaterphenyl: 1.07 eV; *p*-terphenyl: 1.22 eV) using the equation $-E^{HOMO} = E_{oxd}^{onset} + 4.44$ eV.[51]

[49] Only a few examples of poly(biphenylmethylene)s have been described: a) Del Rosso, P. G.; Almassio, M. F.; Antollini, S. S.; Garay, R. O. *Opt. Mater.* **2007**, *30*, 478-485. b) Beinhoff, M.; Bozano, L. D.; Scott, J. C.; Carter, K. R. *Macromolecules* **2005**, *38*, 4147-4156. c) Havelka-Rivard, P. A.; Nagai, K.; Freeman, B. D.; Sheares, V. V. *Macromolecules* **1999**, *32*, 6418-6424. See also: d) Del Rosso, P. G.; Almassio, M. F.; Aramendia, P.; Antollini, S. S.; Garay, R. O. *Eur. Polym. J.* **2007**, *43*, 2584-2593. e) Fáber, R.; Staško, A.; Nuyken, O. *Macromol. Chem. Phys.* **2001**, *202*, 2321-2327.

[50] a) Bohnen, A.; Räder, H. J.; Müllen, K. *Synth. Met.* **1992**, *47*, 37-63. b) Eiras, C.; Foschini, M.; Faria, R. M.; Gonçalves, D. *Mol. Cryst. Liq. Cryst.* **2002**, *374*, 493-496.

[51] Bredas, J. L.; Silbey, R.; Boudreaux, D. S.; Chance, R. R. *J. Am. Chem. Soc.* **1983**, *105*, 6555-6559.

Unfortunately, we were not able to measure the reduction potential of **13**, and therefore, the corresponding LUMO energy level as well of those of *p*-quaterphenyl and *p*-terphenyl could only be estimated from the HOMO energy levels and the optical band gaps ($E^{LUMO} = E^{HOMO} + E_g^{opt}$) (Table 2).

These results show that linking two DPN subunits to *p*-terphenyl increases the energy of the HOMO orbital of *p*-terphenyl from -5.56 eV to -5.37 eV, a value slightly higher than the HOMO orbital of *p*-quaterphenyl (-5.41 eV). A similar situation is observed for the LUMO energy values, pointing to the effective electronic delocalization caused by the homoconjugated DPN subunits.

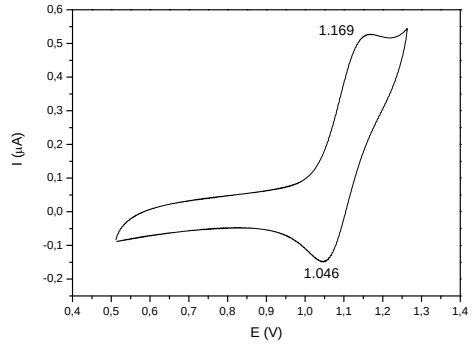

Figure 3. Cyclic voltammogram of compound **13** in 0.1M *n*-Bu_4NClO_4 – CH_2Cl_2.

1.2.2.3 Fluorescent properties

The fluorescence emission spectra of polymers **8**, **11** and **2** as well as of those of reference model compounds **13** and **15** (Tables 1 and 2) measured in CH_2Cl_2 are shown in Figure 4. The emission peaks of all the compounds studied are observed in the UV region, between 366-337 nm in the case of the polymers and at 361 nm and 325 nm in models **13** and **15**, respectively, as expected for compounds with *p*-phenylenes as chromophores.

The influence of including homoconjugated DPN subunits in the backbone structure of the polymers is again very clear by comparing the λ_{em} values of polymer **8** (366 nm), model compound **13** (361 nm), *p*-terphenyl (338 nm) and

p-quaterphenyl (364 nm). The same trend is observed for the case of polymer **11** (337 nm), model compound **15** (325 nm) and biphenyl (315 nm).

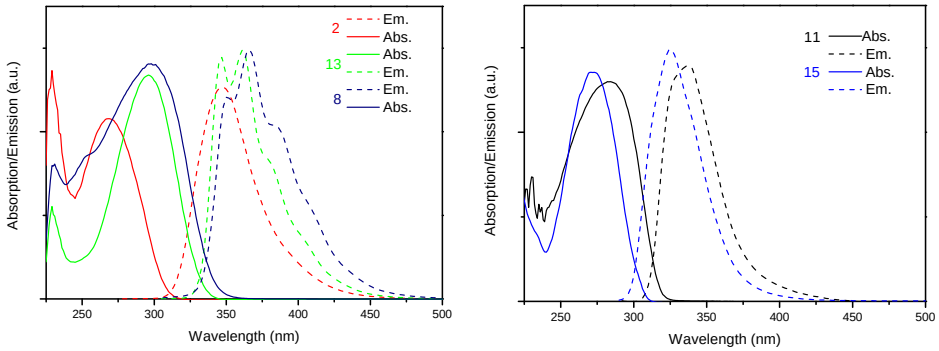

Figure 4. Absorption and emission spectra of polymers **8**, **11** and **2** and reference compounds **13** and **15** in CH_2Cl_2 excited at their respective longest wavelength absorption maximum.

The shapes of the absorption and emission spectra of polymers **11** and **2** and model compound **15** follow the mirror image rule, although in the cases of the emission spectra of **11** additional shoulders in the emission band start to be appreciable.

On the contrary, the shapes of **8** and **13** do not follow the mirror image rule and resemble the shape observed for *p*-quaterphenyl. The breakdown of the mirror image symmetry in the optical/emission spectra of oligo(*p*-phenylene)s has been extensively studied[52] and a clear correlation between the phenylene ring librations and the violation of the mirror symmetry rule has been be established. Therefore, the different shapes observed for the emission of polymers **8** and **2** can be attributable to the lower degree of torsional freedom of the *p*-terphenyl subunit of **2** caused by the alkyl chains, while in polymer **8**, as well as in **13**, the librations of the unsubstituted aryl rings are responsible of the unsymmetrical shapes observed in the emission spectra. It should be mentioned that the librational barrier of the aryl rings in DPN is considerably high (12.5 kcal/mol).[32,35]

The Stokes shifts of polymers **8** (68 nm) and **11**(54 nm) (Table 1) are relatively large and very similar to the values of the corresponding reference

[52] Heimel, G.; Daghofer, M.; Gierschner, J.; List, E. J. W.; Grimsdale, A. C.; Müllen, K.; Beljonne, D.; Brédas, J.-L.; Zojer, E. *J. Chem. Phys.* **2005**, *122*, 54501.

compounds **13** (66 nm) and **15** (53 nm) (Table 2). Therefore, the overlap of the absorption and emission spectra is weak. It should be noted that the Stokes shift in the case of polymer **2** (80 nm) is considerably higher than in polymer **8** (68 nm). Both polymers have a similar structural backbone of poly(terphenylmethylene), but in the case of **2** the alkyl chains linked to the central aryl ring diminish the electronic conjugation in the terphenyl subunit. In this case, the larger Stokes shift is mainly due to the pronounced blue shift of the absorption spectra of **2** (30 nm) caused by its limited conjugation rather than to the red-shift of **8**, that places its λ_{max} value even at lower wavelengths than the λ_{max} of polymer **11**, a poly(biphenylmethylene), while the differences in the emission spectra are not so pronounced (18 nm) and the λ_{em} follow the order **8** (366 nm) > **2** (348 nm) > **11** (337 nm).

1.2.3 Conclusion

Suzuki polycondensation reaction has been used for the synthesis of block copolymers with alternating homoconjugation-conjugation derived from 7,7-diphenylnorbornane (DPN) ((poly(biphenylmethylene)s and poly(terphenylmethylenes)s). The special topology of homoconjugated DPN allows the preparation of conjugated biphenyls or *p*-terphenyls separated by a spacer with geometry halfway between conjugated and π-stacked aryl rings, which contribute to the delocalization of the electrons along the backbone structure of the polymers.

The absorption and emission spectra of the polymers and model compounds demonstrate that the introduction of homoconjugated subunits leads to an extension of the delocalization that modify the electronic properties of the polymers in comparison to other systems in which the conjugated subunits are separated by saturated carbon atoms that act as interrupters of the conjugation.

Also cyclic voltammetry studies, carried out on model compound **13**, shows that homoconjugation enhances the degree of electron delocalization since lower oxidation potentials are observed upon increasing the molecular length by linking two DPN subunits to *p*-terphenyl. Our results show that the delocalization effect caused on oligo *p*-phenylenes by two homoconjugated aryl rings is in the same range than the effect produced by one additional

conjugated aryl ring. The electron delocalization mediated by aromatic homoconjugation observed in our systems differs from the situation observed in homoconjugated acetylenes in which no significant homoconjugative stabilization is observed.[53]

In summary, the polymers described by us can be considered as a new class of delocalized structures with a degree of delocalization between all-conjugated block copolymer[54] and block copolymers with conjugated segments separated by interrupters. The introduction of homoconjugated subunits in these materials may be an efficient method to modulate and control some important properties such as the band gap of the polymers, the dielectric constant,[55] or their optical and electrochemical properties. The synthesis of new polymers with alternating homoconjugation-conjugation and the study of their optical and electronic properties are currently in progress.

[53] For a review on homoconjugated acetylenes, see: de Meijere, A.; Kozhushkov, S. I. In *Macrocyclic Structurally Homoconjugated Oligoacetylenes: Acetylene- and Diacetylene-Expanded Cycloalkanes and Rotaxanes*, in *Top. Curr. Chem.* **1999**, *201*, 1-42.
[54] Scherf, U.; Gutacker, A.; Koenen, N. *Acc. Chem. Res.* **2008**, *41*, 1086-1097.
[55] Maier, G. *Prog. Polym. Sci.* **2001**, *26*, 3-65.

1.2.4 Experimental Section

General Information

^{1}H and ^{13}C NMR spectra were recorded on a 200 MHz spectrometer. Chemical shifts are given in ppm relative to TMS (^{1}H, 0.0 ppm) and $CDCl_3$ (^{13}C, 77.0 ppm). Coupling constants are given in Hertz. UV spectra were measured using hexane as solvent. Cyclic voltammetry experiments were performed with a computer controlled potentiostat in a three-electrode single-compartment cell (5 mL). The platinum working electrode consisted of a platinum wire sealed in a soft glass tube with a surface of A = 0.785 mm^2, which was polished down to 0.5 μm with polishing paste prior to use in order to obtain reproducible surfaces. The counter electrode consisted of a platinum wire and the reference electrode was a Ag/AgCl secondary electrode. All potentials were internally referenced to the ferrocene–ferrocinium couple. For the measurements, concentrations of 5.10^{-3} $mol.L^{-1}$ of the electroactive species were used in freshly distilled and deaerated dichloromethane or acetonitrile and 0.1 M tetrabutylammonium perchlorate (Bu_4NClO_4) which was twice recrystallized from ethanol and dried under vacuum prior to use.

All experiments were carried out under argon atmosphere using standard Schlenk techniques. Anhydrous solvents were distilled under argon from sodium/benzophenone ketyl. Flash chromatography was performed over silica gel 60 (230-400 mesh). All commercially available compounds were used without further purification. 1,4-Benzenediboronic acid bis(pinacol) ester (**7**), AgOTf and $[Pd(PPh_3)_4]$ were purchased from commercial suppliers. The preparation of **3**, **4**, **5** and **6** have been described previously.[40] Iodide **12** was obtained according to the procedure used for diiodide **6**.[40,56] Polymerization reactions have been carried up following the Suzuki policondensation reaction employed by us previously for the synthesis of polymer **2**.[39]

Experimental procedures

2-*endo*-octyl-7-(4-iodophenyl)-7-phenyl-norbornane (12): A solution of 0.25 g (1.00 mmol) of I_2 in 25 mL of $CHCl_3$ was slowly added at 25ºC with vigorous stirring and protected from light to 0.36 g (1.00 mmol) of 2-*endo*-octyl-7,7-diphenylnorbornane (**5**) and 0.26 g (1.00 mmol) of AgOTf in 20 mL of $CHCl_3$. After disappearance of iodine, silver iodide was separated by filtration and the organic solution was washed with saturated $NaHCO_3$ (1 x 20 mL), 10% $Na_2S_2O_3$ (2 x 20 mL), water (1 x 20 mL) and dried over $MgSO_4$. After evaporation of the solvent under vacuum, the mixture of *syn*- and *anti*-(**12**) was purified by flash chromatography (silica gel, hexane/dichloromethane 80:20). Yield 51 %, colorless oil. ^{1}H NMR (200 MHz, $CDCl_3$, 25ºC, TMS): δ= 7.53 (d, ^{3}J(H,H) = 8.4 Hz, 2H), 7.35 (d, ^{3}J(H,H) = 8.4 Hz, 2H), 7.23-7.02 (m, 5H), 2.97-2.92 (m, 2H), 1.90-1.75 (m, 2H), 1.69-1.42 (m, 4H), 1.40-1.10 (m, 14H), 0.88 (t, ^{3}J(H,H) = 6.8 Hz, 3H), 0.81-0.72 (m, 1H) ppm; ^{13}C NMR (50 MHz $CDCl_3$, 25ºC, TMS): δ= 146.1, 145.7, 145.2, 137.4, 137.3, 129.6, 129.4, 128.5, 128.4, 127.3, 127.0, 125.5, 90.5, 65.7, 45.1, 41.8, 37.1, 35.9, 32.8, 31.9, 30.0, 29.6, 29.3, 28.7,

[56] Kobayashi, Y.; Kumadaki, I.; Yoshida, T. *J. Chem. Research* **1977**, 215.

22.7, 20.7, 14.1 ppm. FTIR (film): ῡ = 3059, 3028, 2926, 2872, 2854, 1601, 1580, 1551, 1483, 1460, 1391, 1005, 908, 785, 715, 698 cm^{-1}. MS (EI, 70 eV): m/z (%): 486 (M^+, 100), 361 (39), 360 (70), 332 (53), 293 (41), 206 (80), 205 (94), 193 (58), 192 (86), 191 (51), 167 (45), 166 (29), 165 (48), 115 (43), 91 (75); Elemental analysis (%) calc for $C_{27}H_{35}I$: C 66.66, H 7.25; found: C 66.32, H 7.32.

General procedure for the synthesis of boronates 9, 10 and 14: 1.2 mmol of *n*-BuLi in hexanes (or 2.4 mmol for the preparation of **9**) were slowly added to a solution of 1.15 mmol of iodides **6** or **12** under argon atmosphere at -78ºC. The reaction was stirred for 2 h at -78ºC and then 2.30 mmol (or 4.60 mmol) of trimethyl borate were added. After stirring for 3 h at room temperature the reaction was quenched with water (20 mL) and extracted with Et_2O (3 x 25 mL). The organic solution was washed with saturated aqueous NaCl (1 x 20 mL), dried over $MgSO_4$ and the solvent was removed under vacuum. The residue was dissolved in CH_2Cl_2 (50 mL) and 1.4 mmol (or 2.8 mmol) of pinacol were added. After refluxing for 3 days using a Dean-Stark, the solvent was evaporated under vacuum and the boronates purified by flash chromatography (silica gel, hexane/diethylether 20:1).

Boronate 9: (Yield 66 %): m.p. 217-220ºC; ^{1}H NMR (200 MHz, $CDCl_3$, 25ºC, TMS): δ= 7.64 (d, ^3J(H,H = 6.9 Hz, 4H), 7.40 (d, ^3J(H,H = 6.9 Hz, 4H), 3.12-2.98 (m, 2H), 1.96-1.83 (m, 2H), 1.70-1.45 (m, 4H), 1.35-1.17 (m, 38H), 0.92-0.84 (m, 3H), 0.81-0.75 (m, 1H) ppm; ^{13}C NMR (50 MHz, $CDCl_3$, 25ºC, TMS): δ= 149.2, 148.8, 134.9, 126.9, 126.3, 83.5, 66.5, 44.9, 41.7, 37.1, 35.9, 32.8, 31.9, 30.0, 29.6, 29.3, 28.7, 24.8, 22.7, 20.7, 14.1 ppm; FTIR (film): ῡ = 2980, 2924, 2852, 1604, 1458, 1362, 1325, 1271, 1144, 1091, 908, 858, 734 cm^{-1}. MS (EI, 70 eV): m/z (%): 612 (M^+, 19), 486 (18), 442 (45), 427 (22), 419 (19), 101 (56), 91 (20), 83 (94), 73 (100), 57 (32), 55 (45); Elemental analysis (%) calc for $C_{39}H_{58}B_2O_4$: C 76.48, H 9.54; found: C 76.39, H 9.61.

Boronate 10: (Yield 60 %): m.p. 128-130 ºC; ^{1}H NMR (200 MHz, $CDCl_3$, 25ºC, TMS): δ= 7.65 (d, ^3J(H,H) = 7.4 Hz, 2H), 7.50 (d, ^3J(H,H) = 8.4 Hz, 2H), 7.37 (d, ^3J(H,H) = 7.4 Hz, 2H), 7.12 (d, ^3J(H,H) =8.4 Hz, 2H), 3.15-2.95 (m, 2H), 1.93-1.82 (m, 2H), 1.75-1.40 (m, 4H), 1.38-1.10 (m, 26H), 0.93-0.75 (m, 4H) ppm; ^{13}C NMR (50 MHz, $CDCl_3$, 25ºC, TMS): δ= 149.0, 148.5, 145.7, 137.5, 135.1, 129.6, 129.4, 126.7, 126.5, 90.6, 83.6, 65.9, 45.0, 41.7, 37.2, 35.9, 32.8, 31.9, 29.9, 29.6, 29.3, 28.7, 28.5, 24.8, 22.7, 20.7, 14.1 ppm; FTIR (film): ῡ = 2922, 2851, 1608, 1400, 1361, 1323, 1271, 1143, 1092, 1005, 858, 825, 804, 650 cm^{-1}; MS (EI, 70 eV): m/z (%): 612 (M^+, 22), 486 (29), 485 (31), 419 (19), 217 (25), 101 (35), 83 (35), 73 (100), 72 (28), 57 (25), 55 (27); Elemental analysis (%) calc for $C_{33}H_{46}BIO_2$: C 64.72, H 7.57; found: C 64.78, H 7.60.

Boronate 14: (Yield 65 %): ^{1}H NMR (200 MHz, $CDCl_3$, 25ºC, TMS): δ= 7.67 (d, ^3J(H,H) = 8 Hz, 2H), 7.47-7.34 (m, 4H), 7.18-7.02 (m, 2H), 7.00-6.89 (m, 1H), 3.01-2.88 (m, 2H), 1.96-1.83 (m, 2H), 1.72-1.45 (m, 4H), 1.41-1.10 (m, 26H), 0.95-0.84 (m, 3H), 0.82-0.75 (m, 1H) ppm; ^{13}C NMR (50 MHz, $CDCl_3$, 25ºC, TMS): δ= 149.2, 145.9, 134.9, 128.3, 127.4, 127.2, 126.9, 126.6, 125.3, 83.5, 65.2, 45.1, 41.8, 37.2, 36.0, 32.9, 31.9, 30.0, 29.6, 29.3, 28.7, 24.8, 22.7, 20.7, 14.1 ppm; FTIR (film): ῡ =

2959, 2928, 2852, 1711, 1608, 1398, 1362, 1261, 1144, 1090, 1020, 908, 808, 735, 650 cm^{-1}; MS (EI, 70 eV): m/z (%): 487 ($[M+H]^+$, 40), 486 (M^+,100), 485 (27), 386 (16), 332 (13), 204 (18), 101 (22), 91 (13), 83 (23), 55 (17); Elemental analysis (%) calc for $C_{33}H_{47}BO_2$: C 81.47, H 9.74; found: C 81.53, H 9.80.

4,4''-bis(2-*endo*-octyl-7-phenyl-7-norbornyl)-*p*-terphenyl (13): A mixture of 0.83 g (1.72 mmol) of **12** and 0.42 g (0.86 mmol) of **7** in 20 mL of toluene and 70 mL of 1M solution of $NaCO_3$ was degassed three times using the freeze-pump-thaw technique. 0.01 g (0.0086 mmol) of $[Pd(PPh_3)_4]$ were added and the reaction was heated under argon for 24h, extracted with CH_2Cl_2 (3 x 25 mL) and dried over $MgSO_4$. Evaporation of the solvent and purification of the residue by flash chromatography (silica gel, hexane) yielded 72 % of **13** as a white solid. m.p. 62-64 ºC; ^{1}H NMR (200 MHz, $CDCl_3$, 25ºC, TMS): δ= 7.53 (s, 4H), 7.50-7.40 (m, 12H), 7.27-7.15 (m, 4H), 7.10-7.00 (m, 2H), 3.10-2.95 (m, 4H), 2.03-1.82 (m, 4H), 1.75-1.45 (m, 4H), 1.42-1.06 (m, 32H), 0.95-0.73 (m, 8H) ppm; ^{13}C NMR (50 MHz, $CDCl_3$, 25ºC, TMS): δ= 146.2, 145.8, 145.4, 145.0, 139.4, 137.5, 128.3, 127.8, 127.6, 127.2, 127.0, 126.9, 125.3, 65.8, 45.2, 41.9, 37.2, 36.0, 32.9, 31.9, 31.6, 30.0, 29.6, 29.3, 28.7, 22.7, 20.8, 14.1 ppm; FTIR (film): ῡ = 3082, 3059, 3028, 2926, 2852, 1601, 1488, 1460, 1445, 1004, 812, 762, 711, 698 cm^{-1}; UV/Vis (CH_2Cl_2): λ_{max} (ε) = 295 nm (29800 $mol^{-1}dm^3cm^{-1}$); MS (EI, 70 eV): m/z (%): 795 ($[M+H]^+$, 64), 794 (M^+, 100), 601 (38), 206 (20), 169 (19), 149 (17), 143 (20), 97 (16), 91 (55), 85 (34), 83 (25), 81 (23), 71 (34), 69 (40), 67 (35), 57 (55), 56 (16), 55 (43); Elemental analysis (%) calc for $C_{60}H_{74}$: C 90.62, H 9.38; found: C 90.60, H 9.35.

4,4'-bis(7-phenyl-2-*endo*-octyl-7-norbornyl)biphenyl (15): A mixture of 0.42 g (0.86 mmol) of **12** and 0.42 g (0.86 mmol) of **14** in 20 mL of toluene and 70 mL of 1M solution of $NaCO_3$ was degassed three times using the freeze-pump-thaw technique. 0.01 g (0.0086 mmol) of $[Pd(PPh_3)_4]$ were added and the reaction was heated under argon for 24h, extracted with CH_2Cl_2 (3 x 25 mL) and dried over $MgSO_4$. Evaporation of the solvent and purification of the residue by flash chromatography (silica gel, hexane) yielded 78 % of **15** as colorless oil. ^{1}H NMR (200 MHz, $CDCl_3$, 25ºC, TMS): δ= 7.45-7.30 (m, 12H), 7.25-7.14 (m, 4H), 7.10-6.98 (m, 2H), 3.05-2.93 (m, 4H), 2.00-1.82 (m, 4H), 1.70-1.43 (m, 4H), 1.40-1.02 (m, 32H), 0.98-0.76 (m, 8H) ppm; ^{13}C NMR (50 MHz, $CDCl_3$, 25ºC, TMS): δ= 146.3, 145.8, 145.0, 144.6, 137.8, 128.3, 127.7, 127.4, 127.2, 126.8, 125.3, 65.7, 45.2, 41.9, 37.2, 36.1, 32.9, 31.9, 31.6, 30.0, 29.7, 29.3, 28.7, 22.7, 20.8, 14.1 ppm; FTIR (film): ῡ = 3028, 2926, 2854, 1711, 1599, 1493, 1460, 1379, 908, 814, 735, 700, 650 cm^{-1}; UV/Vis (CH_2Cl_2): λ_{max} (ε) = 270 nm (26000 $mol^{-1}dm^3cm^{-1}$); MS (EI, 70 eV): m/z (%): 719 ($[M+H]^+$, 65), 718 (M^+, 100), 564 (11), 526 (21), 525 (45), 143 (16), 91 (15), 55 (8) ; Elemental analysis (%) calc for $C_{54}H_{70}$: C 90.19, H 9.81; found: C 90.10, H 9.88.

General procedure for the synthesis of polymers 8 and 11 by Suzuki policondensation reaction: A mixture of 0.86 mmol of boronate **7** or **9** and 0.86 mmol of iodide **6** in 20 mL of toluene and 70 mL of 1M solution of $NaCO_3$ was degassed three times using the freeze-pump-thaw technique. 0.01 g (0.0086 mmol) of $[Pd(PPh_3)_4]$ were added and the reaction was heated under argon for three days. The organic solution was separated and concentrated to a volume of 10 mL. Methanol (150

mL) was then added dropwise with vigorous stirring. The white precipitate was separated and purified by repeating the precipitation with methanol. Polymer **11** was also obtained by reaction of 1.76 mmol of **10** and 0.01 g (0.0086 mmol) of $[Pd(PPh_3)_4]$ under the same reaction conditions.

Polymer 8: (Yield 94 %): ^{1}H NMR (200 MHz, $CDCl_3$, 25ºC, TMS): δ= 7.60-7.10 (m, 12H), 3.20-2.90 (m, 2H), 2.00-1.90 (m, 2H), 1.85-1.10 (m, 18H), 0.90-0.80 (m, 4H) ppm; ^{13}C NMR (50 MHz, $CDCl_3$, 25ºC, TMS): δ= 145.3, 144.9, 139.4, 137.6, 128.6, 127.8, 127.6, 127.1, 126.9, 65.5, 45.3, 42.0, 37.2, 36.1, 33.0, 31.9, 31.2, 30.0, 29.7, 29.3, 28.8, 22.7, 20.8, 14.1 ppm; FTIR (film): ῡ = 2922, 2851, 1261, 1101, 1022, 806 cm^{-1}. UV/Vis (CH_2Cl_2): λ_{max} (ε) = 298 nm (14400 $mol^{-1}dm^3cm^{-1}$); Elemental analysis (%) calc for $(C_{33}H_{38})_n$: C 91.19, H 8.81; found: C 91.23, H 8.79; weight-average molecular weight (M_w): 3470 and polydispersity index (PDI): 1.3.

Polymer 11: (Yield 97 %): ^{1}H NMR (200 MHz, $CDCl_3$, 25ºC, TMS): δ= 7.60-7.10 (m, 8H), 3.10-2.95 (m, 2H), 2.00-1.80 (m, 2H), 1.70-1.00 (m, 18H), 0.95-0.75 (m, 4H) ppm; ^{13}C NMR (50 MHz, $CDCl_3$, 25ºC, TMS): δ= 144.9, 144.5, 137.8, 128.6, 128.3, 127.7, 127.4, 126.8, 65.4, 45.3, 42.0, 37.2, 36.0, 32.9, 31.9, 31.6, 30.0, 29.6, 29.3, 28.7, 22.7, 20.8, 14.1 ppm; FTIR (film): ῡ = 2922, 2851, 1261, 1101, 1022, 806 cm^{-1}; UV/Vis (CH_2Cl_2): λ_{max} (ε) = 283 nm (12400 $mol^{-1}dm^3cm^{-1}$); Elemental analysis (%) calc for $(C_{27}H_{34})_n$: C 90.44, H 9.56; found: C 90.45, H 9.60; weight-average molecular weight (M_w): 6440 and polydispersity index (PDI): 1.4.

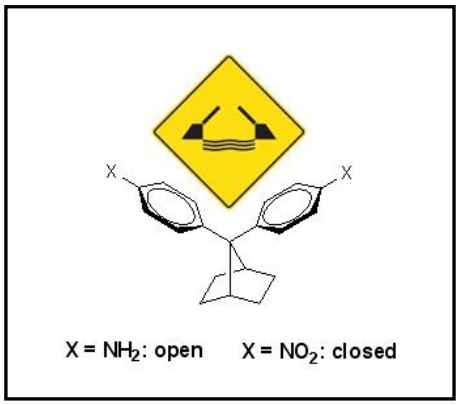

1.3 A Joint Experimental and Computational Investigation on Homoconjugated Push-Pull Chromophores Derived from 7,7-Diphenylnorbornane

We report herein the synthesis, spectroscopic properties and computational studies of novel aromatic homoconjugated compounds derived from 7,7-diphenylnorbornane (DPN). The UV/vis spectra of these compounds show bands corresponding to the respective chromophores as well as new homoconjugation bands and charge transfer absorptions in D-DPN-A push-pull derivatives. Homoconjugation between the aromatic rings strongly depends on the nature of the substitution at the aryl moieties. Therefore, electronic communication by homoconjugation can be easily tuned by controlling the electronic nature and positions of the substituents. The strong homoconjugative interaction is also reflected in the reactivity, NMR spectra and NLO properties of the compounds studied. DFT calculations nicely agree with the experimental data and shed light on the electronic delocalization via homoconjugation.

(*Eur. J. Org. Chem.* **2012**, 2643–2655)

1.3.1 Introduction

Over the past years a considerable effort has been devoted on the design, synthesis and study of the properties of conjugated push-pull molecular chromophores (D-π-A) and their oligomeric and polymeric derivatives.[1,2,3,4,5] Interest in such systems is justified by their important technological applications in molecular electronics and optoelectronics[6] as *e. g.* nonlinear optical (NLO) materials,[6,7] molecular wires,[8] solvatochromic probes,[9] or organic photorefractives.[10] Recently, several strategies have been developed in order to modulate the properties (HOMO-LUMO gap, solubility, processability) of push-pull systems. Thus, nonplanar D-π-A chromophores have been reported and the influence of nonplanarity on their conjugative

[1] R. Gompper, H.-U. Wagner, *Angew. Chem. Int. Ed.* **1988**, 27, 1437-1455.
[2] a) G. Jayamurugan, J.-P. Gisselbrecht, C. Boudon, F. Schoenebeck, W. B. Schweizer, B. Bernet, F. Diederich, *Chem. Commun.* **2011**, *47*, 4520-4522; b) Y.-L. Wu, F. Bureš, P. D. Jarowski, W. B. Schweizer, C. Boudon, J.-P. Gisselbrecht, F. Diederich, *Chem. Eur. J.* **2010**, *16*, 9592-9605; c) F. Bureš, W. B. Schweizer, J. C. May, C. Boudon, J.-P. Gisselbrecht, M. Gross, I. Biaggio, F. Diederich, *Chem. Eur. J.* **2007**, *13*, 5378-5387.
[3] W. Akemann, D. Laage, P. Plaza, M. M. Martin, M. Blanchard-Desce, *J. Phys. Chem. B* **2008**, *112*, 358-368.
[4] a) M. Moreno Oliva, J. Casado, M. M. M. Raposo, A. M. C. Fonseca, H. Hartmann, V. Hernández, J. T. López Navarrete, *J. Org. Chem.* **2006**, *71*, 7509-7520; b) B. Milián, E. Ortí, V. Hernández, J. T. López Navarrete, T. Otsubo, *J. Phys. Chem. B* **2003**, *107*, 12175-12183.
[5] a) *Electronic Materials: The Oligomeric Approach*, (Eds.: K. Müllen, G. Wegner), WILEY-VCH, Weinheim, **1998**; b) *Handbook of Conducting Polymers*, (Eds.: T. A. Skotheim, J. R. Reynolds), CRC Press, **2007**.
[6] a) *Chem. Rev.* **2007**, *107*, issue 4, special issue on organic electronics and optoelectronics; b) *J. Mater. Res.* **2004**, *19*, issue 7, special issue on organic electronics; c) G. S. He, L.-S. Tan, Q. Zheng, P. N. Prasad, *Chem. Rev.* **2008**, *108*, 1245-1330; d) J. W. Verhoeven, H. J. Van Ramesdonk, M. M. Groeneveld, A. C. Benniston, A. Harriman, *Chem. Phys. Chem.* **2005**, *6*, 2251-2260.
[7] a) S. Barlow, S. R. Marder in *Functional Organic Materials* Eds.: T. J. J. Müller, U. H. F. Bunz), WILWY-VCH, Weinheim, **2007**, pp. 393-437; b) *Chem. Phys.* **1999**, *245*, special issue on molecular nonlinear optics; c) J. Zyss, P. Kelley, P. F. Liao, *Molecular Nonlinear Optics: Materials, Physics and Devices*, Academic Press, **1993**.
[8] *Molecular Wires. From design to Properties*, (Ed.: L. de Cola); Thematic issue, *Top. Curr. Chem.* **2005**, *257*, 1-170.
[9] a) P. Milosevic, S. Hecht, *Org. Lett.* **2005**, *7*, 5023-5026; b) F. Würthner, G. Archetti, R. Schmidt, H.-G. Kuball, *Angew. Chem. Int. Ed.* **2008**, *47*, 4529-4532; c) H. Hartmann, K. Eckert, A. Schröder, *Angew. Chem. Int. Ed.* **2000**, *39*, 556-558.
[10] O. Ostroverkhova, W. E. Moerner, *Chem. Rev.* **2004**, *104*, 3267-3314.

properties has been investigated (**1**, Figure 1).[11,12,13] A different approach involves the use of bridges between the donor and acceptor groups with non-conventional electron delocalization, such as cross-conjugated bridges (**2**),[14] spirocompounds (**3**),[15] and also saturated bicyclic connectors.[16] At this respect, aromatic homoconjugated systems have received little attention.

Examples of lateral homoconjugated push-pull systems derived from triptycene have been reported.[17,18] However, electron delocalization by homoconjugation in iptycenes such as trypticene is not clear and remains controversial.[19] Very recently, homoconjugated push-pull systems obtained by [2+2] cycloaddition reaction between 2,3-dichloro-5,6-dicyano-1,4-benzoquinone (DDQ) and *N*,*N*-dialkylanilino (DAA) (**4**, Figure 1) or ferrocene

[11] a) S.-I. Kato, F. Diederich, *Chem. Commun.* **2010**, *46*, 1994-2006; b) B. Breiten, I. Biaggio, F. Diederich, *Chimia* **2010**, *64*, 409-413; c) S.-I. Kato, M. Kivala, W. B. Schweizer, C. Boudon, J.-P. Gisselbrecht, F. Diederich, *Chem. Eur. J.* **2009**, *15*, 8687-8691. See also: d) S. Sergeyev, D. Didier, V. Boitsov, A. Teshome, I. Asselberghs, K. Clays, C. M. L. Vande Velde, A. Plaquet, B. Champagne, *Chem. Eur. J.* **2010**, *16*, 8181-8190.

[12] A. Ortiz, B. Insausty, M. R. Torres, M. Á. Herranz, N. Martín, R. Viruela, E. Ortí, *Eur. J. Org. Chem.* **2008**, 99-108.

[13] R. Gómez, C. Seoane, J. L. Segura, *Chem. Soc. Rev.* **2007**, *36*, 1305-1322.

[14] a) A. B. Ricks, G. C. Solomon, M. T. Colvin, A. M. Scott, K. Chen, M. A. Ratner, M. R. Wasielewski, *J. Am. Chem. Soc.* **2010**, *132*, 15427-15434; b) R. P. Ortiz, R. M. Osuna, V. Hernández, J. T. López Navarrete, B. Vercelli, G. Zotti, V. V. Sumerin, E. S. Balenkova, V. G. Nenajdenko, *J. Phys. Chem. A* **2007**, *111*, 841-851; c) C. A. van Walree, V. E. M. Kaats-Richters, S. J. Veen, B. Wieczorek, J. H. van der Wiel, B. C. van der Wiel, *Eur. J. Org. Chem.* **2004**, 3046-3056.

[15] F. Rizzo, M. Cavazzini, S. Righetto, F. De Angelis, S. Fantacci, S. Quici, *Eur. J. Org. Chem.* **2010**, 4004-4016. See also ref. [20].

[16] R. H. Goldsmith, J. Vura-Weis, A. M. Scott, S. Borkar, A. Sen, M. A. Ratner, M. Wasielewski, *J. Am. Chem. Soc.* **2008**, *130*, 7659-7669.

[17] For recent reviews on iptycenes, see: a) L. Zhao, Z. Li, T. Wirth, *Chem. Lett.* **2010**, *39*, 658-667; b) J. H. Chong, M. J. MacLachlan, *Chem. Soc. Rev.* **2009**, *38*, 3301-3315; c) T. M. Swager, *Acc. Chem. Res.* **2008**, *41*, 1181-1189; d) J.-S. Yang, J.-L. Yan, *Chem. Commun.* **2008**, 1501-1512. See also: V. R. Skvarchenko, V. K. Shalaev, E. I. Klabunovskii, *Russ. Chem. Rev.* **1974**, *43*, 951-966.

[18] a) T. Nakazawa, I. Murata, *J. Am. Chem. Soc.* **1977**, *99*, 1996-1997; b) K. Yamamura, T. Nakazawa, I. Murata, *Angew. Chem. Int. Ed.* **1980**, *19*, 543-546; c) K. Yamamura, K. Nakasuji, H. Yamochi, *Chem. Let.* **1983**, 627-630.

[19] a) X. Gu, Y.-H. Lai, *Org. Lett.* **2010**, *12*, 5200-5203; b) V. J. Chebny, T. S. Navale, R. Shukla, S. V. Lindeman, R. Rathore, *Org. Lett.* **2009**, *11*, 2253-2256; c) T. Doerner, R. Gleiter, F. A. Neugebauer, *Eur. J. Org. Chem.* **1998**, 1615-1623; d) H.-D. Martin, B. Mayer, *Angew. Chem. Int. Ed.* **1983**, *22*, 283-314.

(Fc)-substituted alkynes have been described.[20] The resulting D-A chromophores show strong intramolecular CT interactions and promising third-order nonlinear optical properties.

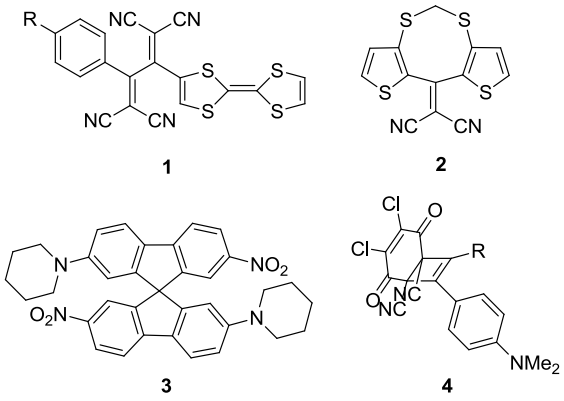

Figure 1. Examples of non planar (**1**), cross-conjugated (**2**), spiro- (**3**), and homoconjugated (**4**) push-pull chromophores.

Aromatic apical homoconjugated compounds derived from 7,7-diphenylnorbornane (DPN) (**5c**, Figure 2) are a family of interesting derivatives featuring non-conventional electron delocalization within the cofacially arranged aryl groups.[21,26] Homoconjugated push-pull systems were synthesized and used for the first time to study the nature of face to face aromatic interactions.[21] Further studies demonstrated that these compounds show remarkable second-order NLO properties, with β_z(1064 nm) values comparable to those measured for linearly conjugated analogous.[22] More recently, the first example of efficient photoinduced energy transfer mediated

[20] S. Kato, M. T. R. Beels, P. La Porta, W. B. Schweizer, C. Boudon, J.-P. Gisselbrecht, F. Diederich, *Angew. Chem. Int. Ed.* **2010**, *49*, 6207-6211.
[21] A. García Martínez, J. Osío Barcina, A. De Fresno Cerezo, R. Gutiérrez Rivas, *J. Am. Chem. Soc.* **1998**, *120*, 673-679.
[22] A. García Martínez, J. Osío Barcina, A. de Fresno Cerezo, G. Rojo, F. Agulló-López, *J. Phys Chem. B* **2000**, *104*, 43-47.

by an homoconjugated bridge in the heterodinuclear D-B-A complex [Ru-DPN-Ir]$^{3+}$ has been reported.[23]

In previous works we have studied electron delocalization in DPN as well as in derived polymers[24] and oligomers[25] by absorption spectroscopy and TD-DFT calculations.[26] The results of these investigations confirm that aromatic homoconjugation in acyclic systems is an effective mechanism for electron delocalization with an effective homoconjugation length for homoconjugated oligomers of 6-7 aryl rings. Our previous calculations also pointed out the importance of transannular interactions in push-pull systems derived from DPN.

Now, in order to check this hypothesis and provide further information on electron delocalization in these aromatic homoconjugated systems, we have performed an extensive joint computational-experimental study in substituted DPN's, with special emphasis on push-pull DPN derivatives. The electronic communication between the donor and acceptor moieties has been studied by UV/Vis and NMR spectroscopy. The experimental results were correlated with DFT and TD-DFT calculations.

1.3.2 Computational details

Geometry optimizations without symmetry constraints were carried out using the Gaussian09 suite of programs[27] at the dispersion corrected meta-

[23] J. Osío Barcina, N. Herrero-García, F. Cucinotta, L. De Cola, P. Contreras-Carballada, R. M. Williams, A. Guerrero-Martínez, *Chem. Eur. J.* **2010**, *16*, 6033-6040.

[24] a) A. García Martínez, J. Osío Barcina, A. de Fresno Cerezo, A.-D. Schlüter, J. Frahn, *Adv. Mater.* **1999**, *11*, 27-31; b) J. Osío Barcina, M. R. Colorado Heras, M. Mba, R. Gómez Aspe, N. Herrero García, *J. Org. Chem.* **2009**, *74*, 7148-7156.

[25] N. Caraballo-Martínez, M. R. Colorado Heras, M. M. Blázquez, J. Osío Barcina, A. García Martínez, M. R. Torres Salvador, *Org. Lett.* **2007**, *9*, 2943-2946.

[26] N. Herrero-García, I. Fernández, J. Osío Barcina, *Chem. Eur. J.* **2011**, *17*, 7327-7335.

[27] Gaussian 09, Revision B.01, M. J. Frisch, G. W. Trucks, H. B. Schlegel, G. E. Scuseria, M. A. Robb, J. R. Cheeseman, G. Scalmani, V. Barone, B. Mennucci, G. A. Petersson, H. Nakatsuji, M. Caricato, X. Li, H. P. Hratchian, A. F. Izmaylov, J. Bloino, G. Zheng, J. L. Sonnenberg, M. Hada, M. Ehara, K. Toyota, R. Fukuda, J. Hasegawa, M. Ishida, T. Nakajima, Y. Honda, O. Kitao, H. Nakai, T. Vreven, J. A. Montgomery,

hybrid functional[28] M06-2X functional in combination with the standard double-ζ plus polarization 6-31+G(d) basis sets.[29] Stationary points were characterized as minima by calculating the Hessian matrix analytically at this level. Calculations of absorption spectra were accomplished by using the time-dependent density functional theory (TD-DFT)[30] method. The assignment of the excitation energies to the experimental bands was performed on the basis of the energy values and oscillator strengths. The B3LYP[31] Hamiltonian was chosen because it was proven to provide reasonable UV/Vis spectra for a variety of chromophores[26,32] including organometallic species.[33] Total first hyperpolarizabilities (β_{tot}) were computed according to the following equation using the different β_{ijk} tensor components:

$$\beta_{tot} = sqrt\left[\begin{matrix}\left(\beta_{xxx} + \beta_{xyy} + \beta_{xzz}\right)^2 + \left(\beta_{yyy} + \beta_{yzz} + \beta_{yxx}\right)^2 \\ +\left(\beta_{zzz} + \beta_{zxx} + \beta_{zyy}\right)^2\end{matrix}\right]$$

Equation 1

Jr., J. E. Peralta, F. Ogliaro, M. Bearpark, J. J. Heyd, E. Brothers, K. N. Kudin, V. N. Staroverov, R. Kobayashi, J. Normand, K. Raghavachari, A. Rendell, J. C. Burant, S. S. Iyengar, J. Tomasi, M. Cossi, N. Rega, J. M. Millam, M. Klene, J. E. Knox, J. B. Cross, V. Bakken, C. Adamo, J. Jaramillo, R. Gomperts, R. E. Stratmann, O. Yazyev, A. J. Austin, R. Cammi, C. Pomelli, J. W. Ochterski, R. L. Martin, K. Morokuma, V. G. Zakrzewski, G. A. Voth, P. Salvador, J. J. Dannenberg, S. Dapprich, A. D. Daniels, Ö. Farkas, J. B. Foresman, J. V. Ortiz, J. Cioslowski, and D. J. Fox, Gaussian, Inc., Wallingford CT, 2009.

[28] Y. Zhao, D. G.Truhlar, *Acc. Chem. Res*. **2008**, *41*, 157 -167.

[29] W. J. Hehre, L. Radom, P. v. R. Scheleyer, J. A. Pople, *Ab Initio Molecular Orbital Theory*, Wiley, New York, **1986**, p. 76, and references therein.

[30] a) M. E. Casida, *Recent Developments and Applications of Modern Density Functional Theory*, Vol. 4, Elsevier, Amsterdam, **1996**; b) M. E. Casida, D. P. Chong, *Recent Advances in Density Functional Methods*, Vol. 1, World Scientific, Singapore, **1995**, p. 155

[31] a) A. D. Becke, *J. Chem. Phys*. **1993**, *98*, 5648-5652; b) C. Lee, W. Yang, R. G. Parr, *Phys. Rev. B* **1988**, *37*, 785-789.

[32] For a review, see: A. Dreuw, M. Head-Gordon, *Chem. Rev*. **2005**, *105*, 4009-4037.

[33] Some recent examples: a) V. N. Nemykin, E. A. Makarova, J. O. Grosland, R. G. Hadt, A. Y. Koposov, *Inorg. Chem*. **2007**, *46*, 9591-9601; b) M. L. Lage, I. Fernández, M. J. Mancheño, M. A. Sierra, *Inorg. Chem*. **2008**, *47*, 5253-5258; c) H. Braunschweig, T. Herbst, D. Rais, S. Ghosh, T. Kupfer, K. Radacki, A. G. Crawford, R. W. Ward, T. B. Marder, I. Fernández, G. Frenking, *J. Am. Chem. Soc.* **2009**, *131*, 8989; d) M. L. Lage, I. Fernández, M. J. Mancheño, M. A. Sierra, *Chem. Eur. J*. **2010**, *16*, 6616-6624. For recent examples of B3LYP and TD-B3LYP calculations on push-pull systems, see: e) P. D. Jarowski, Y.-L. Wu, W. B. Schweizer, F. Diederich, *Org. Lett.* **2008**, *10*, 3347-3350 and references [2a] and [14b].

1.3.3 Results and Discussion

1.3.3.1 Synthesis and structure of DPN's

For this study we have chosen the series of mono- and disubstituted derivatives of DPN (**5** and **6**) and 7-(*o*-fluorophenyl)-7-phenylnorbornane (FDPN, **7**) depicted in Figure 2. The synthesis of these compounds was carried out according to the methodology described previously by us (Scheme 1).[21-26]

One of the advantages of DPN's is that a large variety of different molecules can be prepared following standard and straightforward procedures. Electrophilic aromatic substitution reactions on both DPN and FDPN take place exclusively at the *para* position, since the *ortho* position is sterically hindered by the bridgehead hydrogen atom of norbornane. The only exception to this behaviour was found while attempting the synthesis of **7o,** the FDPN derivative with two *para* nitro groups as substituents (Scheme 2). While nitration reaction of DPN yields the corresponding dinitro derivative **6h** in high yield, reaction of **7c** under the same conditions yields a 25:75 mixture of **7o** and **8** (Scheme 2). Since these compounds are difficult to separate, the synthesis of **7o** was carried out by nitration of the mononitro derivative **7l**.[21]

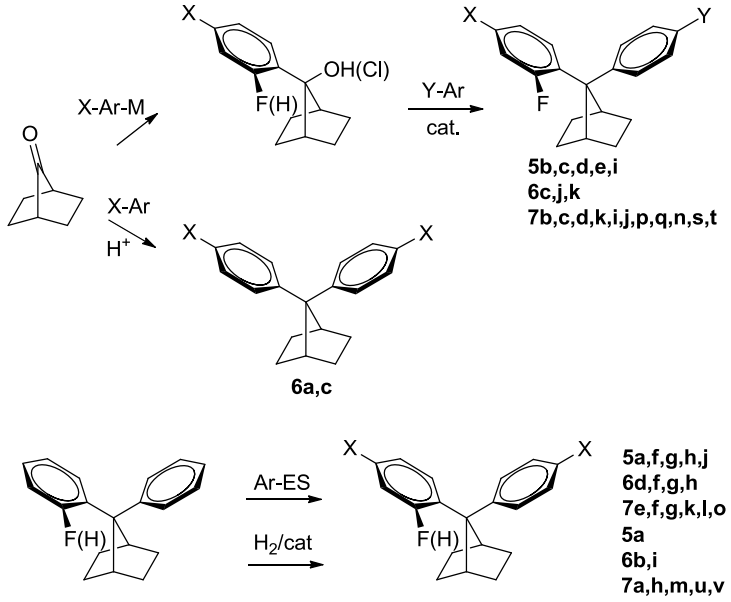

Scheme 1. General synthetic routes for DPN and FDPN derivatives.

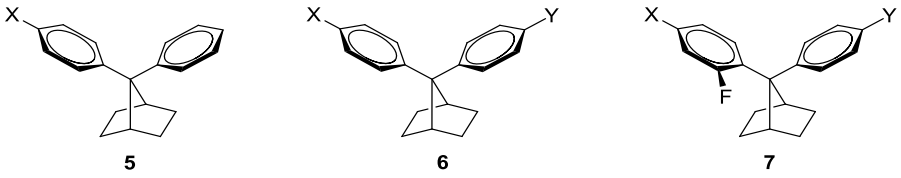

5

5a: X = NH_2
5b: X = OCH_3
5c: X = H
5d: X = Cl
5e: X = Br
5f: X = CO_2H
5g: X = CO_2Et
5h: X = $COCH_3$
5i: X = CF_3
5j: X = NO_2

6

6a: X = Y = NMe_2
6b: X = Y = NH_2
6c: X = Y = OCH_3
6d: X = Y = I
6e: X = Y = CO_2H
6f: X = Y = CO_2Et
6g: X = Y = $COCH_3$
6h: X = Y = NO_2
6i: X = NH_2; Y = NO_2
6j: X = OCH_3; Y = NO_2
6k: X = OCH_3; Y = CF_3

7

7a: X = H; Y = NH_2
7b: X = H; Y = OCH_3
7c: X = H; Y = H
7d: X = H; Y = Cl
7e: X = H; Y = Br
7f: X = H; Y = $COCH_3$
7g: X = H; Y = NO_2
7h: X = NH_2; Y = H
7i: X = OCH_3; Y = H
7j: X = CH_3; Y = H
7k: X = Br; Y = H
7l: X = NO_2; Y = H
7m: X = Y = NH_2
7n: X = Y = OCH_3
7o: X = Y = NO_2
7p: X = CH_3; Y = NO_2
7q: X = OCH_3; Y = NO_2
7r: X = CN; Y = OCH_3
7s: X = Br; Y = OCH_3
7t: X = CH_3; Y = OCH_3
7u: X = OCH_3; Y = NH_2
7v: X = NH_2; Y = NO_2

Figure 2. Mono- and disubstituted derivatives of DPN and FDPN **5**-**7**.

The formation of the *meta*-substituted compound **8** can be explained considering that, in the first step of the nitration reaction, **7g** is obtained as the main reaction product due to the deactivating effect of the fluorine atom (Scheme 2). In the second step, electrophilic aromatic substitution takes place at the *meta* position of the fluorinated ring induced by both the deactivating effects of fluorine and the nitro group of the adjacent homoconjugated aromatic ring. Moreover, nitration of **7g** affords compound **8** in 86% yield. This fact, together with the experimental observation that reaction rate of the second nitration reaction is lower than the first nitration, is a clear evidence of strong transannular homoconjugative interaction in DPN's, similar to that observed in

cyclophanes.[34,35,36] In a previous work we have shown that DPN's can be considered as examples of "open chain cyclophanes" (protophanes).[24b]

Compounds **9a-e** derived from 2,2-diphenylpropane and **10b-c** have been prepared as references for the study of the spectroscopic properties of DPN's (Figure 3). It should be noted that in **10a-c**, the most stable conformation is the orthogonal disposition, since the aryl rings cannot adopt the cofacial conformation because of the restricted mobility of the fused phenyl ring. Therefore, homoconjugative interactions are not expected in these derivatives.

On the other hand, the most stable conformation of 2,2-diphenylpropanes is the helicoidal conformation. The synthesis of these compounds was carried out following the same procedures used for the analogous DPN's starting from the 2,2-diphenylpropane and bicyclic compound **10a**.

[34] a) *Modern Cyclophane Chemistry* (Eds.: R. Gleiter, H. Hopf), Wiley-VCH, Weinheim, **2004**; b) F. Diederich, *Cyclophanes*, Royal Society of Chemistry, Cambridge, **1991**; c) *Cyclophanes* (Ed.: F. Vögtle), Springer, Heidelberg, **1983**.

[35] a) T. Moriguchi, K. Sakata, A. Tsuge, *J. Chem. Soc., Perkin Trans. 2* **2001**, 934-938; b) A. Tsuge, T. Nishimoto, T. Uchida, M. Yasutake, T. Moriguchi, K. Sakata, *J. Org. Chem.* **1999**, *64*, 7246-7248; c) T. Moriguchi, M. Yasutake, K. Sakata, A. Tsuge, *J. Chem. Res. (S)* **1999**, 78-79; d) T. Moriguchi, K. Sakata, A. Tsuge, *J. Chem. Soc., Perkin Trans. 2* **1997**, 2141-2144; e) A. Tsuge, M. Yasutake, T. Moriguchi, K. Sakata, T. Yamato, S. Mataka, M. Tashiro, *Chem. Lett.* **1997**, 413-414; f) A. Tsuge, T. Moriguchi, S. Mataka, M. Tashiro, *Liebigs Ann.* **1996**, 769-771; g) A. Tsuge, T. Moriguchi, S. Mataka, M. Tashiro, *J. Chem. Soc., Perkin Trans. 1* **1993**, 2211-2215.

[36] For recent examples of transannular interactions in cyclophanes, see: a) L. M. Salonen, M. Ellermann, F. Diederich, *Angew. Chem. Int. Ed.* **2011**, *50*, 4808-4842; b) J. K. Klosterman, Y. Yamauchi, M. Fujita, *Chem. Soc. Rev.* **2009**, *38*, 1714-1725; c) M. Fujitsuka, S. Tojo, T. Shinmyozu, T. Majima, *Chem. Communn.* **2009**, 1553-1555; d) M. Shibahara, M. Watanabe, T. Iwanaga, T. Matsumoto, K. Ideta, T. Shinmyozu, *J. Org. Chem.* **2008**, *73*, 4433-4442; e) H. Hopf, *Angew. Chem. Int. Ed.* **2008**, *47*, 9808-9812; f) G. F. Caramori, S. E. Galembeck, *J. Phys. Chem. A* **2007**, *111*, 1705-1712; g) J. W. Hong, H. Y. Woo, B. Liu, G. C. Bazan, *J. Am. Chem. Soc.* **2005**, *127*, 7435-7443; h) K. A. Lyssenko, M. y. Antipin, D. Y. Antonov, *Chem. Phys. Chem.* **2003**, *4*, 817-823.

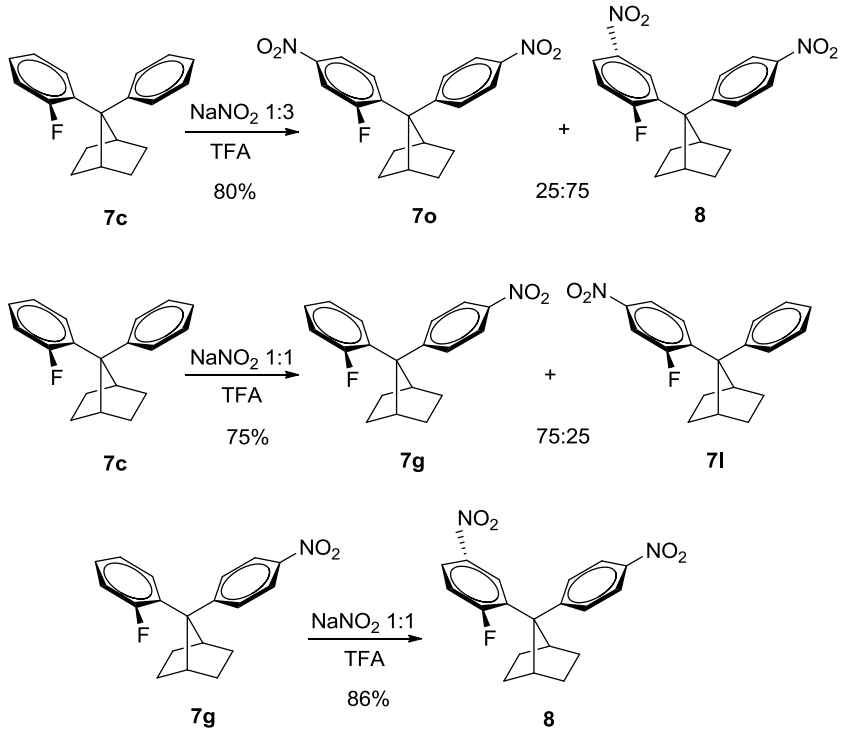

Scheme 2. Synthesis of nitro derivatives of FDPN.

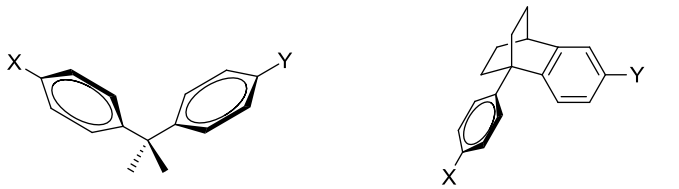

9a: X = H; Y = NH_2
9b: X = H; Y = NO_2
9c: X = NH_2; Y = NH_2
9d: X = NO_2; Y = NO_2
9e: X = NH_2; Y = NO_2

10a: X = H; Y = H
10b: X = NH_2; Y = NH_2
10c: X = NO_2; Y = NO_2

Figure 3. Structures of reference compounds **9** and **10**.

The main structural features of the compounds described in this work are highlighted by the push-pull system **6i**. The crystal structure of **6i** (Figure 4)

confirms the characteristic cofacial arrangement of the aryl groups in DPN's. Thus, the values of the C15-C14-C7-C8 and C9-C8-C7-C14 torsion angles are 92.3^0 and 89.1^0 respectively. On the other hand, the value of the C14-C7-C8 bond angle is 107.8^0 and the distance between the *ipso* carbon atoms of the aryl rings (C14-C8), 2.468 Å, well below the sum of the van der Waals radii for two phenyl rings (3.4 Å).[37a]

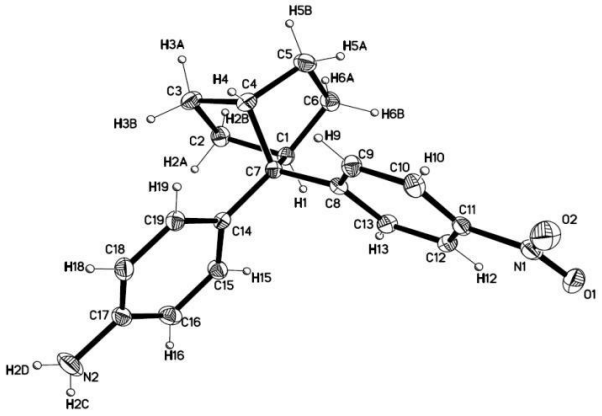

Figure 4. X-ray crystal structure of compound **6i**.

The crystal packing of **6i** (Figure 5) shows some remarkable features. It has been described that nitroanilines crystallize into predictable arrays forming intramolecular hydrogen bonds between the amino and nitro groups. These interactions occur so frequently that can be used to establish hydrogen bond rules which are useful tools to predict and design crystalline materials.[38] However, no nitro-amino hydrogen bonds are detected in the case of **6i**. Instead, short amino-amino contacts are observed. The H2C atom of the amino group interacts with the N2' of the neighbouring molecule: H2C···N2' distance of 2.614 Å, with N2-H2C-N2' angle of 144.6^0 and distance between N2 and N2' amino nitrogen atoms, 3.352 Å. The shorter distance between amino and nitro groups is observed in the case of H2D and O1 (2.994 Å).

[37] a) L. Yu, H.-J. Schneider, *Eur. J. Org. Chem.* **1999**, 1619-1625; b) M. Mantina, A. C. Chamberlin, R.Valero, C. J. Cramer, D. G. Truhlar, *J. Phys. Chem. A* **2009**, *113*, 5806-5812.

[38] a) M. C. Etter, *J. Phys. Chem.* **1991**, *95*, 4601-4610; b) M. C. Etter, *Acc. Chem. Res.* **1990**, *23*, 120-126; c) T. W. Panunto, Z. Urbánczyk-Lipkowska, R. Johnson, M. C. Etter, *J. Am. Chem. Soc.* **1987**, *109*, 7786-7797.

On the other hand, short contacts are detected between the nitro oxygen atoms and H10 and H18 hydrogen atoms of the neighbouring aryl rings of two different molecules (O2···H10 distance = 2.597 Å; O1···H18 distance = 2.618 Å). On the basis of distance criteria, the interaction between the amino groups can be considered as hydrogen bond since the distance (2.614 Å) is shorter than the sum of the van der Waals radii of hydrogen and nitrogen atoms (1.10 Å and 1.55 Å, respectively).[37b]

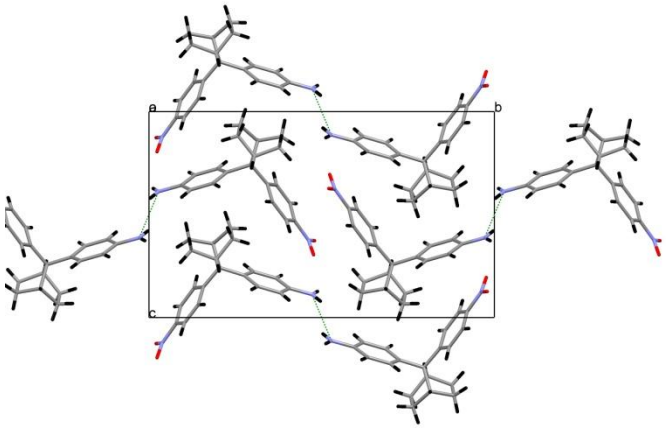

Figure 5. Crystal packing of **6i** showing the amino-amino short contacts.

1.3.3.2 Absorption spectroscopy study

Absorption spectroscopy constitutes an appropriate method to study electron delocalization and transannular interactions in aromatic systems. In previous works we have used UV/Vis spectra to study electron delocalization in homoconjugated DPN's[26] as well as oligomers[25] and polymers[24] derived from DPN. These studies clearly show that aromatic homoconjugation is an effective mechanism for electron delocalization that resembles the situation described for polyphenylenes.

We have also performed TD-DFT calculations on these systems,[26] finding a good agreement between the TD-DFT computed lowest energy vertical transitions and the experimentally observed absorptions. Therefore, TD-DFT

calculations can be used to accurately assign the vertical transitions responsible for the observed spectra in homoconjugated DPN's.

The UV/Vis spectra of DPN's and FDPN's show three important absorption bands: a) the bands of the corresponding chromophores attached to the aryl rings, b) the new homoconjugation bands, and c) charge-transfer bands in push-pull systems with strong electron withdrawing and electron donating groups in their structures. Tables 1-3 show the wavelengths of the absorption maxima of the bands for all compounds studied in this chapter. For those cases where the band appeared as a shoulder, the position of these absorptions has been established by the derivative method.

The influence of electron delocalization by homoconjugation is revealed by the bathocromic shift of the chromophores' bands in comparison to the corresponding spectra of benzene derivatives:[39] compounds **5f** (250 nm) and **6e** (256 nm) and benzoic acid (226 nm); **5g** (250 nm) and **6f** (258 nm) and etoxycarbonylbenzene (228 nm); **5h** (262 nm), **7f** (259 nm) and **6g** (269 nm) and acetophenone (242 nm); **5i** (233 nm) and trifluoromethylbenzene (210 nm); **5j** (289 nm), **7g** (284 nm), **7l** (285 nm) and **6h** (284 nm) and nitrobenzene (251 nm). Furthermore, the position of the band depends on the effect of the substituent placed on the adjacent ring. This effect is similar to the transannular interaction described for cyclophanes.[34-36] Thus, in the series of nitro derivatives **5j**, **6h**, **6i**, **6j** (DPN), **7g**, **7l**, **7o**, **7p** and **7q** (FDPN) there is a correlation between the wavelength of the absorption band of the nitro groups and the corresponding σ_p-Hammett substituent constant[40] of the substituent placed at the opposite aryl ring.

Figure 6 shows the absorption spectra of compounds **7g**, **7o**, **7p** and **7q** as well as the linear relationship between the wavelengths of the absorption maxima of the nitro group and the nature of the substituents placed at the adjacent aryl ring according to their σ_p value. A similar situation is observed with the analogous DPN derivatives.

[39] H.-H. Perkampus, *UV-Vis Atlas of Organic Compounds*, VCH, Weinheim, **1992**.
[40] C. Hansch, A. Leo, R. W. Taft, *Chem. Rev.* **1991**, *91*, 165-195.

Table 1. Absorption spectra (λ_{max}, MeOH) of monosubstituted DPN's and FDPN's.

Compound	λ_{max}/nm ε/M^{-1}.cm^{-1}	Compound	λ_{max}/nm ε/M^{-1}.cm^{-1}	Compound	λ_{max}/nm ε/M^{-1}.cm^{-1}
5[a]	249 (13800)[a]	**5i**	233 (11600)	**7f**	259 (16000)
5b	238 (13800)[a]	**5j**	289 (10000)	**7g**	284 (11800)
5c	229 (13300)[a]	**7a**	249 (10300)[a]	**7h**	246 (10400)[a]
5d	234 (13600)[a]	**7b**	234 (15100)[a]	**7i**	234 (14700)[a]
5e	236 (12800)[a]	**7c**	226 (12300)[a]	**7j**	229 (13700)[a]
5f	250 (15000)	**7d**	232 (16000)[a]	**7k**	234 (16100)[a]
5g	250 (11800)	**7e**	232 (20200)[a]	**7l**	285 (11800)
5h	262 (15200)				

[a] Homoconjugation band.

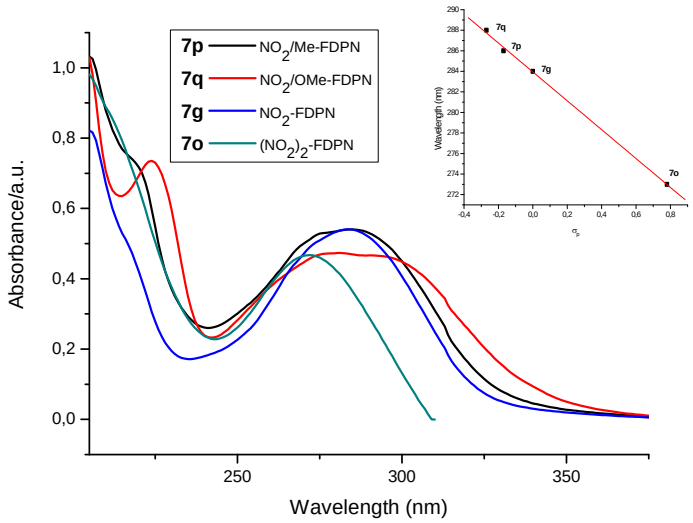

Figure 6. Absorption spectra of NO_2-substituted FDPN's and correlation between the absorption wavelength and the σ_p value of the substituent placed on the adjacent homoconjugated ring.

Table 2. Absorption spectra (MeOH) of disubstituted DPN's and FDPN's with X = Y groups.

Compound	λ_{max}/nm (ε/$M^{-1}.cm^{-1}$)	Compound	λ_{max}/nm (ε/$M^{-1}.cm^{-1}$)
6a	259[b], 272(20000)[a]	**6g**	248(20700), 269(28400)
6b	234(12700), 255(18600)[a]	**6h**	284(16900)
6c	242(18300)[a]	**7m**	237[b], 253(12100)[a]
6d	230(7000), 247(11300)[a]	**7n**	239(16900)[a]
6e	234(10400), 256(15000)	**7o**	273(11900)
6f	235(17400), 258(26700)		

[a] Homoconjugation band. [b] Shoulder.

Gas-phase TD-DFT calculations on compounds **7g**, **7o,p,q** also show the presence of two main absorptions. The band around 300 nm (which is slightly red-shifted in the calculations due to solvatochromism) is ascribed in all cases to the promotion of one electron from the HOMO to the LUMO.

As expected, both frontier orbitals are π molecular orbitals, thus indicating the π-π* nature of this absorption. Inspection of the involved orbitals reveals that the HOMO is mainly centered in the flouro-aryl moiety whereas the LUMO is centered in the adjacent *p*-NO_2-aryl group (Figure 7). For this reason, it is not surprising that a more effective charge transfer (i.e. a red-shift) occurs with better π-donors attached to the *para*-position of the fluoro-aryl fragment in agreement with the above mentioned Hammett plot. Moreover, the band around 230 nm is ascribed to the HOMO-3 to LUMO transition by our TD-DFT calculations. As seen in Figure 7, the HOMO-3 is a delocalized orbital between both aryl substituents thus confirming the homoconjugated nature[26] of this absorption.

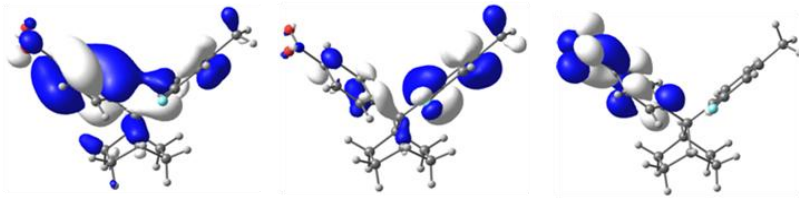

Figure 7. Computed molecular orbitals of compound **7p** (isosurface value of 0.03 au).

In the case of amino-substituted DPN's and FDPN's, the absorption band of the chromophore appears overlapped with the homoconjugation bands in most of the derivatives and can be observed only in compounds where the homoconjugation band is red shifted (vide infra). In these compounds, a similar behaviour is observed: i.e. the absorption band is red shifted in going from compound to **7u** (224 nm) to **7m** (237 nm).

Finally, the effect of homoconjugation in DPN's can be also observed by comparison of the absorption wavelength of the nitro derivatives **5j** (289 nm) and **6h** (284 nm) with the analogous 2,2-diphenylpropanes **9b** and **9d** (276 nm). Similarly, TD-DFT calculations assign this band (for **5j**) to a combination of the HOMO-3 and HOMO-2 to LUMO vertical transitions (calculated excitation energy of 270 nm). The shape of these π molecular orbitals resembles that of HOMO-3 (**7p**), confirming the delocalization of electrons in both aryl moieties due to homoconjugation

One of the most relevant features of the compounds studied in this work is related to the homoconjugation band. We have previously described that DPN shows a characteristic homoconjugation band at 229 nm. The position of this absorption depends on the torsion angle of the aryl rings and the extension of the homoconjugation. Thus, deviations from the cofacial conformation cause hypsochromic shifts of the band. On the other hand, a bathochromic shift is observed in DPN oligomers because of the extension of the homoconjugation.[25,26]

In the substituted DPN's studied herein, the nature of the substituents on the aryl rings exerts a very important effect on the electron delocalization between the aromatic rings. Thus, electron withdrawing groups diminish the electron density and, consequently, the homoconjugative effect is almost imperceptible,

as revealed by the hypsochromic shift of the homoconjugation band with e.g. nitro- substituted DPN's and FDPN's **5j**, **6h**, **7g**, **7l** and **7o**.

In contrast, electron donating groups show the opposite effect, as they increase the electron density and consequently the homoconjugation between the aryl rings. This is observed with methyl-, methoxy- and amino- substituted DPN´s and FDPN's **5a**, **5b**, **6a**, **6b**, **6c**, **7a**, **7b**, **7h**, **7i**, **7j**, **7m** and **7n** in which bathochromic shifts of the corresponding homoconjugation bands are observed (Tables 1-3).

The only exception to this behaviour was found in halogen-substituted DPN's and FDPN's **5d**, **5e**, **6d**, **7d**, **7e** and **7k**. The homoconjugation band in these derivatives is red shifted, pointing to a predominance of the conjugative effect of these atoms on the wavelength of the homoconjugation band, as observed in the absorption bands of halogen substituted benzenes.[39] Strikingly, the homoconjugation band of FDPN (**7c**) is blue shifted in comparison with the band of DPN (**5c**). The reasons for this differential behaviour can be found in the inductive effect of the fluorine atom at the *ortho* position (which is in part responsible for the observed hypsochromic shift of FDPN)[39] and the influence of this atom on the cofaciallity of the aryl rings (which would diminish the homoconjugation between the aryl rings).[26]

The substituents effect on the communication between the aryl groups in homoconjugated derivatives is clearly revealed by comparison with the UV/vis spectra of the orthogonal chromophores **10b** and **10c**. As mentioned above, electron releasing groups such as NO_2 diminish the electron density between the aromatic rings and, consequently, homoconjugation is less effective. The absorption spectra of **10c** shows an absorption maximum at 276 nm, the same wavelength observed for the diphenylpropane derivatives **9b** and **9d**. These bands are characteristic of aromatic nitro derivatives. The spectra of **5j** (289 nm), **6h** (284 nm) and **7o** (273 nm) are quite similar, showing the effect of delocalization by homoconjugation and the deviation from the cofacial conformation in the case of **7o**. The homoconjugation band in these compounds is blue shifted by the NO_2 groups and is difficult to observe.

Interestingly, the situation observed for the amino derivatives is remarkably different. The absorption spectra of the diamino orthogonal derivative **10b** resembles that of aniline, showing an intense strong band at 239 nm (230 nm in

aniline) and a weak absorption (^1L_b band) at 285 nm (281 nm in aniline) (Figure 8).

The spectra of diphenylpropane derivatives **9a** (238 and 289 nm) and **9c** (241 and 289 nm) are similar. While the homoconjugation bands are not observed in these compounds, the spectra of **6b** and **7m** are dominated by the homoconjugation bands at 255 and 253 nm, respectively. Moreover, the homoconjugation band is red shifted up to 272 nm in the case of compound **6a**, in agreement with the higher electron donating nature of the NMe_2 group. These results demonstrate that communication by homoconjugation between aromatic moieties can be easily tuned by controlling the electronic nature of the substituents attached at the aryl rings.

Interestingly, our TD-DFT calculations assign the homoconjugation band in **6b** to the HOMO→LUMO+1 vertical transition (λ_{calc} = 262 nm). Figure 9 nicely shows that this virtual orbital is delocalized between both aryl moieties thus confirming the electronic communication in this species. As expected, no similar delocalized orbital can be found in the non-cofacial analogue **10b**. This provokes that both aryl groups are electronically isolated and therefore, this species behaves quite similarly to aniline.

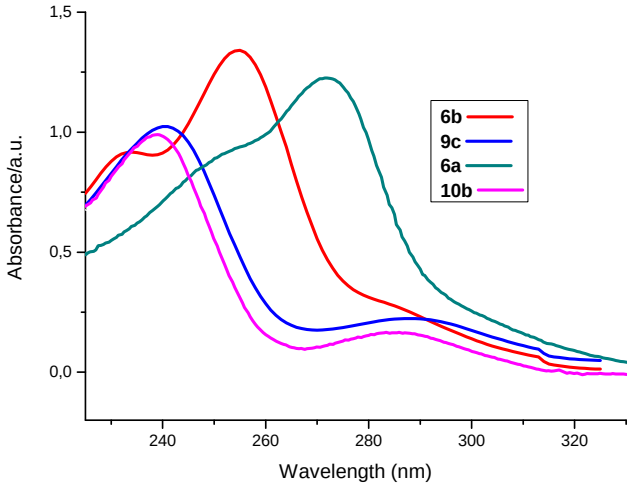

Figure 8. Absorption spectra of amino-substituted compounds.

The position of the homoconjugation bands strongly depends on the nature of the substituents. Figure 10 shows the absorption spectra of MeO-FDPN's with different substituents on the homoconjugated aromatic ring. As can be seen, there is an excellent correlation (r^2 = -0,996) between the position of the homoconjugation band and the σ_p value of the respective group.

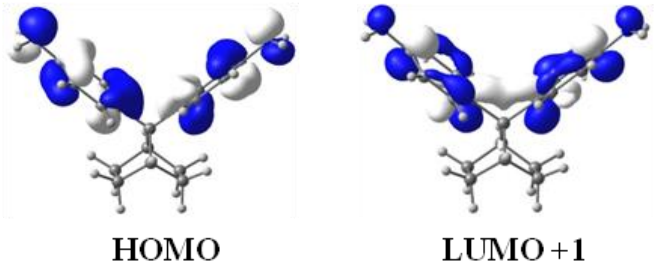

Figure 9. Computed molecular orbitals of compound **6b** (isosurface value of 0.035 au).

Only the bromo-derivative **7s** deviates from this behaviour, as observed before for the halogen-substituted DPN's and FDPN's (vide supra). The same behaviour is observed for the MeO-DPN's **5b**, **6c**, **6j** and **6k** as well as in the series **5a-c**, **6a-c, 7a-c**, **7h-j** and **7m-n**.

The situation observed in push-pull DPN's with strong electron donating and releasing groups is particularly interesting. When both electron withdrawing and electron donor substituents are placed at the *para* positions, besides the chromophore and homoconjugation absorptions, charge transfer bands are observed in the corresponding UV/vis spectra of compounds **6i**, **6j**, **6k**, **7p**, **7q**, **7r** and **7v** (Table 3).

The absorption spectra of compounds **6j**, **6k**, **7p**, **7q** and **7r** are shown in Figure 11. Compounds **6j** and **7q** show broad absorptions corresponding to two overlapping bands between 250-375 nm. These bands are the sum of the charge transfer band and the nitro group absorption.

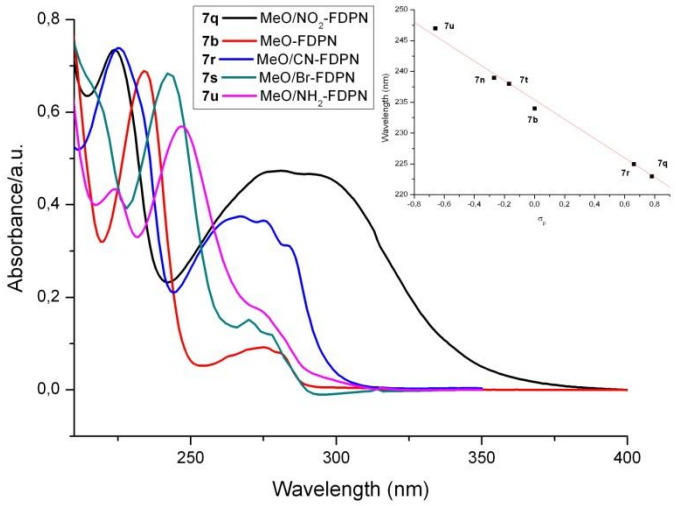

Figure 10. Absorption spectra of MeO-substituted FDPN and correlation between the absorption wavelength and the σ_p value of the substituent placed on the adjacent ring. The absorption spectra of **7n** and **7t** are omitted for clarity.

Table 3. Absorption spectra (MeOH) of disubstituted DPN's and FDPN's with X ≠ Y groups.

Compound	λ_{max}/nm (ε/$M^{-1}.cm^{-1}$)	Compound	λ_{max}/nm (ε/$M^{-1}.cm^{-1}$)
6i	247(13200), 293(9800), 320[b,c]	**7r**	225(12300),[a] 268(7600),288[b,c]
6j	227(12250),[a] 277(8100), 303[b,c]	**7s**	242(16500),[a] 270(6900)
6k	247(9800),[a] 260-290[c,d]	**7t**	237(14300)[a]
7p	286(7800), 275-340[c,d]	**7u**	247(12000)[a]
7q	223(14500),[a] 281(7800),[c,d] 288(7600)	**7v**	250(9300), 250-425[c,d]

[a] Homoconjugation band. [b] Shoulder. [c] Charge transfer band. [d] Overlapping bands.

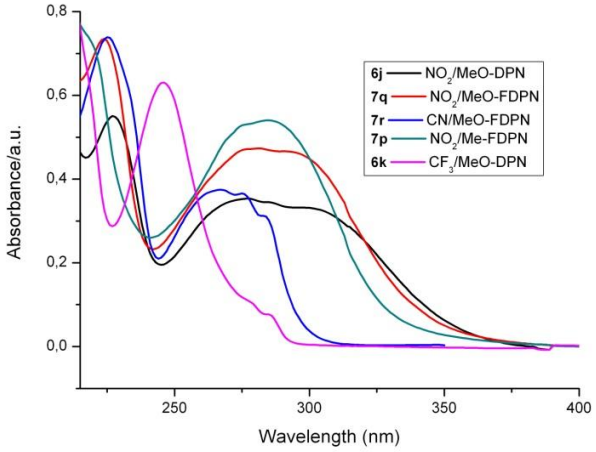

Figure 11. Absorption spectra of compounds **6j**, **6k**, **7p**, **7q** and **7r** showing the charge transfer bands.

A similar situation is observed in **7p**, although in this case a narrower band is observed, in accordance with the lower donating character of the methyl group. In the case of compound **7r**, the charge transfer band is observed between 250-300 nm and in **6k** the residual absorption at longer wavelength can be assigned to the charge transfer band. The cut-off of the CT bands in compounds **6j**, **7p** and **7q** lies between 380-390 nm. Figure 12 shows the absorption spectra of compound **6i**, **7v** and the analogous 2,2-diphenylpropane derivative, **9e**. Comparison of these spectra reveals the presence of a charge transfer band between 300-450 nm in **6i**. This band is not observed or is much less pronounced in **9e** (cut-off 385 nm). The spectrum of **7v** shows a broad absorption band, sum of the NH_2-, NO_2-chromophores and the CT band, with a maximum at 250 nm and cut-off ~ 425 nm.

Previous studies carried out on diphenylmethane and 2,2-diphenylpropane with nitro- and amino groups as substituents describe the presence of a weak charge transfer band as the tail of the long wavelength band of the nitro group.[41] These results nicely illustrate the remarkable effect of homoconjugation in our compounds. In fact, this effect is just the consequence

[41] a) H. Inoue, Y. Mikami, T. Yokotani, Bull. *Chem. Soc. Jpn*. **1973**, *46*, 3614-3615; b) W. N. White, *J. Am. Chem. Soc*. **1959**, *81*, 2912-2913.

of the imposed geometry by the DPN fragment which places both aromatic rings in a cofacial orientation allowing for the observed charge transfer. Obviously, this geometrical constrain is not present in the analogous derivate **9e** or orthogonal chromophores **10** (see Figure 13) and therefore, there is no chance for the electrons to delocalize by homoconjugation.

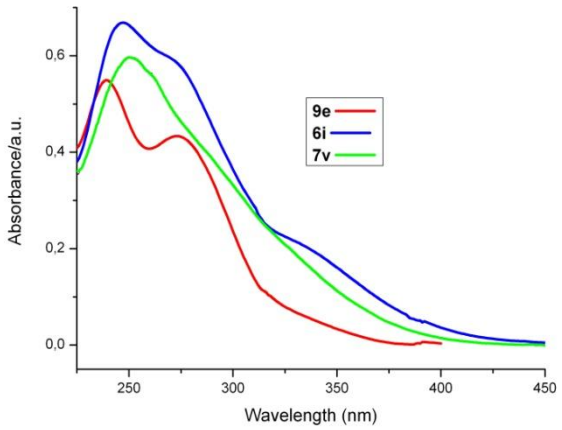

Figure 12. Absorption spectra of compounds **6i** and **9e**.

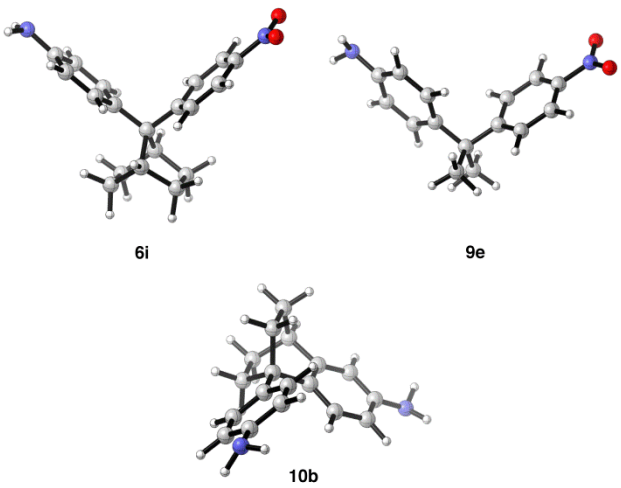

Figure 13. Fully optimized geometries (M06-2X/def2-SVP level) of compounds **6i** and **9e** and **10b.**

Comparison of the absorption spectra of **6i** with the *meta* substituted analogous FDPN leads to some significant conclusions. Partial hydrogenation of **8** (Scheme 3) produces a mixture of *meta*-substituted nitro/amino derivatives **11** and **12**. In the UV/vis spectra of these compounds (**11**, λ_{max} = 283 nm; **12**, λ_{max} = 263 nm) no CT band are observed, showing that charge transfer from the donor to the acceptor groups is favoured by substituents placed at the *para* positions of the aromatic rings. In this regioisomer, the homoconjugative interaction reaches its maximum, according to the homoconjugated resonance structure of **6i** depicted in Scheme 3.

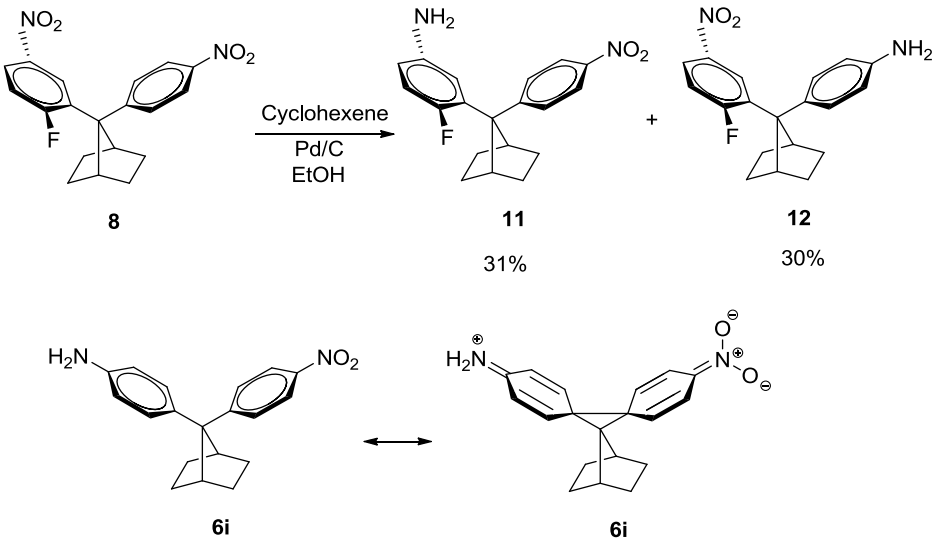

Scheme 3. Synthesis of *meta* FDPN's **11** and **12** and resonance structures of push-pull derivative **6i**.

1.3.3.3 NLO Properties

In a previous work we described the first study reported to date on the NLO properties of homoconjugated compounds.[22] Our results show that push-pull systems derived from DPN and FDPN present significant SHG hyperpolarizabilities. The values of β_z value measured for our DPN's and FDPN's are higher than the obtained for non-homoconjugated analogous and comparable to conjugated push-pull systems. Thus, the β_z(1064 nm) value

measured for compound **6i** was $21x10^{-30}$ esu, three times higher than the observed for **9e** and equal to the measured for *p*-nitroaniline under the same experimental conditions.

Herein we have computed the total first hyperpolarizability (β_{tot}) values of different nitro-substituted DPN's and FDPN's (Table 4). As expected, the computed β_{tot} values are generally higher in DPN's than in their FDPN's counterparts. This is mainly due to the effect of the fluorine atom at the *ortho* position, which slightly modifies the cofacial orientation, leading to a less effective homoconjugation.

Table 4. Computed β_{tot} (B3LYP/def2-SVP//M06-2x/def2-SVP level) for different DPN's and FDPN's.

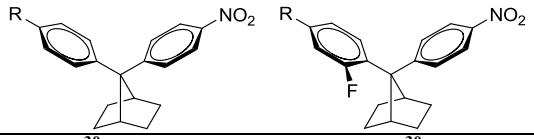

R	**β_{tot} / 10^{-30} esu**	**β_{tot} / 10^{-30} esu**
NH_2	29.85	23.70
OCH_3	23.77	19.50
Br	15.20	12.67
CN	9.67	9.24
NO_2	9.37	9.84

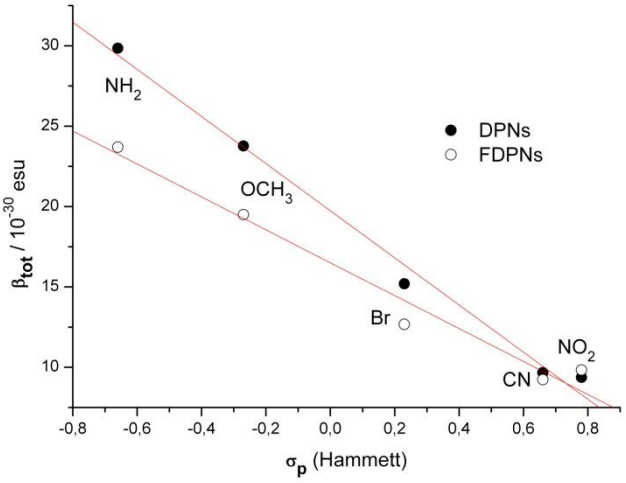

Figure 14. Plots of β_{tot} versus σ_p substituent constants.

Interestingly, push-pull systems exhibit higher β_{tot} values than compounds possessing an electron-withdrawing group at the aryl group adjacent to the *p*-NO_2-aryl fragment. Moreover, the β_{tot} computed for the NH_2-systems is comparable to the β_{tot} value obtained for truly π-conjugated push-pull systems,[42] thus indicating that homoconjugation can be indeed as effective in communicating the donor and acceptor moieties in our DPN's (or FDPN's) as π-conjugation. Not surprisingly, nice linear relationships were obtained when plotting the computed β_{tot} values versus the corresponding σ_p-Hammett substituent constants (Figure 14, correlation coefficient, r^2, of -0.995 and -0.986 for DPN's and FDPN's, respectively) as a consequence of the higher homoconjugation occurring with better π-donor groups.

1.3.3.4 NMR spectroscopy

To complete this study, we have also checked the influence of homoconjugation in DPN's and FDPN's by NMR spectroscopy. The chemical shifts of the most significant protons and carbon atoms of the compounds studied are listed in Table 5. These data show that the effect of a certain group in one of the aryl rings is transferred to the adjacent ring by means of homoconjugation.

In Figure 15, the variation of the chemical shifts of C-7, C-12, C-15 and H-15 with the σ_p value of the respective group X in monosubstituted DPN's **5a**-**j** are shown. Similar graphs are obtained for FDPN's. Although the variations caused by the substituents are, in some cases, not quite significant (e.g. the variations in the chemical shifts in H-15), from the large number of compounds studied some clear trends can be envisaged.

First of all, the most sensitive atom to the influence of groups X is the *ipso* carbon atom placed on the adjacent homoconjugated ring (C-12, correlation coefficient of -0,951). The chemical shifts increments in C-12 are higher and show a better linear correlation than that observed for the C-7 carbon atom of the norbornane structure (r^2 = 0,874). This fact confirms that the effects are transmitted through homoconjugative interactions between the aryl rings and

[42] K. S. Thanthiriwatte, K. M. Nalin da Silva, *J. Mol. Struct. (Theochem)* **2002**, *617*, 169-175, and references therein.

not through bonds via C-7. This phenomenon is similar to the transannular π-electronic effect described in cyclophanes.[34-36]

The effect of substitution is less pronounced in C-15 and H-15, although there is a good correlation with σ_p in both cases (r^2 = 0,983 and r^2 = 0,941, respectively).

Table 5. Selected ^{1}H NMR and ^{13}C NMR data (δ, $CDCl_3$, ppm) of DPN's and FDPN's .

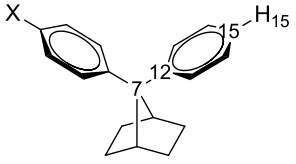

5

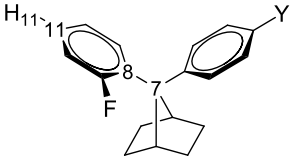

7

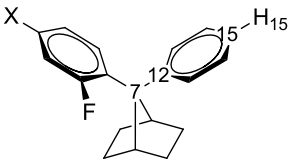

7

Compound	δ_{H15}	δ_{C7}	δ_{C8}	δ_{C11}	δ_{C12}	δ_{C15}
5a	7.04	63.95	-	-	146.63	125.01
5b	7.06	64.04	-	-	146.37	125.18
5c	7.07	64.79	-	-	145.97	125.29
5d	7.09	64.38	-	-	145.45	125.57
5e	7.07	64.44	-	-	145.34	125.58
5f	7.09	65.16	-	-	144.87	125.77
5g	7.09	64.85	-	-	144.94	125.75
5h	7.09	65.08	-	-	144.86	125.75
5i	7.11	64.91	-	-	144.96	125.79
5j	7.12	65.04	-	-	144.09	126.07
7a	-	61.37	133.04	127.15	-	-
7b	-	62.34	132.69	127.14	-	-
7c	-	62.22	132.23	127.47	144.26	125.58
7d	-	61.68	131.92	127.78	-	-
7e	-	61.76	131.90	127.80	-	-
7f	-	62.31	131.36	127.97	-	-
7g	-	62.31	130.68	128.40	-	-
7h	7.09	61.40	-	-	145.08	125.23
7i	7.10	61.51	-	-	144.74	125.45
7j	7.12	61.84	-	-	144.58	125.49
7k	7.12	61.93	-	-	143.64	125.87
7l	7.15	62.64	-	-	142.60	126.41

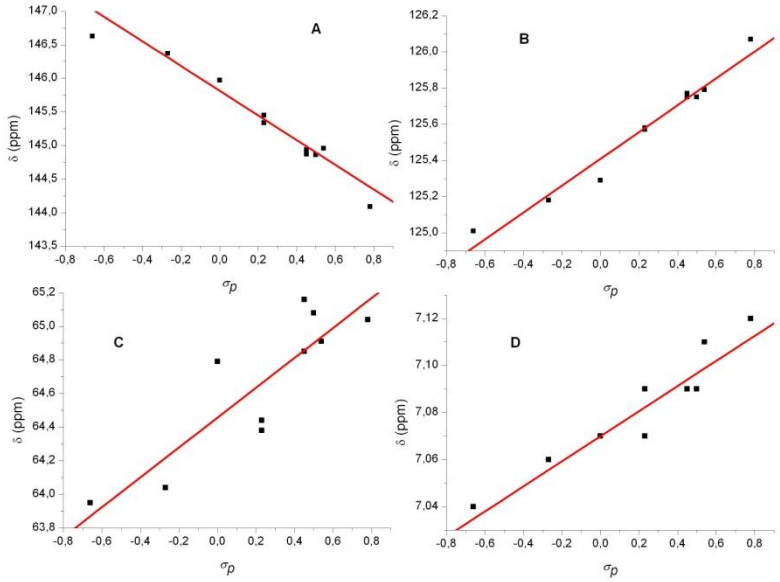

Figure 15. Correlation between NMR chemical shifts (graph A, C-12; graph B, C-15; graph C, C-7; graph D, H-15) and σ_p values in monosubstituted DPN's **5a-j**.

1.3.4 Conclusion

We have synthesized a large family of aromatic homoconjugated compounds with substituents at the *para* and *meta* positions of the aryl rings, in order to carry out the first systematic study of the interactions between the aromatic moieties in this type of chromophores.

The homoconjugative interactions in these compounds are clearly demonstrated by the absorption and NMR spectra, as well as by their reactivity. The UV/vis spectra show new homoconjugative bands whose wavelength maxima strongly depends on the electronic nature of the substituents (measured by their corresponding σ_p value).

TD-DFT calculations assign this homoconjugative bands to transitions involving molecular orbitals which are delocalized on both aryl moieties. On the other hand, the position of the bands of the chromophores placed in one of the aryl rings is influenced by the substituents attached at the *para* position of the cofacially arranged (homoconjugated) aromatic ring. These results are a clear indication of the importance of transannular homoconjugative interactions in the compounds studied in this work. Moreover, push-pull systems show intense intramolecular CT bands which are favoured when the substituents are placed at the *para* positions of the aromatic rings. Substitution at the *meta* position diminishes the homoconjugative interaction.

Finally, NMR spectra show that the transannular interactions are transmitted by homoconjugation between the aromatic rings and not through the C-7 carbon atom of the norbornane framework.

In summary, our joint experimental-computational study shows that homoconjugative interactions constitute indeed an effective way to provoke electronic communication which can be easily tuned by controlling the nature and position of the substituents. Thus, the proper selection of the substituents may lead to new organic materials with remarkable optical properties.

1.3.5 Experimental Section

General Information

^{1}H and ^{13}C NMR spectra were recorded on a 300 MHz spectrometer. Chemical shifts are given in ppm relative to TMS (^{1}H, 0.0 ppm) and $CDCl_3$ (^{13}C, 77.0 ppm). Coupling constants are given in Hertz. All experiments involving organometallic reagents were carried out under argon atmosphere using standard Schlenk techniques. Anhydrous solvents were distilled under argon following standard procedures. Flash chromatography was performed over silica gel 60 (230-400 mesh). All commercially available compounds were purchased from commercial suppliers and used without further purification. The preparation of **5c**, **6d**, **6h-k**, **7a-c**, **7g-j**, **7l-v**, **13a-c**, **14a-b** and **9a-e** has been described previously by us. [21-26] The preparation of **10a** has been reported also.[43]

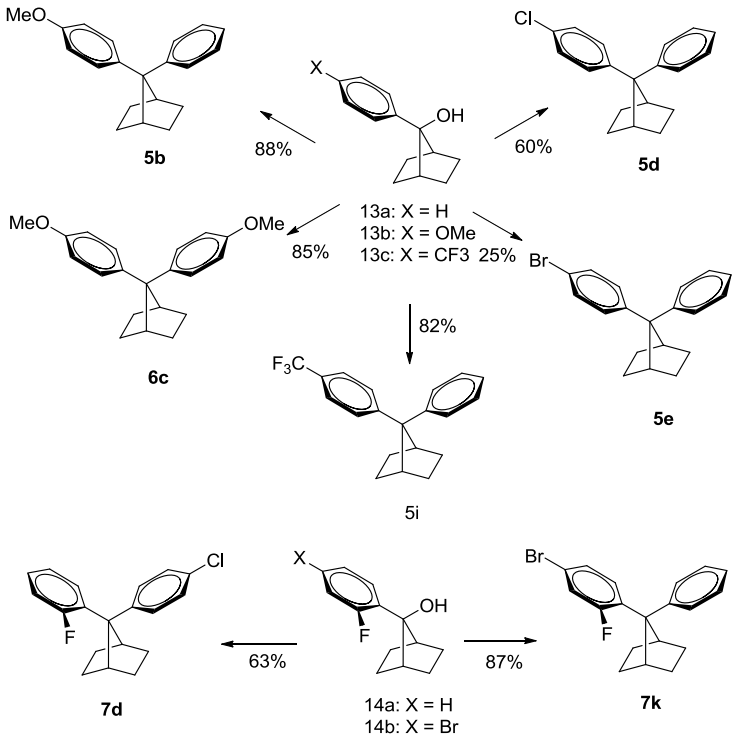

Scheme 4. Synthetic route for the preparation of compounds **5b**, **5d**, **5e**, **5i**, **6c**, **7d** and **7k**. General reaction conditions: alcohols **13a-c** or **14a-b**/aromatic compound (benzene, anisole, chlorobenzene or bromobenzene)/TfOH.

[43] L. Billet, G. Descotes, *Bull. Soc. Chim. Fr.* **1971**, 2626-2628.

General procedure for the synthesis of compounds 5b, 5d, 5e, 5i, 6c, 7d and 7k:[21-26] 13.7 mmol of the corresponding 7-aryl-7-norbornanol **13** or **14** were dissolved in 25 mL of the aromatic derivative and 1.20 mL (13.7 mmol) of TfOH were slowly added at 0ºC with vigorous stirring. After 1 hour (the reactions were monitored by TLC), the reaction mixture was poured on 50 mL of water, washed with saturated $NaHCO_3$ (2x25 mL), water (1x25 mL) and dried over $MgSO_4$. Evaporation of the solvent under reduced pressure and purification of the residue by flash chromatography (silica gel/hexane/CH_2Cl_2) yielded the corresponding DPN or FDPN derivative.

Compound 5b: Yield: 88%. White solid. M.p. 136.1-138.0 ºC. ^{1}H NMR (300 MHz, $CDCl_3$): δ = 7.39 (d, 2H, *J* = 7.2 Hz), 7.32 (d, 2H, *J* = 8.7 Hz), 7.20 (t, 2H, *J* = 7.2 Hz), 7.06 (t, 1H, *J* = 7.2 Hz), 6.75 (d, 2H, *J* = 9.0 Hz), 3.71 (s, 3H), 3.10-3.95 (m, 2H), 1.70-1.60 (m, 4H), 1.35-1.25 (m, 4H) ppm. ^{13}C NMR ($CDCl_3$, 75 MHz): δ = 157.1, 146.4, 138.3, 128.2, 127.1, 125.2, 113.7, 64.0, 55.1, 41.8, 28.5, 28.4 ppm. IR (KBr): ῡ = 3010, 2950, 2870, 1620, 1415, 1255, 1040, 830, 705 cm^{-1}. UV/Vis (MeOH) : λ_{max} (ε) = 238 (13800 $mol^{-1}dm^3cm^{-1}$), 265 (sh), 271 (sh), 280 (sh), 288 (sh) nm. MS (EI, 70 eV) *m/z* (%): 278 (M^+, 100), 277 (23), 209 (22), 197 (45), 121 (24), 115 (29), 91 (34). Elemental analysis calcd (%) for $C_{20}H_{22}O$: C 86.28, H 7.97; found: C 86.05, H 7.81.

Compound 5d: Yield: 60%. White solid. M.p. 122.0-125.0 ºC. ^{1}H NMR (300 MHz, $CDCl_3$): δ = 7.50-7.30 (m, 4H), 7.28-7.15 (m, 4H), 7.09 (t, 1H, J = 7.6 Hz), 3.10-3.00 (m, 2H), 1.80-1.50 (m, 4H), 1.50-1.20 (m, 4H) ppm. ^{13}C NMR ($CDCl_3$, 75 MHz): δ = 145.4, 144.6, 130.9, 128.7, 128.4, 128.3, 127.1, 125.6, 64.4, 41.7, 28.4, 28.3 ppm. IR (CCl_4): ῡ = 3030, 2957, 2873, 1541, 1490, 1093, 1014, 720, 696 cm^{-1}. UV/Vis (MeOH) : λ_{max} (ε) = 234 (13600), 260 nm (1500 $mol^{-1}dm^3cm^{-1}$). MS (EI, 70 eV) *m/z* (%): 284 (M^+ + 2, 140), 282 (M^+, 100), 247 (100), 205 (55), 203 (30), 201 (40), 189 (59), 179 (30), 165 (43), 125 (46), 115 (40), 109 (65), 91 (45), 67 (36), 55 (28). Elemental analysis calcd (%) for $C_{19}H_{19}Cl$: C 80.68, H 6.78; found: C 80.93, H 6.87.

Compound 5e: Yield: 25%. White solid. M.p. 167.0-170.0 ºC. ^{1}H NMR (300 MHz, $CDCl_3$): δ = 7.38 (d, 2H, *J* = 7.3 Hz), 7.35-7.25 (m, 4H), 7.21 (t, 2H, *J* = 7.8 Hz), 7.07 (t, 1H, *J* = 7.3 Hz), 3.10-2.95 (m, 2H), 1.72-1.52 (m, 4H), 1.45-1.25 (m, 4H) ppm. ^{13}C NMR ($CDCl_3$, 75 MHz): δ = 145.3, 145.1, 131.4, 129.1, 128.4, 127.1, 125.6, 119.1, 64.4, 41.7, 28.4, 28.3 ppm. IR (CCl_4): ῡ = 3010, 2970, 2880, 1550, 1495, 1020, 720, 705 cm^{-1}. UV/Vis (MeOH): λ_{max} (ε) = 236 nm (12800 $mol^{-1}dm^3cm^{-1}$). MS (EI, 70 eV) *m/z* (%): 328 (M^+ + 2, 31), 326 (M^+, 31), 247 (71), 205 (35), 204 (27), 193 (31), 192 (80), 191 (55), 189 (25), 179 (35), 178 (35), 169 (37), 166 (27), 165 (58), 143 (30), 141 (26), 129 (45), 128 (28), 117 (40), 115 (49), 101 (29), 95 (28), 91 (100), 77 (22), 51 (19), 41 (29). Elemental analysis calcd (%) for $C_{19}H_{19}Br$: C 69.71, H 5.85; found: C 69.66, H 5.79.

Compound 5i: Yield: 82%. White solid. M.p. 120.0-122.5 ºC. ^{1}H NMR (300 MHz, $CDCl_3$): δ = 7.53 (d, 2H, *J* = 9.0 Hz), 7.45 (d, 2H, *J* = 9.0 Hz), 7.40 (d, 2H, *J* = 8.4 Hz), 7.22 (t, 2H, *J* = 7.0 Hz), 7.11 (t, 1H, *J* = 7.5 Hz), 3.12-3.00 (m, 2H), 1.70-1.50 (m, 4H), 1.42-1.28 (m, 4H) ppm. ^{13}C NMR ($CDCl_3$, 75 MHz): δ = 150.1 (q, *J* = 1.4 Hz), 145.0, 128.5, 127.6, 127.5 (q, *J* = 47.0 Hz), 127.3, 125.8, 125.3 (q, *J* = 3.9 Hz), 124.0 (q, *J* =

272.0 Hz), 64.9, 41.7, 28.3, 28.2 ppm. IR ($CHCl_3$): ϑ = 3010, 2960, 2880, 1610, 1340, 1210, 1120, 830, 700 cm^{-1}. UV/Vis (MeOH) : λ_{max} (ε) = 233 (11600 $mol^{-1}dm^3cm^{-1}$), 263 (sh), 273 (sh) nm. MS (EI, 70 eV) *m/z* (%): 316 (M^+, 100), 274 (21), 273 (22), 271 (18), 248 (31), 247 (51), 235 (20), 183 (17), 179 (16), 165 (16), 115 (28), 91 (34), 81 (15). Elemental analysis calcd (%) for $C_{20}H_{19}F_3$: C 75.91, H 6.06; found: C 76.08, H 6.15.

Compound 6c: Yield: 85%. White solid. M.p. 194.8-197.0 º C. ^{1}H NMR (300 MHz, $CDCl_3$): δ = 7.29 (d, 4H, *J* = 6.7 Hz), 6.74 (d, 4H, *J* = 6.7 Hz), 3.70 (s, 6H), 3.02-2.95 (m, 2H), 1.70-1.55 (m, 4H), 1.35-1.20 (m,4H) ppm. ^{13}C NMR ($CDCl_3$, 75 MHz): δ = 157.0, 138.7, 128.0, 113.6, 63.3, 55.4, 41.9, 28.5 ppm. IR (KBr): ϑ = 3010, 2970, 2880, 1610, 1515, 1450, 1300, 1250, 1180, 1040, 830 cm^{-1}. UV/Vis (MeOH): λ_{max} (ε) = 224 (sh), 242 (18300), 272 (3500), 283 nm (1500 $mol^{-1}dm^3cm^{-1}$). MS (EI, 70 eV) *m/z* (%): 308 (M^+, 80), 277 (55), 227 (50), 200 (23), 159 (23), 145 (30), 121 (100), 91 (25). Elemental analysis calcd (%) for $C_{21}H_{24}O_2$: C 81.77, H 7.85; found: C 81.88, H 7.97.

Compound 7d: Yield: 63%. White solid. M.p. 117.0-119.0 ºC. ^{1}H NMR (300 MHz, $CDCl_3$): δ = 7.50-7.35 (m, 3H), 7.20 (d, 2H, *J* = 8.5 Hz), 7.13-6.97 (m, 2H), 6.88 (ddd, 1H, *J* = 12.0, 8.0, 1.4 Hz), 3.35 (dt, *J* = 4.3, 4.3 Hz), 3.10-2.95 (m, 1H), 1.84-1.65 (m, 2H), 1.55-1.20 (m, 6H) ppm. ^{13}C NMR ($CDCl_3$, 75 MHz): δ = 161.7 (d, *J* = 246.7 Hz), 142.8, 131.9 (d, *J* = 13.6 Hz), 131.3, 129.4 (d, *J* = 5.6 Hz), 129.1, 129.1, 128.3, 127.8 (d, *J* = 8.8 Hz), 124.1 (d, *J* = 3.2 Hz), 116.3 (d, *J* = 23.9), 61.7 (d, *J* = 2.5 Hz), 42.5, 41.3 (d, *J* = 8.1 Hz), 28.9, 28.3, 28.1, 27.2 ppm. IR (CCl_4): ϑ = 3033, 2958, 2875, 1548, 1485, 1220, 1093, 1014, 761 cm^{-1}. UV/Vis (MeOH): λ_{max} (ε) = 232 (16000), 258 (1500), 264 (1800), 271 nm (1500 $mol^{-1}dm^3cm^{-1}$). MS (EI, 70 eV) *m/z* (%): 302 (M^+ + 2, 14), 300 (M^+, 46), 282 (35), 265 (51), 247 (36), 232 (47), 223 (49), 221 (28), 219 (52), 210 (30), 209 (27), 203 (27), 201 (28), 197 (25), 191 (25), 183 (44), 165 (36), 149 (38), 143 (28), 133 (33), 129 (41), 127 (34), 125 (59), 117 (37), 115 (57), 108 (100), 101 (37), 91 (52), 81 (35), 41 (35). Elemental analysis calcd (%) for $C_{19}H_{18}ClF$: C 75.85, H 6.03; found: C 75.69, H 6.12.

Compound 7k: Yield 87%. White solid. M.p. 135.5-138.0 ºC. ^{1}H NMR (300 MHz, $CDCl_3$): δ = 7.44 (d, 2H, J = 8.1 Hz), 7.37 (t, 1H, J = 8.46 Hz), 7.12 (t, 2H, J = 8.09 Hz), 7.20-7.04 (m, 3H), 3.39 (dt, 1H, J = 4.1, 4.1 Hz), 3.08-3.00 (m, 1H), 1.82-1.65 (m, 2H), 1.60-1.20 (m, 6H) ppm. ^{13}C NMR ($CDCl_3$, 75 MHz): δ = 160.6 (d, *J* = 251.5 Hz), 143.6, 131.9 (d, *J* = 13.6 Hz), 130.8 (d, *J* = 6.8 Hz), 128.3, 127.5, 127.5, 127.3 (d, *J* = 3.2 Hz), 125.9, 119.8 (d, *J* = 27.9 Hz), 119.5 (d, *J* = 10.0 Hz), 61.9 (d, *J* = 3.1 Hz), 42.5, 41.1 (d, *J* = 8.4 Hz), 28.8, 28.4, 28.0, 27.2 ppm. IR (CCl_4): ϑ = 3020, 2958, 2875, 1598, 1566, 1481, 1396, 866, 721 cm^{-1}. UV/Vis (MeOH): λ_{max} (ε) = 234 (16100), 263 (1800), 270 (2000), 277 nm (1800 $mol^{-1}dm^3cm^{-1}$). MS (EI, 70 eV) *m/z* (%): 346 (M^+ + 2, 29), 344 (M^+, 37), 278 (23), 276 (24), 265 (59), 263 (34), 223 (23), 222 (27), 211 (30), 210 (84), 209 (62), 207 (20), 197 (47), 196 (41), 189 (58), 187 (57), 183 (57), 170 (19), 157 (21), 144 (21), 133 (24), 129 (33), 116 (36), 115 (48), 107 (24), 104 (34), 94 (28), 91 (100), 81 (42), 79 (26), 77 (24), 65 (23), 51 (27), 41 (43). Elemental analysis calcd (%) for $C_{19}H_{18}BrF$: C 66.08, H 5.26; found: C 65.89, H 5.15.

Synthesis of compound 7e:[44] 16 mg (1.00 mmol) of bromine were slowly added to a mixture of 270 mg (1.00 mmol) of FDPN and 510 mg (2.00 mmol) of AgTfO in 25 mL of $CHCl_3$ at 25 ºC, in the dark. After 24 h (the reaction was monitored by TLC), the silver halide was separated by filtration and the organic solution was washed with 20 mL of saturated $NaCO_3H$, 20 mL of 10% NaS_2O_3 and dried over $MgSO_4$. Evaporation of the solvent at reduced pressure an purification of the residue by flash chromatography (silica gel, hexane) yielded 210 mg (62%) of **7e**. White solid. M.p. 125.0-128.0 ºC. ^{1}H NMR (300 MHz, $CDCl_3$): δ = 7.46 (td, 1H, *J* = 7.4 Hz), 7.35 (s, 4H), 7.15-7.00 (m, 2H), 6.88 (ddd, 1H, *J* = 12.1, 8.1, 1.5 Hz), 3.41-3.32 (m, 1H), 3.08-3.00 (m, 1H), 1.84-1.65 (m, 2H), 1.55-1.20 (m, 6H) ppm. ^{13}C NMR ($CDCl_3$, 75 MHz): δ = 161.7 (d, *J* = 246.7 Hz), 143.3, 131.9 (d, *J* = 13.6 Hz), 131.2, 129.5, 129.5, 129.4 (d, *J* = 5.6 Hz), 127.8 (d, *J* = 8.7 Hz), 124.1 (d, *J* = 3.2 Hz), 119.4, 116.3 (d, *J* = 23.9 Hz), 61.8 (d, *J* = 2.5 Hz), 42.5, 41.3 (d, *J* = 8.1 Hz), 28.9, 28.3, 28.1, 27.2 ppm. IR ($CHCl_3$): ῡ = 3060, 2958, 2876, 1600, 1456, 1010, 669 cm^{-1}. UV/Vis (MeOH): λ_{max} (ε) = 232 (20200), 264 (2700), 272 (2400 $mol^{-1}dm^3cm^{-1}$), 279 (sh) nm. MS (EI, 70 eV) *m/z* (%): 346 (M^+ + 2, 33), 344 (M^+, 35), 278 (30), 276 (30), 265 (65), 263 (39), 223 (58), 210 (87), 196 (37), 183 (60), 169 (38), 161 (16), 143 (41), 135 (46), 115 (43), 109 (100), 91 (30), 81 (48), 67 (25), 41(50). Elemental analysis calcd (%) for $C_{19}H_{18}BrF$: C 66.08, H 5.26; found: C 66.14, H 5.16.

[44] Kobayashi, Y.; Kumadaki, Y.; Yoshida, T. *J. Chem. Res.* **1977**, 215.

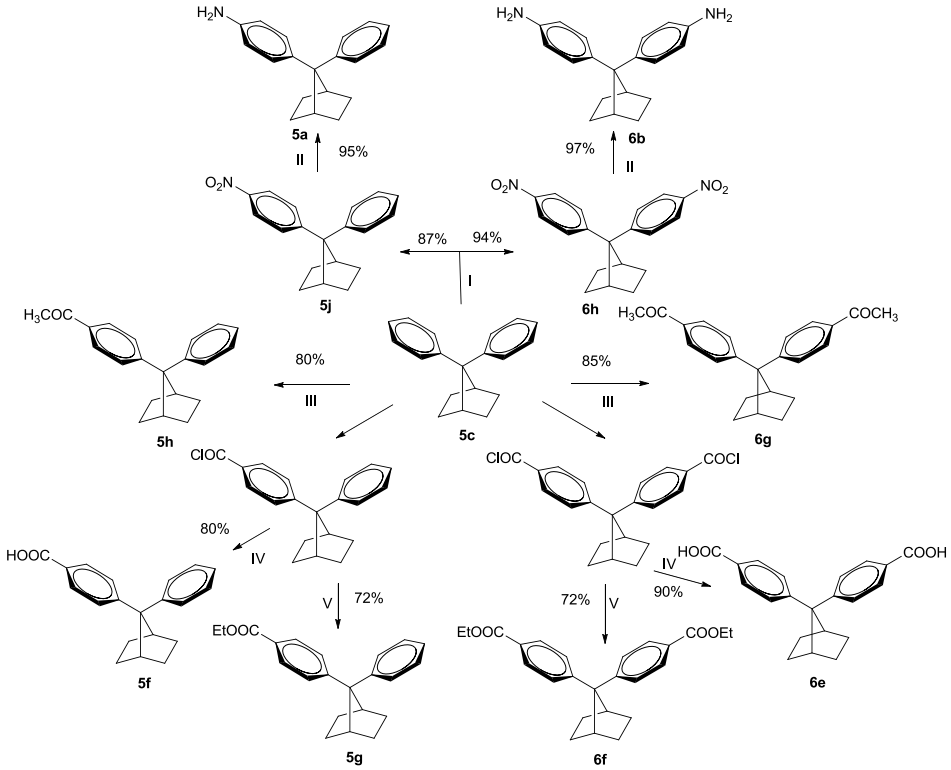

Scheme 5. Synthetic route for the preparation of compounds **5a**, **5f-h**, **5j**, **6b**, **6e** and **6f-h**. I) $NaNO_2$/TFA; II) H_2/Pd/C 10%; III) $CH_3COCl/AlCl_3$; IV) a) $(COCl)_2/AlCl_3$, b) H_2O; V) a) $(COCl)_2/AlCl_3$, b) EtOH.

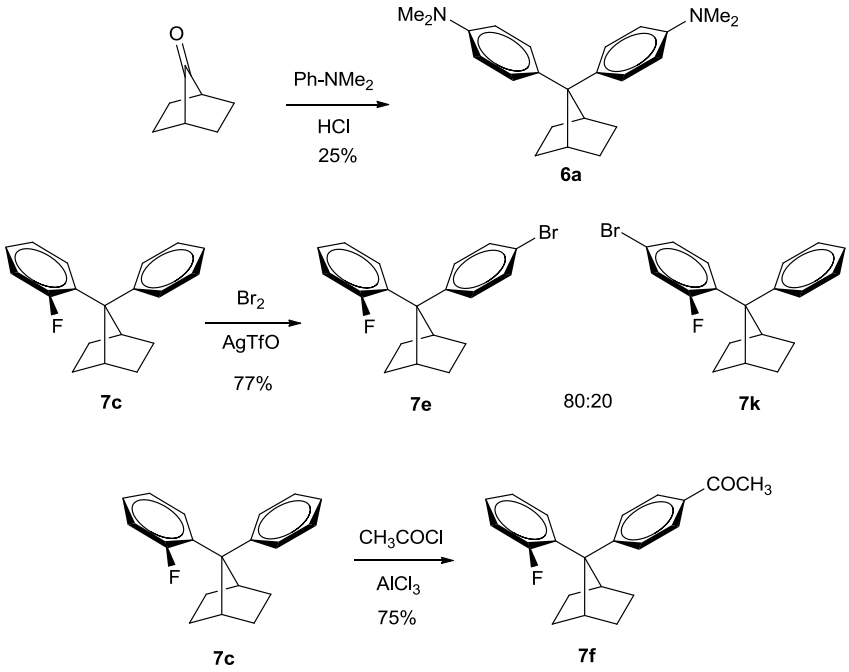

Scheme 6. Synthetic route for the preparation of compounds **6a**, **7e**, and **7k**.

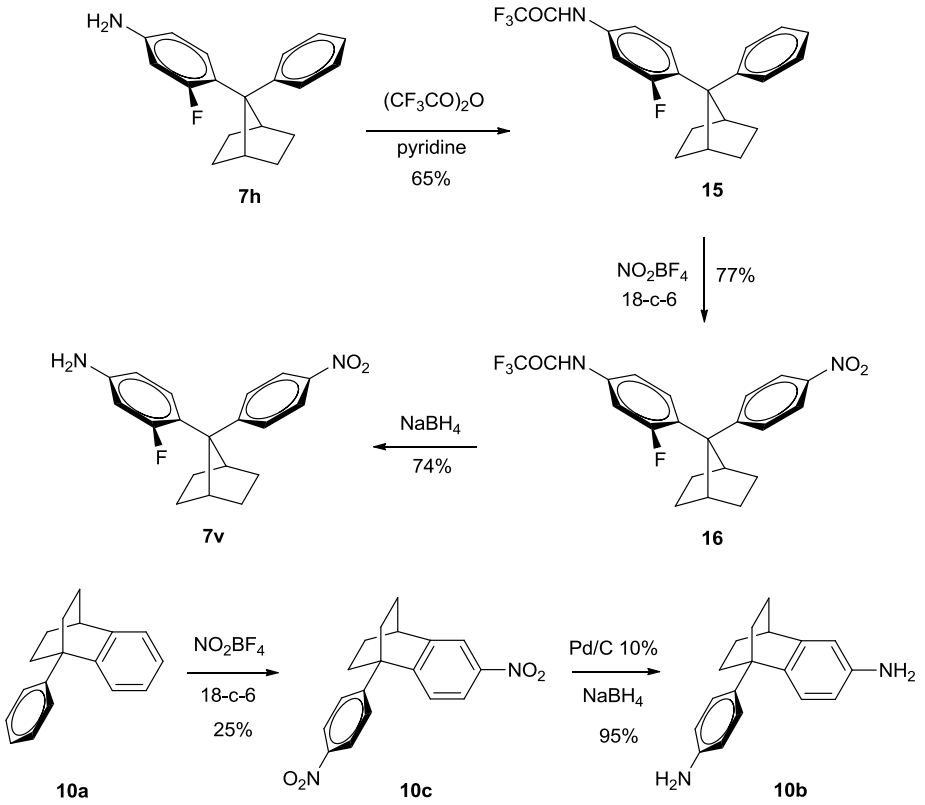

Scheme 7. Synthetic route for the preparation of compounds **7v**, **10c**, and **10b**.

General procedure for the synthesis of compounds 5j, **6h** and **8:**[45] 80 mg (1.1 mmol, **5j**) or 160 mg (2.2 mmol, **6h** and **8**) of $NaNO_2$ were added to a solution of 1 mmol of DPN (**5j** and **6h**) or FDPN (**8**) in 20 mL of TFA at 0 ºC. After 20 h at 25 ºC the reaction mixture was diluted with 50 mL of CH_2Cl_2, washed with saturated $NaHCO_3$ (1x25 mL), water (2x30 mL) and dried over $MgSO_4$. Evaporation of the solvent under reduced pressure and purification of the residue by flash chromatography (silica gel/hexane/CH_2Cl_2) yielded the corresponding nitro derivative.

Compound 5j: Yield: 87%. White solid. M.p. 173.0-173.8 ºC. ^{1}H NMR (300 MHz, $CDCl_3$): δ = 8.08 (d, 2H, *J*= 9.0 Hz), 7.58 (d, 2H, *J*= 9.0 Hz), 7.40 (d, 2H, *J*= 7.8 Hz), 7.24 (t, 2H, *J*= 7.8 Hz), 7.12 (t, 1H, *J*= 7.8 Hz), 3.15-3.05 (m, 2H), 1.72-1.62 (m, 2H), 1.60-1.50 (m, 2H), 1.45-1.30 (m, 4H) ppm. ^{13}C NMR ($CDCl_3$, 75 MHz): δ = 153.8,

[45] Uemura, A. Toshimitsu, M. Okano, *J. Chem. Soc., Perkin Trans. 1*, **1978**, 1076-1079.

145.8, 144.1, 128.6, 128.0, 127.3, 126.1, 123.8, 65.0, 41.8, 28.2, 28.1 ppm. IR (KBr): ϋ = 3070, 2950, 2860, 1600, 1515, 1350, 1110, 845, 705 cm^{-1}. UV/Vis (MeOH): λ_{max} (ε) = 223 (sh), 289 nm (10000 $mol^{-1}dm^3cm^{-1}$). MS (EI, 70 eV) *m/z* (%): 293 (M^+, 94), 277 (22), 276 (41), 264 (29), 263 (100), 262 (37), 251 (33), 225 (41), 208 (25), 204 (35), 203 (30), 202 (34), 192 (65), 191 (63), 190 (29), 189 (38), 186 (29), 182 (40), 179 (27), 178 (54), 166 (30), 165 (71), 152 (28), 141 (27), 129 (39), 128 (43), 115 (89), 107 (27), 106 (30), 91 (98), 81 (38), 77 (39), 51 (30). Elemental analysis calcd (%) for $C_{19}H_{19}NO_2$: C 77.78, H 6.53, N 4.78; found: C 77.81, H 6.66, N 4.69.

Compound 6h: Yield: 94%. White solid. M.p. 263.8-264.5 ºC. ^{1}H NMR (300 MHz, $CDCl_3$): δ = 8.12 (d, 4H, *J* = 9.0 Hz), 7.58 (d, 4H, *J* = 9.0 Hz), 3.18-3.10 (m, 2H), 1.65-1.55 (m, 4H), 1.50-1.40 (m, 4H). ^{13}C NMR ($CDCl_3$, 75 MHz): δ = 151.7, 146.0, 128.1, 124.0, 65.4, 41.9, 28.0. IR (KBr): ϋ = 3020, 2975, 2860, 1615, 1530, 1350, 850, 710 cm^{-1}. UV/Vis (MeOH): λ_{max} (ε) = 284 nm (16900 $mol^{-1}dm^3cm^{-1}$). MS (EI, 70 eV) *m/z* (%): 338 (M^+, 14), 308 (37), 279 (36), 278 (100), 277 (41), 197 (37), 189 (24), 186 (30), 185 (28), 149 (28), 144 (24), 130 (33), 106 (69). Elemental analysis calcd (%) for $C_{19}H_{18}N_2O_4$: C 67.43, H 5.36, N 8.28; found: C 67.48, H 5.44, N 8.32.

Compound 8: Yield: 60%. White solid. M.p. 188-189 ºC. ^{1}H NMR (300 MHz, $CDCl_3$): δ = 8.42 (dd, 1H, *J* = 6.6, 2.9 Hz), 8.14 (d, 2H, *J*= 9.1 Hz), 8.07 (ddd, 1H, *J* = 9.0, 4.2, 2.9 Hz), 7.65 (dd, 2H, *J* = 9.1, 1.5 Hz), 7.08 (dd, 1H, *J* = 9.1, 9.0 Hz), 3.51-3.38 (m, 1H), 3.29-3.17 (m, 1H), 1.90-1.62 (m, 2H), 1.60-1.31 (m, 6H) ppm. ^{13}C NMR ($CDCl_3$, 75 MHz): δ = 164.4 (d, *J* = 258.5 Hz), 150.1, 146.4, 143.0 (d, *J* = 2.9 Hz), 132.8 (d, *J* = 16.0 Hz), 128.7, 128.7, 125.6 (d, *J* = 7.5 Hz), 124.4 (d, *J* = 10.8 Hz), 123.9, 117.5 (d, *J* = 29.5 Hz), 62.4 (d, *J* = 2.7 Hz), 43.0, 41.3 (d, *J* = 7.5 Hz), 28.6, 28.1, 27.8, 27.0 ppm. IR (KBr): ϋ = 2958, 1522, 1512, 1350 cm^{-1}. UV/Vis (MeOH): λ_{max} (ε) = 276 nm (16000 $mol^{-1}dm^3cm^{-1}$). MS (EI, 70 eV) *m/z* (%): 356 (M^+, 100), 339 (59), 297 (46), 267 (34), 207 (34), 81 (54), 67 (36). Elemental analysis calcd (%) for $C_{19}H_{17}FN_2O_4$: C 64.02, H 4.81, N 7.86; found: C 64.21, H 4.69, N 7.73.

General procedure for the synthesis of compounds 16 and **10c:**[46] 130 mg (1 mmol, **16**) or 260 mg (2 mmol, **10c**) of NO_2BF_4 were added to a solution of 1 mmol of compound **15** or **10a** and 7.9 mg (0.03 mmol) of 18-crown-6 in 15 mL of CH_2Cl_2 under argon atmosphere at 0 ºC. After 4 h at 25 ºC, the reaction mixture was washed with water (2x25 mL) and dried over $MgSO_4$. Evaporation of the solvent under reduced pressure and purification of the residue by flash chromatography (silica gel/hexane/Et_2O 10:1) yielded the corresponding nitro derivative.

Compound 16: Yield: 77%. Yellow solid. M.p. 68.0-70.0 ºC. ^{1}H NMR (300 MHz, $CDCl_3$): δ = 8.10 (d, 2H, *J* = 9.0 Hz), 7.98 (bs, 1H), 7.61 (dd, 2H, *J* = 9.0, 1.5 Hz), 7.55-7.43 (m, 1H), 7.36 (dd, 1H, *J* = 12.9, 2.2 Hz), 7.20 (dd, 1H, *J* = 8.4, 2.2 Hz), 3.47-3.34 (m, 1H), 3.14-3.02 (m, 1H), 1.90-1.15 (m, 8H) ppm. ^{13}C NMR ($CDCl_3$, 75 MHz): δ = 160.7 (d, *J* = 248.3 Hz), 154.7 (d, *J* = 37.6 Hz), 151.5, 146.1, 135.1 (d, *J* = 11.5 Hz), 130.1 (d, *J* = 6.6 Hz), 129.0 (d, *J* = 14.1 Hz), 128.5, 128.5, 123.7, 116.2 (d, *J* = 3.2 Hz), 115.5 (q, *J* = 288.8 Hz), 109.1 (d, *J* = 29.6 Hz), 62.2 (d, *J* = 2.8 Hz), 42.7,

[46] B. Masci, *J. Chem. Soc., Chem. Commun.* **1982**, 1262-1263.

41.3 (d, *J* = 7.6 Hz), 28.8, 28.2, 28.0, 27.1 ppm. IR (film): ῡ = 3325, 2959, 2878, 1717, 1620, 1605, 1543, 1520, 1425, 1348, 1209, 1175 cm^{-1}. MS (EI, 70 eV) *m/z* (%): 423 (M^+ + H, 24), 422 (M^+, 100), 405 (53), 392 (32), 363 (27), 354 (73), 333 (21), 321 (33), 220 (28), 91 (17), 81 (41), 57 (27), 55 (30). Elemental analysis calcd (%) for $C_{21}H_{18}F_4N_2O_3$: C 59.70, H 4.30, N 6.63; found: C 59.58, H 4.49, N 6.51.

Compound 10a:[43] ^{1}H NMR (300 MHz, $CDCl_3$): δ = 7.58-7.46 (m, 4H), 7.44-7.36 (m, 1H), 7.33-7.22 (m, 2H), 7.16 (td, *J* = 7.6, 1.8 Hz, 1H), 6.73 (d, *J* = 7.6 Hz, 1H), 3.21 (m, 1H), 2.13-1.95 (m, 6H), 1.8-1.6 (m, 2H) ppm. ^{13}C NMR ($CDCl_3$, 75 MHz): δ = 146.4, 144.7, 144.2, 128.2, 127.9, 126.4, 125.9, 125.6, 123.6, 123.6, 42.9, 35.1, 32.1, 27.2 ppm.

Compound 10c: Yield: 25%. White solid. ^{1}H NMR (300 MHz, $CDCl_3$): δ = 8.33 (d, *J* = 7.0 Hz, 2 H), 8.11 (d, *J* = 2.4 Hz, 1 H), 7.96 (dd, *J* = 8.4, 2.4 , 1 H), 7.61 (d, *J* = 7.0 Hz, 2 H), 6.71 (d, *J* = 8.4 Hz, 1 H), 3.35-3.29 (m, 1 H), 2.14-2.0 (m, 4 H), 2.0-1.88 (m, 2 H), 1.73-1.59 (m, 2 H) ppm. ^{13}C NMR ($CDCl_3$, 75 MHz): δ = 152.1, 151.1, 147.0, 146.7, 145.4, 128.8, 124.0, 123.8, 121.4, 119.1, 44.1, 35.1, 31.8, 26.4 ppm. IR (KBr): ῡ = 3081, 2928, 2864, 1598, 1520, 1347, 1103, 850, 742 cm^{-1}. UV/Vis (MeOH): λ_{max} (ε) = 276 nm (19000 $mol^{-1}dm^3cm^{-1}$). MS (EI, 70 eV) *m/z* (%): 324 (M^+, 100), 296 (56), 295 (86), 279 (26), 250 (38), 249 (95), 204 (34), 203 (67), 202 (94), 189 (29), 136 (17), 101 (14), 77 (25). Elemental analysis calcd (%) for $C_{18}H_{16}N_2O_4$: C 73.94, H 5.52, N 9.59; found: C 74.12, H 5.71, N 9.82.

General procedure for the synthesis of compounds 5a and **6b:** A solution of 1 mmol of the corresponding nitroderivative in 150 mL of Et_2O was hydrogenated (1 atm.) with 60 mg of 5% Pd/C. The catalyst was separated by filtration and after evaporation of the solvent at reduced pressure the residue was purified by flash chromatography (silica gel/hexane/Et_2O).

Compound 5a: Yield: 95%. Yellow oil. ^{1}H NMR (300 MHz, $CDCl_3$): δ = 7.38 (d, 2H, *J* = 9.0 Hz), 7.26-7.15 (m, 4H), 7.04 (t, 1H, *J* = 9.0 Hz), 6.57 (d, 2H, *J* = 9.0 Hz), 3.23 (bs, 2H), 3.05-2.95 (m, 2H), 1.80-1.65(m, 4H), 1.40-1.20(m, 4H) ppm. ^{13}C NMR ($CDCl_3$, 75 MHz): δ = 146.6, 143.5, 136.4, 128.2, 128.0, 127.0, 125.0, 115.2, 64.0, 41.7, 28.5, 28.4 ppm. IR (CCl_4): ῡ = 3460, 3370, 3020, 2980, 2870, 1600, 1500, 1160, 690 cm^{-1}. UV/Vis (MeOH): λ_{max} (ε) = 249 nm (13800 $mol^{-1}dm^3cm^{-1}$). MS (EI, 70 eV) *m/z* (%): 263 (M^+, 100), 186 (24), 182 (37), 130 (15), 115 (25), 106 (25), 91 (19). Elemental analysis calcd (%) for $C_{19}H_{21}N$: C 86.64, H 8.04, N 5.32; found: C 86.48, H 8.22, N 5.28.

Compound 6b: Yield: 97%. Yellow solid. M.p. 201.6-202.8 ºC. ^{1}H NMR (300 MHz, $CDCl_3$): δ = 7.16 (d, 4H, *J* = 8.7 Hz), 6.54 (d, 4H, *J* = 8.4 Hz), 3.39 (bs, 4H), 2.98-2.90 (m, 2H), 1.72-1.58 (m, 4H), 1.80-1.40 (m, 4H) ppm. ^{13}C NMR ($CDCl_3$, 75 MHz): δ = 143.3, 137.1, 127.8, 115.2, 63.1, 41.7, 28.5 ppm. IR (CCl_4): ῡ = 3450, 3350, 3020, 2980, 2870, 1620, 1510, 1275, 1180, 790, 760 cm^{-1}. UV/Vis (MeOH): λ_{max} (ε) = 234 (12700), 255 nm (18600 $mol^{-1}dm^3cm^{-1}$). MS (EI, 70 eV) *m/z* (%): 278 (M^+, 100), 277 (42), 197 (36), 185 (27), 144 (20), 130 (32), 106 (64), 91 (6), 77 (13). Elemental

analysis calcd (%) for $C_{19}H_{22}N_2$: C 81.96, H 7.97, N 10.07; found: C 82.12, H 7.73, N 10.18.

General procedure for the synthesis of compounds 11 and **12:**[47] 40 mg of 10% Pd/C were added to a solution of 360 mg (1 mmol) of **8** and 0.61 mL (6 mmol) of cyclohexene in 20 mL of EtOH. The reaction mixture was refluxed 1 h (the reaction was monitored by TLC) and the catalyst was separated by filtration. After evaporation of the solvent at reduced pressure, the mixture of compounds obtained was separated by flash chromatography (silica gel, hexane/Et_2O 10:1).

Compound 11: Yield: 31%. Yellow solid. M.p. 138.0-140.0 ºC. ^{1}H NMR (300 MHz, $CDCl_3$): δ = 8.08 (d, 2H, *J* = 9.0 Hz), 8.14 (dd, 2H, *J* = 9.0, 1.5 Hz), 6.79-6.63 (m, 2H), 6.42 (ddd, 1H, *J* = 8.5, 3.9, 2.9 Hz), 3.43-3.34 (m, 3H), 3.04-2.96 (m, 1H), 1.95-1.77 (m, 1H), 1.70-1.52 (m, 2H), 1.47-1.35 (m, 5H) ppm. ^{13}C NMR ($CDCl_3$, 75 MHz): δ = 154.3 (d, *J* = 237.5 Hz), 152.1, 145.9, 142.6 (d, *J* = 2.0 Hz), 131.1 (d, *J* = 14.7 Hz), 128.6, 128.6, 123.5, 116.9 (d, *J* = 25.5 Hz), 115.5 (d, *J* = 4.9 Hz), 114.8 (d, *J* = 8.5 Hz), 62.4 (d, *J* = 2.8 Hz), 42.6, 41.4 (d, *J* = 8.4 Hz), 28.9, 28.3, 28.2, 27.2 ppm. IR (film): ϋ = 3447, 3371, 3018, 2960, 1593, 1518, 1497, 1350, 1215 cm^{-1}. UV/Vis (MeOH): λ_{max} (ε) = 283(9300 mol^{-1}dm^{3}cm^{-1}). MS (EI, 70 eV) *m/z* (%): 326 (M^+, 100), 283 (15), 258 (17), 138 (27), 124 (14), 81 (10). Elemental analysis calcd (%) for $C_{19}H_{19}FN_2O_2$: C 69.91, H 5.87, N 8.59; found: C 69.86, H 5.99, N 8.45.

Compound 12: Yield: 30%. Yellow solid. M.p. 138.0-140.0 ºC. ^{1}H NMR (300 MHz, $CDCl_3$): δ = 8.37 (dd, 1H, *J* = 6.6, 2.9 Hz), 7.97 (ddd, 1H, *J* = 9.0, 4.1, 2.9 Hz), 7.23 (dd, 2H, *J* = 8.6, 1.5 Hz), 7.01 (dd, 1H, *J* = 9.0, 8.5 Hz), 6.57 (d, 2H, *J* = 8.6 Hz), 3.65-3.48 (bs, 2H), 3.37-3.27 (m, 1H), 3.09 (t, 1H, *J* = 3.8 Hz), 1.86-1.61 (m, 2H), 1.61-1.18 (m, 6H) ppm. ^{13}C NMR ($CDCl_3$, 75 MHz): δ = 164.4 (d, *J* = 258.3 Hz), 144.6, 144.2 (d, *J* = 2.5 Hz), 135.1 (d, *J* = 16.1 Hz), 132.8, 128.6, 128.5, 125.5 (d, *J* = 8.2), 123.2 (d, *J* = 10.8 Hz), 117.2 (d, *J* = 27.0 Hz), 115.1, 61.6 (d, *J* = 3.0 Hz), 42.8, 41.2 (d, *J* = 8.2 Hz), 28.8, 28.5, 28.0, 27.2 ppm. IR (film): ϋ = 3476, 3387, 2963, 2939, 1533, 1514, 1475, 1352 cm^{-1}. UV/Vis (MeOH): λ_{max} (ε) = 263 nm (11000 mol^{-1}dm^{3}cm^{-1}). MS (EI, 70 eV) *m/z* (%): 326 (M^+, 100), 271 (20), 245 (35), 225 (15), 106 (12), 93 (11). Elemental analysis calcd (%) for $C_{19}H_{19}FN_2O_2$: C 69.91, H 5.87, N 8.59; found: C 70.12, H 5.76, N 8.71.

Synthesis of compound 15: 320 mg (1.5 mmol) of trifluoroacetic anhydride were added to a solution of 280 mg (1.00 mmol) of **7h** and 240 mg (3.0 mmol) of pyridine in 25 mL of CH_2Cl_2. After 2 h at 25 ºC the reaction mixture was washed with water (2x25 mL) and dried over $MgSO_4$. Evaporation of the solvent at reduced pressure and purification by flash chromatography (silica gel, hexane/Et_2O 10:1) yielded 250 mg (65%) of **15**. Yellow solid. M.p. 140.0-142.0 ºC. ^{1}H NMR (300 MHz, $CDCl_3$): δ = 7.75 (bs, 1H), 7.56-7.40 (m, 3H), 7.35-7.05 (m, 5H), 3.40 (dt, 1H, *J* = 3.9, 3.9 Hz), 3.05 (t, 1H, *J* = 3.2 Hz), 1.85-1.61 (m, 2H), 1.61-1.20 (m, 6H) ppm. ^{13}C NMR ($CDCl_3$, 75 MHz): δ = 160.6 (d, *J* = 248.1 Hz), 154.6 (d, *J* = 37.6 Hz), 143.8, 134.1 (d, *J* = 11.2

[47] I. D. Entwistle, R. A. W. Johnstone, T. J. Povall, *J. Chem. Soc., Perkin Trans. I* **1975**, 1300-1301.

Hz), 130.9 (d, *J* = 14.1 Hz), 130.3 (d, *J* = 7.0 Hz), 128.3, 128.3, 127.6, 127.5, 125.9, 115.8 (d, *J* = 3.2 Hz), 115.6 (q, *J* = 288.8 Hz), 108.9 (d, *J*= 29.7 Hz), 62.0 (d, *J* = 2.9 Hz), 42.6, 41.2 (d, *J* = 8.0 Hz), 28.9, 28.5, 28.1, 27.3 ppm. IR (film): ῡ = 3298, 3206, 2955, 2914, 2872, 1705, 1204, 1184 cm^{-1}. MS (EI, 70 eV) *m/z* (%): 378, (M^+ + H, 24) 377 (M^+, 100), 335 (26), 309 (36), 308 (19), 296 (40), 220 (27), 115 (17), 91 (29), 84 (28), 51 (22), 49 (55). Elemental analysis calcd (%) for $C_{21}H_{19}F_4NO$: C 66.82, H 5.08, N 3.71; found: C 66.89, H 5.19, N 3.64.

Synthesis of compound 7v:[48] 15 mg (4.00 mmol) of $NaBH_4$ were added to a solution of 210 mg (0.50 mmol) of **16** in 50 mL of EtOH at 25 ºC under argon atmosphere. After 24 h, 25 mL of water were added and the reaction mixture was extracted with CH_2Cl_2 (3x20 mL). The organic solution was dried over $MgSO_4$ and the solvent was evaporated under reduced pressure. Purification of the residue by flash chromatography (silica gel, hexane/Et_2O 10:4) yielded 120 mg (74%) of **7v** as a yellow solid. M.p. 50.0-52.0 ºC. ^{1}H NMR (300 MHz, $CDCl_3$): δ = 8.08 (d, 2H, *J* = 9.0 Hz), 7.58 (dd, 2H, *J* = 9.0, 1.5 Hz), 7.19 (t, 1H, *J* = 8.6 Hz), 6.37 (dd, 1H, *J* = 8.6, 2.4 Hz), 6.22 (dd, 1H, *J* = 13.5, 2.4 Hz), 3.64 (bs, 2H), 3.34 (dt, 1H, *J* = 3.6, 3.6 Hz), 3.07-2.95 (m, 1H), 1.93-1.07 (m, 8H) ppm. ^{13}C NMR ($CDCl_3$, 75 MHz): δ = 161.5 (d, *J* = 245.4 Hz), 152.9, 146.8 (d, *J* = 11.5 Hz), 145.7, 130.0 (d, *J* = 7.45 Hz), 128.3, 128.2, 123.5, 120.4 (d, *J* = 14.4 Hz), 111.1 (d, *J*= 2.3 Hz), 102.8 (d, *J* = 27.3 Hz), 61.6 (d, *J* = 2.7 Hz), 42.6, 41.4 (d, *J* = 8.2 Hz), 28.8, 28.3, 28.1, 27.2 ppm. IR (film): ῡ = 3018, 2961, 2928, 1630, 1593, 1350, 1261 cm^{-1}. UV/Vis (MeOH): λ_{max} (ε) = 250 nm (9300 $mol^{-1}dm^3cm^{-1}$). MS (EI, 70 eV) *m/z* (%): 326 (M^+, 100), 309 (28), 271 (17), 258 (18), 225 (22), 224 (19), 124 (25), 111 (17), 57 (17). Elemental analysis calcd (%) for $C_{19}H_{19}FN_2O_2$: C 69.91, H 5.87, N 8.59; found: C 69.83, H 5.97, N 8.63.

Synthesis of compound 10b:[49] Yield: 95%. ^{1}H NMR (300 MHz, $CDCl_3$): δ = 7.24 (d, *J* = 6.6, Hz, 2 H), 6.75 (d, *J* = 6.6, Hz, 2 H), 6.60 (d, *J* = 2.3 Hz, 1 H), 6.47 (d, *J* = 8.0 Hz, 1 H), 6.40 (dd, *J* = 8.0, 2.3 Hz, 1 H), 3.82-3.13 (m, 4 H), 3.06-2.89 (m, 1 H), 2.07-1.77 (m, 6 H), 1.77-1.43 (m, 2 H) ppm. ^{13}C NMR ($CDCl_3$, 75 MHz): δ = 145.3, 144.5, 144.4, 137.2, 135.3, 128.6, 124.4, 115.0, 112.1, 111.1, 41.4, 35.2, 32.6, 27.3 ppm. IR (KBr): ῡ = 3426, 3354, 3217, 3012, 2933, 2862, 1622, 1518, 1492, 1279, 824 cm^{-1}. UV/Vis (MeOH): λ_{max} (ε) = 239 nm (11000 $mol^{-1}dm^3cm^{-1}$). MS (EI, 70 eV) *m/z* (%): 264 (M^+, 99), 263 (13), 236 (90), 235 (100), 221 (37), 218 (20), 149 (26), 106 (19), 69 (29), 57 (8). Elemental analysis calcd (%) for $C_{18}H_{20}N_2$: C 81.77, H 7.63, N 10.60; found: C 81.60, H 7.79, N 10.58.

General procedure for the synthesis of compounds 5h, **6g**, and **7f:** 150 mg (1.10 mmol, **5h** and **7f**) or 290 mg (2.20 mmol, **6g**) of $AlCl_3$ were added to a solution of 90 mg (1.1 mmol, **5h**, **7f)** or 180 mg (2.2 mmol, **6g**) of CH_3COCl in 25 mL of CH_2Cl_2 at -20 ºC with vigorous stirring. After 30 min, a solution of 1 mmol of the corresponding DPN or FDPN derivative in 5 mL of CH_2Cl_2 was slowly added. The reaction mixture was stirred 3 h, poured into 50 mL of ice water and extracted with CH_2Cl_2 (3x20 mL). The organic solution was dried over $MgSO_4$ and the solvent was evaporated under

[48] Z. H. Kuzdin, P. Lyzwa, J. Luczak, G. Andrijewski, *Synthesis*, **1997**, 44-46.
[49] M. Petrini, R. Ballini, G. Rosini, *Synthesis* **1987**, 713-714.

reduced pressure. The residue was purified by flash chromatography (silica gel, hexane/CH_2Cl_2 10:4).

Compound 5h: Yield: 80%. White solid. M.p. 137.5-140.0 ºC. ^{1}H NMR (300 MHz, $CDCl_3$): δ = 7.81 (d, 2H, *J* = 8.0 Hz), 7.51 (d, 2H, *J* = 8.0 Hz), 7.41 (d, 2H, *J* = 8.0 Hz), 7.21 (t, 2H, *J* = 7.3 Hz), 7.09 (t, 1H, *J* = 7.8 Hz), 3.15-3.05 (m, 2H), 2.51 (s, 3H), 1.72-1.52 (m, 4H), 1.45-1.20 (m, 4H) ppm. ^{13}C NMR ($CDCl_3$, 75 MHz): δ = 197.8, 151.8, 144.9, 134.5, 128.6, 128.5, 127.5, 127.3, 125.8, 65.1, 41.6, 28.3, 26.5 ppm. IR (CCl_4): ϑ = 3010, 2980, 2880, 1680, 1605, 1410, 1275 cm^{-1}. UV/Vis (MeOH): λ_{max} (ε) = 262 nm (15200 mol^{-1}dm^{3}cm^{-1}). MS (EI, 70 eV) *m/z* (%): 290 (M^+, 14), 91 (11), 43 (100). Elemental analysis calcd (%) for $C_{21}H_{22}O$: C 86.85, H 7.64; found: C 87.04, H 7.57.

Compound 6g: Yield: 85%. White solid. M.p. 263.0-266.0 ºC. ^{1}H NMR (300 MHz, $CDCl_3$): δ = 7.83 (d, 4H, *J* = 8.4 Hz), 7.51 (d, 4H, *J* = 8.4 Hz), 3.18-3.08 (m, 2H), 2.51 (s, 6H), 1.69-1.58 (m, 4H), 1.45-1.30 (m, 4H) ppm. ^{13}C NMR ($CDCl_3$, 75 MHz): δ = 197.6, 150.5, 134.8, 128.7, 127.6, 65.3, 41.7, 28.2, 26.5 ppm. IR (KBr): ϑ = 3010, 2980, 2880, 1690, 1605, 1410, 1275, 970, 855, 830 cm^{-1}. UV/Vis (MeOH): λ_{max} (ε) = 248 (20700), 269 nm (18300 mol^{-1}dm^{3}cm^{-1}). MS (EI, 70 eV) *m/z* (%): 332 (M^+, 10), 289 (8), 151 (8), 43 (100). Elemental analysis calcd (%) for $C_{23}H_{24}O_2$: C 83.09, H 7.28; found: C 82.92, H 7.33.

Compound 7f: Yield: 75%. White solid. M.p. 107.0-109.0 ºC. ^{1}H NMR (300 MHz, $CDCl_3$): δ = 7.83 (d, 2H, *J* = 8.5 Hz), 7.57 (d, 2H, *J* = 8.2 Hz), 7.49 (td, 1H, *J* = 7.6, 2.0 Hz), 7.15-6.95 (m, 2H), 6.88 (ddd, 1H, *J* = 12.0, 7.9, 1.4 Hz), 3.40 (dt, 1H, *J* = 4.3, 4.3 Hz), 3.12-3.05 (m, 1H), 2.50 (s, 3H), 1.82-1.20 (m, 8H) ppm. ^{13}C NMR ($CDCl_3$, 75 MHz): δ = 197.8, 160.8 (d, *J* = 246.9 Hz), 149.9, 134.7, 131.4 (d, *J* = 13.5 Hz), 129.5 (d, *J* = 5.4 Hz), 128.4, 128.0 (d, *J* = 8.7 Hz), 128.0, 127.9, 124.2 (d, *J* = 3.2 Hz), 116.3 (d, *J* = 23.9 Hz), 62.3 (d, *J* = 2.6 Hz), 42.5, 41.2 (d, *J* = 8.2 Hz), 28.8, 28.3, 28.1, 27.2, 26.5 ppm. IR (C Cl_4): ϑ = 3035, 2958, 2875, 1683, 1602, 1487, 1357, 1271 cm^{-1}. UV/Vis (MeOH): λ_{max} (ε) = 259 nm (16600 mol^{-1}dm^{3}cm^{-1}). MS (EI, 70 eV) *m/z* (%): 308(M^+, 14), 225(9), 43(100). Elemental analysis calcd (%) for $C_{21}H_{21}FO$: C 81.78, H 6.87; found: C 81.94, H 6.68.

General procedure for the synthesis of compounds 5f-g and 6e-f:[50] 140 mg (1.10 mmol, **5f** and **5g**) or 280 mg (2.20 mmol, **6e** and **6f**) of oxalyl chloride were added to a solution of 150 mg (1.10 mmol, **5f** or **5g**) or 300 mg (2.20 mmol, **6e** or **6f**) of $AlCl_3$ in 30 mL of CH_2Cl_2 at -20 ºC. After 30 min, a solution of 250 mg (1 mmol) of DPN in 5 mL of CH_2Cl_2 was slowly added. The reaction mixture was stirred 4 h, poured into 50 mL of ice water and extracted with CH_2Cl_2 (3x20 mL). The organic solution was dried over $MgSO_4$ and the solvent was evaporated under reduced pressure. The residue was refluxed in chlorobenzene for 6 h and the solvent was evaporated at reduced pressure. The reaction product, without further purification, was refluxed for 2 h with NaEtO/EtOH in the case of esters **5g** and **6f**, or H_2O/EtOH in the case of acids **5g** and

[50] Grützmacher, H.-F.; Mehdizadeh, A.; Mülverstedt, A. *Chem. Ber.* **1994**, *127*, 1163-1166.

6e. After extraction with Et_2O (3x25 mL), the reaction products were purified by flash chromatography (silica gel, hexane/$CHCl_3$).

Compound 5f: Yield: 80%. White solid. M.p. 230.0-235.0 ºC. ^{1}H NMR (300 MHz, $CDCl_3$): δ = 7.95 (d, 2H, *J* = 8.4 Hz), 7.53 (d, 2H, *J* = 8.7 Hz), 7.42 (d, 2H, *J* = 7.2 Hz), 7.23 (t, 2H, *J* = 7.2 Hz), 7.09 (t, 1H, *J* = 7.5 Hz), 3.16-3.06 (m, 2H), 1.72-1.52 (m, 4H), 1.40-1.20 (m, 4H) ppm. ^{13}C NMR ($CDCl_3$, 75 MHz): δ = 172.0, 152.4, 144.9, 130.4, 128.5, 127.4, 127.3, 126.2, 125.8, 65.2, 41.7, 28.2 ppm. IR (CCl_4): ϑ̃ = 3010, 2980, 2890, 1690, 1605, 1420, 1280 cm^{-1}. UV/Vis (MeOH): λ_{max} (ε) = 250 nm (15000 mol^{-1}dm^{3}cm^{-1}). MS (EI, 70 eV) *m/z* (%): 292 (M^+, 64), 248 (22), 247 (100), 211 (28), 205 (39), 193 (21), 191 (26), 179 (42), 178 (35), 165(48), 143 (20), 129 (42), 128 (28), 117 (27), 115 (89), 91 (96), 81 (23), 77 (30), 44 (41), 41 (38). Elemental analysis calcd (%) for $C_{20}H_{20}O_2$: C 82.15, H 6.90; found: C 82.28, H 6.85.

Compound 5g: Yield: 72%. White solid. M.p. 83.0-86.0 ºC. ^{1}H NMR (300 MHz, $CDCl_3$): δ = 7.89 (d, 2H, *J* = 8.7 Hz), 7.51 (d, 2H, *J* = 8.7 Hz), 7.42 (d, 2H, *J* = 8.7 Hz), 7.23 (t, 2H, *J* = 8.7 Hz), 7.09 (t, 1H, *J* = 8.7 Hz), 4.33 (q, 2H, *J* = 7.2 Hz), 3.15-3.05 (m, 2H), 1.72-1.52 (m, 4H), 1.40-1.20 (m, 7H) ppm. ^{13}C NMR ($CDCl_3$, 75 MHz): δ = 167.2, 152.0, 144.9, 129.7, 128.4, 127.4, 127.3, 127.3, 125.7, 64.9, 60.8, 41.6, 28.3, 14.3 ppm. IR (KBr): ϑ̃ = 3010, 2960, 2880, 1715, 1610, 1285, 1115, 775, 715 cm^{-1}. UV/Vis (MeOH): λ_{max} (ε) = 245 (sh), 250 nm (11800 mol^{-1}dm^{3}cm^{-1}). MS (EI, 70 eV) *m/z* (%): 320 (M^+, 30), 248 (21), 247 (100), 205 (32), 191(28), 179 (20), 178 (24), 165 (36), 143 (22), 129 (33), 117 (35), 115 (51), 91 (77), 77 (15), 41 (19). Elemental analysis calcd (%) for $C_{22}H_{24}O_2$: C 82.45, H 7.55; found: C 82.42, H 7.67.

Compound 6e: Yield: 90%. White solid. M.p. > 350 ºC (d). ^{1}H NMR (300 MHz, [D_6]DMSO): δ = 12.80 (bs, 2H), 7.79 (d, 4H, *J* = 8.7 Hz), 7.64 (d, 4H, *J* = 8.7 Hz), 3.30-3.24 (m, 2H), 1.58-1.40 (m, 4H), 1.40-1.20 (m, 4H) ppm. ^{13}C NMR (75 MHz, [D_6]DMSO): δ = 172.1, 151.8, 130.8, 129.5, 128.8, 66.5, 42.7, 29.0 ppm. IR (KBr): ϑ̃ = 3010, 2960, 2880, 1690, 1605, 1420, 1280, 1190, 770 cm^{-1}. UV/Vis (MeOH): λ_{max} (ε) = 234 (10400), 256 nm (15000 mol^{-1}dm^{3}cm^{-1}). MS (EI, 70 eV) *m/z* (%): 336 (M^+, 17), 292 (26), 291 (100), 205 (25), 191 (19), 189 (18), 179 (24), 178 (26), 165 (29), 143 (20), 135 (25), 129 (36), 128 (20), 117 (26), 115 (60), 91 (51), 81 (46), 77 (24), 44 (72), 41 (31). Elemental analysis calcd (%) for $C_{21}H_{20}O_4$: C 74.97, H 6.00; found: C 74.82, H 6.13.

Compound 6f: Yield: 72%. White solid. M.p. 132.5-133.0 ºC. ^{1}H NMR (300 MHz, $CDCl_3$): δ = 7.90 (d, 4H, *J* = 8.7 Hz), 7.48 (d, 4H, *J* = 8.7 Hz), 4.33 (q, 4H, *J* = 7.2 Hz), 3.15-3.05 (m, 2H), 1.70-1.55 (m, 4H), 1.42-1.26 (m, 10H) ppm. ^{13}C NMR ($CDCl_3$, 75 MHz): δ = 166.4, 150.3, 129.8, 128.0, 127.3, 65.3, 60.7, 41.7, 28.2, 14.3 ppm. IR (CCl_4): ϑ̃ = 3040, 2970, 2880, 1720, 1610, 1275, 1115, 1025, 850, 725 cm^{-1}. UV/Vis (MeOH): λ_{max} (ε) = 235 (17400), 258 nm (26700 mol^{-1}dm^{3}cm^{-1}). MS (EI, 70 eV) *m/z* (%): 392 (M^+, 11), 347 (18), 320 (24), 319 (100), 205 (17), 191 (19), 165 (25), 143 (24), 129 (30), 117 (31), 115 (30), 91 (28), 77 (10), 41 (16). Elemental analysis calcd (%) for $C_{25}H_{28}O_4$: C 76.49, H 7.19; found: C 76.57, H 7.25.

Synthesis of compound 6a: A mixture of 1.27 g (11.50 mmol) of 7-norbornanone,[51] 3.55 ml (28.70 mmol) of *N*,*N*-dimethylaniline and 5 mL of cc. HCl was refluxed for 48 h with vigorous stirring. The reaction mixture was neutralizated with 10% NaOH and extracted with CH_2Cl_2 (3x20 mL). The organic solution was washed with water (3x25 mL) and dried over KOH. The solvent was evaporated at reduced pressure and the residue purified by flash chromatography (silica gel, hexane/Et_2O 7:3) yielding 0.96 g (25%) of **6a**. Yellow solid. M.p. 232.0-235.0 ºC. ^{1}H NMR (300 MHz, $CDCl_3$): δ = 7.24 (d, 4H, *J* = 9.9 Hz), 6.60 (d, 4H, *J* = 9.9 Hz), 3.00-2.90 (m, 2H), 2.84 (s, 12H), 1.70-1.60 (m, 4H), 1.32-1.22 (m, 4H) ppm. ^{13}C NMR ($CDCl_3$, 75 MHz): δ = 148.0, 135.3, 127.6, 112.7, 62.8, 41.7, 40.7, 28.7 ppm. IR (KBr): ῡ = 3050, 2980, 2880, 1620, 1525, 1360, 1180, 830, 820 cm^{-1}. UV/Vis (MeOH): λ_{max} (ε) = 259 (sh), 272 nm (20000 $mol^{-1}dm^3cm^{-1}$). MS (EI, 70 eV) *m/z* (%): 334 (M^+, 100), 333 (49), 290 (33), 253 (33), 213 (33), 167 (31), 146 (21), 139 (33), 138 (35), 134 (74), 131 (59), 126 (42), 118 (31), 117 (32), 44 (19), 42 (26). Elemental analysis calcd (%) for $C_{23}H_{30}N_2$: C 82.58, H 9.05, N 8.38; found: C 82.71, H 9.20, N 8.27.

Selected UV/vis spectra:

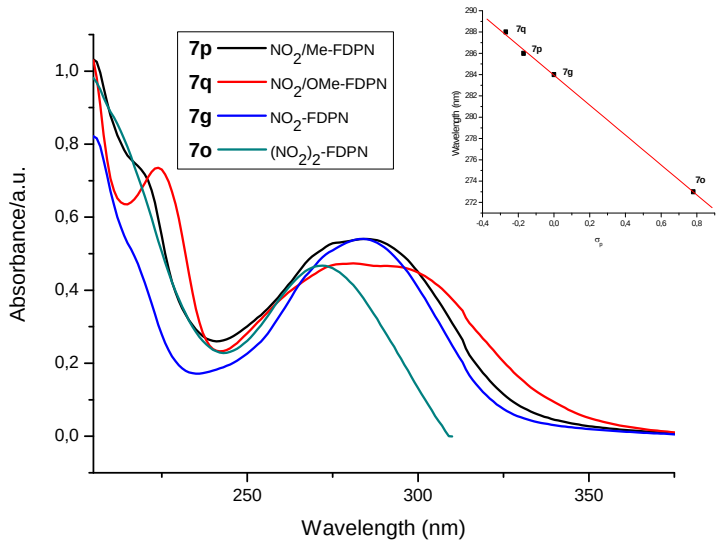

Figure 16.

[51] (a) P. G. Gassman, P. G. Pape, *J. Org. Chem.* **1964**, *29*, 160-163. (b) P. G. Gassman, J. L. Marshall, *Org. Synth.* **1968**, *48*, 68-72.

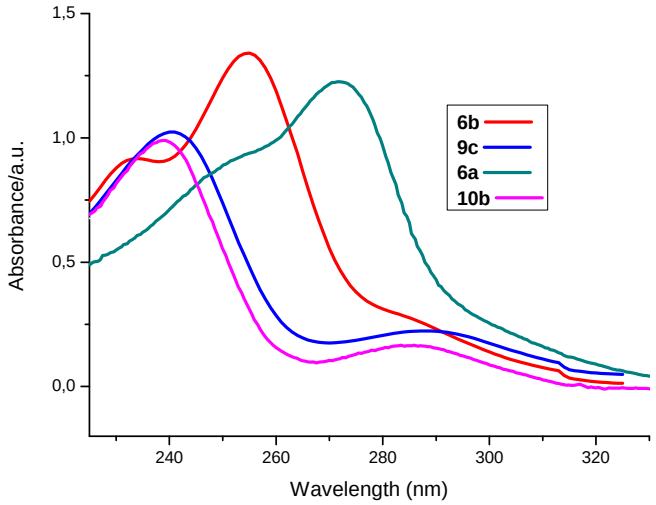

Figure 17.

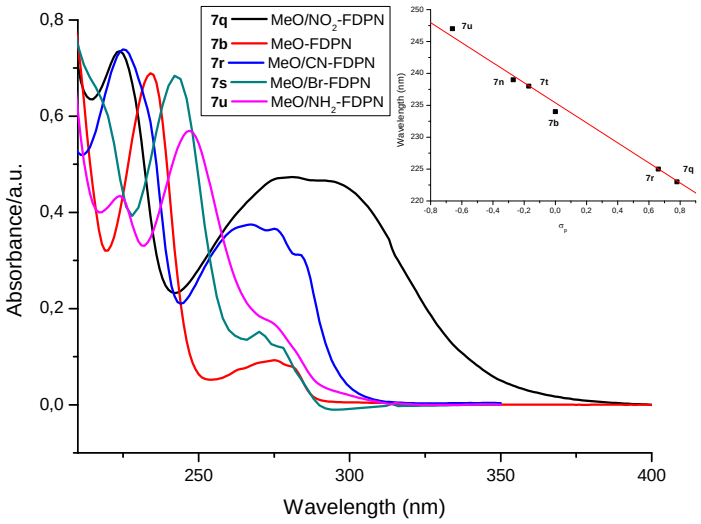

Figure 18.

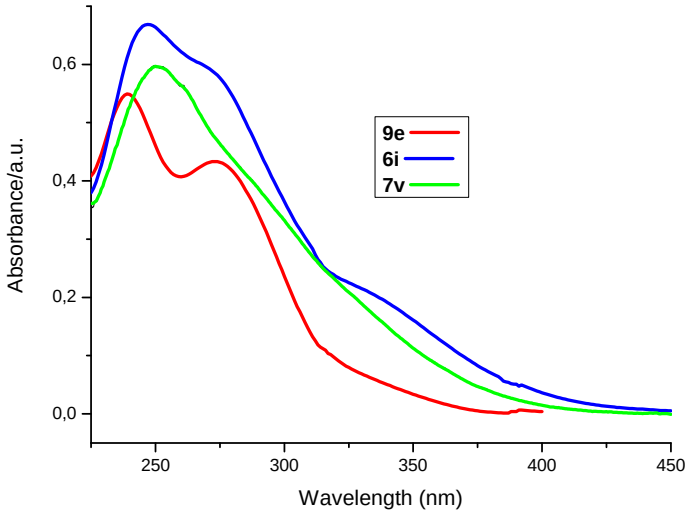

Figure 19.

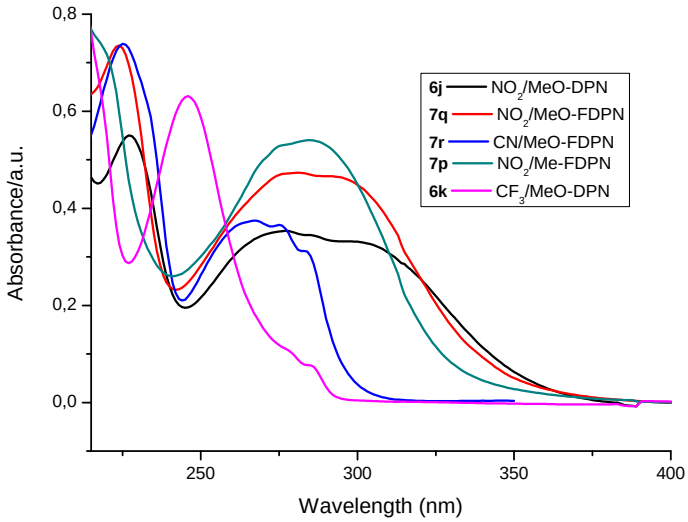

Figure 20.

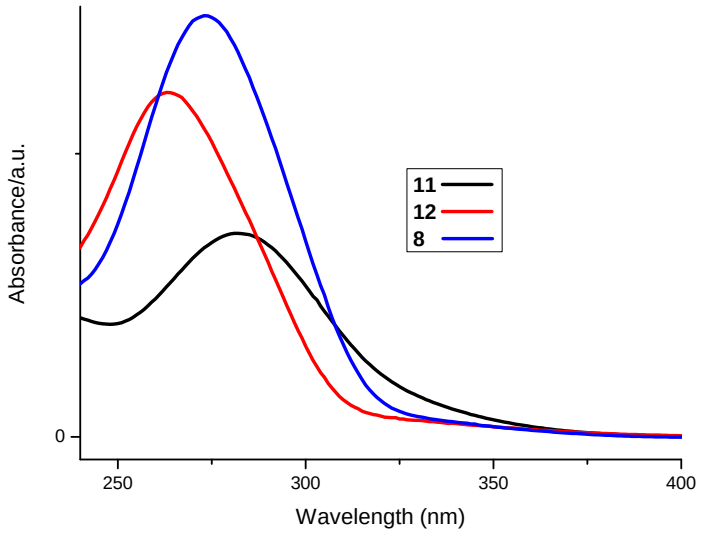

Figure 21.

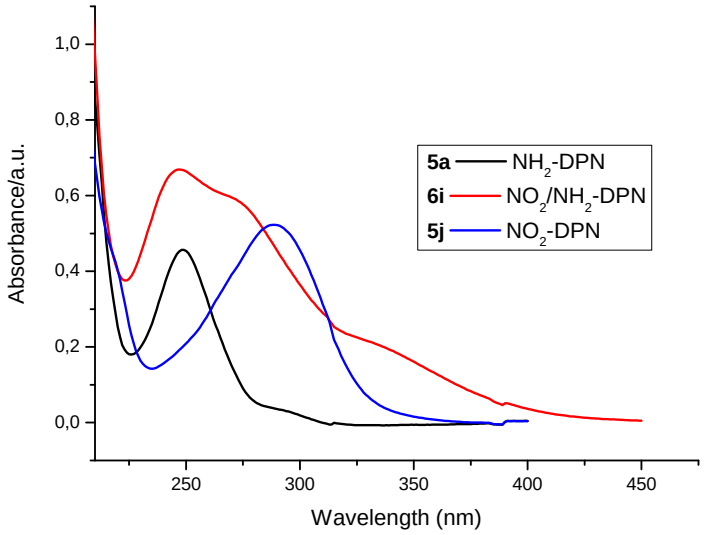

Figure 22.

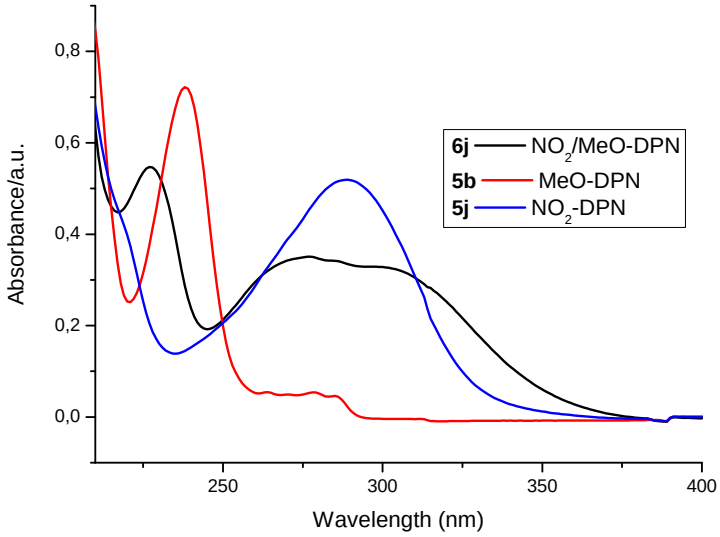

Figure 23.

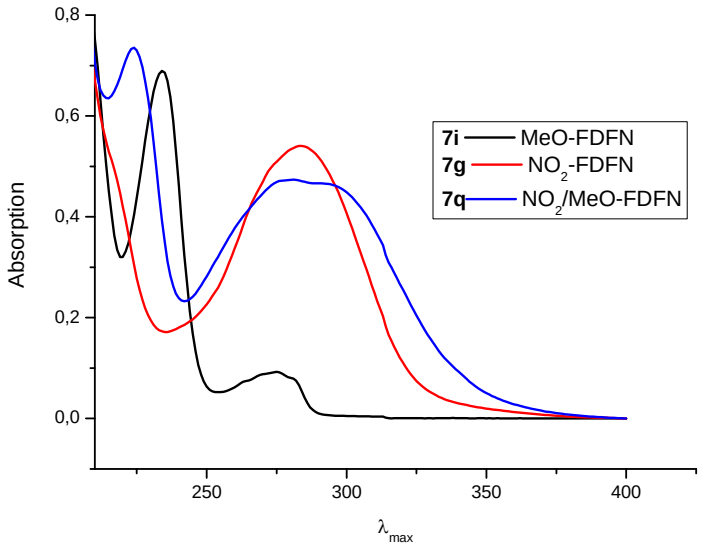

Figure 24.

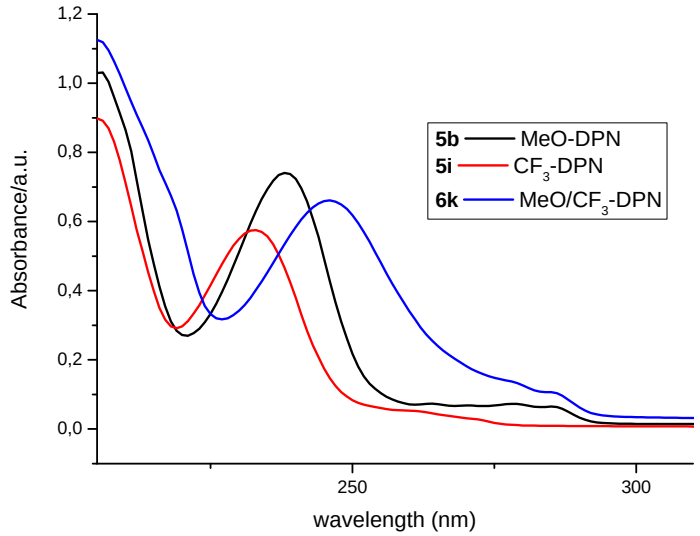

Figure 25.

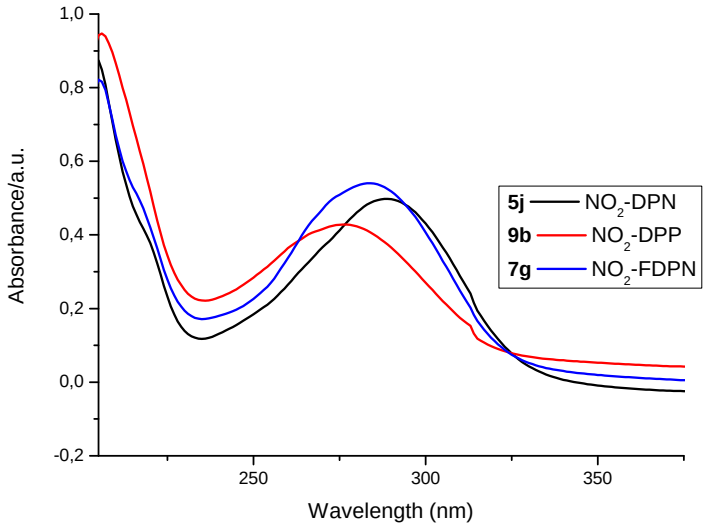

Figure 26.

NMR correlations:

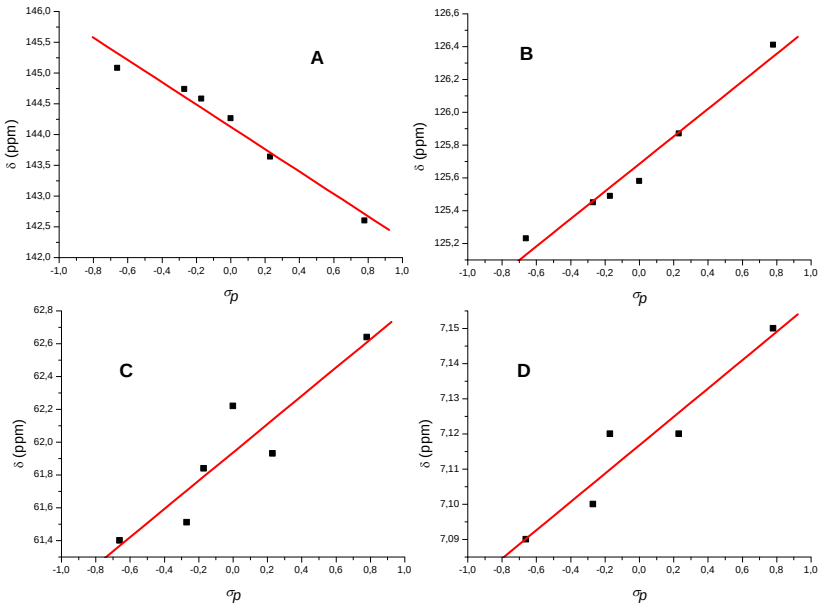

Figure 27. Correlation between NMR chemical shifts (graph A, C-12; graph B, C-15; graph C, C-7; graph D, H-15) and σ_p values in monosubstituted FDPN's **7c** and **7h-l**.

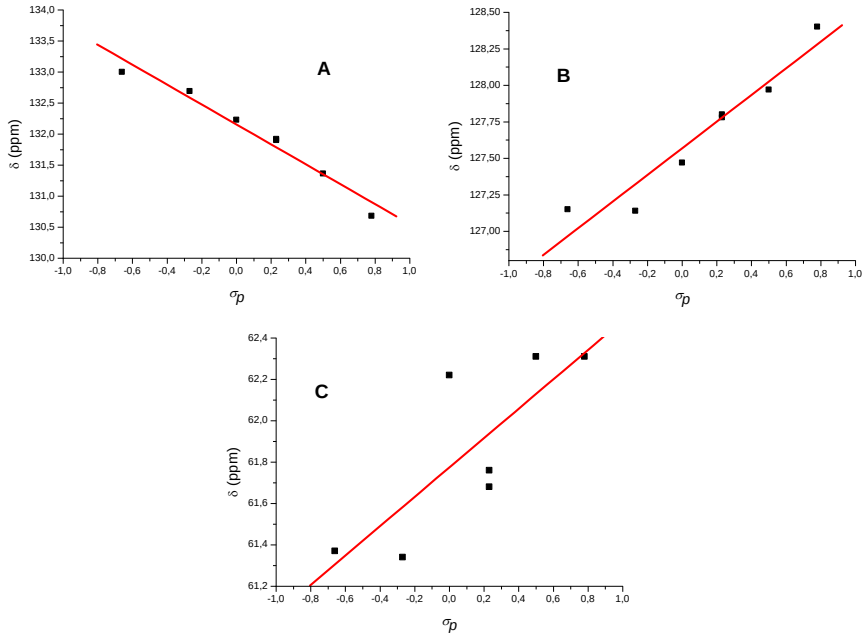

Figure 28. Correlation between NMR chemical shifts (graph A, C-8; graph B, C-11; graph C, C-7) and σ_p values in monosubstituted FDPN's **7a-g**.

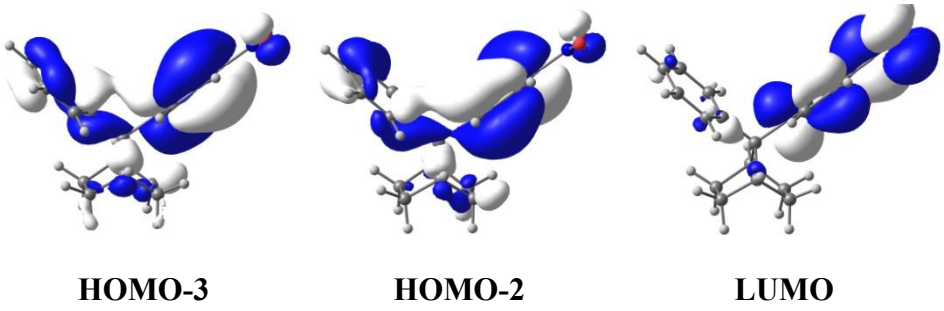

Figure 29. Molecular orbitals of **5j** responsible for the homoconjugation band

III. CAPÍTULO 2

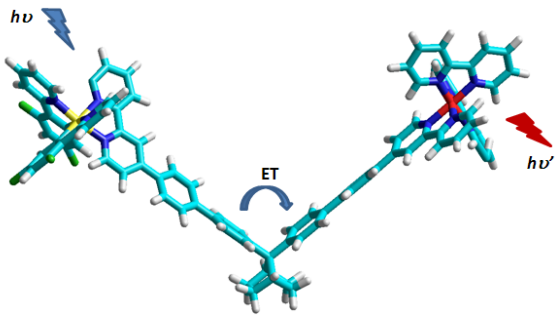

2.1 Efficient Photoinduced Energy Transfer Mediated by Aromatic homoconjugated bridges

A new D-B-A dyad consisting of Ruthenium(II) and Iridium(III) species separated by an homoconjugated bridge derived from 7,7-diphenylnorbornane $[Ir\text{-}Nor\text{-}Ru]^{3+}$ *has been synthesized. The photophysical and electrochemical properties of the heterodinuclear complex have been compared with those of the analogous homodinuclear complexes* $[Ru\text{-}Nor\text{-}Ru]^{4+}$ *and* $[Ir\text{-}Nor\text{-}Ir]^{2}$*. Transient absorption spectra on the nanosecond and sub-picosecond timescales show for the first time that an homoconjugated bridge can mediate efficiently in the photoinduced energy transfer from the Iridium (III) to the Ruthenium(II) center according to a Dexter-type mechanism.*

(*Chem. Eur. J.* **2010**, *16*, 6033 – 6040)

2.2.1 Introduction

The design of supramolecular multicomponent systems for photoinduced energy/electron transfer is an important field of research with applications in the development of electroluminescent displays, molecular scale devices and solar energy conversion systems.[1] In donor-bridge-acceptor (D-B-A) dyads, not only the chromophores but also the bridge plays a fundamental role in mediating the energy transfer process and the search of bridges with molecular wire behavior still remains a challenge.[2] The electronic coupling between donor and acceptor, which is a main determining factor for the (Dexter) energy/electron transfer processes, can be provided by various types of electronic interactions that are inherent to the intervening medium between donor and acceptor.

Whereas much attention is focused on π-conjugated bridges,[2,3] also σ-conjugation (through σ bond interaction),[4] cross-conjugated pathways,[5] helical bridges (through foldamer coupling),[6] π-stacked systems[7] and hexa-arylbenzenes with toroidal delocalization[8] are modes for electronic communication that can be very effective (as compared to through (vacuum) space separation).

---

[1] a) V. Balzani, F. Scandola, *Supramolecular Photochemistry*, Horwood, Chichester, **1993**; b) V. Balzani, A. Credi, M. Venturi, *Molecular Devices. Concepts and Perspectives for the Nanoworld*, Wiley-VCH, Weinheim, **2008**.

[2] *Molecular Wires. From design to Properties*, (Ed.: L. de Cola); Thematic issue, *Top. Curr. Chem.* **2005**, *257*, 1-170.

[3] W. B. Davis, W. A. Svec, M. A. Ratner, M. R. Wasielewski, *Nature* **1998**, *396*, 60-63.

[4] a) R. M. Williams, M. Koeberg, J. M. Lawson, Y.-Z. An, Y. Rubin, M. N. Paddon-Row, J. W. Verhoeven, *J. Org. Chem.* **1996**, *61*, 5055-5062; b) H. Oevering, M. N. Paddon-Row, M. Heppener, A. M. Oliver, E. Cotsaris, J. W. Verhoeven, N. S. Hush, *J. Am. Chem. Soc.* **1987**, *109*, 3258-3269.

[5] a) B. C. van der Wiel, R. M. Williams, C. A. van Walree, *Org. Biomol. Chem.* **2004**, *2*, 3432-3433. For a review on cross-conjugation, see: b) M. Gholami, R. R. Tykwinski, *Chem. Rev.* **2006**, *106*, 4997-5027.

[6] M. Wolffs, N. Delsuc, D. Veldman, N. V. Anh, R. M. Williams, S. C. J. Meskers, R. A. J. Janssen, I. Huc, A. P. H. J. Schenning, *J. Am. Chem. Soc.* **2009**, *131*, 4819-4829.

[7] a) T. A. Zeidan, Q. Wang, T. Fiebig, F. D. Lewis *J. Am. Chem. Soc.* **2007**, *129*, 9848-9849; b) M. Smeu, R. A. Wolkow, H. Guo *J. Am. Chem. Soc.* **2009**, *131*, 11019-11029.

[8] a) C. Lambert, *Angew. Chem. Int Ed.* **2005**, *44*, 7337-7339; b) S. V. Rosokha, I. S. Neretin, D. Sun, J. K. Kochi, *J. Am. Chem. Soc.* **2006**, *128*, 9394-9407.

Next to σ-, π-, spiro-,[9] toroidal and cross-conjugation (Figure 1), an unexplored area for D-B-A systems is provided by aromatic homoconjugation. Homoconjugation can be defined as the orbital overlap of two π-systems separated by a non-conjugated group, such as CH_2 (IUPAC).[10] Homoconjugative interactions between double and triple bonds have been extensively studied.

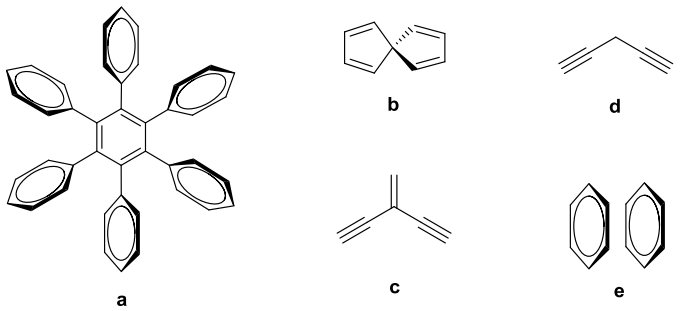

Figure 1. Examples of systems showing a): toroidal conjugation, b) spiro-conjugation, c) cross-conjugation, d) homoconjugation and e) π-stacking.

Electron delocalization in homoconjugated alkenes is well established in the case of cationic homoaromatic compounds in which the positive charge is the driving force for delocalization.[10e,f] However, the situation in neutral homoconjugated molecules remains controversial, even in the case of homoaromatic compounds.[10a-f,h] Surprisingly, homoconjugative interactions between aromatic rings have received less attention. In that respect, it has been

[9] T. P. I. Saragi, T. Spehr, A. Siebert, T. Fuhrmann-Lieker, J. Salbeck, *Chem. Rev.* **2007**, *107*, 1011-1065.

[10] For a review on homoconjugated acetylenes, see: a) A. de Meijere, S. I. Kozhushkov, *Top. Curr. Chem.* **1999**, *201*, 1-42. See also: b) A. de Meijere, S. I. Kozhushkov, R. Boese, T. Haumann, D. S. Yufit, J. A. K. Howard, L. S. Khaikin, M. Traetteberg, *Eur. J. Org. Chem.* **2002**, 485-492. For recent studies on homobenzene, see: c) Z. Chen, H. Jiao, J. I. Wu, R. Herges, S. B. Zhang, P. von R. Schleyer, *J. Phys. Chem. A* **2008**, *112*, 10586-10594; d) F. Stahl, P. von R. Schleyer, H. Jiao, H. F. Schaefer III, K.-H. Chen, N. Allinger, *J. Org. Chem.* **2002**, *67*, 6599-6611. For a review on homoaromaticity, see: e) R. V. Williams, *Chem. Rev.* **2001**, *101*, 1185-1204. See also: f) C. Lepetit, B. Silvi, R. Chauvin, *J. Phys. Chem. A* **2003**, *107*, 464-473. For inorganic molecules with homoconjugation/homoaromaticity, see: g) Q. Zhang, S. Yue, X. Lu, Z. Chen, R. Huang, L. Zheng, P. von R. Schleyer, *J. Am. Chem. Soc.* **2009**, *131*, 9789-9799. Stabilizing homoconjugative interactions between double and triple bonds are described in: h) R. Gleiter, R. Merger, H. Irngartinger, *J. Am. Chem. Soc.* **1992**, *114*, 8927-8932.

argued that in diphenylmethane, the simplest candidate for aromatic homoconjugated compounds, the saturated methylene group should act as a barrier to conduction.[11] Diphenylmethane can be described as a free rotator whose most stable conformation is the helical disposition, thus avoiding homoconjugative interactions between the aromatic rings.[12] This situation can be modified by forcing the aryl rings to adopt a cofacial conformation as we have found in the case of 7,7-diphenylnorbornane (DPN) (**1**) (Figure 2).[12,13]

We have shown that in oligomers and polymers derived from DPN, aromatic homoconjugation contributes to the electron delocalization along the backbone structure.[13a-c] These results show that the delocalization mediated by aromatic homoconjugation is more effective than in homoconjugated acetylenes, where no significant homoconjugative stabilization is observed.[10a,b] In order to gain further understanding of the role played by the bridging unit, we report now the synthesis and photophysical properties of the first example of a D-B-A dyad with aromatic homoconjugated bridge **5** as well as its homodinuclear analogs **3** and **4** (Figure 2).

[11] a) D. K. James, J. M. Tour, *Top. Curr. Chem.* **2005**, *257*, 33-62. For examples of block copolymers with diphenylmethane subunits acting as conjugation interrupters, see: b) K.-Y. Peng, S.-A. Chen, W.-S. Fann, *J. Am. Chem. Soc.* **2001**, *123*, 11388-11397; c) P. G. Del Rosso, M. F. Almassio, S. S. Antollini, R. O. Garay, *Opt. Mater.* **2007**, *30*, 478-485; d) M. Beinhoff, L. D. Bozano, J. C. Scott, K. R. Carter, *Macromolecules* **2005**, *38*, 4147-4156; e) P. G. Del Rosso, M. F. Almassio, P. Aramendia, S. S. Antollini, R. O. Garay, *Eur. Polym. J.* **2007**, *43*, 2584-2593.

[12] A. García Martínez, J. Osío Barcina, *The Diphenylmethane Moiety* in *Encyclopedia of Supramolecular Chemistry*, (Eds.: J. L. Atwood, J. W. Steed), Marcel Dekker, New York, **2004**, 452-456.

[13] a) J. Osío Barcina, M. R. Colorado Heras, M. Mba, R. Gómez Aspe, N. Herrero García, *J. Org. Chem.* **2009**, *74*, 7148-7156; b) N. Caraballo-Martínez, M. R. Colorado Heras, M. M. Blázquez, J. Osío Barcina, A. García Martínez, M. R. Torres Salvador, *Org. Lett.* **2007**, *9*, 2943-2946; c) A. García Martínez, J. Osío Barcina, A. de Fresno Cerezo, A.-D. Schlüter, J. Frahn, *Adv. Mater.* **1999**, *11*, 27-31; d) A. García Martínez, J. Osío Barcina, A. de Fresno Cerezo, R. Gutiérrez Rivas, *J. Am. Chem. Soc.* **1998**, *120*, 673-679.

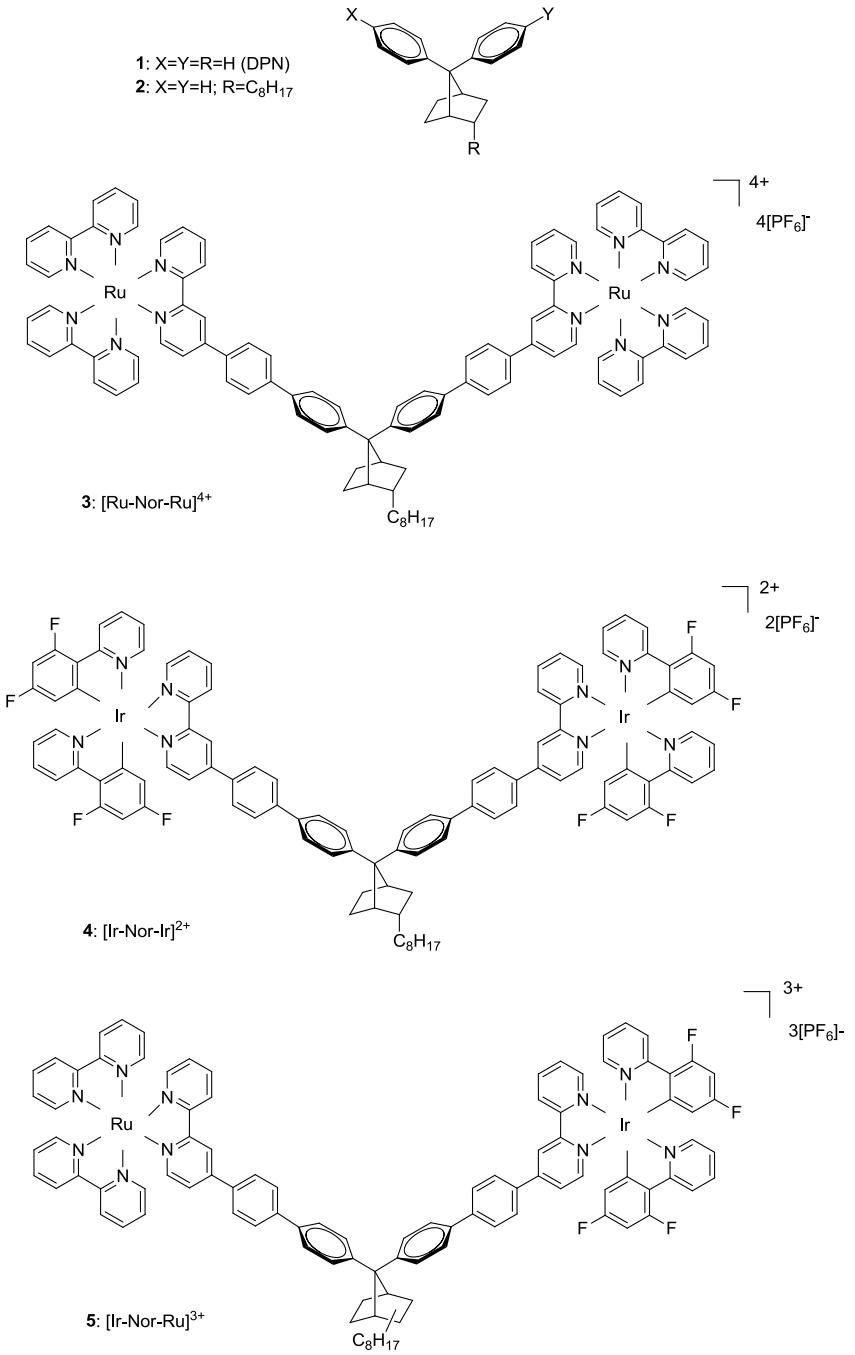

Figure 2. Structures of DPN and complexes **3**, **4** and **5**.

2.2.2 Results and Discussion

As chromophores for this study, we have chosen complexes containing Ru(II)[14] and Ir(III)[15] species due to the effective molecular wire behaviour that has been observed in dinuclear Ir(III)/Ru(II) complexes with conjugated *p*-phenylene bridges.[16] Iridium complexes forming part of supramolecules for the monitoring of energy and electron transfer processes have been widely studied, and the literature presents several examples of interesting wire-like molecules based on bis-terpyridine linear geometries.[15] Additionally, iridium metal complexes are being extensively studied for the potential and very promising application in electroluminescent devices thanks to their high photo-stability and emission tunability.[17]

The synthesis of compounds **3**, **4** and **5** (Figure 2) has been carried out following the methodology described previously for the preparation of DPN derivatives and Ir(III)/Ru(II) complexes (Scheme 1). Alkyl chain (C_8H_{17}) is introduced in the norbornane skeleton (**2**) in order to increase the solubility of the derivatives during the synthetic route.

[14] S. Campagna, F. Puntoriero, F. Nastasi, G. Bergamini, V. Balzani, *Top. Curr. Chem.* **2007**, *280*, 117-214.

[15] a) L. Flamigni, A. Barbieri, C. Sabataini, B. Ventura, F. Barigelletti, *Top. Curr. Chem.* **2007**, *281*, 143-203. b) L. Flamigni, J.-P. Collin, J.-P. Sauvage, *Acc. Chem. Res.* **2008**, *41*, 857-871.

[16] a) S. Welter, F. Lafolet, E. Cecchetto, F. Vergeer, L. De Cola, *Chem. Phys. Chem.* **2005**, *6*, 2417-2427. See also: b) M. Cavazzini, S. Quici, C. Scalera, F. Puntoriero, G. La Ganga, S. Campagna, *Inorg. Chem.* **2009**, *48*, 8578-8592; c) C. Sabatini, A. Barbieri, F. Barigelletti, K. J. Arm, J. A. G. Williams, *Photochem. Photobiol. Sci.* **2007**, *6*, 397-405; d) K. J. Arm, J. A. G. Williams, *Chem. Commun.* **2005**, 230-232; e) M. Cavazzini, P. Pastorelli, S. Quici, F. Loiseau, S. Campagna, *Chem. Commun.* **2005**, 5266-5268.

[17] For representative examples, see: a) A. B. Tamayo, S. Garon, T. Sajoto, P. I. Djurovich, I. M. Tsyba, R. Bau, M. E. Thompson, *Inorg. Chem.* **2005**, *44*, 8723-8732; b) W. J. Finkenzeller, M. E. Thompson, H. Yersin, *Chem. Phys. Lett.* **2007**, *444*, 273-279; c) J. Li, P. I. Djurovich, B. D. Alleyne, M. Yousufuddin, N. N. Ho, J. C. Thomas, J. C. Peters, R. Bau, M. E. Thompson, *Inorg. Chem.* **2005**, *44*, 1713-1727; d) A. Guerrero-Martínez, Y. Vida, D. Dominguez-Gutierrez, R. Q. Albuquerque, L. De Cola, *Inorg. Chem.* **2008**, *47*, 9131-9133.

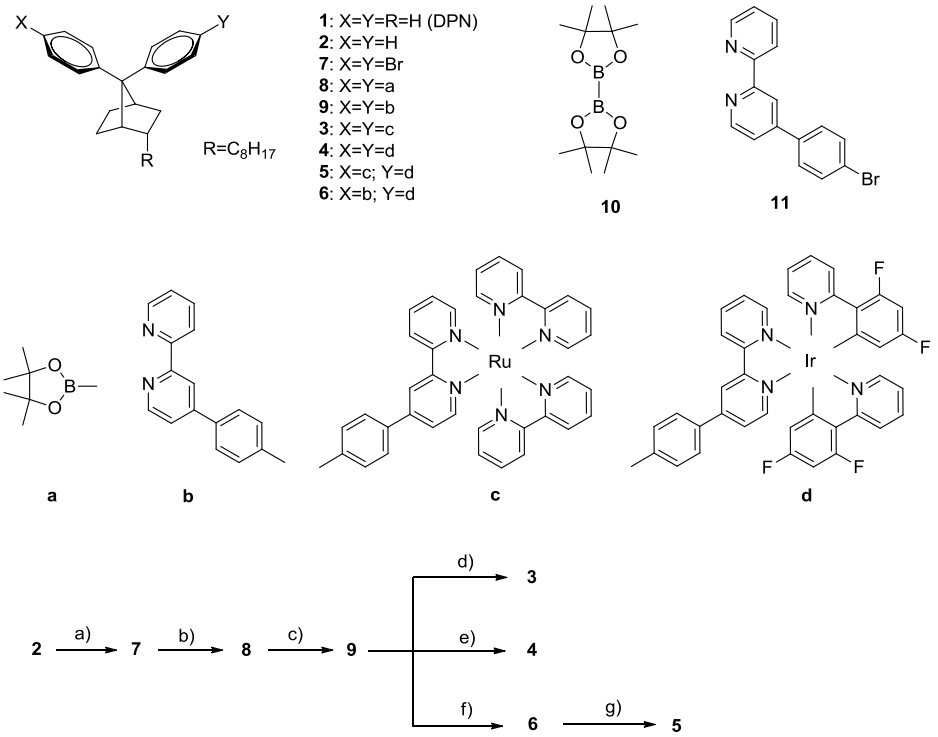

Scheme 1. a) Br_2 (88%); b) **10**/ $PdCl_2(dppf)$/KAcO/DMSO (87%); c) **11**/ $Pd(PPh_3)_4$/ Na_2CO_3/toluene/H_2O (54%); d) $[Ru(bpy)_2Cl_2]$/DME/ethylene glycol (2:1)/ultrasound (85%); e) $[Ir(ppyFF)_2(\mu\text{-}Cl)]_2$/ethylene glycol/$CHCl_3$ (3:1) (66 %); f) $[Ir(ppyFF)_2(\mu\text{-}Cl)]_2$/ethylene glycol/$CHCl_3$ (3:1) (51 %); g) $[Ru(bpy)_2Cl_2]$/ ethylene glycol/$CHCl_3$ (3:1)/ultrasound (62%).

1.1.2.1 Photophysical properties

1.1.2.1.1 Absorption and emission spectroscopy

The absorption spectra of the homodinuclear complexes $[Ir\text{-}Nor\text{-}Ir]^{2+}$ and $[Ru\text{-}Nor\text{-}Ru]^{4+}$, and the heterodinuclear compound $[Ir\text{-}Nor\text{-}Ru]^{3+}$ in diluted (optical density < 0.1) air-equilibrated acetonitrile at 293 K closely resemble the sum of the individual spectra of the mononuclear units $[Ir(ppyFF)_2(bpy)]^+$ and $[Ru(bpy)_3]^{2+}$ (see Figure 3).

The spectrum of $[Ir\text{-}Nor\text{-}Ru]^{3+}$ shows both absorption bands of the two homodinuclear species. The intense peaks at 246 nm and 288 nm can be assigned to spin-allowed ligand-centered, ^{1}LC, transitions involving the fluorinated phenylpyridines (ppyFF) and the peripheral bipyridines (bpy),[18,19] together with transitions associated to the preferred cofacial disposition of the aryl ring in the DPN subunit.[13]

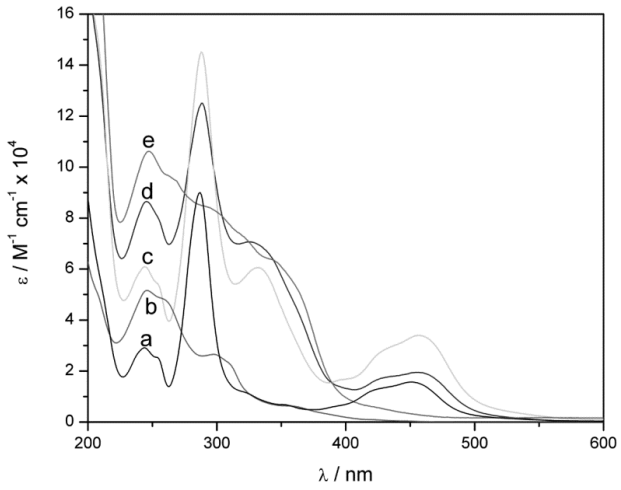

Figure 3. Absorption spectra of $[Ru(bpy)_3]^{2+}$ (a), $[Ir(ppyFF)_2(bpy)]^+$ (b), $[Ru\text{-}Nor\text{-}Ru]^{4+}$ (c), $[Ir\text{-}Nor\text{-}Ru]^{3+}$ (d), and $[Ir\text{-}Nor\text{-}Ir]^{2+}$ (e) in dilute acetonitrile solution at 298 K.

Moreover, the broad band centred around 326 nm can be assigned to spin-allowed π-π* transitions localized on the DPN substituted bridging bipyridines,[16a] which includes the weaker spin-allowed Ir-based MLCT transitions, as also observed for $[Ir\text{-}Nor\text{-}Ir]^{2+}$ complex.[18,20]

Additionally, in the visible region (400-550 nm) we can find the typical spin-allowed Ru-based MLCT absorption band,[14] that is half as intense as observed for the $[Ru\text{-}Nor\text{-}Ru]^{4+}$ complex.

[18] a) S. O. Garces, K. A. King, R. J. Watts, *Inorg. Chem.* **1988**, *27*, 3464-3471; b) K. Ichimura, T. Kobayashi, K. A. King, R. J. Watts, *J. Phys. Chem.* **1987**, *91*, 6104-6106.
[19] See e.g. K. Kalyanasundaram, Photochemistry of Polypyridine and Porphyrin Complexes, Academic Press, London, **1994**.
[20] F. Lafolet, S. Welter, Z. Popovic, L. De Cola, *J. Mater. Chem.* **2005**, *15*, 2820-2828.

In order to quantify possible energy-transfer processes after excitation of the energy donor component (see below), we have to consider that no selective excitation on the iridium MLCT band is possible, due to the full overlap in the absorption bands of the two ruthenium and iridium homodinuclear species (Figure 3). However, the dinuclear complexes spectra show an iso-absorptive point at about 332 nm, in which the Ir and Ru moieties absorb the same fraction of incident light.

Figure 4a shows the emission spectra of $[Ir\text{-}Nor\text{-}Ir]^{2+}$, $[Ir\text{-}Nor\text{-}Ru]^{3+}$, $[Ru\text{-}Nor\text{-}Ru]^{4+}$, and the reference compound $[Ir(ppyFF)_2(bpy)]^{+}$, recorded upon excitation at 332 nm, at room temperature from dilute acetonitrile solutions (optical density < 0.1).

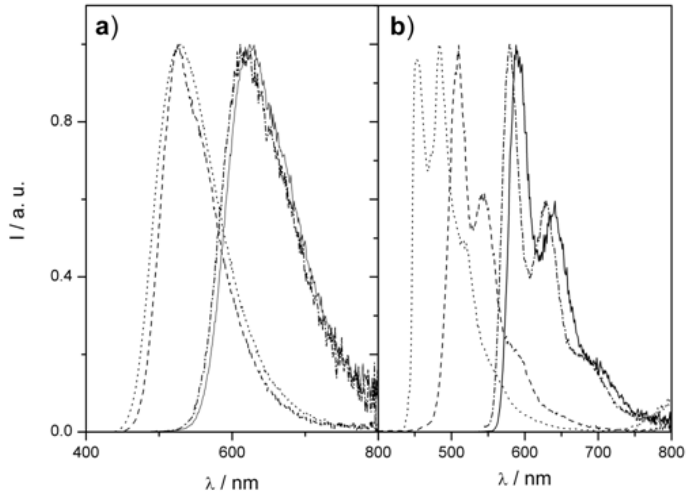

Figure 4. Emission spectra of $[Ir(ppyFF)_2(bpy)]^{+}$ (•••••), $[Ir\text{-}Nor\text{-}Ir]^{2+}$(-----), $[Ru\text{-}Nor\text{-}Ru]^{4+}$ (-•-•-), and $[Ir\text{-}Nor\text{-}Ru]^{3+}$ (—) in (a) dilute acetonitrile solution at 298 K, and (b) a butyronitrile rigid matrix at 77 K (λ_{exc} = 332 nm).

The luminescence spectrum of the homodinuclear complex $[Ir\text{-}Nor\text{-}Ir]^{2+}$ exhibits an emission centered at 526 nm, which originates from a state with mixed ^{3}MLCT – ^{3}LC character, mostly located on the bipyridine ligand, as for the parent compound $[Ir(ppyFF)_2(bpy)]^{+}$.[15a] It is noteworthy that $[Ir\text{-}Nor\text{-}Ir]^{2+}$ complex shows a 20 nm blue-shifted emission, when compared to similar homodinuclear iridium complexes with full extended π-conjugation,[16a] since the presence of a sp^3 carbon, bearing the DPN subunit, diminishes the

conjugation in the bridge between the two iridium centers, thus causing a raise in the LUMO orbital energy.[13a]

The homodinuclear complex $[Ru\text{-}Nor\text{-}Ru]^{4+}$ displays an emission band centered at 625 nm, slightly red-shifted as compared to $[Ru(bpy)_3]^{2+}$,[14] due to the larger conjugation on one of the bipyridines, that lowers its LUMO level and consequently the energy of the ^{3}MLCT transition.[16a]

Keeping the excitation wavelength at 332 nm, we have recorded the luminescence spectrum of the heterodinuclear complex $[Ir\text{-}Nor\text{-}Ru]^{3+}$, which shows the complete quenching of the iridium-based emission, and a broad band centered at 625 nm, as observed for $[Ru\text{-}Nor\text{-}Ru]^{4+}$ complex. No significant difference in the Ru-based emission intensities are observed for $[Ir\text{-}Nor\text{-}Ru]^{3+}$ and $[Ru\text{-}Nor\text{-}Ru]^{4+}$ complexes after excitation at 332 nm, which implies very efficient energy transfer (see Table 1 and below).

Table 1. Photophysical data

	298 K[a]					**77 K[b]**			
	Ir^{III}		**Ru^{II}**			**Ir^{III}**		**Ru^{II}**	
	λ_{max}/ nm	**τ / ns[d]**	**λ_{max}/ nm**	**τ / ns[d]**	**$10^2 . \phi$**	**λ_{max}/ nm**	**τ / µs[d]**	**λ_{max}/ nm**	**τ/ µs[d]**
$[Ir\text{-}Nor\text{-}Ir]^{2+}$	526	150	-	-	1.8	508	37.0	-	-
$[Ru\text{-}Nor\text{-}Ru]^{4+}$	-	-	625	197	7.4	-	-	593	5.9
$[Ir\text{-}Nor\text{-}Ru]^{3+}$	-	[c]	625	200	7.4	[c]	-	590	5.8
$[Ir(ppyFF)_2(bpy)]^+$	529	140	-	-	2.2	484	4.4	-	-
$[Ru(bpy)_3]^{2+}$	-	-	619	619	6.2	-	-	579	5.7

[a] In aerated acetonitrile, λ_{exc} = 332 nm. [b] In a butyronitrile rigid matrix, λ_{exc} = 332 nm. [c] Too low in intensity to be detected accurately by [d]. [d] Time-correlated single-photon counting method.

In Figure 4b the low-temperature emission spectra at diluted conditions are shown, reflecting the same trend observed at room temperature. Both $[Ir\text{-}Nor\text{-}Ir]^{2+}$ and $[Ru\text{-}Nor\text{-}Ru]^{4+}$ complexes exhibit structured emission profiles, with maxima at respectively at 508 nm and 580 nm; the first emission band is 18 nm blue-shifted when compared to the room temperature emission, while the Ru-based homodinuclear complex shows a larger hypsochromic shift of 45 nm. This behaviour matches the statement of a mixed ^{3}LC – ^{3}MLCT state for the

$[Ir\text{-}Nor\text{-}Ir]^{2+}$ complex emission, which in rigid matrix, due to the strong destabilization of the ^{3}MLCT state, is predominantly a ligand centered emission, whereas the $[Ru\text{-}Nor\text{-}Ru]^{4+}$ emission retains its ^{3}MLCT character.[21]

The emission spectrum of the heterodinuclear $[Ir\text{-}Nor\text{-}Ru]^{3+}$ complex is essentially identical to that of $[Ru\text{-}Nor\text{-}Ru]^{4+}$ compound, even at this low temperature, showing again the complete intramolecular quenching of the iridium unit emission.

All the photophysical data related to the emission spectra of the complexes are listed in Table 1, including the emission quantum yields and the time-resolved measurements. The lifetimes of the Ru-based emission in the heterodimetallic complex at room temperature and in the frozen matrix are very similar to those of complexes $[Ru(bpy)_3]^{2+}$ and $[Ru\text{-}Nor\text{-}Ru]^{4+}$,[14] which shows analogous excited states. However, the marked lifetime differences of the iridium centered emission at 77 K in the case of the complex $[Ir\text{-}Nor\text{-}Ir]^{2+}$ and the iridium parent compound $[Ir(ppyFF)_2(bpy)]^+$, has been ascribed to a low energy, long lived emission due to a ^{3}LC state localized on the homoconjugated bridge unit of iridium homodinuclear complexes,[16a] which at low temperature becomes the lowest excited state.

Electrochemical characterizations were performed by cyclic voltammetry in 10^{-3}M acetonitrile solutions, containing 0.1M *t*-Bu_4NPF_6 as supporting electrolyte, where characteristic electrochemical features of iridium and ruthenium complexes were observed.[14,22]

1.1.2.1.2 Transient absorption spectroscopy

The nanosecond transient absorption spectra of $[Ir(ppyFF)_2(bpy)]^+$, $[Ir\text{-}Nor\text{-}Ir]^{2+}$ and $[Ir\text{-}Nor\text{-}Ru]^{3+}$ complexes were recorded upon excitation at 330 nm at room temperature in deaerated acetonitrile solutions (Figure 5). The transient absorption spectra of the dinuclear iridium complex register a long-lived broad

[21] M. G. Colombo, A. Hauser, H. U. Güdel, *Inorg. Chem.* **1993**, *32*, 3088-3092.
[22] a) P. Coppo, E. A. Plummer, L. De Cola, *Chem. Commun.* **2004**, 1774-1775; b) A. B. Tamayo, B. D. Alleyne, P. I. Djurovich, S. Lamansky, I. Tsyba, N. N. Ho, R. Bau, M. E. Thompson, *J. Am. Chem. Soc.* **2003**, *125*, 7377-7387.

absorption, stretching from 400 to 820 nm (Figure 5a), which arises from several contributions, such as the bpy radical anion and the ligand-centred triplet state. The absence of such long-lived transient absorption bands in deaerated $[Ir(ppyFF)_2(bpy)]^+$ solutions (Figure 5b), indicates the formation of the excited state of the bpy-oligophenylene-DPN ligand for **4**.

In the case of the $[Ir\text{-}Nor\text{-}Ru]^{3+}$ complex, the transient spectra (Figure 5c) exhibit two features in the region from 400-850 nm. The negative absorption at 460 nm is related to the bleaching of the Ruthenium centred ground state, whereas no bands attributed to the Iridium component are observed. The broad feature in the region from 500-850 nm is assigned to the formation of the radical anion of the bpy-oligophenylene-DPN ligand.

All bands decay monoexponentially with lifetimes slightly longer than those registered by time-resolved emission measurements, due to the existence of possible underlying long lived absorbing species that modifies the evolution at the selected wavelengths. Since it was not possible to monitor the energy transfer processes on the nanosecond time-scale for the iridium-ruthenium mixed metal complexes,[16a] sub-picosecond transient absorption spectroscopy was performed.

Figure 6a shows the femtosecond transient absorption data matrix obtained for an acetonitrile solution of the $[Ir\text{-}Nor\text{-}Ru]^{3+}$ complex after laser excitation at 370 nm,[23] where several processes can be observed. Positive transient absorptions are shown in red shades and negative bands are shown in purple-blue. After laser excitation, a broad band is formed between 500 and 800 nm, corresponding to the iridium centred excited state, which decays abruptly within the first 150 ps of the measurement. Concomitantly with this decay, two new bands appear: a positive absorption below 400 nm, ascribed to the reduced bipyridine radical anion on the ruthenium moiety and a negative transient absorption, located between 400 and 500 nm, which originates from the bleaching of the ruthenium centred ground state. As the process evolves, this state is depleted, while the ^{3}MLCT excited state is formed, and the band becomes more negative over time.

[23] For description and optical layout see SI of: J. Baffreau, S. Leroy-Lhez, N. Van Anh, R. M. Williams, P. Hudhomme, *Chem. Eur. J.* **2008**, 14, 4974-4992.

By overlaying transient absorption spectra at different time delays we obtain Figure 6b. For comparison, the sub-picosecond transient absorption spectra of the two homodinuclear complexes were also recorded, showing characteristic features for these types of systems. [20,24]

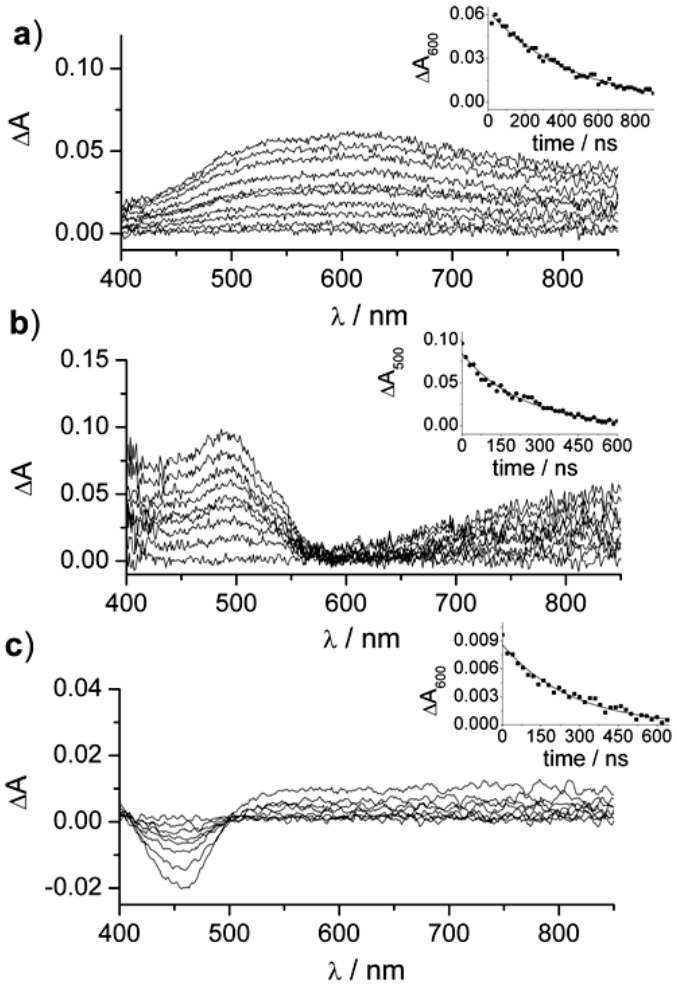

Figure 5. Transient absorption spectra and decay kinetics of a) $[Ir\text{-}Nor\text{-}Ir]^{2+}$, b) $[Ir(ppyFF)_2(bpy)]^{+}$, c) $[Ir\text{-}Nor\text{-}Ru]^{3+}$ complexes in acetonitrile solution at 293 K (λ_{exc} = 332 nm, <5 mJ pulse-1, 2 ns half width at half maximum, FWHM). The insets show the decay for a) and c) at 600 nm, and b) at 500 nm.

[24] a) J. K. McCusker, *Acc. Chem. Res.* **2003**, *36*, 876-887; b) S. Welter, N. Salluce, P. Belser, M. Groeneveld, L. De Cola, *Coord. Chem. Rev.* **2005**, *249*, 1360-1371.

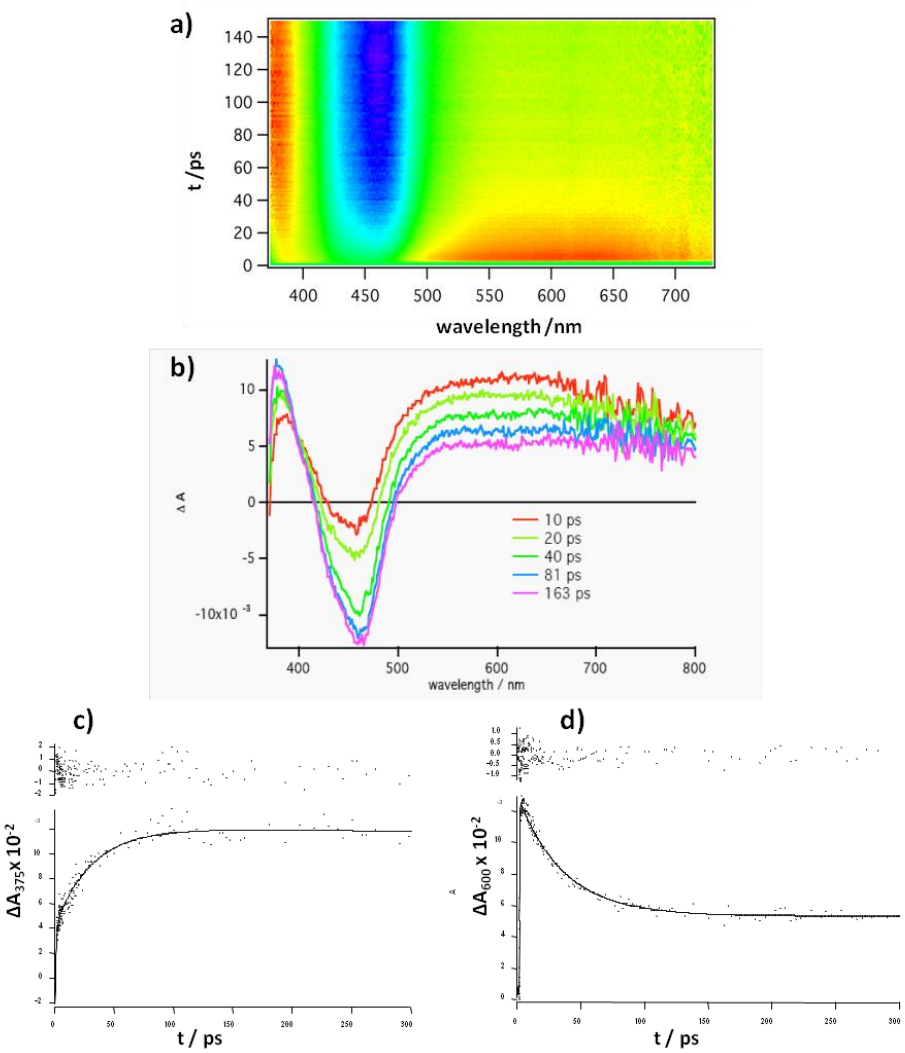

Figure 6. (a) Sub-picosecond transient absorption data matrix of [Ir-Nor-Ru]$^{3+}$ complex in acetonitrile (λ_{exc} = 370 nm, 130 fs FWHM). Dark-lined grey is negative, light grey is positive. b) Overlay of several sub-picosecond absorption spectra at different time delays. c) Kinetics profiles at 375 nm and d) at 600 nm.

The analysis of the kinetics of the energy transfer process in the [Ir-Nor-Ru]$^{3+}$ system was obtained from the band evolution at 375 nm, that shows a complete quenching of the iridium centred excited state takes place within the

first 150 ps of the measurement (Figure 6c). A reasonable complementarity is observed in Figure 6d that shows a decay of the signal at 600 nm as time proceeds. We ascribe this fast component to the energy transfer occurring from the higher lying iridium triplet state to the lower lying ruthenium triplet state. The energy transfer rate has been calculated from $k_{ET} = 1/\tau - 1/\tau_0$, where τ_0 is the iridium lifetime given by the time-resolved emission measurements, and τ is the quenched lifetime obtained from the kinetic analysis (30.9 ps). A global fit procedure using TIMP was applied to the data-matrix,[25] evaluating all ~300 kinetic traces, resulting in an energy transfer rate of $k_{ET} = 3.24 \times 10^{10}$ s^{-1}. Taking into account an unquenched lifetime of 150 ns (see Table 1) and a quenched lifetime of 30.9 ps, an energy transfer efficiency of 99.98 % has been calculated ($\eta=1-\tau_q/\tau_{ref}$).

Although there are several examples based on iridium/ruthenium and ruthenium/osmium bimetallic complexes interconnected by linear polyphenylene conjugated spacers,[2,16a] no examples of energy transfer processes in organometallic based homoconjugated systems have been reported to our knowledge. Thus, a reasonable comparison between these full extended π conjugated complexes and the homoconjugated $[Ir\text{-}Nor\text{-}Ru]^{3+}$ compound, in terms of the k_{ET} dependence with the intermetallic distance, can be done. Regarding the estimated Ir-Nor(C7)-Ru distance and the energy transfer rate between the metal units (29.7 Å, 3.24×10^{10} s^{-1}), an intermediate behaviour is observed respect to previously reported binuclear complex bearing a bridge consisting of four phenylene groups such as $[Ir\text{-}ph_4\text{-}Ru]^{3+}$ (28.3 Å, 3.6×10^{11} s^{-1}) complex,[16a] in which energy transfer proceeds via a clear Dexter mechanism.[26]

Even though the observed energy transfer process for the $[Ir\text{-}Nor\text{-}Ru]^{3+}$ compound is slower than in the $[Ir\text{-}ph_4\text{-}Ru]^{3+}$ case, due to the higher energy of the triplet state localized on the homoconjugated spacer, the rate of this process is fast in relation with other full extended π conjugated species.[24] Within a Dexter-type energy transfer mechanism (double electron transfer), several

[25] a) I. H. M. van Stokkum, D. S. Larsen, R. van Grondelle, *Biochim. Biophys. Acta: Bioenergetics* **2004**, *1657*, 82-104; b) I. H. M. van Stokkum, R. H. Lozier, *J. Phys. Chem. B* **2002,** *106*, 3477-3485; c) K. M. Mullen, I. H. M. van Stokkum, *J. Stat. Software* **2007**, *18*, issue 3, special volume .

[26] F. Barigelletti, L. Flamigni, M. Guardigli, A. Juris, M. Beley, S. Chodorowski-Kimmes, J.-P. Collin, J.-P. Sauvage, *Inorg. Chem.* **1996**, *35*, 136-142.

bridge related aspects are of key importance. The mixing of donor and acceptor orbitals with the bridge orbitals, which is governed by symmetry and the energy gap, is essential,[2,3,4] since electronic coupling is required. As such the donor-bridge coupling is rather combination specific and comparison with different donor chromophores is less useful.

It should be noted that electron delocalization in aromatic homoconjugated systems is less effective than in conjugated compounds,[13] and therefore the energy band gap is higher for homoconjugated bridges.[13a] This result indicates that the energy transfer takes place according to a Dexter-type mechanism which formally consists of a double electron exchange between donor excited-state and acceptor.[27]

2.2.3 Conclusion

In conclusion, the photophysical behaviour of $[Ir\text{-}Nor\text{-}Ru]^{3+}$ demonstrates that energy transfer between donor/acceptor components through aromatic homoconjugation is an effective mechanism, and could be used for vectorial energy and electron-transport over very long distances (e.g. 3 nm).

This is the first example reported to date of effective photoinduced energy transfer mediated by aromatic homoconjugated bridges and provides a new tool to tune the properties of D-B-A systems by changing the structural features of the bridging unit. Work is currently in progress in our laboratories to design novel D-B-A systems with aromatic homoconjugated bridges and to study the possibility of molecular wire behaviour in these complexes.

[27] D.L. Dexter, *J. Chem. Phys.* **1953**, *21*, 836-850.

2.2.4 Experimental Section

General Information

^{1}H and ^{13}C NMR spectra were recorded on a 300 MHz spectrometer. Chemical shifts are given in ppm relative to TMS (^{1}H, 0.0 ppm) and $CDCl_3$ (^{13}C, 77.0 ppm). Coupling constants are given in Hertz.
All experiments were carried out under argon atmosphere using standard Schlenk techniques. Anhydrous solvents were distilled under argon following standard procedures. Flash chromatography was performed over silica gel 60 (230-400 mesh). All commercially available compounds were purchased from commercial suppliers and used without further purification. The preparation of **2**,[13b] **11**,[28] $Ru(bpy)_2Cl_2$,[29] and $[Ir(ppyFF)_2Cl_2]$[30] have been described previously. Boronate **8**[13a] was obtained following a modified procedure starting from dibromide **7** instead of the analogous diiodide.

Experimental procedures

Dibromide 7: Bromine in excess (0.2 mL) was slowly added over 387 mg of **2** (1.1 mmol) at room temperature and the reaction mixture was stirred during 45 minutes. Then 10% $NaHSO_3$ solution was slowly added until disappearance of the red colour. The resulting slurry was extracted with CH_2Cl_2 (3x15 mL), washed with water (1x15 mL) and dried over $MgSO_4$. The solvent was removed under reduced pressure and the residue was purified by flash chromatography (silica gel, hexane) to give 489 mg (88%) of the desired product. ^{1}H NMR (300 MHz, $CDCl_3$): δ = 7.33 (m, 4H), 7.23 (m, 4H), 2.98-2.79 (m, 2H), 1.89-1.76 (m, 2H), 1.71-1.40 (m, 4H), 1.40-1.08 (m, 14H), 0.88 (t, *J* = 6.6 Hz, 3H), 0.80 (d, *J* = 7.1 Hz, 1H); ^{13}C NMR (75 MHz, $CDCl_3$): δ = 144.8, 144.4, 131.7, 131.6, 129.1, 128.9, 119.4, 65.3, 45.3, 42.0, 37.2, 35.8, 32.8, 32.0, 30.0, 29.7, 29.3, 28.7, 28.6, 22.7, 20.7, 14.2; MS (ESI, *m/z*): 516 (M^+, 6), 518 (M^+ + 2, 11), 520 (M^+ + 4, 6); Elemental analysis (%) calc for $C_{27}H_{34}Br_2$: C 62.56, H 6.61; found: C 62.54, H 6.60.

Boronate 8: A dry Schlenk flask placed under argon was charged with a mixture of 40 mg (0.08 mmol) of **7**, 41 mg (0.16 mmol) of **10**, 45 mg (0.46 mmol) of anhydrous potassium acetate and 2 mL of anhydrous DMSO. Oxygen was removed through three freeze-pump-thaw cycles and 5 mg ($6.1x10^{-3}$ mmol) of $PdCl_2$(dppf) were added over a mild flow of argon. The reaction was heated at 100 ºC for 15 h and the cooled residue was filtered through a short column containing a mixture of celite and fluorisil. The column was washed with hexane and the resulting solution washed with CH_2Cl_2 (3x15 mL) and water until disappearance of red colour. After drying over $MgSO_4$ and

[28] a) S. Altobello, C. A. Bignozzi, S. Caramori, G. Larramona, S. Quici, G. Marzanni, R. Lakhmiri, *J. Photochem. Photobiol. A* **2004**, *166*, 91. b) R. A. Kipp, Y. Li, J. A. Simon, R. H. Schmehl, *J. Photochem. Photobiol. A* **1999**, *121*, 27.
[29] a) P. A. Lay, A. M. Sargeson, H. Taube, *Inorg. Synth.* **1986**, *24*, 291. b) B. P. Sullivan, D. J. Salmon, T. J. Meyer, *Inorg. Chem.* **1978**, *17*, 3334.
[30] Y. You, S. H. Kim, H. K. Jung, S. Y. Park, *Macromolecules* **2006**, *39*, 349.

removal of the solvent under reduced pressure, 41 mg (87%) of **8** were obtained and used in the next step without further purification.[13a]

Ligand 9: A dry Schlenk flask placed under argon was charged with a mixture of 168 mg (0.27 mmol) of **8**, 153 mg (0.49 mmol) of **11**, 5 mL of toluene and 5 mL of 1.5 M aqueous solution of Na_2CO_3. Oxygen was removed through three freeze-pump-thaw cycles and 29 mg (0.02 mmol) of $Pd(PPh_3)_4$ were added over a mild flow of argon. After heating at 95 ºC for 63 h, the reaction mixture was extracted with CH_2Cl_2 (3x15 mL) and dried over $MgSO_4$. The solvent was removed under pressure and the residue purified by flash chromatography (silica gel, CH_2Cl_2/MeOH 40:1). 109 mg (54%) of **9** were obtained. ^{1}H NMR (300 MHz, $CDCl_3$): δ = 8.72 (m, 6H), 8.47 (d, *J* = 7.9 Hz, 2H), 7.90-7.80 (m, 6H), 7.76 (dd, *J* = 8.3 and 1.8 Hz, 4H), 7.67-7.60 (m, 10H), 7.44-7.40 (m, 2H), 3.13-3.08 (m, 2H), 2.0-1.90 (m, 2H), 1.75-1.25 (m, 4H), 1.25-1.10 (m, 14H), 0.90-0.80 (m, 4H); ^{13}C NMR (75 MHz, $CDCl_3$): δ = 156.5, 156.0, 149.5, 149.2, 149.1, 145.9, 145.4, 141.8, 137.3, 137.1, 136.6, 128.0, 127.8, 127.5, 127.2, 127.1, 123.9, 121.4, 118.9, 65.7, 45.4, 42.1, 37.3, 36.1, 33.0, 31.9, 31.3, 30.1, 29.7, 29.4, 28.8, 22.7, 20.9, 14.1; MS (FAB, *m/z*): 822 $(M + 2H)^+$; Elemental analysis (%) calc for $C_{59}H_{56}N_4$: C 86.30, H 6.87; found: C 86.26, H 6.85.

[Ru-Nor-Ru] (3): 43 mg (0.05 mmol) of **9** and 48 mg (0.1 mmol) of $[Ru(bpy)_2Cl_2]$ were dissolved in 7.5 mL of a DME/ethylene glycol mixture (2:1) and heated in an ultrasonic bath using ethylene glycol as external solvent. After 30 minutes (the reaction was monitored by TLC) the solvents were removed under vacuum by bulb-to-bulb distillation and the residue was purified by flash chromatography (silica gel, CH_3CN/MeOH/H_20/NaCl 4:1:1:0.1). Organic solvents were evaporated and excess NH_4PF_6 dissolved in MeOH (saturated solution) was added to the resulting aqueous solution. After anionic exchange, the red microcrystalline solid was filtered over celite and washed with water. Elution of the solid with acetone and evaporation of the solvent yielded 95 mg (85%) of complex **3**. ^{1}H NMR (300 MHz, CD_3CN): δ = 8.88 (s, 2H), 8.81 (d, *J* = 8.3 Hz, 2H), 8.63 (dd, *J* = 8.0 and 3.7 Hz, 8H), 8.24-8.12 (m, 10H), 8.06 (d, *J* = 8.3 Hz, 4H), 7.97-7.72 (m, 26H), 7.58-7.47 (m, 10H), 3.27-3.17 (m, 2H), 1.90-1.75 (m, 2H), 1.70-1.40 (m, 4H), 1.40-1.10 (m, 14H), 0.95-0.85 (m, 4H); MS (ESI, *m/z*): 969.2 $[M^+ - 2PF_6]$, 597.8 $[M^+ - 3PF_6]$; HRMS (ESI, *m/z*): $[M^+ - 4PF_6]$ calc for $C_{99}H_{88}N_{12}Ru_2$: 412.13354; found: 412.13378.

[Ir-Nor-Ir] (4): 90 mg (0.11 mmol) of **9** and 134 mg (0.06 mmol) of $[Ir(ppyFF)_2(\mu\text{-}Cl)]_2$ dissolved in 28 mL of a $CHCl_3$/MeOH mixture (3:1) were refluxed under argon for 4 h. After evaporation of the solvents the residue was purified by flash chromatography (silica gel, CH_2Cl_2/MeOH 9:1). The solvents were removed under vacuum and the solid dissolved in a minimal amount of $CHCl_3$. Complex **6** was precipitated as hexafluorophosphate salt by adding a saturated solution of NH_4PF_6 in MeOH. The solid was filtered over celite, washed with water and diethyl ether and eluted with acetonitrile. Evaporation of the solvent yielded 164 mg (66%) of **4**. ^{1}H NMR (300 MHz, CD_3CN): δ = 8.79 (d, *J* = 1.5 Hz, 2H), 8.74 (d, *J* = 8.2 Hz, 2H), 8.35 (m, 4H), 8.20 (td, *J* = 7.9 and 1.4 Hz, 2H), 8.08-7.88 (m, 12H), 7.84-7.80 (m, 6H), 7.71-7.62 (m, 12H), 7.57 (t, *J* = 6.6 Hz, 2H), 7.10 (dd, *J* = 12.3 and 6.1 Hz, 4H), 6.73 (t, *J* = 11.1 Hz, 4H), 5.77 (dd, *J* = 8.6 and 2.4 Hz), 3.27-3.16 (m, 2H), 1.90-1.35 (m,

6H), 1.35-1.20 (m, 14H), 0.94-0.82 (m, 4H); MS (ESI, *m/z*): 2111.5 [M^+ - PF_6], 983.3 [M^+ - $2PF_6$]; HRMS (ESI, *m/z*): [M^+ - $2PF_6$] calc for $C_{103}H_{80}N_8F_8Ir_2$: 983.28183; found: 983.28223.

[Ir-Nor-bpyph] (6): 99 mg (0.12 mmol) of **9** and 73 mg (0.06 mmol) of $[Ir(ppyFF)_2(\mu\text{-}Cl)]_2$ dissolved in 56 mL of a $CHCl_3$/MeOH mixture (3:1) were refluxed under argon for 4 h. After evaporation of the solvents the residue was purified by flash chromatography (silica gel, CH_2Cl_2/MeOH 9:1). The solvents were removed under vacuum and the solid dissolved in a minimal amount of $CHCl_3$. Complex **6** was precipitated as hexafluorophosphate salt by adding a saturated solution of NH_4PF_6 in MeOH. The solid was filtered over celite, washed with water and diethyl ether and eluted with acetonitrile. Evaporation of the solvent yielded 94 mg (51%) of **6**. ^{1}H NMR (300 MHz, $CDCl_3$): δ = 8.79-8.68 (m, 5H), 8.54 (d, *J* = 8.1 Hz, 1H), 8.39 (d, *J* = 9.1 Hz, 1H), 8.33 (d, *J* = 9.4 Hz, 1H), 8.02 (t, *J* = 7.9 Hz, 1H), 7.93-7.57 (m, 13H), 7.54-7.31 (m, 11H), 7.23 (t, *J* = 6.1 Hz, 1H), 7.15 (t, *J* = 7.3 Hz, 2H), 7.04 (t, *J* = 6.3 Hz, 1H), 6.94-6.79 (m, 1H), 6.71-6.53 (m, 2H), 5.71 (dd, *J* = 8.2 and 2.2 Hz, 2H), 3.16-3.02 (m, 2H), 2.05-1.35 (m, 6H), 1.35-1.20 (m, 14 H), 0.86-0.76 (m, 4H); MS (ESI, *m/z*): 1393.5 [M^+ - PF_6]; HRMS (ESI, *m/z*): [M^+ - PF_6] calc for $C_{81}H_{68}F_4N_6Ir$: 1393.50708; found: 1393.50788.

[Ir-Nor-Ru] (5): Complex **5** was obtained following the procedure described for **3** by reacting 81 mg (0.053 mmol) of **6** and 37 mg (0.076 mmol) of $[Ru(bpy)_2Cl_2]$ disolved in 28 mL of a ethylene glycol/$CHCl_3$ mixture (3:1). Purification of the resulting solid was achieved by flash chromatography (silica gel, CH_2Cl_2/MeOH 9:1). After evaporation of the solvents the residue was dissolved in a minimal amount of $CHCl_3$ and precipitated adding saturated NH_4PF_6 solution in MeOH. The complex was filtered over celite, washed with water and diethyl ether and eluted with acetonitrile. Evaporation of the solvent yielded 74 mg (62%) of **5**. ^{1}H NMR (300 MHz, CD_3CN): δ = 8.80 (s, 1H), 8.78 (s, 1H), 8.75 (d, *J* = 8.7 Hz, 1H), 8.71 (d, *J* = 8.1 Hz, 1H), 8.53 (dd, *J* = 8.0 and 3.5 Hz, 4H), 8.36 (m, 2H), 8.21 (t, *J* = 7.9 Hz, 1H), 8.15-7.89 (m, 13H), 7.88-7.61 (m, 22H), 7.56 (t, *J* = 6.5 Hz, 1H), 7.49-7.38 (m, 5H), 7.11 (dd, *J* = 12.5 and 6.4 Hz, 2H), 6.73 (t, *J* = 12.1 Hz, 2H), 5.78 (dd, *J* = 8.6 and 2.4 Hz, 2H), 3.25-3.16 (m, 2H), 1.90-1.40 (m, 6H), 1.40-1.20 (m, 14H), 0.95-0.85 (m, 4H); MS (ESI, *m/z*): 976.2 [M^+ - $2PF_6$], 602.5 [M^+ - $3PF_6$]; HRMS (ESI, *m/z*): [M^+ - $3PF_6$] calc for $C_{101}H_{84}N_{10}F_4RuIr$: 602.51631; found: 602.51664.

Electrochemistry

Electrochemical measurements were performed in 10^{-3}M acetonitrile solutions, containing 0.1M *t*-Bu_4NPF_6 as supporting electrolyte (redox potentials versus $E_{1/2}$ (Fc/Fc^+) in Table 2).

Cyclic voltammograms of $[Ir\text{-}Nor\text{-}Ir]^{2+}$ show, in the anodic scan, the presence of a reversible process at $E_{1/2}$ = +1.24 V, as similarly observed for the reference system $[Ir(ppyFF)_2bpy]^+$, then assigned to the Iridium-centred oxidation.[22]

The voltammograms of $[Ru\text{-}Nor\text{-}Ru]^{4+}$ and $[Ir\text{-}Nor\text{-}Ru]^{3+}$ show both a reversible oxidation wave at $E_{1/2}$ = +0.87 V and $E_{1/2}$ = +0.89 V respectively, due to the Ruthenium-centred oxidation process.[14] At higher values, for the heterodinuclear

complex, around $E_{1/2}$ = +1.32 V, we could observe the irreversible, under our experimental conditions, potential wave of the Iridium-centred oxidation.

In the cathodic scan, the homodinuclear $[Ir\text{-}Nor\text{-}Ir]^{2+}$ complex undergoes two reduction processes, centered at $E_{1/2}$ = -1.69 V and at $E_{1/2}$ = -2.40 V. The first reduction takes place on the phenyl-substituted bipyridines and it is indeed slightly shifted to a less negative potential when compared to the reference compound $[Ir(ppyFF)_2bpy]^+$, due to the increased π conjugation on the bipyridine ligand; interestingly, a similar trend was observed in ref. [22], where this shift toward less negative potentials was even larger ($E_{1/2}$ = -1.69 V) because of the presence of a fully conjugated phenylene bridge between the two central cores. The reduction occurring at $E_{1/2}$ = -2.40 V, as for the reference complex, takes place on the fluorinated phenylpyridines, and it is barely visible due to adsorption phenomena at the electrode surface.

Common features of the homobinuclear complexes are observed in the anodic and cathodic scans of the $[Ir\text{-}Nor\text{-}Ru]^{3+}$ complex, in which the voltammogram shows two reversible processes, centered at $E_{1/2}$ = -1.86 V and at $E_{1/2}$ = -2.19 V, and one irreversible reduction waves beyond $E_{1/2}$ = -2.40 V.

Table 2. Redox potentials of complexes $[Ru\text{-}Nor\text{-}Ru]^{4+}$ and $[Ir\text{-}Nor\text{-}Ir]^{2+}$, and the reference complexes $[Ru(bpy)_3]^{2+}$ and $[Ir(ppyFF)_2bpy]^+$.

	Oxidation processes		**Reduction processes**		
	Ir^{III}/Ir^{IV}/V	Ru^{II}/Ru^{III}/V	1 / V	2 / V	3 / V
$[Ru(bpy)_3]^{2+}$ [a]	-	0.89	-1.72	-1.95	-2.26
$[Ru\text{-}Nor\text{-}Ru]^{4+}$ [b]	-	0.87	-1.71	-1.91	-2.23
$[Ir(ppyFF)_2bpy]^+$[a]	1.23	-	-1.71	-2.39 [c]	-
$[Ir\text{-}Nor\text{-}Ir]^{2+}$ [b]	1.24	-	-1.69	-2.40 [c]	-
$[Ir\text{-}Nor\text{-}Ru]^{3+}$ [b]	1.32 [d]	0.89	-1.86	-2.19	-2.43 [c]

[a] From ref. [16a]. [b] Conditions: 10^{-3}M solutions in acetonitrile (containing 0.1M *t*-Bu_4NPF_6) at 293 K; Pt disk electrode; scanning rate = 50 $mV.s^{-1}$; redox potentials versus $E_{1/2}$ (Fc/Fc^+). [c] Adsorption on the electrode. [d] Irreversible process.

Femtosecond transient absorption spectra

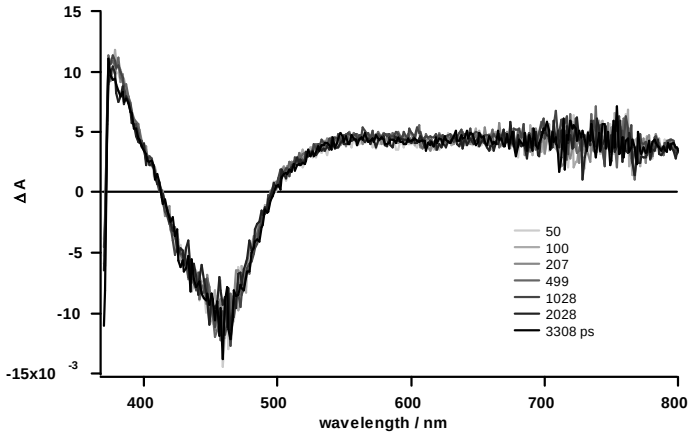

Figure 7. Transient absorption spectrum of [Ru-Nor-Ru]$^{4+}$ in acetonitrile after laser light excitation at 370 nm.

The transient absorption spectrum of the ruthenium binuclear complex shows characteristic features for these type of complexes (Figure 7).[24] Between 400 and 500 nm an intense negative band, corresponding to the bleaching of the ground state, can be observed. Above 500 nm a very broad absorption band extends to the infrared region, characteristic of highly delocalized excited states. This signal has been assigned to the MLCT transition involving the biphenyl appended bipyridine. Another positive band can be observed below 400 nm that is assigned to the reduced bpy. This assignment is done after comparison with the transient spectra of the parent compound $Ru(bpy)_3^{2+}$.[24]

The lifetime of the excited state of this compound is very long when compared to the employed time window. A trace measured at 600 nm shows the immediate formation of the excited state after laser light excitation. The excited state does not decay within our time window, Figure 8.

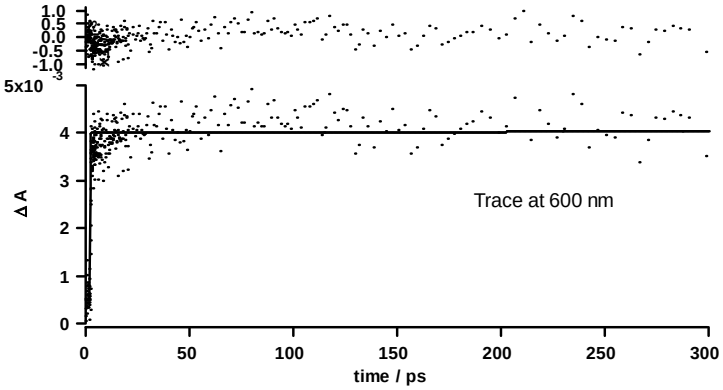

Figure 8. Trace at 600 nm showing the formation of the excited state at 600 nm after laser light excitation.

Figure 8 shows the transient absorption spectrum of the iridium bimetallic complex. Again, a very broad absorption band is observed, indicating the presence of a delocalized excited state on the biphenyl appended ligand.[20] No negative bands, related to the bleaching of the ground state, are observed, probably due to an overlap of signals in the 400 nm region of the spectrum as the indentation in the transient signal indicates in this area. Also in this case, as shown in Figure 10, the excited state decays with a long lifetime and then can not be observed within the employed time window.

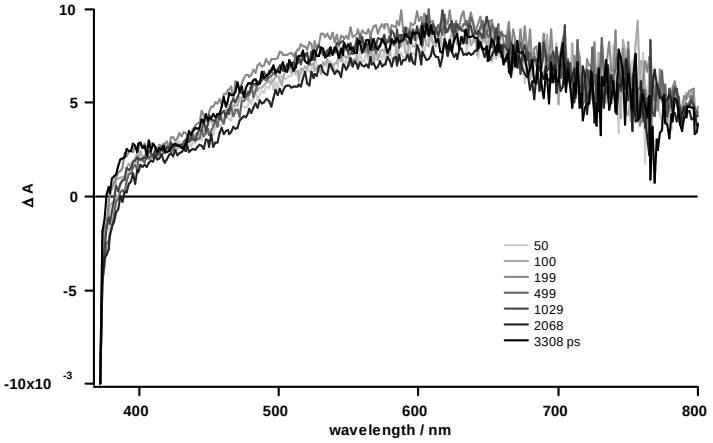

Figure 9. Transient absorption spectrum of $[Ir\text{-}Nor\text{-}Ir]^{3+}$ in acetonitrile after laser light excitation at 370 nm.

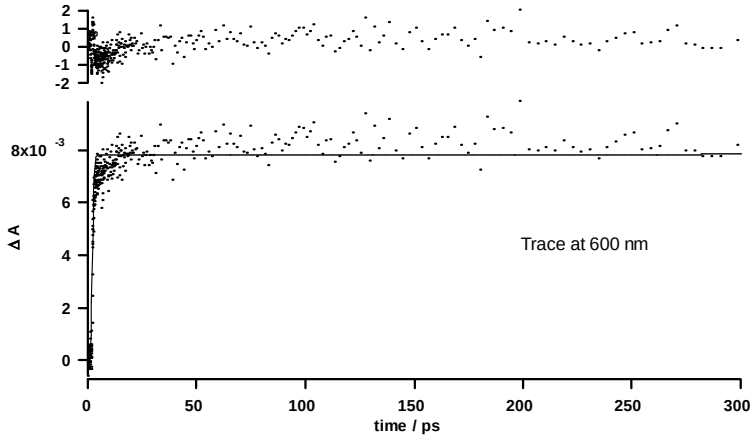

Figure 10. Trace at 600 nm showing the formation of the excited state at 600 nm after laser light excitation.

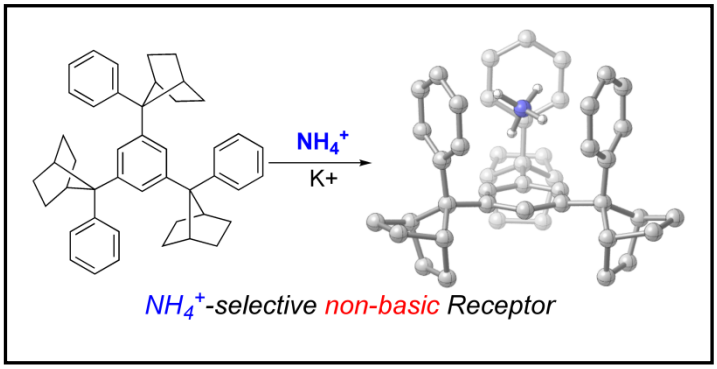

2.2 Rational Design of a non-Basic Molecular Receptor for Selective NH_4^+/K^+ Complexation.

*A new molecular receptor (**1**) for ammonium recognition has been designed and constructed only with carbon atoms. This molecular receptor can coexist in two different isoenergetic conformations but, upon complexation, the conformers are no longer isoenergetic, and a basket shaped conformation becomes clearly more stable. The preorganized tetrahedral structure of this basket shaped molecule favours the complexation of ammonium ions by N-H···π interactions with the four phenyl groups of the host. A similar behaviour is not observed in a similar, but less preorganized, reference molecule. ESI-MS competition experiments show that **1** is able to bind NH_4^+ over K^+ selectively. This is the first example of a neutral molecular receptor that shows a remarkable NH_4^+/K^+ selectivity. DFT-calculations provide insight into the nature of host-guest interactions of both **1**·NH_4^+ and **1**·K^+ complexes as well as in the mechanism involved in multiple cation-π interactions and the influence of these interactions on the conformational stability and the selective binding of the host.*

Chem. Eur. J. **2012,** *18*, **DOI:** 10.1002/chem.201201642

2.2.1 Introduction

The design of artificial synthetic receptors for the molecular recognition of ammonium and alkylammonium ions has been one of the most important challenges from the very beginning of Supramolecular Chemistry. The importance and variety of ammonium ions in chemistry and molecular biology has been the driving force of the enormous effort devoted to the development of efficient molecular receptors for selective ammonium complexation.[1,2,3,4,5]

A major problem encountered in the design of ammonium ion receptors is that related to the interference from potassium ion. Although ammonium ion prefers a tetrahedral coordination in contrast to the octahedral preference of potassium, the similar diameter of both guests (286 pm for NH_4^+ and 266 pm for K^+) makes the selective recognition of ammonium over potassium difficult. Several strategies have been developed in order to overcome this problem, resulting in a series of molecular receptors that show high NH_4^+/K^+ selectivity.[6,7,8,9,10,11,12] However, all the hosts described until now posses several

[1] T. Schrader, M. Maue, in *Functional Synthetic Receptors*, (Eds.: T. Schrader, A. D. Hamilton), WILEY-VCH, Weinheim, **2005**, pp. 111-164.
[2] *Encyclopedia of Supramolecular Chemistry* (Eds.: J. L. Atwood, J. W. Steed), Marcel Dekker, New York, **2004**.
[3] *Comprehensive Supramolecular Chemistry*, (Eds.: J. L. Atwood, J. E. D. Davies, D. D. MacNicol, F. Vögtle), Vol. 1, *Molecular Recognition: Receptors for Cationic Guests*, Pergamon, **1996**.
[4] J. W. Steed, J. L. Atwood, *Supramolecular Chemistry*, John Wiley & Sons, Chichester, **2009**.
[5] A. Späth, B. König, *Beilstein J. Org. Chem.* **2010**, *6*, 1-111.
[6] A. Lélias-Vanderperre, J.-C. Chambron, E. Espinosa, P. Terrier, E. Leize-Wagner, *Org. Lett.* **2007**, *9*, 2961-2964.
[7] J. Kim, Y. K. Kim, N. Park, J. H. Hahn, K. H. Ahn, *J. Org. Chem.* **2005**, *70*, 7087-7092.
[8] a) J. Chin, J. Oh, S. Y. Jon, S. H. Park, C. Walsdorff, B. Stranix, A. Ghoussoub, S. J. Lee, H. J. Chung, S.-M. Park, K. Kim, *J. Am. Chem. Soc.* **2002**, *124*, 5374-5379; b) S. Y. Jon, J. Kim, M. Kim, S. H. Park, W. S. Jeon, J. Heo, K. Kim, *Angew. Chem. Int. Ed.* **2001**, *40*, 2116-2119; c) K. H. Ahn, S.-G. Kim, J. Jung, K.-H. Kim, J. Kim, J. Chin, K. Kim, *Chem. Lett.* **2000**, 170-171; d) J. Chin, C. Walsdorff, B. Stranix, J. Oh, H. J. Chung, S.-M. Park, K. Kim, *Angew. Chem. Int. Ed.* **1999**, *38*, 2756-2759.
[9] A. Rahman, N.-H. Kwon, M.-S. Won, M.-H. Hyun, Y.-B. Shim, *Anal. Chem.* **2004**, *76*, 3660-3665.
[10] S.Sasaki, T. Amano, G. Monma, T. Otsuka, N. Iwasawa, D. Citterio, H. Hisamoto, K. Suzuki, *Anal. Chem.* **2002**, *74*, 4845-4848.
[11] K. S. Oh, C.-W. Lee, H. S. Choi, S. J. Lee, K. S. Kim, *Org. Lett.* **2000**, *2*, 2679-2681.

heteroatoms in their structure and, therefore, hydrogen bonds are the main noncovalent interactions involved in the ammonium ion recognition or, at least, they play an important role as secondary forces.

To our knowledge, no molecular receptor for selective ammonium recognition based exclusively on cation-π (or N-H···π) interactions[13] has been described until now. Such a receptor should have a preorganized cavity size able to complex ammonium ion and four complementary aromatic rings disposed in a tetrahedral arrangement in order to facilitate the selective binding of ammonium over potassium ion by N-H···π interactions, since the positive charge of NH_4^+ is located predominantly on the hydrogen atoms. In this paper, we report the synthesis and complexation behaviour of the first neutral molecular receptor that shows a remarkable NH_4^+/K^+ selectivity based exclusively on N-H···π interactions.

2.2.2 Results and Discussion

With the conditions mentioned above in mind, we have designed and synthesized the tripodal basket-shaped[14,15] molecular receptor **1** (Scheme 1).
The non preorganized compound **5** has been prepared also as a reference for the study of the complexation properties of **1**. In previous works we have shown that the inclusion of the preorganized 7,7-diphenylnorbornane subunit

[12] H.-S. Kim, H. J. Park, H. J. Oh, Y. K. Koh, J.-H. Choi, D.-H. Lee, G. S. Cha, H. Nam, *Anal. Chem.* **2000**, *72*, 4683-4688.
[13] a) J. C. Ma, D. A. Dougherty, *Chem. Rev.* **1997**, *97*, 1303-1324; b) G. W. Gokel, S. L. De Wall, E. S. Meadows, *Eur. J. Org. Chem.* **2000**, 2967-2978; c) E. A. Meyer, R. K. Castellano, F. Diederich, *Angew. Chem. Int. Ed.* **2003**, *42*, 1210-1250; d) L. M. Salonen, M. Ellermann, F. Diederich, *Angew. Chem. Int. Ed.* **2011**, *50*, 4808-4842.
[14] For reviews and highlights on tripodal receptors, see: a) S. E. Gibson, M. P. Castaldi, *Angew. Chem. Int. Ed.* **2006**, *45*, 4718-4720; b) C. Moberg, *Angew. Chem. Int. Ed.* **2006**, *45*, 4721-4723; c) B. Kuswandi, Nuriman, W. Verboom, D. N. Reinhoudt, *Sensors*, **2006**, *6*, 978-1017; d) C. Moberg, *Angew. Chem. Int. Ed.* **1998**, *37*, 248-268.
[15] For recent examples of molecular baskets, see: a) J. Hornung, D. Fankhauser, L. D. Shirtcliff, A. Praetorius, W. B. Schweizer, F. Diederich, *Chem. Eur. J.* **2011**, *17*, 12362-12371; b) S. Rieth, J. D. Badjić, *Chem. Eur. J.* **2011**, *17*, 2562-2565; S. Stojanović, D. A. Turner, C. M. Hadad, J. D. Badjić, *Chem. Sci.* **2011**, *2*, 752-759; d) H. Cui, N. G. Akhmedov, J. L. Petersen, K. K. Wang, *J. Org. Chem.* **2010**, *75*, 2050-2056; e) X. Bao, S. Rieth, S. Stojanović, C. M. Hadad, J. D. Badjić, *Angew. Chem. Int. Ed.* **2010**, *49*, 4816-4819.

instead of diphenylmethane in supramolecular structures exerts a dramatic influence on the stability of the corresponding complexes.[16]

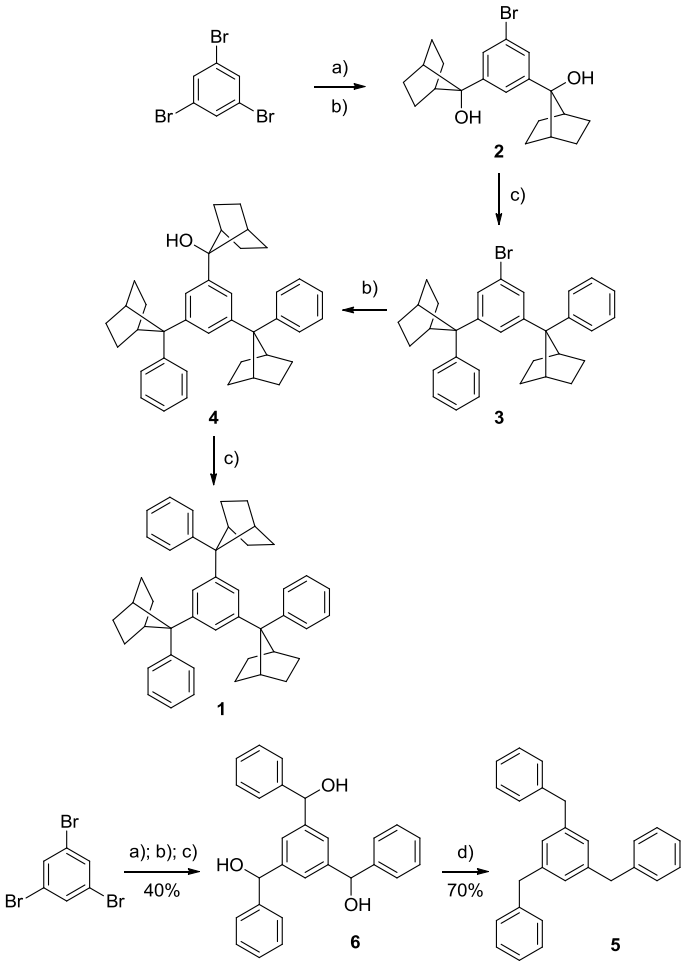

Scheme 1. Synthesis of molecular basket **1**: a) BuLi/Et_2O; 7-norbornanone. b) BuLi/Et_2O; 7-norbornanone; H_2O. c) Benzene/TfOH. d) *t*BuLi/THF; 7-norbornanone; H_2O.

The aryl rings in **1** are forced to adopt a cofacial conformation by the steric hindrance of the norbornane moieties, as can be observed in other 7,7-

[16] a) A. García Martínez, J. Osío Barcina, M. R. Colorado Heras, A. de Fresno Cerezo, M. R. Torres Salvador, *Chem. Eur. J.* **2003**, *9*, 1157-1165; b) A. García Martínez, J. Osío Barcina, A. de Fresno Cerezo, *Chem. Eur. J.* **2001**, *7*, 1171-1175.

diphenylnorbornanes described by us,[17] thus resulting in a preorganized tetrahedral aromatic receptor. On the contrary, in compound **5** no preferred conformation is observed since diphenylmethane derivatives behave as free rotators.[18]

On the other hand, molecular receptor **1** may exist as two stable conformations, i.e. the C_3-symmetric basket-shaped conformation (**1a**) with the three lateral phenyl rings oriented in the same direction and the C_1-symmetric alternate or partial-basket conformation (**1b**). X-ray crystal studies reveal that in the solid state **1** crystallizes in the *P*1 space group adopting the alternate conformation **1b** where phenyl groups A and B are oriented in a direction opposite to ring C (Figure 1). All three phenyl groups are disposed cofacially respect to the central aryl ring. The values of the corresponding torsion angles are C18-C13-C4-C10: 85.89^o and C13-C4-C10-C6: 88.96^o (ring A), C26-C12-C7-C5: 98.92^o and C12-C7-C5-C11: 95.40^o (ring B), and C19-C9-C2-C1: 74.56^o and C9-C2-C1-C11: 71.53^o (ring C).

[17] a) N. Herrero-García, I. Fernández, J. Osío Barcina, *Chem. Eur. J.* **2011**, *17*, 7327-7335; b) J. Osío Barcina, N. Herrero-García, F. Cucinotta, L. De Cola, P. Contreras-Carballada, R. M. Williams, A. Guerrero-Martínez, *Chem. Eur. J.* **2010**, *16*, 6033-6040; c) J. Osío Barcina, M. R. Colorado Heras, M. Mba, R. Gómez Aspe, N. Herrero García, *J. Org. Chem.* **2009**, *74*, 7148-7156; d) N. Caraballo-Martínez, M. R. Colorado Heras, M. M. Blázquez, J. Osío Barcina, A. García Martínez, M. R. Torres Salvador, *Org. Lett.* **2007**, *9*, 2943-2946; e) A. García Martínez, J. Osío Barcina, A. de Fresno Cerezo, A.-D. Schlüter, J. Frahn, *Adv. Mater.* **1999**, *11*, 27-31; f) A. García Martínez, J. Osío Barcina, A. De Fresno Cerezo, R. Gutiérrez Rivas, *J. Am. Chem. Soc.* **1998**, *120*, 673-679.

[18] See: A. García Martínez, J. Osío Barcina, in *The Diphenylmethane Moiety*, pp. 452-456, in ref. 2.

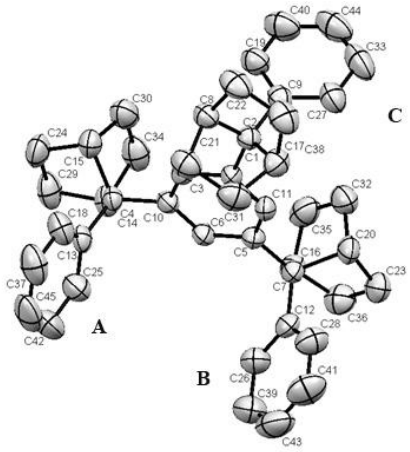

Figure 1. Crystal structure of **1** (hydrogen atoms are omitted for clarity).

Crystal packing shows that **1** crystallizes with one molecule of acetone (Figure 2). The oxygen atom of acetone exhibits CH···O interactions with the bridgehead hydrogen atoms of norbornanes A and B (CH···O distances 2.696 and 2.583 Å, respectively), thus contributing to stabilize the conformation observed in the crystal structure. Also of note is that methyl groups of acetone are oriented towards the A and B phenyl groups of the neighbouring molecule forming linear arrays. The shortest CH···π distances are 3.032 and 3.025 Å, only slightly higher than the sum of the van der Waals radii of a hydrogen atom and a phenyl group (2.9 Å), pointing to CH···π interactions as forces that contribute to the crystal packing structure.

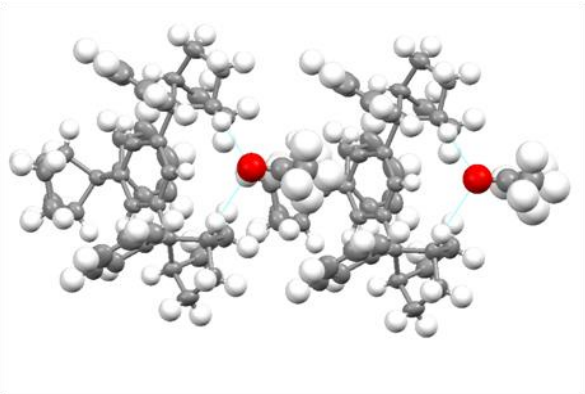

Figure 2. Crystal packing of **1** showing the CH···O interactions with acetone.

In solution, a rapid equilibrium exists between the basket-shaped conformation **1a** and the alternate conformation **1b**. Density functional theory (DFT) calculations at the M062X/TZVP//M062X-def2-SVP level[19] show that these conformations are almost degenerated (ΔE = 0.2 kcalmol^{-1}) (Figure 3). Therefore, the conformation observed in the solid state can be attributed to favourable packing forces and not to the stability of the conformers. The computed low rotation barrier which converts **1a** into **1b** ($\Delta E^{\neq}$ = 8.6 kcal.mol^{-1}) suggests that **1** can coexist in both conformations at room temperature. This barrier energy is comparable to the rotational barrier of the phenyl group in 7,7-diphenylnorbornane (11.2 kcal.mol^{-1}).[17a,d] Moreover, a similar situation has been reported for 7,7-diphenylnorbornane oligomers where an equilibrium between the isoenergetic Z- and U-shaped conformations has been described.[17a,d]

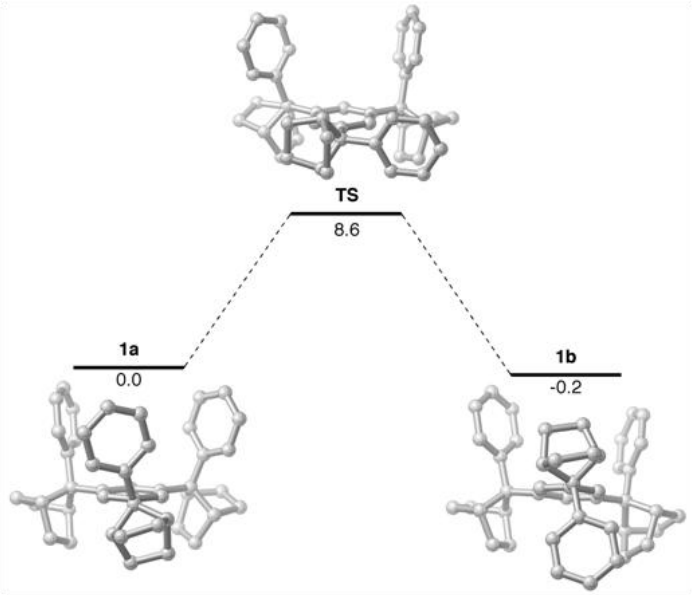

Figure 3. Computed isomerization process for compound **1** (hydrogen atoms are omitted for clarity). Gas-phase energy values (at the M062X/TZVP//M062X/def2-SVP level) are given in kcalmol^{-1}.

[19] All calculations were carried at the dispersion-corrected meta-hybrid M062x functional using the def2-SVP basis sets. Single point energy calculations were performed at the M062x/TZVP level over the M062x/def2-SVP geometries. For the complexation energies, the basis set superposition error were taken into account for the TZVP basis set energy values.

In order to check the complexation properties of **1**, we carried out two different competition experiments and investigated the results by positive ESI-MS spectrometry. Electrospray spectrometry has proven to be an appropriate tool for the study of supramolecular complexes and non-covalent interactions,[20,21,22] particularly in the case of ammonium receptors.[6,7]

First, we investigated the differential behaviour of compounds **1** and **5**. Interestingly, when an equimolecular mixture of **1**, **5** and NH_4PF_6 was examined, only the corresponding peak of the **1** + NH_4^+ complex at *m/z* = 606 was detected. The relative ESI-MS response factor ($R = R_{[\mathbf{1} + NH4+]}/ R_{[\mathbf{5} + NH4+]} =$ 10.3) confirms the higher affinity of **1** in the complexation of NH_4^+.This results shows very clearly the importance of the preorganization afforded by the norbornane frameworks in molecular receptor **1** in comparison to compound **5**, as reported previously by us for the case of 7,7-diphenylnorbornane derived macrocycles and complexes.[16]

In a second experiment we studied the selective complexation of NH_4^+ over K^+ by receptor **1**. The competition experiment using an equimolecular mixture of **1**, NH_4PF_6 and KPF_6 showed the peaks of the 1:1 complexes [**1**·NH_4^+] and [**1**·K^+] at *m/z* = 606 and *m/z* = 627, respectively. The relative intensity of these peaks (I[**1**·NH_4^+] / I[**1**·K^+] = 5.1) shows that receptor **1** has a clear preference for binding NH_4^+ over K^+. This result is comparable or even better than the reported for cage-type basic molecular receptors.[6,7] To our knowledge, this is the first example of a molecular receptor based only on carbon atoms that shows a remarkable NH_4^+/K^+ selectivity since no heteroatoms that could coordinate with NH_4^+ are present in the structure of **1**. This fact demonstrates the importance of the tetrahedral disposition of the phenyl groups in molecular receptor **1**, that should favour the selective complexation of NH_4^+ over K^+ by NH···π interactions.

---

[20] M. Kogej, C. A. Schalley, in *Analytical Methods in Supramolecular Chemistry*, (Ed.: C. Schalley), WILEY-VCH, Weinheim, **2007**, pp. 104-162.

[21] a) N. B. Cech, C. G. Enke, *Mass Spectrom. Rev.* **2001**, *20*, 362-387; b) F. Inokuchi, Y. Miyahara, T. Inazu, S. Shinkai, *Angew. Chem. Int. Ed.* **1995,** *34*, 1364-1366; c) H. Konishi, K. Takahashi, M. Nakamura, H. Sakamoto, K. Kimura, *J. Incl. Phenom. Macrocycl. Chem.* **2006**, *54*, 147-152.

[22] Although several reports claim that ESI-MS reflect the situation of complexes in solution (See: E. Leize, A. Jaffrezic, A. Van Dorsselaer, *J. Mass Spectrom.* **1996**, *31*, 537-544, and ref. 6), extrapolation of the data obtained in gas phase to the situation in solution must be made carefully (see ref. 20, pp. 118).

To gain further insight into the complexation properties of receptor **1**, we computationally explored the different species formed upon complexation of ammonium and potassium cations with compound **1**.[23]

Figure 4a shows the M062x/def2-SVP optimized geometries of the corresponding 1:1 complexes, where the guest molecule interacts with 2 to 4 aryl fragments of the host molecule **1**. The complexation energies gathered in Figure 4b (which include the basis set superposition error at the M062x/TZVP level)[20] clearly indicate that, as expected, the more aryl groups interacting with the guest molecule the more exothermic the formation of the complex is. Moreover, although conformer **1b** is slightly more stable than conformer **1a** (by only 0.2 kcalmol^{-1}, see above), the basket shaped conformation becomes more stable upon complexation with both NH_4^+ and K^+ due to the presence of an additional guest-aryl group interaction.

Interestingly, from the data in Figure 4b, it becomes obvious that the complexation of NH_4^+, either with **1a** or **1b**, is always favoured over the complexation of K^+ ($\Delta E \approx 4$ kcalmol^{-1}), which reflects the greater selectivity of our receptor **1** towards the binding of ammonium over potassium cations, as experimentally observed.

[23] DFT calculations have been successfully used in studies of cation-π interactions of NH_4^+ and alkaline metals cations with benzene and several molecular receptors: a) L. K. Engerer, T. P. Hanusa, *J. Org. Chem.* **2011**, *76*, 42-49; b) Y. Wang, Z. Xu, Y. Gao, L. Zhang, H. Li, *J. Phys. Chem. A* **2009**, *113*, 7097-7102; c) R. Wu, T. B. McMahon, *J. Am. Chem. Soc.* **2008**, *130*, 12554-12555; d) A. B. Rozhenko, W. W. Schoeller, M. C. Letzel, B. Decker, C. Agena, J. Mattay, *Chem. Eur. J.* **2006**, *12*, 8995-9000; e) R. Sa, W. Zhu, J. Shen, Z. Gong, J. Cheng, K. Chen, H. Jiang, *J. Phys. Chem. B* **2006**, *110*, 5094-5098; f) A. T. Macias, J. E. Norton, J. D. Evanseck, *J. Am. Chem. Soc.* **2003**, *125*, 2351-2360; g) W.-L. Zhu, X.-J. Tan, C. M. Puah, J.-D. Gu, H.-L. Jiang, K.-X. Chen, C. E. Felder, I. Silman, J. L. Sussman, *J. Phys. Chem. A* **2000**, *104*, 9573-9580; h) Y. Inoue, S. Sugio, J. Andzelm, N. Nakamura, *J. Phys. Chem. A* **1998**, *102*, 646-648. See also: i) E. A. Orabi, G. Lamoureux, *J. Chem. Theory Comput.* **2012**, *8*, 182-193; j) F. B. Sayyed, C. H. Suresh, *J. Phys. Chem. A* **2011**, *115*, 9300-9307; k) M. S. Marshall, R. P. Steele, K. S. Thanthiriwatte, C. D. Sherrill, *J. Phys. Chem. A* **2009**, *113*, 13628-13632; l) D. Kim, S. Hu, P. Tarakeshwar, K. S. Kim, *J. Phys. Chem. A* **2003**, *107*, 1228-1238; m) A. Mohajeri, E. Karimi, *THEOCHEM* **2006**, *774*, 71-76.

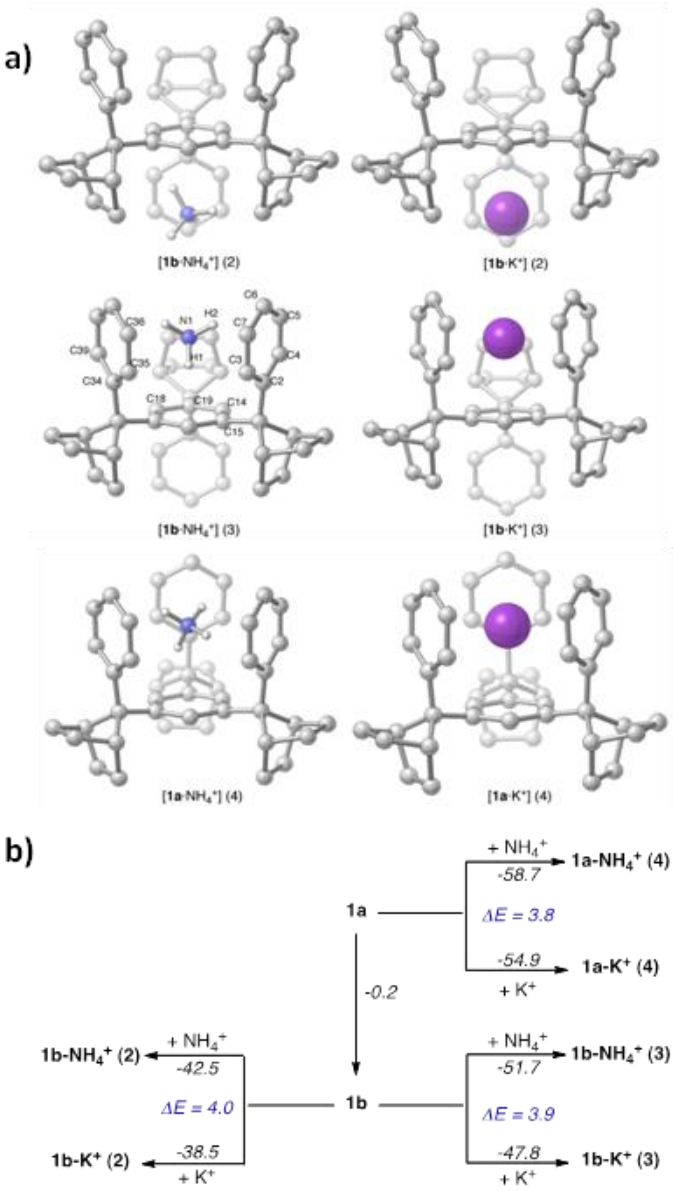

Figure 4. (a) M062x/def2-SVP optimized geometries of complexes [**1a**·NH_4^+], [**1b**·NH_4^+], [**1a**·K^+], and [**1b**·K^+]. (b) Complexation energies (in kcalmol^{-1}, as *E* = *E*(complex) – *E* (**1**) – *E*(cation)) computed at the M062x/TZVP//M062x/def2-SVP level (including the corresponding basis set superposition error).

Therefore, it can be concluded that receptor **1** is an excellent model compound for the study not only of multiple cation-π interactions (which are known to play a fundamental role in supramolecular complexes and biological systems involving ion channels)[24] but also for the study of the relationship between the binding strength and the position and number of the aryl groups in the molecular receptor.

The nature of the host-guest interaction in the ammonium complexes has been addressed next by means of the second-order perturbation theory (SOPT) of the Natural Bond Orbital (NBO) method.[25] As instance, for complex [**1b**·NH_4^+](**3**), a good number of stabilizing two-electrons delocalizations from the occupied π(C=C)-molecular orbitals of the aryl-groups to the vacant σ*(N-H) molecular orbitals were found. The corresponding associated second-order perturbation energies ($\Delta E^{(2)}$) are gathered in Table 1, which shows that the more significant π→σ* interaction occur from the aryl group at the base of the cavity. Similar π→σ* delocalizations can be also found in the analogues ammonium complexes depicted in Figure 4a.

The conformational flexibility of receptor **1** allows the calculation of the interaction energies (N^+-H···π and K^+···π interactions) between the cationic guests and the flipping phenyl groups in our dynamic model compound by means of molecular balances.[16b,26] Thus, on going from [**1a**·NH_4^+](4) to [**1b**·NH_4^+](3), the NH_4^+···π interaction energy with the flipping phenyl rig can be obtained from the energy difference between complexes [**1a**·NH_4^+](4) and [**1b**·NH_4^+](3).

---

[24] a) S. A. Pless, J. D. Galpin, A. P. Niciforovic, C. A. Ahern, *Nat. Chem. Biol.* **2011**, *7*, 617-623; b) R. C. Dumbar, J. D. Steill, J. Oomens, *J. Am. Chem. Soc.* **2011**, *133*, 9376-9386; c) A. T. Macias, J. E. Norton, J. D. Evanseck, *J. Am. Chem. Soc.* **2003**, *125*, 2351-2360; d) K. Murayama, K. Aoki, *Chem. Commun.* **1997**, 119-120. For studies of cation-π interactions in ammonium ion complexation by enzyme π-pockets, see: e) L. M. Salonen, C. Bucher, D. W. Banner, W. Haap, J.-L. Mary, J. Benz, O. Kuster, P. Seiler, W. B. Schweizer, F. Diederich, *Angew. Chem. Int. Ed.* **2009**, *48*, 811-814; f) M. Zürcher, F. Diederich, *J. Org. Chem.* **2008**, *73*, 4345-4361. See also: g) U. Akgun, S. Khademi, *Proc. Natl. Acad. Sci.USA* **2011**, *108*, 3970-3975.

[25] a) J. P. Foster, F. Weinhold, *J. Am. Chem. Soc*. **1980**, *102*, 7211-7218; b) A. E. Reed, F. J. Weinhold, *J. Chem. Phys*. **1985**, *83*, 1736-1740; c) A. E. Reed, R. B. Weinstock, F. Weinhold, *J. Chem. Phys*. **1985**, *83*, 735-746; d) A. E. Reed, L. A. Curtiss, F. Weinhold, *Chem. Rev*. **1988**, *88*, 899-926.

[26] I. K. Mati, S. L. Cockroft, *Chem. Soc. Rev.* **2010**, *39*, 4195-4205.

Table 1. Second-order perturbation energies ($\Delta E^{(2)}$) associated to the stabilizing $\pi \rightarrow \sigma^*$ interactions in complex [**1b**·NH_4^+](**3**).[a]

Interaction	$\Delta E^{(2)}$ / kcalmol^{-1}
π (C2=C3) $\rightarrow$ σ^* (N1-H1)	-0.84
π (C14=C15) $\rightarrow$ σ^*(N1-H1)	-4.97
π (C18=C19) $\rightarrow$ σ^*(N1-H1)	-0.38
π (C34=C39) $\rightarrow$ σ^*(N1-H1)	-0.10
π (C35=C36) $\rightarrow$ σ^*(N1-H1)	-0.32
π (C4=C5) $\rightarrow$ σ^*(N1-H2)	-1.39
π (C6=C7) $\rightarrow$ σ^*(N1-H2)	-1.96
π (C18=C19) $\rightarrow$ σ^*(N1-H2)	-0.11
π (C34=C39) $\rightarrow$ σ^*(N1-H2)	-0.13

[a] All data have been computed at the M062x/def2-SVP level.

This value is then corrected by the energy difference between conformations **1a** and **1b**, resulting in the following equation: $E_{\text{N-H}\cdots\pi}$ = ($E_{[\mathbf{1a}\cdot\text{NH4+}](4)}$ - $E_{[\mathbf{1b}\cdot\text{NH4+}](3)}$) − ($E_{\mathbf{1a}}$ - $E_{\mathbf{1b}}$). For the $K^+\cdots\pi$ interaction energy a similar equation is obtained: $E_{K^+\cdots\pi}$ = ($E_{[\mathbf{1a}\cdot\text{K+}](4)}$ - $E_{[\mathbf{1b}\cdot\text{K+}](3)}$) − ($E_{\mathbf{1a}}$ - $E_{\mathbf{1b}}$). The values obtained for the interaction energies according to these equations are very similar: $E_{\text{N-H}\cdots\pi}$ = -7.2 kcalmol^{-1} and $E_{K^+\cdots\pi}$ = -7.1 kcalmol^{-1}.

On the other hand, the interaction energies between the cationic guests and the new interacting phenyl group on going from [**1b**·NH_4^+](3) (or [**1b**·K^+](3)) to [**1b**·NH_4^+](2) (or [**1b**·NH_4^+](2)) can be obtained directly from the energy difference between the two complexes. The values obtained for the N^+-H$\cdots\pi$ and $K^+\cdots\pi$ interaction energies in this case are also very similar, 9.2 and 9.3 kcalmol^{-1} respectively. It should be noted that the experimental values of the NH_4^+·benzene and the K^+·benzene interaction energies are almost the same, -19.3 kcalmol^{-1} and -19.2 kcalmol^{-1} respectively,[13] a result in agreement with our calculations.

All these data afford some interesting conclusion about the characteristics of multiple cation-π interactions in our model compound. The contribution of the phenyl groups to the stability of the complexes is different in each case, being less important ($\approx$ 2 kcalmol^{-1}) the contribution of the fourth group (on going

from **1b**·guest (3) to **1b**·guest (2)) than the afforded from the third phenyl group (on going from **1a**·guest (4) to **1b**·guest (3)).

2.2.3 Conclusion

In summary, the first receptor based only on a carbonated skeleton able to bind selectively NH_4^+ over K^+ in its preorganized cavity has been rationally designed. This molecular receptor can coexist in two different and almost isoenergetic conformations, which are able to form 1:1 complexes with NH_4^+ and K^+ through multiple cation-π interactions. Strikingly, both conformers exhibit a remarkable greater selectivity for NH_4^+ over K^+ through genuine NH···π interactions, as revealed by DFT-calculations. Upon complexation, the conformers are no longer isoenergetic, and the basket shaped conformation becomes clearly more stable. The molecular receptor described in this work provides interesting information about multiple cation-π interactions and the influence of these interactions on the conformational stability and the selective binding of the host. Further studies towards the synthesis of novel non-heteroatom based receptors are currently underway in our laboratories.

2.2.4 Experimental Section

General Information

^{1}H and ^{13}C NMR spectra were recorded on a 300 MHz spectrometer. Chemical shifts are given in ppm relative to TMS (^{1}H, 0.0 ppm) and $CDCl_3$ (^{13}C, 77.0 ppm). Coupling constants are given in Hertz. All experiments involving organometallic reagents were carried out under argon atmosphere using standard Schlenk techniques. Anhydrous solvents were distilled under argon following standard procedures. Flash chromatography was performed over silica gel 60 (230-400 mesh). All commercially available compounds were purchased from commercial suppliers and used without further purification. The preparation of **2** was carried out following the sequential metal-halogen exchange reaction described in the literature.[27] 7-Norbornanone was synthesized according to a described procedure.[28] Compound **5** has been described elsewhere.[29]

Experimental procedures

Compound 2: BuLi (9.9 mL 1.6 M in hexanes, 15.9 mmol) was slowly added at -78 ºC to a solution of 5 g (15.9 mmol) of 1,3,5-tribromobenzene in 25 mL of Et_2O. After 20 min, 1.74 g (15.9 mmol) of 7-norbornanone dissolved in 10 mL of Et_2O were added dropwise into the flask. The reaction mixture was stirred for 4 h at 25 ºC and then, cooled at -78 ºC before adding BuLi (9.9 mL 1.6 M in hexanes, 15.9 mmol). After 20 min, 1.74 g (15.9 mmol) of 7-norbornanone dissolved in 10 mL of Et_2O wee again added into the flask. The reaction mixture was stirred for 4 h, quenched with 50 mL of water and extracted with Et_2O (3 x 20 mL). The combined organic layer was washed with water (2 x 25 mL) and dried over $MgSO_4$. Evaporation of the solvent at reduced pressure and purification of the residue by flash chromatography (silica gel, hexane/Et_2O 7:3) yielded **2** (1.5 g, 25%) as a white solid. ^{1}H NMR (300 MHz, $CDCl_3$): δ = 7.57 (d, 1H, *J* = 1.4 Hz), 7.55 (t, 2H, *J* = 1.4 Hz), 2.34 (s, 4H), 2.14 (m, 4H), 1.78 (s, 2H), 1.50-1.22 (m, 10H) ppm; ^{13}C NMR (75 MHz, $CDCl_3$): δ = 145.5, 130.0, 125.3, 123.0, 88.0, 42.5, 28.7, 27.7 ppm; MS (70 eV): *m/z* (%) = 378 (30) [M^+ + 2], 376 (30) [M^+], 360 (6), 358 (4), 323 (15), 321 (16), 297 (100), 295 (95), 293 (91), 267 (86), 265 (84), 187 (52), 168 (38), 131 (46), 111 (74), 3 (88); Elemental analysis (%) calc for $C_{20}H_{25}BrO_2$: C 63.65, H 6.68; found: C 63.46, H 6.71.

---

[27] a) L. S. Chen, G. J. Chen, C. Tamborski, *J. Organometallic. Chem.* **1981**, *215*, 281-291. b) L. S. Chen, C. Tamborski, *J. Fluorine Chem.* **1995**, *75*, 117-120. c) G. J. Chen, C. Tamborski, *J. Organometallic. Chem.* **1983**, *251*, 149-158.

[28] a) P. G. Gassman, P. G. Pape, *J. Org. Chem.* **1964**, *29*, 160-163. b) P. G. Gassman, J. L. Marshall, *Org. Synth.* **1968**, *42*, 287.

[29] a) K. S. Choi, M. K. Park, B. H. Han, *Bull. Korean Chem. Soc.* **1998**, *19*, 1257-1261; b) T. Fujimoto, S. Tani, K. Takano, M. Ogawa, M. Nagasawa, *Macromolecules* **1978**, *11*, 673-677.

Compound 3: 210 mg (0.56 mmol) of **2** were dissolved in 15 mL of anhydrous benzene and 182 mg (1.2 mmol) of trifluoromethanesulfonic acid were slowly added at 0 ºC.[16,17] After 10 min (the evolution of the reaction was monitored by TLC) the reaction was quenched with 10% $NaHCO_3$ and extracted with Et_2O (3 x 15 mL). The organic solution was washed with 10% $NaHCO_3$ (2 x 25 mL), water (1 x 25 mL) and dried over $MgSO_4$. Evaporation of the solvent at reduced pressure and purification of the residue by flash chromatography (silica gel, hexane/Et_2O 9:1) yielded **3** (193 mg, 70%) as a white solid. ^{1}H NMR (300 MHz, $CDCl_3$): δ = 7.46 (m, 1H), 7.35 (d, 4H, *J* = 8.4 Hz), 7.21 (t, 4H, *J* = 8.0 Hz), 7.20 (s, 2H), 7.07 (t, 2H, *J* = 7.3 Hz), 3.02 (s, 4H), 1.69-1.47 (m, 8H), 1.35-1.26 (m, 8H) ppm; ^{13}C NMR (75 MHz, $CDCl_3$): δ = 148.0, 145.2, 128.3, 127.5, 127.3, 125.7, 125.3, 122.1, 64.8, 41.8, 28.3, 28.3 ppm; MS (70 eV): *m/z* (%) = 498 (77) [M^+ + 2], 496 (77) [M^+], 418 (82), 417 (95), 327 (73), 325 (74), 171 (100), 129 (89), 91 (92); Elemental analysis (%) calc for $C_{32}H_{33}Br$: C 77.24, H 6.69; found: C 77.08, H 6.72.

Compound 4: *t*BuLi (1.17 mL 1.7 M in pentane, 2 mmol) was slowly added to a solution of 500 mg (1 mmol) of **3** in 30 mL of THF at -78 ºC. After 4 min, a solution of 110 mg (1 mmol) of 7-norbornanone in 5 mL of THF was added dropwise. The reaction mixture was stirred for 8 h, diluted with 50 mL of water and extracted with Et_2O (3 x 25 mL). The organic solution was dried over $MgSO_4$ and after evaporation of the solvent, the residue was purified by flash chromatography (silica gel, hexane/Et_2O 9:1) to yield **4** (360 mg, 68%) as a white solid. ^{1}H NMR (300 MHz, $CDCl_3$): δ = 7.48 (m, 1H), 7.38 (d, 4H, *J* = 8.4 Hz), 7.25 (d, 2H, *J* = 1.6 Hz), 7.18 (t, 4H, *J* = 7.8 Hz), 6.98 (t, 2H, *J* = 7.3 Hz), 2.99 (s, 4H), 2.25 (s, 2H), 2.05 (m, 2H), 1.85-1.75 (m, 3H), 1.61-1.51 (m, 4H), 1.45-1.16 (m, 15H) ppm; ^{13}C NMR (75 MHz, $CDCl_3$): δ = 146.3, 146.1, 142.1, 128.6, 127.5, 126.2, 125.6, 123.7, 88.3, 65.3, 42.6, 42.1, 28.8, 28.7, 27.8 ppm; MS (70 eV): *m/z* (%) = 528 (17) [M^+], 446 (62), 445 (100), 417 (36), 357 (57), 171 (68), 129 (59), 91 (79); Elemental analysis (%) calc for $C_{39}H_{44}O$: C 88.58, H 8.39; found: C 88.63, H 8.41.

Compound 1: Compound **1** (365 mg, 90%) was obtained as a white solid following the same procedure described for **3**, using 364 mg (0.69 mmol) of **4** and 103 mg (0.69 mmol) of TfOH. ^{1}H NMR (300 MHz, $CDCl_3$): δ = 7.35 (d, 6H, *J* = 7.2 Hz), 7.17 (s, 3H), 7.16 (t, 6H, *J* = 7.3 Hz), 7.01 (t, 3H, *J* = 7.3 Hz), 3.03 (s, 6H), 2.94 (m, 6H), 1.69-1.58 (m, 6H), 1.42-1.23 (m, 12H), 1.23-1.13 (m, 6H) ppm; ^{13}C NMR (75 MHz, $CDCl_3$): δ = 146.2, 145.1, 128.0, 127.1, 125.0, 123.4, 64.9, 41.7, 28.4, 28.4 ppm; MS (70 eV): *m/z* (%) = 588 (56) [M^+], 418 (35), 417 (82), 349 (73), 348 (95), 258 (78), 257 (100), 179 (93), 165 (82), 129 (56), 91 (95); Elemental analysis (%) calc for $C_{45}H_{48}$: C 91.78, H 8.22; found: C 91.81, H 8.20.

Compound 5: A mixture of 500 mg (1.5 mmol) of 1,3,5-tribromomethylbenzene, 184 mg (0.76 mmol) of $AlCl_3$, 0.2 mL of CH_3NO_2 and 40 mL of benzene[30] was stirred at 25 ºC for 5 h. The reaction mixture was poured into 75 mL of 1% HCl and extracted with Et_2O (3 x 15 mL). The combined organic layer was washed with water (2 x 20 mL) and

[30] S. Mataka, Y. Tsuda, K. Takahashi, M. Tashiro, *Org. Prep. Proced. Int.* **1981**, *13*, 93-96.

dried over $MgSO_4$. After evaporation of the solvent at reduced pressure, the residue was purified by flash chromatography (silica gel, hexane/Et_2O 9:1) to give **5** (110 mg, 70%) as a white solid. ^1H NMR (300 MHz, $CDCl_3$): δ = 7.35-7.10 (m, 15H), 6.91 (s, 3H), 3.93 (s, 6H) ppm; ^{13}C NMR (75 MHz, $CDCl_3$): δ = 141.3, 141.2, 128.9, 128.4, 127.6, 126.0, 41.8 ppm. MS (70 eV): *m/z* (%) = 348 (85) [M^+], 257 (100), 179 (66), 165 (39), 91 (86), 69 (40), 57 (56).

ESI-MS spectrum of 1 + NH_4PF_6 + KPF_6

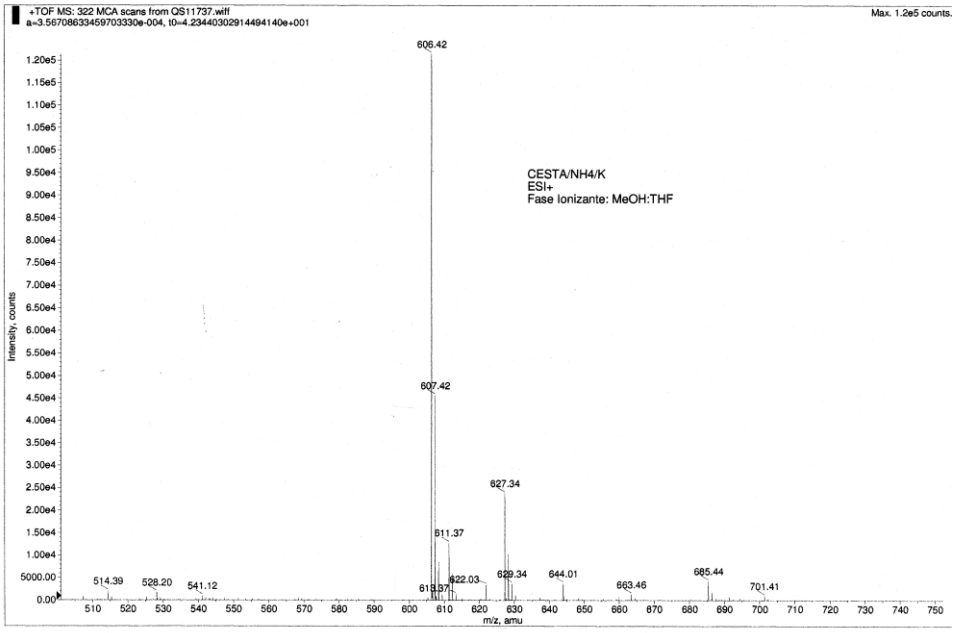

Figure 5. ESI-MS spectrum of **1** + NH_4PF_6 + KPF_6 (10^{-4} M, THF/MeOH 1:1). [**1** + NH_4^+]: *m/z* = 606.42; [**1** + K^+]: *m/z* = 627.34.

Response factors of receptors 1 and 5

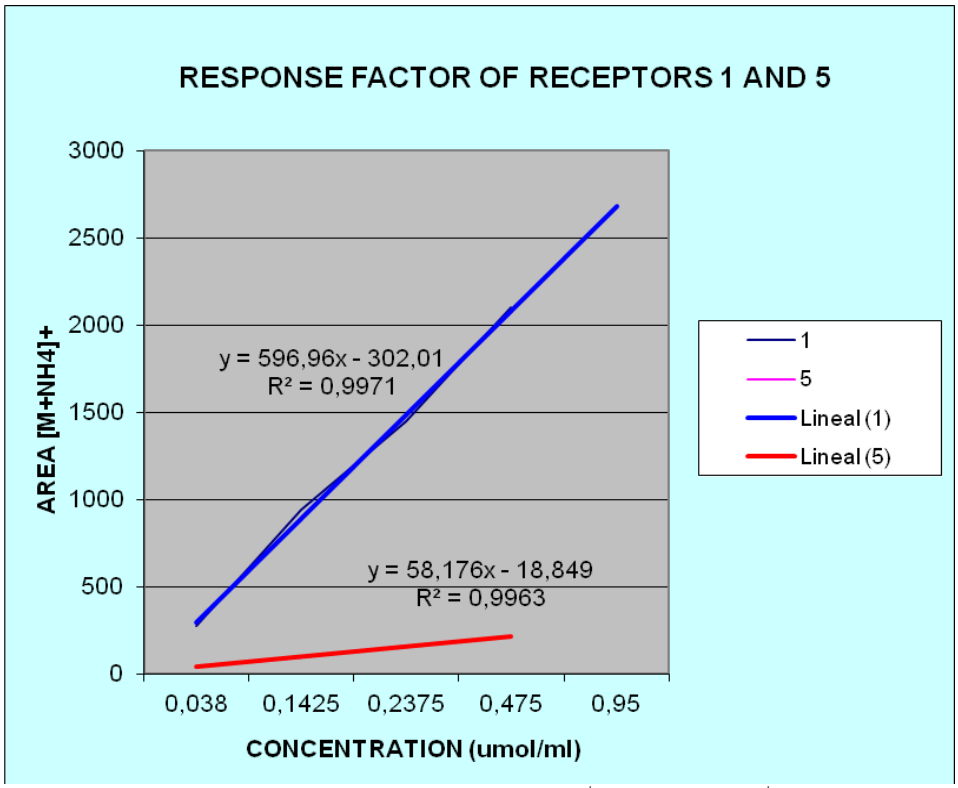

Figure 6. ESI-MS response factors of [**1** + NH_4^+] and [**5** + NH_4^+]. Relative response factor $R = R_{[\mathbf{1} + NH4+]} / R_{[\mathbf{5} + NH4+]} = 10.3$.

Computational Details

Geometry optimizations without symmetry constraints were carried out using the Gaussian09 suite of programs[31] at the M06-2X[32]/def2-SVP[33] level of theory. Stationary points and saddle point **TS** were characterized as minima or transition state by calculating the Hessian matrix analytically at this level. Single point energy calculations were performed using the same functional with the triple-ζ plus polarization TZVP basis set on the geometries optimized at the M06-2X/def2-SVP level. This level is denoted as M06-2X/TZVP//M06-2X/def2-SVP. The basis set superposition error (BSSE) values were calculated for the TZVP basis set for the different ammonium and potassium complexes using the counterpoise procedure.[34]

[31] Gaussian 09, Revision B.1, M. J. Frisch, G. W. Trucks, H. B. Schlegel, G. E. Scuseria, M. A. Robb, J. R. Cheeseman, G. Scalmani, V. Barone, B. Mennucci, G. A. Petersson, H. Nakatsuji, M. Caricato, X. Li, H. P. Hratchian, A. F. Izmaylov, J. Bloino, G. Zheng, J. L. Sonnenberg, M. Hada, M. Ehara, K. Toyota, R. Fukuda, J. Hasegawa, M. Ishida, T. Nakajima, Y. Honda, O. Kitao, H. Nakai, T. Vreven, J. A. Montgomery, Jr., J. E. Peralta, F. Ogliaro, M. Bearpark, J. J. Heyd, E. Brothers, K. N. Kudin, V. N. Staroverov, R. Kobayashi, J. Normand, K. Raghavachari, A. Rendell, J. C. Burant, S. S. Iyengar, J. Tomasi, M. Cossi, N. Rega, J. M. Millam, M. Klene, J. E. Knox, J. B. Cross, V. Bakken, C. Adamo, J. Jaramillo, R. Gomperts, R. E. Stratmann, O. Yazyev, A. J. Austin, R. Cammi, C. Pomelli, J. W. Ochterski, R. L. Martin, K. Morokuma, V. G. Zakrzewski, G. A. Voth, P. Salvador, J. J. Dannenberg, S. Dapprich, A. D. Daniels, Ö. Farkas, J. B. Foresman, J. V. Ortiz, J. Cioslowski, and D. J. Fox, Gaussian, Inc., Wallingford CT, 2009.

[32] Y. Zhao, D. G. Truhlar, *Theor. Chem. Acc.* **2008**, *120*, 215-241.

[33] F. Weigend, R. Ahlrichs, *Phys. Chem. Chem. Phys.* **2005**, *7*, 3297-3305

[34] S. Simon, M. Duran, J. J. Dannenberg, *J. Chem. Phys.* **1996**, *105*, 11024-11031.

IV. DISCUSIÓN GENERAL

En este capítulo se presenta, en español, una discusión integradora de los resultados descritos en apartados anteriores, comparando las conclusiones de los mismos y valorando la consecución de los objetivos propuestos al comienzo del trabajo. Se incluye también una breve mención a resultados relacionados aún sin publicar.

IV.1 Capítulo 1

IV.1.1 Estudio de la deslocalización electrónica por homoconjugación en compuestos aromáticos y sistemas poliméricos.

Para estudiar si es posible la deslocalización electrónica en moléculas aromáticas mediante homoconjugación, así como las similitudes y diferencias que este fenómeno presenta en comparación con los sistemas aromáticos conjugados, se ha sintetizado una gran variedad de derivados del DPN. También se han preparado algunos compuestos que sirven de referencia para este estudio, con estructuras similares, pero en los que la deslocalización electrónica no es posible. El conjunto de estos compuestos puede dividirse en dos grandes grupos: por una parte moléculas pequeñas u oligómeros cortos[299] y por otra parte sistemas poliméricos.[300] En la Figura 1 pueden verse las moléculas y oligómeros homoconjugados utilizados para este estudio (**1**-**10**) así como los compuestos de referencia análogos (**11**-**14**). En la Figura 2 se describen los polímeros homoconjugados sintetizados (**15** y **16**). Las características de estos polímeros se comparan con las de **17**, obtenido previamente en nuestro grupo de investigación,[301] así como también con los compuestos **9** y **10**, cuyas estructuras forman parte de las de los polímeros **15** y **16**.

[299] N. Herrero-García, I. Fernández, J. Osío Barcina, *Chem. Eur. J.* **2011**, *17*, 7327-7335.
[300] J. Osío Barcina, M. R. Colorado Heras, M. Mba, R. Gómez Aspe, N. Herrero García, *J. Org. Chem.* **2009**, *74*, 7148-7156.
[301] A. García Martínez, J. Osío Barcina, A. de Fresno Cerezo, A.-D. Schlüter, J. Frahn, *Adv. Mater.* **1999**, *11*, 27-31.

Como instrumento para el estudio de la deslocalización electrónica se ha empleado principalmente la espectroscopia UV-vis y, en algunos casos los correspondientes potenciales de oxidación. El estudio experimental se completa con cálculos computacionales DFT.

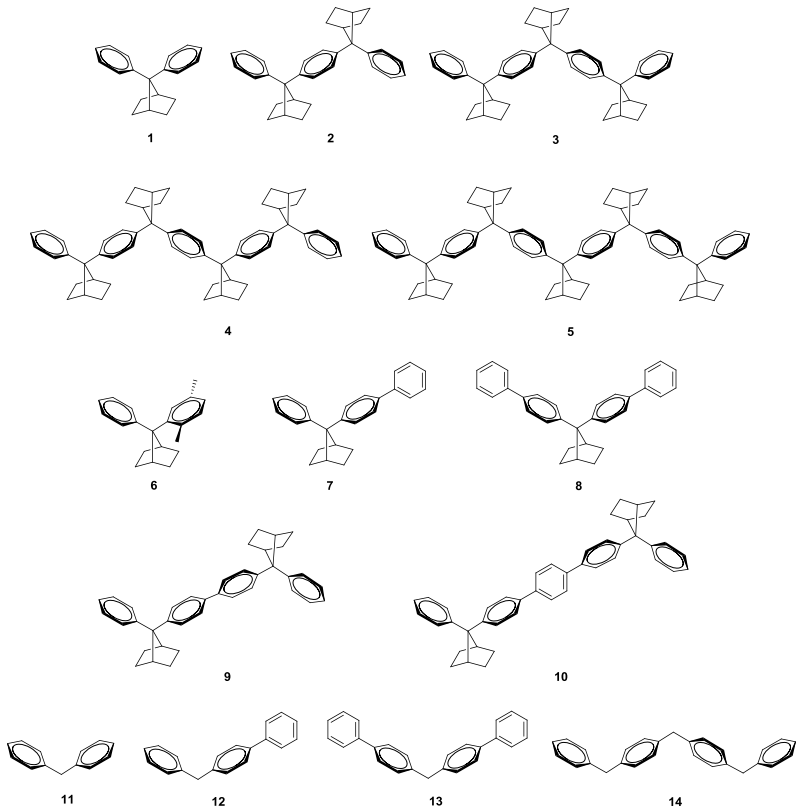

Figura 1. Estructura de los compuestos homoconjugados estudiados y de las moléculas empleadas como referencia.

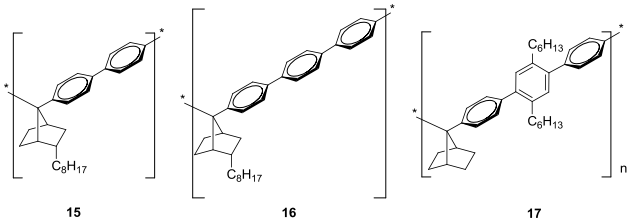

Figura 2. Estructura de los polímeros homoconjugados estudiados.

Los datos de la espectroscopia UV-vis de los compuestos estudiados y de los cálculos TD-DFT llevados a cabo se recogen en la Tabla1.

Tabla 1. Datos de UV-vis (λ_{max}) de los compuestos **1**-**13**.

	λ_{exp}/ nm[a]	λ_{calc}/ nm[b]	Transición[c]	δ_r (BLA) [d]		λ_{exp}/ nm[a]	λ_{calc}/ nm[b]	Transición [c]
1	228	237 (0.18)	HOMO→ LUMO (5.75)	0.0039	**8**	268	292 (0.70)	HOMO→ LUMO (4.70)
2	242[e]	255 (0.42)	HOMO→ LUMO (5.38)	0.0077	**9**	272	288 (0.98)	HOMO→ LUMO (4.74)
	222	220 (0.02)	HOMO-5→ LUMO	0.0068	**10**	295	316 (1.51)	HOMO→ LUMO (4.34)
3	248[e]	265 (0.63)	HOMO→ LUMO (5.21)	0.0076	**12**	251	265 (0.65)	HOMO→ LUMO (5.06)
	232	232 (0.01)	(banda de combinación)	0.0077	**13**	257	276 (0.67)	HOMO→ LUMO (4.94)
4	250[e]	272 (0.84)	HOMO→ LUMO (5.12)		**14**	--	246 (0.13)	(banda de combinación)
	231	240	HOMO-1 →LUMO+1					
5	--	273 (1.07)	HOMO→ LUMO (5.06)					
6	218	234 (0.08)	HOMO-1 →LUMO(46%)[f] HOMO →LUMO (29%)					
7	259	274 (0.67)	HOMO→LUMO (4.94)					

[a] Datos experimentales a temperatura ambiente (MeOH). [b] Valores calculados (TD-B3LYP/def2-SVP) en fase gaseosa de las energías de excitación verticales; los valores de la fuerza de los osciladores se indican entre paréntesis. [c] Las diferencias de energía HOMO-LUMO (en eV) se indican entre paréntesis. [d] Valores calculados de la alternancia en las longitudes de enlace (BLA). [e] En hexano. [f] Contribución relativa de la transición.

El análisis de los datos aportados por la espectroscopia UV-vis permite llegar a una serie de conclusiones acerca de la deslocalización electrónica en los compuestos homoconjugados estudiados:

1. La deslocalización electrónica en el DPN (**1**) se traduce en una nueva banda (banda de homoconjugación) en el espectro UV-vis centrada a 228 nm. Esta banda no se observa en el difenilmetano (**11**). En la Figura 3 pueden verse los orbitales HOMO-3 y LUMO del DPN que muestran claramente la deslocalización electrónica existente entre los anillos aromáticos. Los cálculos TD-B3LYP/def2-SVP llevados a cabo reproducen muy bien los datos experimentales asignando la banda de homoconjugación del DPN a la transición entre los orbitales HOMO y LUMO (Figura 3).

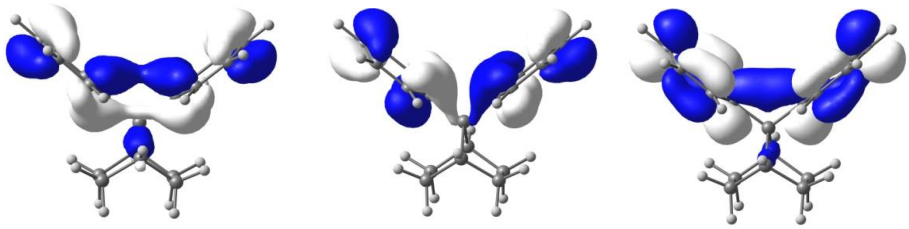

HOMO-3 **HOMO** **LUMO**

Figura 3. Orbitales HOMO, HOMO-3 y LUMO del DPN.

2. Se ha comprobado que la posición de la banda de homoconjugación en derivados del DPN es muy sensible a pequeñas variaciones del ángulo torsional C_{ipso}-C_7-$C_{ipso'}$-$C_{orto'}$. Así, se observa un desplazamiento hipsocrómico e hipocrómico (λ_{max} = 218 nm, ε = 10900) de la correspondiente banda de homoconjugación en el derivado **6**. El impedimento estérico de los grupos metilo en este compuesto produce una desviación de la cofacialidad en los anillos aromáticos (el ángulo torsional en el caso de **6** es 77.4º), con la consiguiente disminución de la homoconjugación, situación que se ve reflejada en la banda de absorción. Esto explica que en el caso del difenilmetano (ángulo torsional en estado sólido 63.5º) las interacciones homoconjugativas entre los fenilos sean muy pequeñas y no se reflejen en su espectro UV-vis. En la Figura 4 puede verse la variación del valor de λ_{max} (calculada) con el ángulo torsional. Como puede observarse, desviaciones pequeñas de la cofacialidad tienen un efecto muy notable sobre la posición de la banda de homoconjugación.

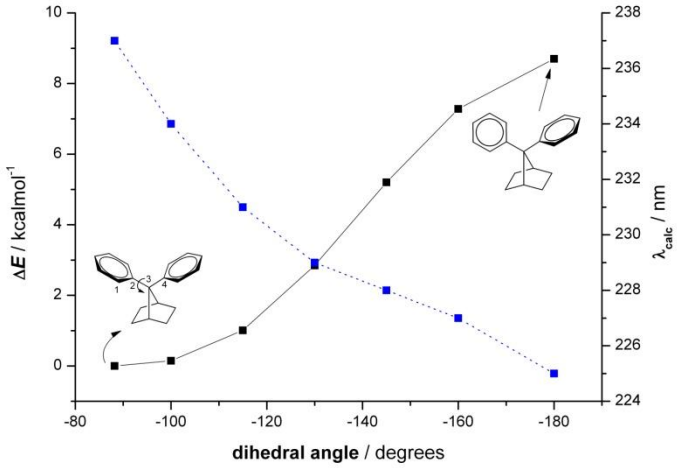

Figura 4. Variación del valor de λ_{max} (calculada, azul) del DPN con el ángulo torsional C_{ipso}-C_7-$C_{ipso'}$-$C_{orto'}$.

3. La extensión de la deslocalización electrónica por homoconjugación al pasar del DPN a los correspondientes oligómeros, dímero (**2**) (λ_{max} = 242 nm), trímero (**3**) (λ_{max} = 248 nm) y tetrámero (**4**) (λ_{max} = 250 nm) produce un desplazamiento batocrómico e hipercrómico de la banda de homoconjugación, comportamiento idéntico al observado en derivados conjugados. Se observa además la aparición de nuevas bandas en el espectro UV-vis a menor longitud de onda en el caso de de los oligómeros (Tabla 1, Figura 5). Por otra parte, el espectro UV-vis del trímero del difenilmetano (**14**) es prácticamente idéntico al del difenilmetano, sin que se observe ningún indicio de banda de homoconjugación.

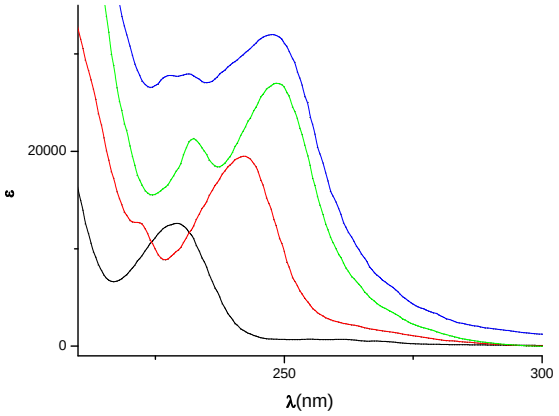

Figura 5. Espectros UV-vis del DPN (negro) y de los correspondientes dímero (rojo), trímero (verde) y tetrámero (azul).

Los resultados obtenidos permiten estimar por primera vez la longitud de homoconjugación efectiva para el caso de derivados aromáticos homoconjugados, que resulta estar en torno a 5-6 subunidades de DPN. Los datos experimentales coinciden muy bien con los calculados para los mismos sistemas (Figura 6). Este resultado es muy parecido al descrito para oligofenilenos conjugados unidos por la posición *orto*.[302]

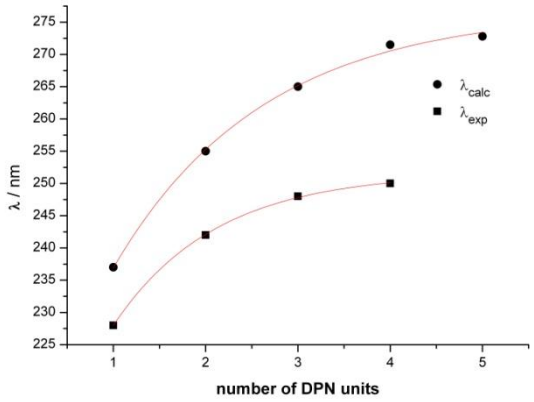

Figura 6. Valores de λ_{max} (experimentales y calculados) en oligómeros del DPN.

[302] J. He, L. C. Jason, S. H. Wadumethrige, K. Thakur, L. Dai, S. Zou, R. Rathore, S. Hartley, *J. Am. Chem. Soc.* **2010**, *132*, 13848-13857.

Los cálculos TD-DFT también reproducen muy bien los datos experimentales de la espectroscopia UV-vis (Tabla 1), asignando las bandas de homoconjugación a transiciones HOMO-LUMO. En la Figura 7 pueden verse los orbitales frontera del trímero del DPN, **3**. Se observa claramente la deslocalización electrónica entre los fenilos homoconjugados en el orbital LUMO, de manera similar a lo descrito para el DPN (Figura 3). Además, los cálculos TD-DFT explican la aparición de las bandas adicionales a menor longitud de onda observadas en el caso de los oligómeros (Tabla 1).

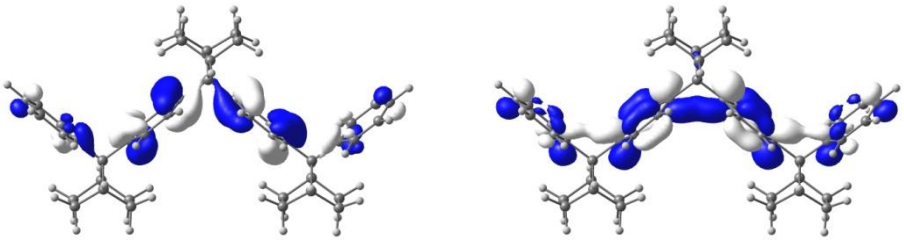

HOMO **LUMO**

Figura 7. Orbitales HOMO y LUMO del trímero del DPN.

4. Los espectros UV-vis de derivados homoconjugados con sustituyentes bifenilo (**7** y **8**) también ponen de manifiesto el efecto de la deslocalización electrónica por homoconjugación. La banda de homoconjugación en estos compuestos aparece solapada con la del bifenilo en el caso de **7** y como un hombro en torno a 239 nm (determinado mediante la primera derivada) en el caso de **8**, es decir, desplazada batocrómicamente con respecto al DPN. La comparación de los valores de λ_{max} de **7** (259 nm) y **8** (268 nm) con los del bifenilo (247 nm) (Figura 8) muestran una vez más el efecto de la homoconjugación aromática.

Los cálculos TD-DFT asignan estas bandas a transiciones HOMO-LUMO (Tabla 1). En la figura 9 pueden verse los orbitales frontera de **7** y **8**. En ambos casos es patente la deslocalización electrónica en los correspondientes orbitales LUMO. Es importante señalar que los espectros UV-vis de los compuestos análogos derivados del difenilmetano (**12** y **13**), preparados como referencia, son diferentes a los de los derivados homoconjugados **7** y **8** y a su vez, parecidos a los del bifenilo, con valores de λ_{max} de 251 nm (**12**) y 257 nm (**13**).

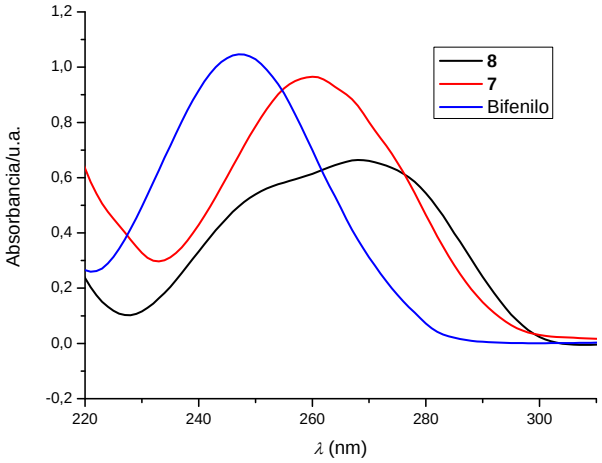

Figura 8. Espectros UV-vis de los derivados del DPN **7**, **8** y del bifenilo (referencia).

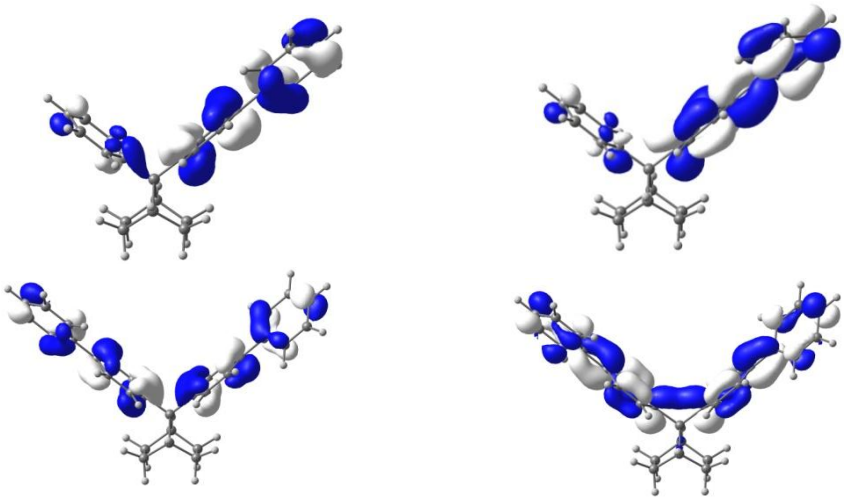

HOMO **LUMO**

Figura 9. Orbitales frontera de los compuestos **7** y **8**.

5. En la Introducción de esta Memoria se comentó la gran importancia que tienen actualmente los polímeros conjugados. Una vez demostrado que la deslocalización electrónica puede tener lugar de forma eficaz en moléculas y oligómeros homoconjugados, nos ha parecido interesante extender este estudio

a sistemas poliméricos. Para ello se han preparado los polímeros **15** y **16**, comparándose sus propiedades con las del polímero **17**, preparado previamente en nuestro grupo de investigación.

La característica más destacable de estos polímeros es que alternan homoconjugación y conjugación en sus estructuras. La subunidad conjugada en el caso de **15** (bifenilo) es más corta que la que se encuentra en el caso de **16** (terfenilo), por lo que la importancia de la deslocalización por homoconjugación es mayor en el caso de **15**.

Por otra parte, la diferencia entre **16** y **17** estriba en que en el caso del polímero **17**, la introducción de cadenas alquílicas en la subunidad de terfenilo, necesarias para aumentar la solubilidad, disminuyen la coplanaridad de los anillos y, por tanto, la deslocalización electrónica. Nosotros hemos pensado eludir esta limitación introduciendo las cadenas alquílicas en la estructura del norbornano en **15** y **16**.

Se han sintetizado también los compuestos **9** y **10**, presentes como subunidades monoméricas en las estructuras de los polímeros estudiados. La información obtenida a partir de estas moléculas y de los hidrocarburos bifenilo, *p*-terfenilo y *p*-cuaterfenilo servirán para completar el estudio de los polímeros. Los resultados obtenidos se resumen en las Tablas 2 y 3 (ver también la Tabla 1).

Del análisis de los resultados de la Tabla 2 se deduce que la homoconjugación aromática contribuye de manera eficaz a la deslocalización electrónica en estos compuestos.

Así se desprende de los datos de UV-vis, donde se observa un desplazamiento batocrómico de la bandas de absorción del bifenilo (247 nm) y del terfenilo (274 nm) en comparación con **9** (272 nm) y **10** (295 nm).

Estos resultados parecen indicar que el grado de deslocalización electrónica provocado por dos fenilos homoconjugados es similar al de un anillo conjugado, dado que el espectro UV-vis de **9** se asemeja más al del *p*-terfenilo, mientras que el de **10** es similar al del *p*-cuaterfenilo (292 nm) (Figura 10). Esta semejanza se observa también en los correspondientes espectros de emisión, en los que puede observarse que tanto **9** como **10** presentan desplazamientos de Stokes considerables (53 y 66 nm, respectivamente), con valores muy similares a los del *p*-terfenilo y *p*-cuaterfenilo (64 y 72 nm) (Figura 10).

Por último, los valores de las diferencias de energía entre los orbitales HOMO-LUMO así como los correspondientes potenciales de oxidación también ponen de manifiesto el efecto de la deslocalización electrónica en estos derivados homoconjugados y su paralelismo con los patrones conjugados *p*-terfenilo y *p*-cuaterfenilo.

Los cálculos DFT realizados con **9** y **10** están de acuerdo con los datos experimentales. En la Figura 11 se muestran los orbitales frontera de ambos compuestos. Al igual que en sistemas mencionados anteriormente, la deslocalización electrónica entre los fenilos homoconjugados puede apreciarse claramente en los correspondientes orbitales LUMO. Las bandas observadas en los espectros UV-vis se corresponden con transiciones HOMO-LUMO entre estos orbitales, según los cálculos TD-DFT llevados a cabo.

Tabla 2. Propiedades de los compuestos **9** y **10**, y de las referencias bifenilo, *p*-terfenilo y *p*-cuaterfenilo.

	λ_{abs} [a,b]	λ_{em} [a,b]	**Desplaza-miento de Stokes**[b]	λ_{onset} [b]	E_g^{opt} **(eV)**	$E_{oxd}^{1/2}$**(V)**	E^{HOMO} **(eV)**	E^{LUMO} **(eV)**
9	272	325	53	310	4.00	-	-	-
10	295	361	66	335	3.70	1.11[c]	-5.37	-1.67
						1.18, 1.43[d]		
Bifenilo	247	315	68	278	4.46	-	-	-
p-Terfenilo	274	338	64	312	3.97	1.44[d] (1.5[e])	-5.56	-1.59
p-Cuaterfenilo	292	364	72	334	3.71	1.09[c]	-5.41	-1.70

[a] En CH_2Cl_2. [b] En nm. [c] En CH_2Cl_2 con $n$$Bu_4NClO_4$ 0.1 M como electrolito; los potenciales se midieron empleando un electrodo Ag/AgCl como referencia; los valores de los potenciales *vs.* Fc/Fc^+. [d] En CH_3CN con $n$$Bu_4NClO_4$ 0.1 M como electrolito; los potenciales se midieron empleando un electrodo Ag/AgCl como referencia; los valores de los potenciales *vs.* Fc/Fc^+. [e] Lit.

Tabla 3. Propiedades de los polímeros **15**, **16** y **17**.

	Rto. (%)	M_w [a]	M_n [a]	PDI [a]	λ_{abs} [b]	λ_{em} [b]	Desplazamiento de Stokes [b]	λ_{onset} [b]	E_g^{opt} (eV)
15	97	6440	4650	1.4	283	337	54	319	3.89
16	94	3470	2600	1.3	298	366	68	342	3.62
17	94	21600	8820	2.4	268	348	80	308	4.02

[a] Determinado por GPC en THF. [b] En nm.

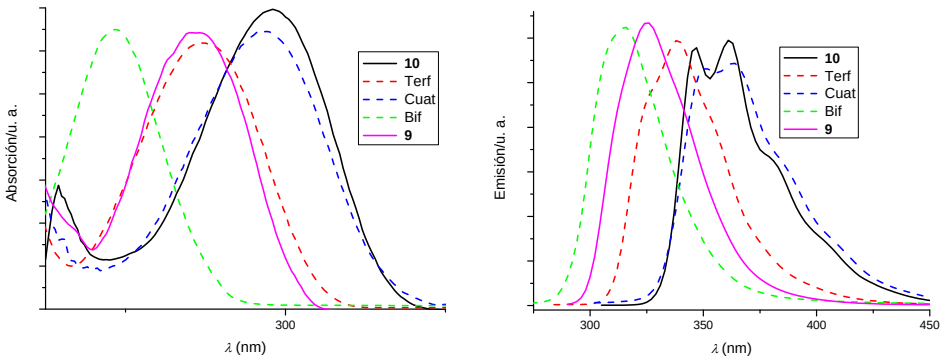

Figura 10. Espectros de absorción y emisión de los compuestos **9** y **10** y de las referencias bifenilo, *p*-terfenilo y *p*-cuaterfenilo.

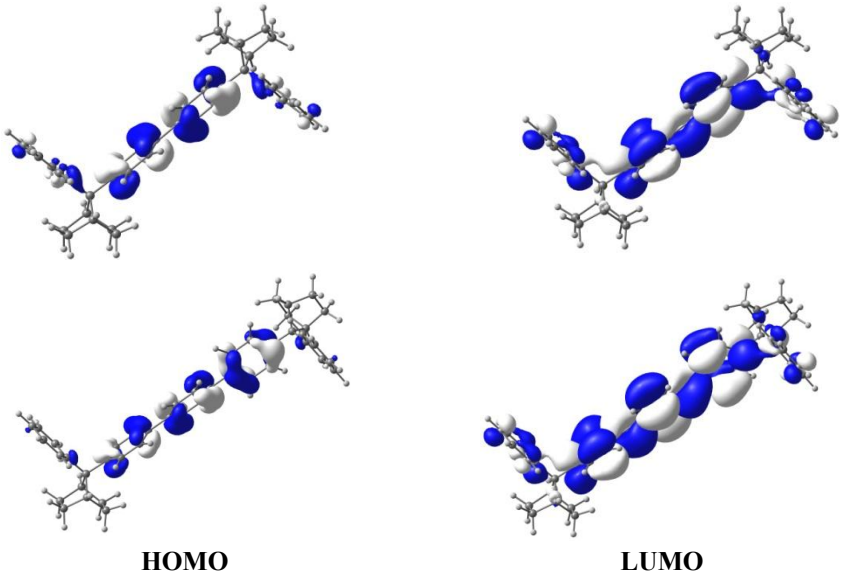

HOMO **LUMO**

Figura 11. Orbitales frontera de **9** y **10**.

Una vez estudiados los compuestos de referencia **9** y **10**, se procedió a investigar las propiedades de los correspondientes polímeros **15**, **16** y **17**, obtenidos mediante reacciones de policondensaciónde Suzuki[303] (Tabla 3). De la comparación de los datos experimentales obtenidos a partir de los espectros UV-vis y de emisión (Figura 12) puede concluirse que al pasar de los monómeros a los correspondientes polímeros se produce un incremento de la deslocalización electrónica, más apreciable en el caso del polímero con subunidades de bifenilo (**15**).

Por otra parte, y como cabía esperar, un aumento de la conjugación en la subunidad de terfenilo al pasar del polímero **17** a **16** se traduce en un desplazamiento batocrómico de la correspondiente banda de absorción en el espectro UV-vis (298 nm *vs.* 268 nm). Sin embargo, el polímero **17** muestra el mayor valor del desplazamiento de Stokes de los tres estudiados.

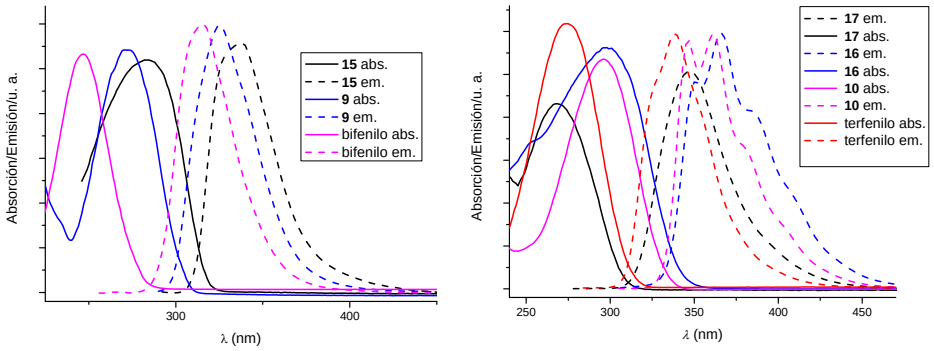

Figura 12. Espectros UV-vis y de emisión de los polímeros **15**, **16** y **17** y de las moléculas referencia **9** y **10**.

En resumen, el conjunto de resultados, tanto experimentales como computacionales, descritos en esta parte de la presente Memoria permiten concluir que la homoconjugación aromática constituye un mecanismo muy eficaz de deslocalización electrónica, tanto en moléculas como en oligómeros y polímeros homoconjugados. Esta es la primera vez que se describe y explica con detalle este fenómeno, que puede ser la base para el diseño de una gran variedad de sistemas con deslocalización electrónica no convencional. La importancia de estos resultados es más destacable si se tiene en cuenta que en

[303] J. Sakamoto, M. Rehahn, G. Wegner, A. D. Schlüter, *Macromol. Rapid Commun.* **2009**, *30*, 653-687; b) *Conjugated Polymer Synthesis*, Ed.: Y. Chujo, Wiley-VCH, Weinheim, **2010**.

sistemas homoconjugados neutros formados por dobles y/o triples enlaces no se produce deslocalización electrónica.

Por otra lado, nuestros estudios señalan que la deslocalización electrónica por homoconjugación aromática es muy sensible a variaciones estructurales pequeñas, por ejemplo en los ángulos torsionales que afectan a la cofacialidad de las moléculas. Esto explica la falta de deslocalización en el difenilmetano y en derivados del tripticeno.

IV.1.2 Estudio de la deslocalización electrónica por homoconjugación en compuestos con sustituyentes. Sistemas push-pull.

Una vez investigada la deslocalización electrónica en hidrocarburos, parece lógico extender este estudio a sistemas sustituidos. Esto permitiría analizar la influencia de la sustitución en la homoconjugación aromática y cómo puede modularse la deslocalización electrónica mediante el empleo de diferentes sustituyentes. De especial interés dentro de este grupo de derivados son los sistemas con sustituyentes dadores y aceptores de electrones en la misma molécula (sistemas push-pull) debido a sus importantes aplicaciones (Ver introducción del capítulo I).

Con objeto de llevar a cabo este estudio hemos sintetizado una familia muy amplia de derivados del DPN con diferentes sustituyentes (Figura 13) y hemos estudiado su reactividad y sus espectros UV-vis y de RMN. El estudio se completa con cálculos computacionales DFT.

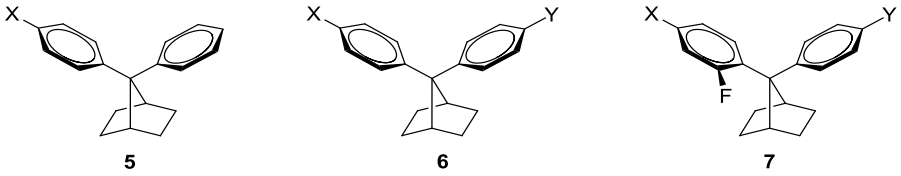

5

5a: X = NH_2
5b: X = OCH_3
5c: X = H
5d: X = Cl
5e: X = Br
5f: X = CO_2H
5g: X = CO_2Et
5h: X = $COCH_3$
5i: X = CF_3
5j: X = NO_2

6

6a: X = Y = NMe_2
6b: X = Y = NH_2
6c: X = Y = OCH_3
6d: X = Y = I
6e: X = Y = CO_2H
6f: X = Y = CO_2Et
6g: X = Y = $COCH_3$
6h: X = Y = NO_2
6i: X = NH_2; Y = NO_2
6j: X = OCH_3; Y = NO_2
6k: X = OCH_3; Y = CF_3

7

7a: X = H; Y = NH_2
7b: X = H; Y = OCH_3
7c: X = H; Y = H
7d: X = H; Y = Cl
7e: X = H; Y = Br
7f: X = H; Y = $COCH_3$
7g: X = H; Y = NO_2
7h: X = NH_2; Y = H
7i: X = OCH_3; Y = H
7j: X = CH_3; Y = H
7k: X = Br; Y = H
7l: X = NO_2; Y = H
7m: X = Y = NH_2
7n: X = Y = OCH_3
7o: X = Y = NO_2
7p: X = CH_3; Y = NO_2
7q: X = OCH_3; Y = NO_2
7r: X = CN; Y = OCH_3
7s: X = Br; Y = OCH_3
7t: X = CH_3; Y = OCH_3
7u: X = OCH_3; Y = NH_2
7v: X = NH_2; Y = NO_2

Figura 13. Estructura de los derivados sustituidos sintetizados.

También se han sintetizado una serie de derivados análogos, no homoconjugados, que servirán como referencias en este estudio (Figura 14). En el caso de los compuestos derivados del difenilpropano (**9a-e**), la comunicación entre los anillos aromáticos por homoconjugación no existe o es muy débil debido a la inestabilidad de la conformación cofacial, mientras que en los derivados del sistema biciclo[2.2.2]octano la conformación cofacial está imposibilitada por razones estructurales. Estos derivados representan una situación opuesta a la del DPN.

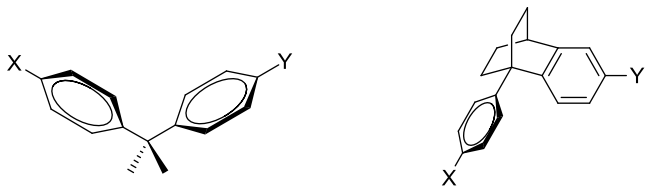

9a: X = H; Y = NH_2
9b: X = H; Y = NO_2
9c: X = NH_2; Y = NH_2
9d: X = NO_2; Y = NO_2
9e: X = NH_2; Y = NO_2

10a: X = H; Y = H
10b: X = NH_2; Y = NH_2
10c: X = NO_2; Y = NO_2

Figura 14. Moléculas no homoconjugadas sintetizadas como referencias.

Del conjunto de datos experimentales obtenidos con estos derivados cabe obtener las siguientes conclusiones:

1. Los espectros UV-vis de los compuestos estudiados muestran tres bandas de absorción importantes: a) la banda del cromóforo unido al anillo aromático, b) la banda de homoconjugación y c) bandas de transferencia de carga en el caso de sistemas push-pull.

La extensión de la deslocalización por homoconjugación se pone claramente de manifiesto al comparar los espectros UV-vis de los derivados del DPN y del *o*-fluoro-DPN (FDPN) monosustituidos con los derivados del benceno con los mismos sustituyentes, observándose desplazamientos batocrómicos de las bandas de absorción de los cromóforos del orden de 20-35 nm. Por otra parte, la posición de estas bandas en derivados disustituidos depende del sustituyente situado en el otro anillo aromático, existiendo una relación lineal entre los valores de λ_{max} y los de σ_p de los sustituyentes, observándose desplazamientos batocrómicos con sustituyentes dadores de electrones, que aumentan la homoconjugación, y el efecto contrario con grupos desactivantes. En la Figura 15 puede verse este efecto para el caso de NO_2-FDPNs con grupos -NO_2, -Me, -H y -OMe en el anillo homoconjugado. La misma relación se observa en el caso de los DPNs análogos.

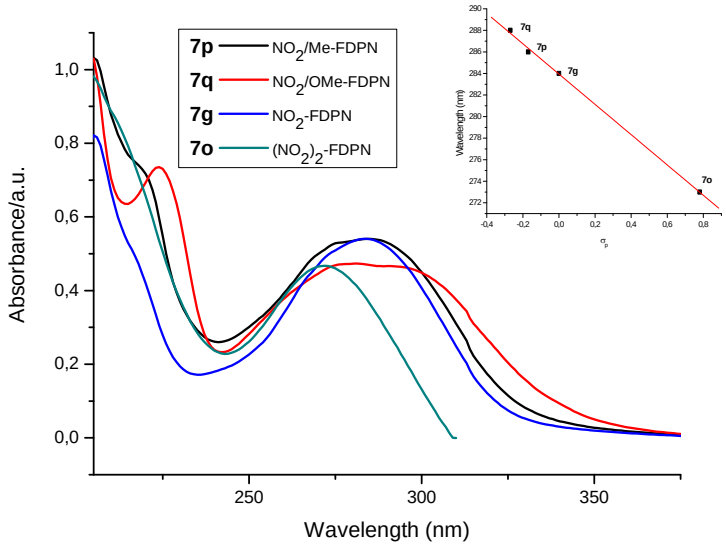

Figura 15. Espectros de absorción de NO_2-FDPNs y correlación de los valores de λ_{max} *vs.* σ_p de los sustituyentes.

Los cálculos TD-DFT aportan información muy relevante que permite interpretar los datos experimentales y confirmar las interacciones homoconjugativas presentes en estos derivados. Así, en el caso de los compuestos descritos en la Figura 15, los cálculos confirman la presencia de dos bandas importantes. Por una parte, la banda que aparece a mayor longitud de onda se asigna en todos los casos a transiciones electrónicas entre los orbitales HOMO y LUMO. En la Figura 16 pueden verse los orbitales para el caso del derivado del NO_2-FDPN con un sustituyente -Me en el fenilo homoconjugado. Como puede observarse, el orbital HOMO está centrado principalmente en el anillo con -F y -Me, mientras que el orbital LUMO lo está en el fenilo sustituido con el grupo -NO_2. Por otra parte, la banda de homoconjugación, muy visible a 223 nm en el caso del derivado FDPN-OMe y que aparece como un hombro en el caso del FDPN-Me se atribuye, de acuerdo con nuestros cálculos TD-DFT, a una transición electrónica desde los orbitales HOMO-3 y LUMO. En la Figura 16 puede verse el orbital HOMO-3 de FDPN-Me involucrado en esta transición. Se trata de un orbital con deslocalización entre los dos anillos aromáticos, lo que confirma la naturaleza

homoconjugativa de esta banda de absorción. Por último, la comparación de los espectros UV-Vis de los compuestos NO_2-DPN y NO_2-DPN-NO_2 con los derivados análogos del difenilpropano **9b** y **9d** muestran asimismo el efecto de la homoconjugación, observándose desplazamientos batocrómicos de las correspondientes bandas de 19 nm.

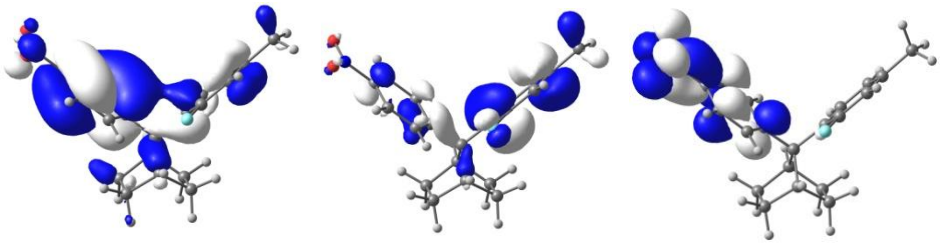

HOMO-3 **HOMO** **LUMO**

Figura 16. Orbitales HOMO-3, HOMO y LUMO del compuesto FDPN-Me.

2. La banda más característica en los espectros UV-vis de los derivados del DPN estudiados es la de homoconjugación. La posición de esta banda presenta una fuerte dependencia de la naturaleza de los sustituyentes unidos a los anillos aromáticos. Así, sustituyentes desactivantes provocan una menor interacción homoconjugativa entre los fenilos al disminuir la densidad electrónica en los anillos aromáticos. Como consecuencia, la banda de homoconjugación en estos derivados experimenta un desplazamiento hipsocrómico, que puede hacer que la banda de homoconjugación no sea fácil de distinguir al aproximarse su longitud de onda a la zona del ultravioleta lejano (~ 200 nm).

Por el contrario, el incremento de la densidad electrónica provocado por sustituyentes dadores de electrones favorece las interacciones homoconjugativas y provoca desplazamientos batocrómicos de la banda de homoconjugación. El caso más notable de los estudiados es el del derivados del DPN con dos grupos –NMe_2 en el que la banda de homoconjugación aparece a 272 nm. En la Figura 17 pueden verse los espectros UV-vis de este compuesto, del $(NH_2)_2$-DPN y de los compuestos de referencia derivados del difenilpropano y del biciclo[2.2.2]octano, **9c** y **10b**.

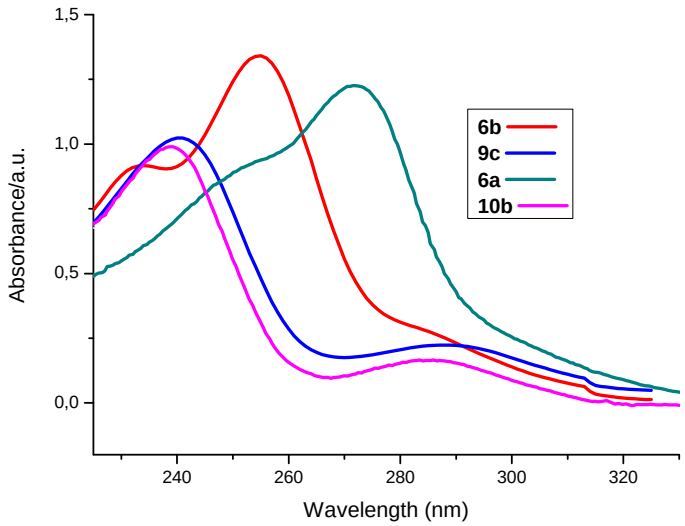

Figura 17. Espectros UV-vis de los compuestos $(Me_2N)_2$-DPN (**6a**) , $(NH_2)_2$-DPN (**6b**) y de las referencias **9c** y **10b**.

El efecto de la homoconjugación resulta evidente ya que en el caso de **9c** y **10b**, sus espectros son muy similares, con bandas a 241 nm y 239 nm respectivamente, y a su vez, parecidos al espectro de la anilina (230 nm), es decir, sin bandas de homoconjugación. Por el contrario, el espectro de $(NH_2)_2$-DPN presenta dos bandas, una a ~ 233 nm, similar a la banda de la anilina y a las descritas para **9c** y **10b**, y una segunda banda a 255 nm (banda de homoconjugación).

Los cálculos TD-DFT realizados en el caso de $(NH_2)_2$-DPN indican que la banda de homoconjugación corresponde a una transición entre los orbitales HOMO y LUMO + 1 (Figura 18). Como puede verse, el orbital LUMO + 1 está deslocalizado entre los dos anillos aromáticos. Este orbital deslocalizado está ausente en el caso de **10b**.

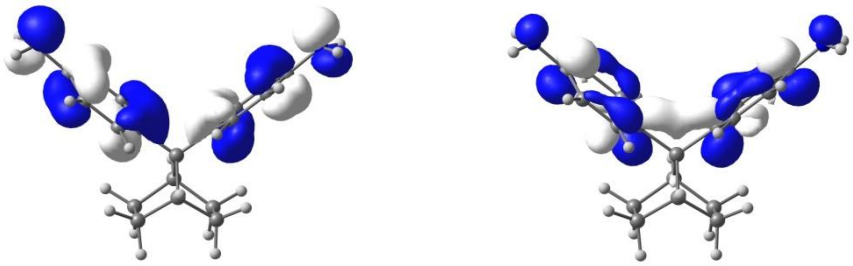

HOMO **LUMO + 1**

Figura 18. Orbitales HOMO y LUMO + 1 del compuesto $(NH_2)_2$-DPN (**6b**).

Otro aspecto importante de los espectros de los derivados homoconjugados es la variación de la posición de la banda de homoconjugación con los sustituyentes. En la Figura 19 puede observarse cómo varía la longitud de onda de la banda de homoconjugación en una serie de derivados del MeO-DPN. La correlación entre la posición de la banda y el valor de σ_p de los sustituyentes es muy buena (r^2 = -0.996).

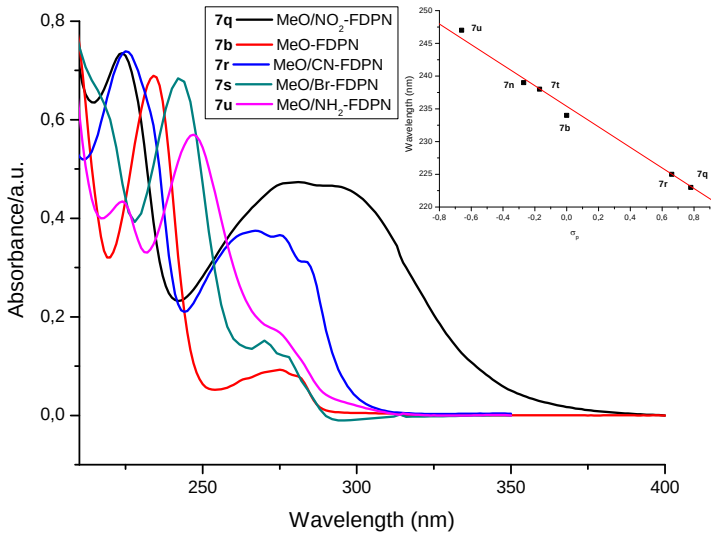

Figura 19. Espectros UV-vis de MeO-DPNs y correlación entre los valores de λ_{max} *vs.* σ_p de los sustituyentes.

3. El último aspecto destacable de los espectros UV-vis de los compuestos homoconjugados estudiados es la aparición de bandas de transferencia de carga en sistemas con un sustituyente activante en uno de los fenilos y otro desactivante en el otro anillo aromático (sistemas push-pull). Los ejemplos más significativos de estas bandas de transferencia de carga pueden verse en la Figura 20.

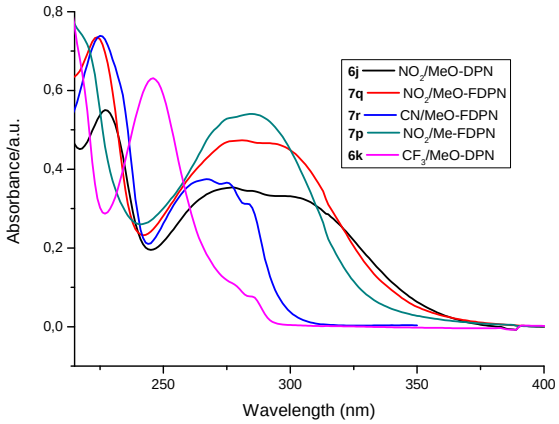

Figura 20. Espectros UV-vis de sitemas push-pull homoconjugados.

También en esta ocasión la homoconjugación desempeña un papel muy importante en la aparición de la transferencia de carga. En la Figura 21 pueden verse los espectros de los compuestos NO_2-DPN-NH_2 (**6i**), NO_2-FDPN-NH_2 (**7v**) y del análogo derivados del difenilpropano (**9e**). Mientras que la banda de transferencia de carga es claramente visible en el caso de NO_2-DPN-NH_2, entre 300-450 nm, tan solo aparece como una absorción residual, menos intensa y solapada con la banda del cromóforo Ph–NO_2, en el caso de **9e**. Este resultado puede explicarse considerando que la homoconjugación entre los anillos aromáticos hace disminuir la diferencia de energía entre los orbitales implicados en el proceso de transferencia de carga. Por otra parte, este fenómeno estaría favorecido por la cofacialidad de los anillos aromáticos en los DPNs así como por la estabilidad de la especie resultante debido a una mayor deslocalización electrónica en el caso de derivados homoconjugados sustituidos en la posición *para* (Figura 22).

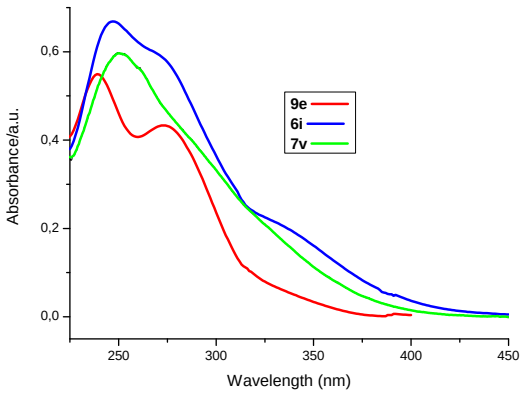

Figura 21. Espectros UV-vis de NO_2-DPN-NH_2 (**6i**), NO_2-FDPN-NH_2 (**7v**) y del análogo derivados del difenilpropano (**9e**)

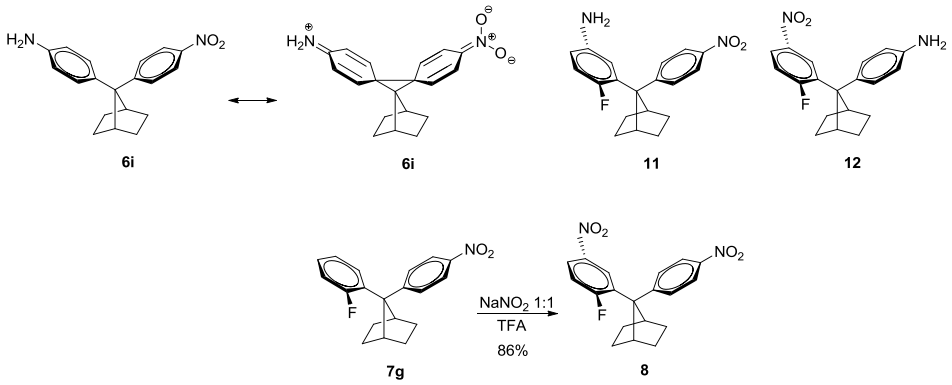

Figura 22. Estructura y síntesis de sistemas push-pull sustituidos en la posición *meta*.

Estas suposiciones se ven confirmadas por el hecho de que los espectros de los derivados análogos al NO_2-DPN-NH_2 con uno de los grupos en posición *meta* (**11** y **12**) (Figura 22) no se observan bandas de transferencia de carga. La síntesis de estos compuestos se llevó a cabo a partir del dinitroderivado **8**. A su vez, este se obtuvo por nitración de **7g**, que conduce al isómero *meta* por la suma de los efectos desactivantes del flúor y del anillo aromático homoconjugado con un grupo NO_2. Este resultado pone de manifiesto el efecto de la homoconjugación también en la reactividad de los derivados del DPN.

El efecto de la homoconjugación no solo es patente en las propiedades ópticas y la reactividad de los compuestos estudiados. También se pone de

manifiesto al estudiar los espectros de RMN. El efecto que ejercen los sustituyentes de un anillo aromático sobre los desplazamientos químicos (^{1}H y ^{13}C) de las señales del anillo homoconjugado se transmiten principalmente a las posiciones *ipso* y *para*, y no al C7 del norbornano, como cabría esperar si estos efectos se transmitieran a través de los enlaces.

Por último hay que destacar que los sistemas push-pull descritos en este apartado han demostrado poseer propiedades ONL muy interesantes y similares a la de compuestos conjugados con los mismos sustituyentes.[304] Nuestros cálculos DFT (B3LYP/def2-SVP//M06-2x/def2-SVP) permiten reproducir los resultados experimentales descritos previamente por nosotros, lo cual permitirá predecir las propiedades ONL de otros derivados homoconjugados.

Del conjunto de resultados descritos en esta parte de la Memoria puede concluirse que la deslocalización electrónica por homoconjugación en sistemas con sustituyentes se pone de manifiesto en su reactividad, sus propiedades ópticas y ONL y en sus espectros de RMN. Los cálculos DFT realizados ayudan a explicar los datos experimentales obtenidos de los espectros UV-vis así como la deslocalización electrónica entre los anillos aromáticos. Por otra parte, la homoconjugación en estos compuestos depende en gran medida del tipo y la posición de los sustituyentes presentes en los anillos, lo cual permite controlar el grado de comunicación entre ellos.

IV.2 Capíulo 2

IV.2.1 Aplicaciones de sistemas homoconjugados en el diseño de cables moleculares y OLEDs

Una vez investigados los aspectos básicos de la homoconjugación aromática en moléculas con y sin sustituyentes, así como en oligómeros y polímeros homoconjugados, nos ha parecido interesante iniciar el estudio de las aplicaciones de estos sistemas. La eficacia de la deslocalización electrónica en

[304] A. García Martínez, J. Osío Barcina, A. de Fresno Cerezo, G. Rojo, F. Agulló-López, *J. Phys Chem. B* **2000**, *104*, 43-47.

los derivados del DPN, similar a la encontrada en compuestos conjugados, los convierte en candidatos idóneos para llevar a cabo este estudio.

Una de las aplicaciones de los compuestos conjugados más interesantes desarrolladas en los últimos años es la de su utilización como cables moleculares, capaces de intervenir o mediar en el transporte de electrones o de energía entre dos extremos de una molécula, formando díadas D-B-A (D = dador de electrones o energía; B = puente, molécula conjugada; A = aceptor de electrones o energía). Hasta la fecha se ha investigado el comportamiento de un número muy elevado de puentes conjugados, pero no de sistemas homoconjugados, por lo que decidimos iniciar este estudio como parte del presente trabajo. Para ello se han sintetizado los complejos descritos en la Figura 23.[305]La elección del complejo bimetálico heteronuclear Ir -Nor-Ru (**5)** se basó en los buenos resultados descritos para sistemas D-B-A en los que intervienen complejos de Ir(III) y Ru(II), como dadores y aceptores, respectivamente, en procesos de transferencia de energía.[306] Los complejos homonucleares de Ru(II), Ru-Nor-Ru (**3**), e Ir(III), Ir-Nor-Ir (**4**), se sintetizaron como referencias para el estudio del comportamiento de **5**. En la Figura 24 pueden verse los espectros de absorción y emisión de estos complejos.

Los espectros de absorción y emisión de los complejos Ru-Nor-Ru e Ir-Nor-Ir son muy similares a los de las referencias $[Ru(bpy)_3]^{2+}$ e $[Ir(ppyFF)_2(bpy)]^{+}$ con bandas de absorción (λ_{max}) a 288 nm (Ru-Nor-Ru) y 247, 298 y 350 nm (Ir-Nor-Ir) y bandas de emisión a 625 nm (Ru-Nor-Ru) y 526 nm (Ir-Nor-Ir) (Tabla 4). Por otra parte, el espectro de absorción del complejo heteronuclear Ir-Nor-Ru (Figura 25) es la suma de los espectros de los complejos homonucleares, con bandas a 246, 288, 326 y 400-550 nm.

Para estudiar la transferencia de energía en el complejo Ir-Nor-Ru se utilizó una λ_{exc} de 332 nm. A esta longitud de onda los complejos de Ir y Ru absorben la misma fracción de radiación. El espectro de emisión de Ir-Nor-Ru (Figura 25, Tabla 4) muestra tan solo una banda a 625 nm, correspondiente a la emisión del complejo de Ru(II). No hay rastro de la emisión por parte del

[305] J. Osío Barcina, N. Herrero-García, F. Cucinotta, L. De Cola, P. Contreras-Carballada, R. M. Williams, A. Guerrero-Martínez, *Chem. Eur. J.* **2010**, *16*, 6033-6040.
[306] S. Welter, F. Lafolet, E. Cecchetto, F. Vergeer, L. De Cola, *Chem. Phys. Chem.* **2005**, *6*, 2417-2427.

complejo de Ir(III), lo cual indica que se ha producido la total desactivación (quenching) de la emisión de este centro o, lo que es lo mismo, que ha tenido lugar una transferencia de energía muy eficaz desde el Ir al Ru.

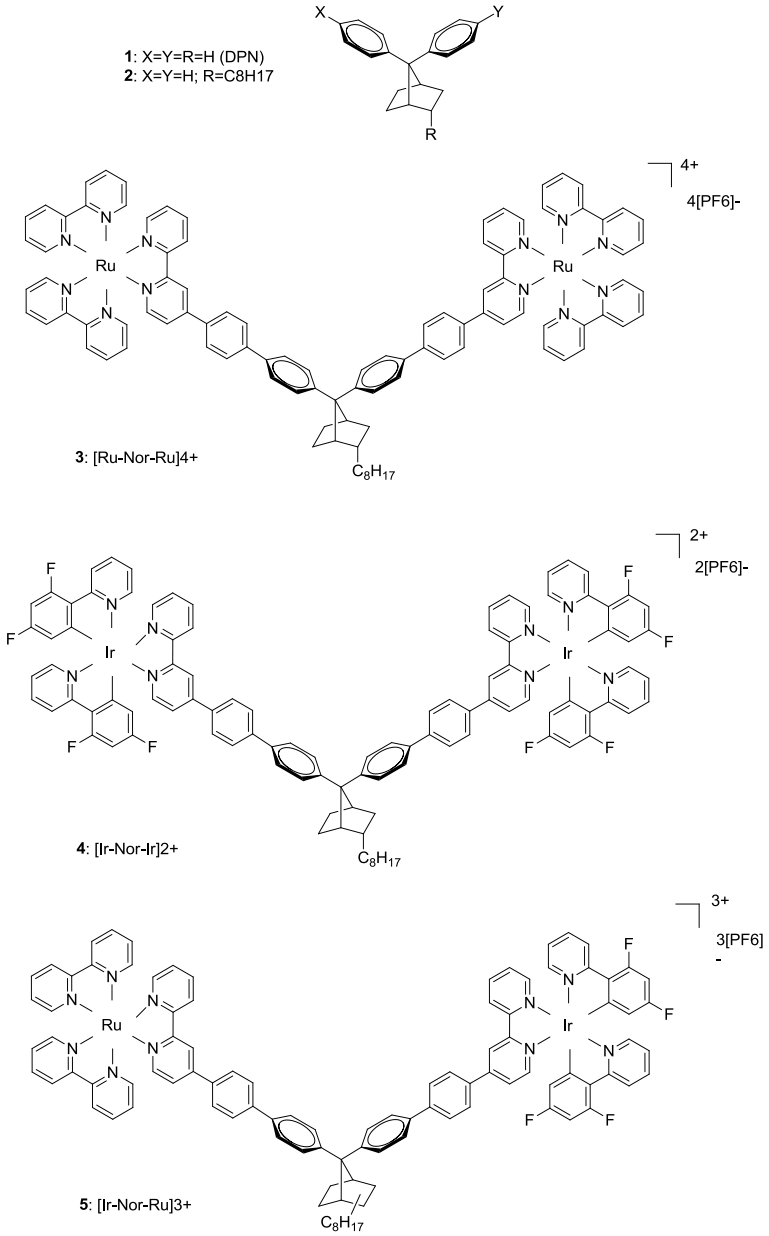

Figura 23. Estructura de los complejos metálicos estudiados.

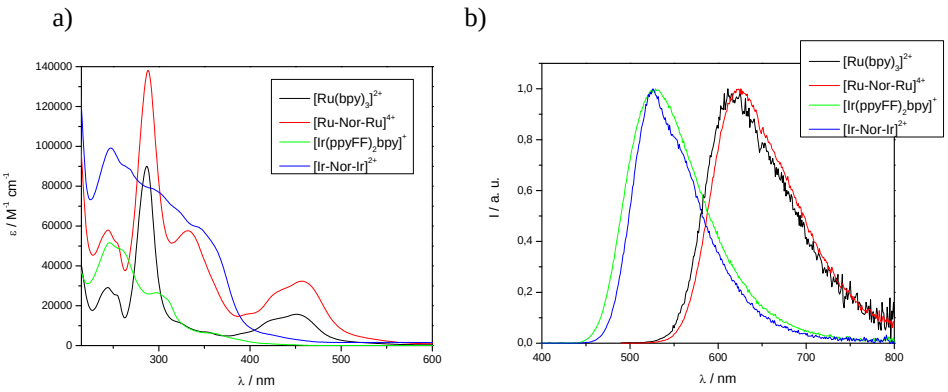

Figura 24. Espectros de absorción (a) y emisión (λ_{exc} =332 nm) (b) (acetonitrilo diluido, 298 K) de los complejos Ru-Nor-Ru e Ir-Nor-Ir.

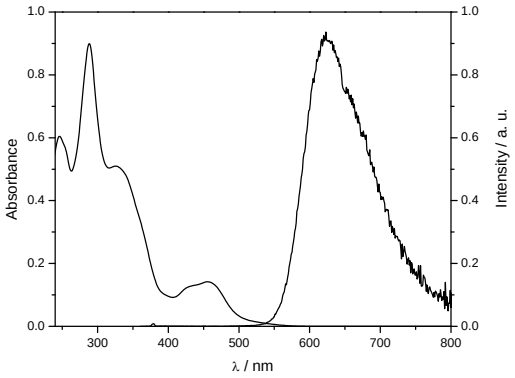

Figura 25. Espectros de absorción y emisión del complejo bimetálico heteronuclear Ir-Nor-Ru (acetonitrilo, 293 K).

Tabla 4. Datos fotofísicos de los complejos estudiados.

	298 K [a]					77 K [b]			
	Ir^{III} λ_{max} [nm]	τ [ns] [d]	Ru^{II} λ_{max} [nm]	τ [ns] [d]	$10^2 \times \phi$	Ir^{III} λ_{max} [nm]	τ [μs] [d]	Ru^{II} λ_{max} [nm]	τ [μs] [d]
$[Ir\text{-}Nor\text{-}Ir]^{2+}$	526	150	-	-	1.8	508	37.0	-	-
$[Ru\text{-}Nor\text{-}Ru]^{4+}$	-	-	625	197	7.4	-	-	593	5.9
$[Ir\text{-}Nor\text{-}Ru]^{3+}$	-	[c]	625	200	7.4	[c]	-	590	5.8
$[Ir(ppyFF)_2(bpy)]^+$	529	140	-	-	2.2	484	4.4	-	-
$[Ru(bpy)_3]^{2+}$	-	-	619	156	6.2	-	-	579	5.7

[a] En acetonitrilo, λ_{exc} = 332 nm. [b] En matriz rígida de acetonitrilo, λ_{exc} = 332 nm. [c] Intensidad demasiado baja para poder medirse con precision mediante [d]. [d] Determinado mediante el método de recuento de fotones individuals correlacionados temporalmente (time-correlated single-photon counting method).

Para seguir la evolución del proceso de transferencia de energía en el complejo Ir-Nor-Ru se recurrió a la espectroscopia de absorción de transitorios en la escala de sub-picosegundos (no fue posible hacerlo en la escala de tiempos de nanosegundos). Los resultados obtenidos se exponen en la Figura 26.

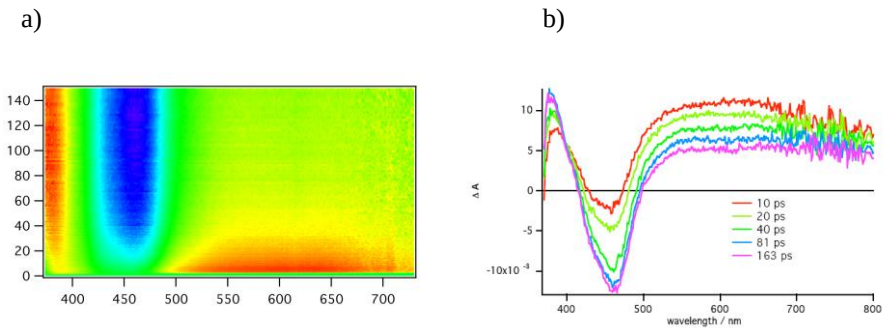

Figura 26. Espectros de absorción de transitorios en la escala de sub-picosegundos del complejo Ir-Nor-Ru.

En la Figura 26a se muestran los datos de la espectroscopia de absorción transitoria a intervalos de tiempo de femtosegundos. En color azul se aparecen

las bandas negativas mientras que en rojo aparecen las positivas. Tras la excitación, se observa la formación de una banda ancha entre 500-800 nm correspondiente al estado excitado centrado en el Ir. Esta banda decae rápidamente durante los primeros 150 ps al mismo tiempo que aparecen dos bandas nuevas: una positiva por debajo de 400 nm, y otra negativa entre 400-500 nm. Esta última banda se corresponde con la pérdida de intensidad de la emisión del centro de Ru.

La figura 26b se obtiene por superposición de varios espectros de absorción transitoria. La cinética del proceso de transferencia de energía se obtuvo a partir de la evolución de la banda a 375 nm, que muestra que la desactivación completa del centro de Ir tiene lugar durante los primeros 150 ps. La velocidad de la transferencia de energía resultó ser k_{ET} = 3.24 x 10^{10} s^{-1} y la eficacia del proceso del 99.98%.

Estos datos demuestran que, aunque la velocidad de la transferencia de energía es algo menor que en díadas con puentes conjugados debido a que la deslocalización electrónica no es tan eficaz en compuestos homoconjugados, la transferencia de energía tiene lugar mediante un mecanismo de tipo Dexter.

En resumen, los resultados obtenidos permiten afirmar que los sistemas homoconjugados pueden emplearse para el transporte eficaz de energía y electrones a distancias largas (~ 3 nm). Nuestros datos son los primeros descritos que emplean este tipo de puentes homoconjugados.

En este capítulo se exponen también resultados previos, no publicados, que forman parte de los estudios llevados a cabo en la presente Memoria. En concreto, se ha estudiado la aplicación del complejo Ru-Nor-Ru descrito anteriormente en la construcción de OLEDs.

Una de las aplicaciones más relevantes de los compuestos orgánicos conjugados es su utilización en el diseño de diodos orgánicos emisores de luz (OLED's).[307,308,309,310,311,312,313] El empleo de materiales orgánicos en estos dispositivos presenta ventajas importantes en comparación con los análogos inorgánicos como son su facilidad de procesado y la enorme variedad estructural de las moléculas orgánicas, lo que permite estudiar en profundidad la relación estructura-propiedades en estos dispositivos.

En la Figura 27 se representa de manera esquemática la estructura interna típica de un OLED. Básicamente, éste consiste en una serie de capas de materiales orgánicos situadas entre un ánodo, con frecuencia de óxido de titanio y estaño (ITO), y un cátodo metálico de Mg-Ag o Li-Al. Al aplicarse un voltaje externo al dispositivo se produce la migración de electrones y huecos desde las respectivas capas de materiales orgánicos hacia la capa emisora. La formación y consiguiente relajación de los excitones produce la emisión de luz.

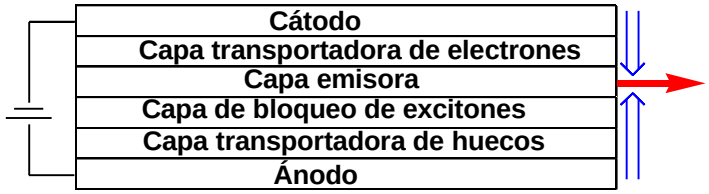

Figura 27. Representación esquemática típica de un OLED.

[307] Yersin, H. *Highly Efficient OLEDs with Phosphorescent Materials*; Wiley-VCH: Weinheim, Germany, **2008**.
[308] *Organic Light-Emitting Devices. Synthesis, Properties and Applications*, (Eds: K. Müllen, U. Scherf), Wiley-VCH, Weinheim, **2006.**
[309] *Organic Electroluminescence*, Kafafi Z. H., Ed.; Taylor Francis, Boca Raton, **2005**.
[310] J. Liu, Q. Pei, *Curr. Org. Chem.* **2010**, *14*, 2133-2144.
[311] Z. Ma, P. Sonar, Z.-K. Chen, *Curr. Org. Chem.* **2010**, *14*, 2034-2069.
[312] A. C. Grimsdale, *Curr. Org. Chem.* **2010**, *14*, 2196-2217; h) C. Li, Z. Bo, *Polymer* **2010**, *51*, 4273-4292.
[313] Chiu, C.-W.; Chow, T. J.; Chuen, C.-H.; Lin, H.-M.; Tao, Y.-T. *Chem. Mater.* **2003**, *15*, 4527.

Hasta ahora se ha utilizado una gran variedad de compuestos orgánicos en el diseño de OLED's, incluyendo complejos metálicos con ligados orgánicos conjugados.[314] Sin embargo, la utilización de sistemas homoconjugados en estos dispositivos permanece inexplorada hasta la fecha, en vista de lo cual, y dadas las buenas propiedades que han demostrado poseer los complejos metálicos homoconjugados descritos previamente, hemos decidido comenzar el estudio de la utilización de los mismos en el diseño de OLEDs. Este trabajo se está llevando a cabo en colaboración con el Prof. Miguel Clemente, del Instituto de Ciencia Molecular de la Universidad de Valencia. Los resultados obtenidos hasta la fecha con el complejo homoconjugado Ru-Nor-Ru (Figura 28) son muy prometedores.

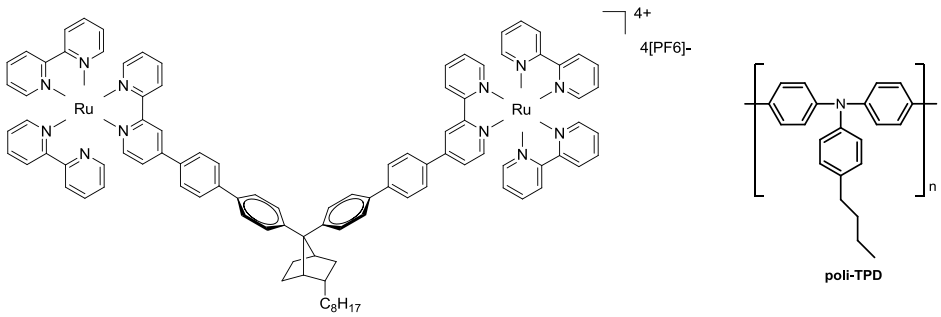

Figura 28. Estructura del complejo Ru-Nor-Ru y del polímero poli-TPD utilizados en la preparación de OLEDs.

Para el estudio con el complejo Ru-Nor-Ru se han preparado dispositivos con la siguiente estructura (Figura 29):[315a]

- Sustrato de ITO
- Capa de polimero (polyTPD de 70-80 nm) depositado por spin coating
- Pelicula LB del complejo Ru-Nor-Ru mezclado con una molecula anfifilica (SME, metil estearato)
- Capa evaporada de Ba/Ag para cerrar el circuito

[314] R. C. Evans, P. Douglas, C. J. Winscom, *Coord. Chem. Rev.* **2006**, *250*, 2093-2126.
[315] a) H. J. Bolink, E. Baranoff, M. Clemente-León, E. Coronado, N. Lardiés, A. López-Muñoz, D. Repetto, Md. K. Nazeeruddin, *Langmuir* **2010**, *26*, 11461-11468; b) H. J. Bolink, E. Baranoff, M. Clemente-León, E. Coronado, A. López-Muñoz, D. Repetto, M. Sessolo, Md. K. Nazeeruddin, *Langmuir* **2009**, *25*, 79-83.

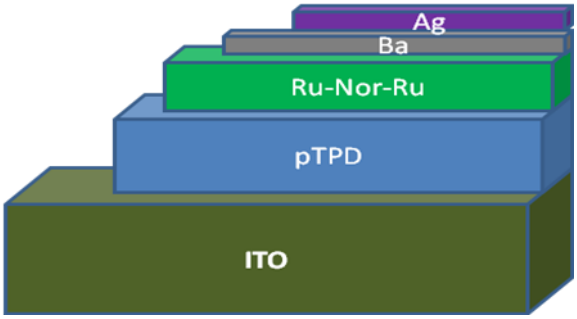

Figura 29. Arquitectura de los dispositivos estudiados.

El aspecto más novedoso de los dispositivos diseñados en este caso es que para hacer la capa emisora se ha empleado la técnica LB en lugar de las más habituales como son la evaporación o el spin-coating.[17] El polímero semiconductor poli-TPD se emplea con mucha frecuencia en la construcción de OLEDs como capa transportadora de huecos. Por otra parte, la técnica LB presenta la ventaja de que es muy fácil cambiar de contraión, lo que permite estudiar el efecto que diferentes iones tienen sobre las propiedades emisoras del OLED. En la figura 30 se muestran los resultados obtenidos hasta la fecha con los contraiones F^-, BF_4^-, PF_6^-, $(SiW_{12}O_{40})^{4-}$.

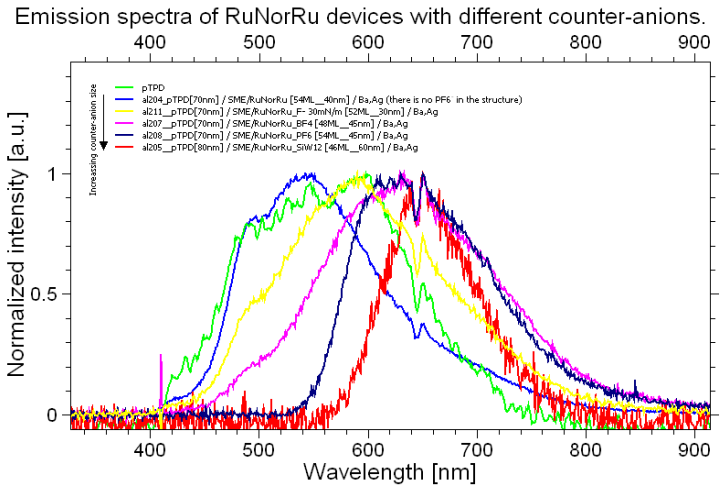

Figura 30. Espectros de emisión de los dispositivos preparados con diferentes contraiones.

Como puede observarse en la Figura 30, el color de la luz emitida al aplicar el voltaje depende del contraión utilizado en cada caso. Este es un resultado muy interesante ya que podría controlarse la longitud de onda de la luz emitida por el dispositivo mediante un sencillo cambio del contraión.

IV.2.2 Diseño de receptores moleculares para la complejación selectiva NH_4^+/K^+

Tanto el diseño de receptores moleculares selectivos como el estudio de las interacciones no covalentes involucradas en la formación de los correspondientes complejos receptor-huésped siguen siendo retos importantes en Química Supramolecular.

En nuestro grupo de investigación hemos venido utilizando el DPN como subunidad estructural de diversos tipos de compuestos para el estudio de interacciones aromáticas (cara-cara y lado-cara),[316,317] interacciones no covalentes CH···π y OH···π,[318] y en el diseño de receptores moleculares que formen complejos estables con cationes metálicos, como el catión Ag^+.[319] La base de estos estudios estriba en el elevado grado de preorganización que presentan el DPN y sus derivados. Esta preorganización no solo hace posible la deslocalización electrónica entre los anillos aromáticos, sino que convierte al DPN en un sustituto ventajoso del difenilmetano, subunidad muy utilizada en Química Supramolecular. Hay que tener en cuenta que los factores de carácter entrópico, como por ejemplo el grado de libertad conformacional del receptor, desempeñan un papel fundamental a la hora de diseñar sustratos complementarios con el huésped y que formen con éste complejos estables.

En esta ocasión nos propusimos diseñar un receptor molecular neutro, es decir, sin heteroátomos básicos como el oxígeno o el nitrógeno que puedan

[316] A. García Martínez, J. Osío Barcina, A. De Fresno Cerezo, R. Gutiérrez Rivas, *J. Am. Chem. Soc.* **1998**, *120*, 673-679.
[317] A. García Martínez, J. Osío Barcina, A. de Fresno Cerezo, *Chem. Eur. J.* **2001**, *7*, 1171-1175.
[318] J. Osío Barcina, I. Fernández, M. R. Colorado Heras, *Eur. J. Org. Chem.* **2012**, 940-947.
[319] A. García Martínez, J. Osío Barcina, M. R. Colorado Heras, A. de Fresno Cerezo, M. R. Torres Salvador, *Chem. Eur. J.* **2003**, *9*, 1157-1165.

interaccionar con el huésped, capaz de complejar de manera selectiva el ión amonio frente al catión potasio. El diseño de este tipo de receptores es uno de los problemas clásicos en Química Supramolecular debido a que ambos cationes tienen tamaños muy similares y geometrías esféricas. Por otra parte, este receptor, al estar constituido exclusivamente por hidrocarburos aromáticos sería un buen modelo para el estudio de las interacciones catión-π ($NH_4^+\cdots\pi$ y $K^+\cdots\pi$) involucradas en la formación de los complejos.

Con estas ideas previas diseñamos y sintetizamos el receptor **1** (Figura 32). En este compuesto, debido a la presencia de subunidades de DPN, los anillos aromáticos se encuentran situados en una conformación tetrahédrica, formando un receptor con geometría de "cesta molecular", lo cual debería favorecer la complejación de iones NH_4^+ frente al K^+ mediante el establecimiento de interacciones N-H$\cdots\pi$. También se obtuvo el compuesto **5**, derivado del difenilmetano, como referencia menos preorganizada.

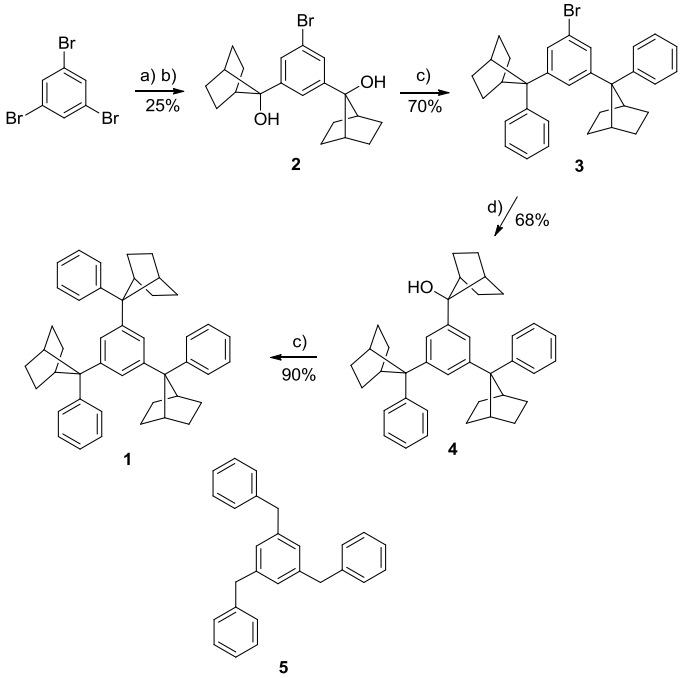

Figura 31. Estructuras y síntesis de la cesta molecular **1** y del compuesto de referencia **5**.

El análisis por rayos-X de la estructura de **1** en estado sólido confirma que los fenilos laterales se sitúan en conformación cofacial con respecto al fenilo central (Figura 33), adoptando una conformación alternada con dos de los fenilos en sentido contrario con respecto al tercero.

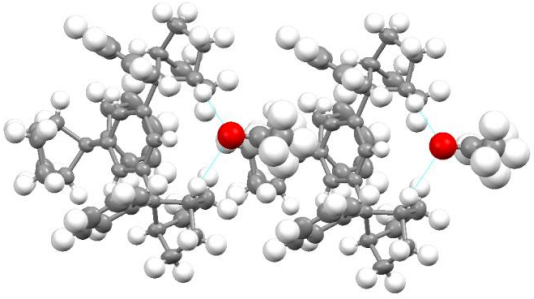

Figura 32. Estructura cristalina de **1**.

De acuerdo con cálculos DFT (M06-2X/TZVP/M062x-def2-SVP) las dos conformaciones representativas de **1**, la conformación cesta y la alternada son prácticamente isoenergéticas (Figura 34), existiendo un equilibrio rápido entre ambas en disolución. Este resultado está de acuerdo con observaciones previas descritas por nosotros para otros derivados del DPN.

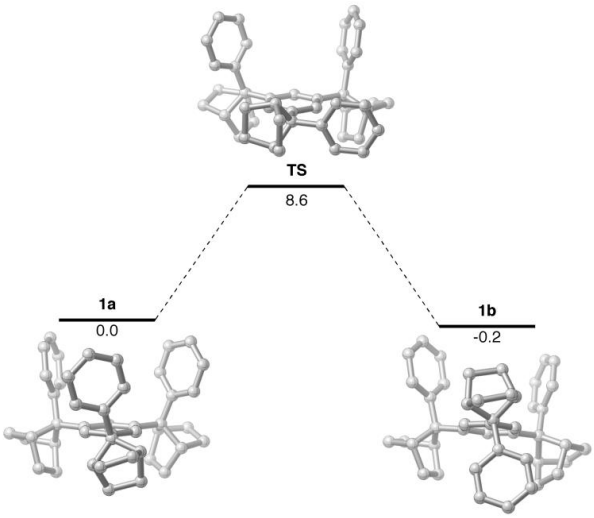

Figura 33. Proceso de isomerización del receptor **1**. Datos obtenidos mediante cálculos DFT (M06-2X/TZVP/M06-2X-def2-SVP).

Una vez comprobados los aspectos estructurales de la cesta molecular **1**, procedimos a estudiar su comportamiento como receptor molecular. Para ello se llevaron a cabo dos experimentos de competencia, cuyos resultados se analizaron empleando espectrometría de masas con ionización por electrospray (ESI-MS). En un primer experimento se analizó una mezcla equimolecular de los compuestos **1**, **5** y NH_4PF_6. En este caso solo se detectó la presencia del pico a *m/z* = 606, correspondiente al complejo **1**·NH_4^+. Este resultado pone de manifiesto la importancia de la preorganización y confirma nuestra hipótesis de partida en el sentido de la idoneidad del empleo de DPNs en la construcción de receptores moleculares en lugar de difenilmetano.

En un segundo experimento de competencia se analizó una disolución con cantidades equimoleculares del receptor **1** y las sales NH_4PF_6 y KPF_6. Se detectó la formación de los complejos **1**·NH_4^+ (*m/z* = 606) y **1**·K^+ (*m/z* = 627). La intensidad relativa de los picos (I[**1**·NH_4^+]/I[**1**·K^+] = 5.1) (Figura 34) pone de manifiesto que la cesta molecular **1** muestra una clara preferencia por el catión amonio frente al potasio, de acuerdo con nuestra idea inicial según la cual un receptor preorganizado, con anillos aromáticos en disposición tetrahédrica complementarios con los enlaces N-H del ión NH_4^+ favorecería la complejación receptor·NH_4^+. Este es un resultado muy notable ya que constituye el primer ejemplo de receptor molecular hidrocarbonado que muestra una elevada selectividad NH_4^+/K^+, basada tan solo en interacciones catión···π.

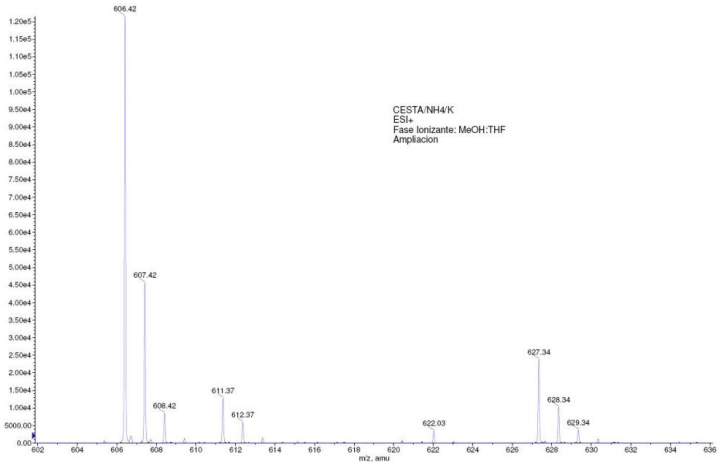

Figura 34. Espectro ESI-MS de la disolución **1**:NH_4PF_6:KPF_6 (1:1:1) en MeOH/THF (1:1).

a)

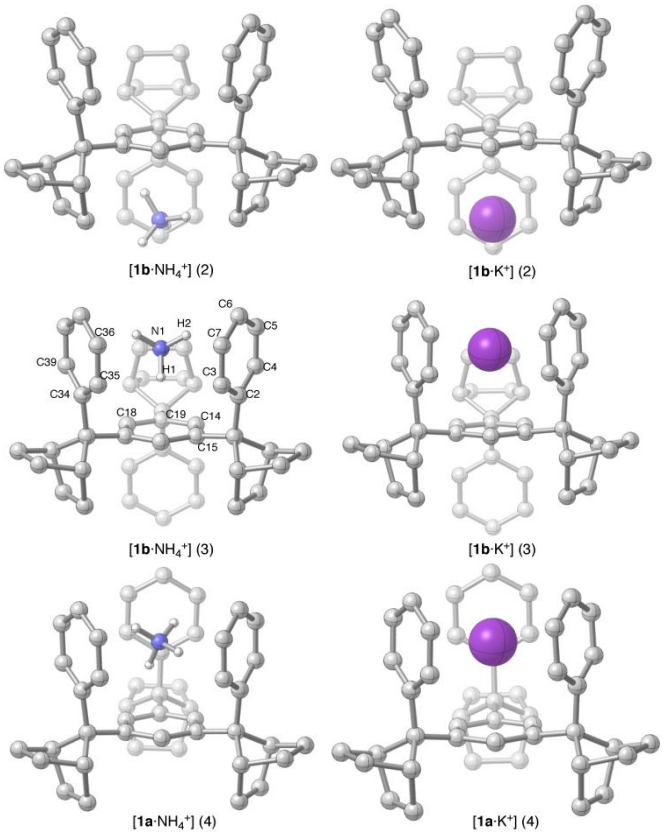

(b)

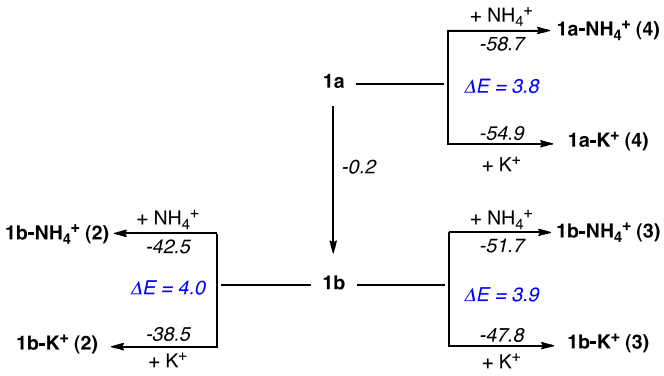

Figura 35. a) Geometrías optimizadas (M06-2X/def2-SVP) de los complejos [1a·NH_4^+], [1b·NH_4^+], [1a·K^+], y [1b·K^+]. b) Energías de complejación: E = E(complejo) – E (1) – E(catión), en kcalmol^{-1}) (M06-2X/TZVP//M06-2X/def2-SVP, incluyendo los correspondientes errores de superposición de bases)

Una vez más los cálculos computacionales DFT aportan información muy relevante que ayuda a interpretar los datos experimentales. En la Figura 35 se muestran los resultados obtenidos con los diferentes complejos que pueden formarse en el experimento de competencia.

Se han calculado las geometrías y las energías de los complejos que pueden intervenir en el proceso de complejación y que dan lugar a la selectividad NH_4^+/K^+ observada. Los cationes más estables son aquellos en los que el receptor adopta la conformación de cesta estableciendo cuatro interacciones catión·π con los respectivos huéspedes. Por tanto, tras la complejación el equilibrio entre las dos conformaciones isoenergéticas (cesta y alternada) de **1** se desplaza hacia la conformación que da lugar a los complejos más estables. Por otra parte, en todos los casos estudiados los complejos **1**·NH_4^+ resultan ser más estables que los complejos **1**·K^+, independientemente del número de interacciones catión·π que intervengan. La contribución de las interacciones NH·π en el complejo **1**·NH_4^+, responsables en última instancia de la selectividad observada, queda puesta de manifiesto por los cálculos NBO llevados a cabo que indican la presencia de interacciones entre los orbitales ocupados π(C=C) de los fenilos y los orbitales vacíos σ*(N-H).

Por último, los datos de las energías de complejación recogidos en la Figura 35 permiten estudiar las interacciones múltiples catión·π que se producen en los complejos y estimar la contribución de cada grupo arilo a medida que pasamos desde los sistemas menos estables, con dos interacciones catión·π, a los complejo más estables con el receptor en conformación de cesta. De acuerdo con estos datos, la contribución de un tercer fenilo al pasar de **1b**·catión (2) a **1b**·catión (3) es ~ 9.2 $kcalmol^{-1}$, mientras que la del cuarto fenilo al pasar de **1a**·catión (4) es ~ 7.1 $kcalmol^{-1}$. Por tanto el conjunto de datos aportados por los cálculos computacionales suministran información relevante acerca del mecanismo de complejación en sistemas en los que se establecen interacciones múltiples catión·π, muy importantes en sistemas biológicos.

En resumen, en esta parte del trabajo presentado se describe el primer ejemplo de un receptor molecular sin centros básicos que muestra una selectividad NH_4^+/K^+ elevada. Las uniones receptor·huésped en los complejos estudiados se establecen únicamente a través de interacciones catión·π. Los cálculos DFT realizados aportan información muy relevante que permite

interpretar los mecanismos de complejación y la selectividad observada en nuestro receptor molecular.

V. CONCLUSIONES

V. Conclusiones

A continuación se exponen las conclusiones más relevantes que pueden extraerse del trabajo llevado a cabo en la presente Tesis Doctoral:

- De los estudios llevados a cabo en el presente trabajo se deduce que, al contrario de lo observado en sistemas formados por dobles o triples enlaces, la homoconjugación aromática permite la comunicación electrónica entre los anillos aromáticos de forma muy eficaz.

- La deslocalización electrónica observada en los sistemas estudiados es comparable a la descrita en oligofenilenos conjugados y se pone de manifiesto tanto en la reactividad como en las propiedades espectroscópicas de las moléculas, oligómeros y polímeros estudiados.

- La deslocalización electrónica en sistemas homoconjugados puede modularse fácilmente mediante la introducción de sustituyentes en diferentes posiciones de las moléculas.

- Los cálculos computacionales DFT realizados confirman los resultados experimentales y aportan información muy relevante que ayuda a interpretar el fenómeno de la homoconjugación aromática. Asi, las bandas de homoconjugación observadas en los espectros UV-vis se asignan a transiciones HOMO-LUMO que involucran a orbitales moleculares con deslocalización electrónica entre los anillos aromáticos.

- Se describe el primer ejemplo de transferencia de energía fotoinducida en sistemas dador-puente-aceptor en el que la subunidad puente está formada por moléculas homoconjugadas. Los estudios llevados a cabo muestran que la transferencia de energía se produce mediante un mecanismo tipo Dexter con una eficacia del 99.98%.

- Se describe el primer ejemplo de un receptor molecular hidrocarbonado que muestra una selectividad NH_4^+/K^+ elevada, basada exclusivamente en interacciones catión-π. Los cálculos DFT llevados a cabo aportan información importante acerca del origen de la selectividad observada,

así como del mecanismo de complejación en sistemas receptor-huésped en los que están involucradas interacciones no covalentes múltiples.